University of Nevada, Reno

Evaluation of Existing Subsurface Cooling Systems Worldwide and Development of Efficient Cooling Methods and Systems Based on Renewable Energy Sources

A dissertation submitted in partial fulfillment of the
Requirements for the degree of
Doctor of Philosophy in Mineral Resources Engineering

by

Jon Eric Fox

Dr. Karoly (Charles) Kocsis/Dissertation Advisor

May 2021

THE GRADUATE SCHOOL

We recommend that the dissertation
prepared under our supervision by

JON ERIC FOX

entitled

Evaluation of Existing Subsurface Cooling Systems Worldwide and Development of Efficient Cooling Methods and Systems Based on Renewable Energy Sources

be accepted in partial fulfillment of the
requirements for the degree of

DOCTOR OF PHILOSOPHY

Karoly (Charles) Kocsis, Ph.D.
Advisor

Rajagopala Kallu, Ph.D.
Committee Member

Robert Watters, Ph.D.
Committee Member

Pengbo Chu, Ph.D.
Committee Member

Sergiu Dascalu, Ph.D.
Graduate School Representative

David W. Zeh, Ph.D., Dean
Graduate School

May 2021

Abstract:

As relatively hot mineral deposits are being developed to considerable depth, the issue of mitigating heat will require substantial cooling capacity in some cases. For deep deposits to be mined at increasing depths, mechanical cooling systems used to maintain an acceptable underground climate will most surely become increasingly complex and expensive, which most certainly preclude practical solutions without fresh innovation.

In most subsurface operations, bulk air-cooling methods, the main source of potential cooling energy comes from cold-water applications. The cold water can come from ice (stowed or transported), in situ reservoirs or refrigerated water chillers in either low or high-pressure systems. The main issue with ice is the service temperature is limited to freezing point of water, at 0 °C. In respect to cooling capacity considerations, it is important to highlight that most industrial applications of refrigerants are capable of maintaining the liquid phase state far below 0 °C.

This dissertation primarily investigates the practical use of low-pressure, chilled propylene glycol, which has a freezing point of -68 °C, in a closed circuit as the source of cooling the intake air for deep and hot mines. Air-cooling power is available by means of passing intake airflow across plate heat exchangers through which low pressure chilled propylene glycol is pumped. A key factor to the design and operation of an efficient and sustainable cooling system is that

the tanks of propylene glycol are chilled during favorable atmospheric conditions when the tanks can be exposed to the cold of the night.

Planning for sustainable cooling potential requires protected space to successfully maintain chilled propylene glycol in storage until needed. Stored propylene glycol should be judiciously cared for, safely kept from the ill effects of heat, in order to remain useful for bulk air-cooling. Maximizing the chilled temperature of the propylene glycol reservoir tanks means that atmospheric conditions will be monitored closely during the chilling phase. Storage facilities would maintain restricted airflow while minimizing possibilities for heat transfer during the storage phase.

Secondly, this dissertation investigates the use of ice accumulated in underground access tunnels as the source of renewable air-cooling. The current market trend in profitable mining operations involves continued mining activity below a viable mineral deposit which was initially developed with an open pit. Due to the scale of this type of operation, a popular current trend from the surface mining perspective is to use very large haul trucks bringing ore up a long ramp system which daylights in the open pit. This type of ramp mine access drift is driven into the most stable strata surrounding the open pit. This mining arrangement is the proposed application for bulk air cooling via stowed ice reservoirs. The proposed ice storage arrangement would work successfully in any lower latitude mining operations that experience a cold winter season.

Snow is produced under favorable atmospheric conditions using commercial snow making equipment typically found at ski resorts. Regulators with air locks would be installed on either end of each gallery to maintain minimum velocities during snow and ice accumulation. Using compressed air and water, snow is blown, during near-freezing conditions across snow fences arranged in an array aligned with the airflow. Snow fences are employed to maximize the snow deposition potential.

The system will use wastewater from the mine and recycle water during operation as the ice melts into storage sumps. Water quality monitoring will be required since nucleation agents will need to be added to the reservoir water before spraying application. In order to maintain the highest level of safety, continual monitoring of ground conditions will be maintained during the operation and maintenance of the renewable cooling ice storage facility. Additional geotechnical measures will be necessary to ensure pit portal integrity due to the addition of the stowed ice reservoirs.

Sustainable cooling systems could reduce or eliminate the need for mechanical cooling if installed with favorable conditions. Successful installations will prioritize environmental management to favor long time span usage of sustainable cooling systems.

Acknowledgments:

I would like to express my deepest appreciation and gratitude to my advisor, Dr. Karoly (Charles) Kocsis. Without the guidance and support of Dr. Kocsis, the completion of my graduate studies would not have been possible. Dr. Kocsis has advocated for me and taught me a vast amount about the value of health and safety of our underground workforce and ventilation related mine design issues throughout my time at the University of Nevada, Reno.

Along with Dr. Kocsis, I would like to thank my committee members, Dr. Rajagopala Kallu, Dr. Pengbo Chu, Dr. Robert Watters and Dr. Sergiu Dascalu for their support throughout my graduate school process.

Special acknowledgments are needed for the engineers and mine sites that made all the work I completed possible. Special thanks are also due to Vale and Cheryl Allen for their time, effort and the opportunities they presented and continue so since early 2015.

I need to thank my family, my brother Edgar, and specifically my wife, Lisa. Their guidance, love and unwavering support allow me to accomplish tasks I never thought possible.

Thank you all.

Table of Contents

Table of Tables

Table of Figures

1. Problem Statement

In order to ensure the health and safety of the underground workforce, the quality of air delivered to the workplace is vitally important (MSHA, 2012). Sufficient airflow also needs to be delivered to remove waste heat, noxious fumes and fugitive dust that will adversely affect the performance of mining equipment (McPherson, 1984). Both workers and equipment will suffer from poor performance due to prolonged exposure to relatively hot working environments.

For an underground mine's atmosphere to be a safe, healthy and ultimately a highly productive workplace is a challenge in our current economic environment. In order for deep deposits to be mined at increasing depths, mechanical cooling systems used to maintain an acceptable underground climate may become increasingly complex and expensive (Butterworth and Sheer, 2011).

As relatively hot mineral deposits are being developed to considerable depth, the issue of mitigating heat will require significant cooling capacity at extremely high capital and operating costs. In many deep underground mines the heat transferred to the ventilating air from strata, auto-compression and mining equipment will dictate whether deep ore reserves will be mined or left in place. In addition, an increased energy demand from the massive mechanical cooling systems and associated refrigeration plants will generate a large amount of greenhouse gas emissions (GHG), thus increasing the carbon footprint of many underground mines. Consequently, the need to develop environmental-friendly and efficient mine ventilation and cooling systems able to provide appropriate work conditions in deep and hot underground mines is of paramount importance. Development and implementation of efficient cooling methods and systems based on renewable-energy sources coupled to forward thinking and innovative practical solutions would significantly reduce ventilation and air cooling costs, while minimizing the carbon footprint of many underground mines world-wide.

1.1 Contaminants Underground

The production of dust and fumes by mining operations is a necessary evil (McPherson, 1993). Drilling, blasting, loading and haulage activities liberate quantities of heat, dust and noxious fumes that have numerous negative health and safety consequences. Diesel equipment is very inefficient by nature and tremendous amounts of waste heat are generated by the operation of the internal combustion engine in the underground environment (Carpenter, Roghanchi and Kocsis, 2015). Diesel particulate matter is carcinogenic and has other ill effects on equipment and other installations within the mining infrastructure. Much of the desired airflow in a mine tends to be dedicated to the diffusion of diesel fumes (Howes, 2010).

1.2 Heat

The temperature of a mine’s intake air gradually increases as a function of depth and the distance the air travels through the underground openings (Schlotte and Walasiak, 2011). A major heat source in underground mines is the geothermal heat from the strata. The geothermal flow of heat is emanating from the core of the earth, and it is transferred to the mine air, as it passes through the rock formations (Brake and Bates, 2002).

Heat sources in deep underground mines include:

- Steep geothermal gradient (strata heat)
- Diesel and electric equipment
- Geothermally hot inflow water

Other sources of heat in underground mines are auto-compression as air flows through shafts and slopes when the potential energy is converted into thermal energy, explosive detonation, human metabolism and influx of thermal water (Hardcastle and Kocsis, 2002).

The effects of heat on the health and safety of mineworkers has been historically underestimated in the mining industry (Mine Safety and Health Administration, 2012). Miners are usually not complaining about heat problems until it's too late. Multitudes of occupational errors and poor decisions can be attributed to hot or humid workplaces (Department of Industry and Resources, 1997). Injuries and accidents are far more likely to happen when a miner is having a hard time maintaining their focus. Excessive heat exposure will negatively affect the performance of mine workers and the overall productivity of the mine (Roghanchi and Kocsis, 2018). Having a cool, comfortable environment for the miner will help them stay alert and on task.

The consequences of heat exposure include: heat-related illnesses, fatigue and fainting, loss of concentration, performance reduction, and production loss (Roghanchi, 2017). Heat-related illnesses include:

1) Heat stress and strain,
2) Heat cramps,
3) Heat exhaustion,
4) Heat stroke.

When heat is identified as a health problem it is really too late since the worker might have already passed through the heat stroke phase (ISO 7243, 1989). Delivering cooler air to the workplace is an appropriate way to approach air quality that ensures safety and health in underground workplaces.

1.3 Greenhouse Gas Effects on Global Warming

Serious changes are happening to our environment, as the direct result of global warming (Trewin and Baddour, 2018). Glaciers are retreating at unprecedented rates while rising sea levels are the direct result of rapidly melting polar ice caps leading to rapid acidification of the artic oceans (AMAP, 2019). Wildfires are increasing at an alarming rate, increasing the total carbon dioxide content of the atmosphere (Goss, Swain, Abatzoglou, Sarhadi, Kolden, Williams and Diffenbaugh, 2020). Global warming is a scientific fact that must be embraced if our society is to be responsibly sustained.

The Paris Climate Accord has voluntarily engaged 195 countries to help maintain the earth’s atmosphere to within less than 2°C pre-industrial average climate temperatures (UNFCCC, 2015). Within the USA under some previous administrations, many states and local governments independently pledged commitments, along with the Federal government, to the goals of the Paris agreement. Under other administrations, some of these policies have been reversed or are losing momentum. However, much support remains present in state and local governments in the USA to remain committed to the goals of the Paris agreement. The mining industry needs to comply with local and state jurisdictions to combat the overall global carbon footprint by taking significant measures to limit fossil fuel based energy consumption.

Along with climate change, various sources impact the total heat load in a mine site (Hanna, Kjellstrom, Bennett and Dear, 2011), (Kjellstrom, Lemke, Hyatt and Otto, 2014), (Song, Wang, Hu, Yue, Zhang, Liu, Tian and Shang, 2017). Saving electrical energy consumption reduces the amount of required operating kilowatt hours, thereby lowering greenhouse gases and the carbon footprint of sustainable mining operations. Minimization of the carbon footprint for any industrial operation will decrease the additional carbon dioxide attributing to an overall greenhouse gas effect on global warming.

The ability to effectively use renewable energy sources in large part revolve around the ability to store that energy for use later (Simon, 2020). Development of storage facilities with minimal environmental controls required to maintain said energy harvesting facility is a win-win for all earth's citizens. This is to say that energy storage facilities designed to use the least amount of energy will help minimize the carbon footprint for sustainable mining projects.

Harvesting energy from our environment is the core of sustainable and renewable energy system designs (Simon, 2020). Alignment with the ideas and pursuit of effective sustainable energy plans would potentially save millions of dollars in both capital and operating expenses. Using the cold of wintertime to cool down refrigerant in the most cost-effective method possible, and storing the chilled refrigerant until summertime is the fundamental concept of new renewable air conditioning methods for underground mines presented in this dissertation.

2. Objectives

Development of innovative methods for underground mine air conditioning systems by employing renewable energy sources is the primary objective of this research. Harvesting energy is at the core of sustainable cooling system designs. Using the cold of wintertime to cool down refrigerant in the simplest, most cost-effective method possible, will potentially save millions of dollars in both capital and operating costs.

Vale's Creighton mine in Northern Ontario, Canada is one of the deep and hot operations world-wide that employs a natural renewable energy-based air cooling system (Acuna and Lowndes, 2013). Many research studies have been undertaken to quantify this renewable cooling capacity (Twort, Lowndes, Pickering, 2009) and model the airflow using various novel methods (Johnson, 2000) (Kurnia, Sasmito, and Mujumdar, 2014).

The Natural Heat Exchange Area (NHEA) at Creighton mine is the result of airflow coursing into the underground operation on the 1100 level after filtering through the open pit above, which was partially backfilled with waste rock. Ice accumulates within the backfill during the winter months, as regulators are adjusted to limit the airflow entering the mine from the NHEA. Various ventilation engineering studies and feasibility studies were conducted for the Creighton mine. The main fan failure analysis project was conducted by SRK, along with engineers from Bluhm Burton Engineering (BBE, a South African-based engineering firm that specializes in air conditioning systems for the mining industry), involved validation of the seasonal natural cooling capacity.

Canmet MINING also conducted research on renewable energy source systems through the ice stope project at Vale's Stobie Mine, which resulted in the Modular Thermal Transfer Unit (MMTU). This trial project employed ice formed by spraying water as a fine mist into a shipping container during the frigid winter months. The design concept involved filling the container with ice on the surface, then relocating the container into an enclosure connected to the intake shaft to cool the mine's intake air during summer. This trial was only partially successful, since the particular winter chosen experienced an unusually warm February. However, research work conducted by Canmet MINING in collaboration with Vale showed that innovative use of the environment and responsible care of natural resources available at the mine site will inevitably lead to a sustainable mine.

When industry truly values the health and safety of every underground worker, we state without a doubt the intention that productivity lies ultimately with the most valuable asset a mining company can engender: the first–person workforce that enables efficient production and development of the targeted orebodies. The ethics behind sustainability can thusly engender ownership never before experienced in industrial mining operations. Stakeholders could reap benefits in the long-term due to the perceived value of the employee by the operator. Health programs, including air quality (e.g. temperatures, contaminant concentrations) monitoring, help reinforce the employee's view of mining operations perceived value of said employee.

2.1 Renewable Cooling Power for Deep Mines

In many subsurface mines where bulk air-cooling methods are used, the main source of potential cooling energy comes from cold-water applications (Hartman, Mutmansky, Ramani and Wang, 1992). The cold water can come from ice (stowed or transported), in situ reservoirs or refrigerated water chillers in either low or high-pressure systems. The main issue with ice is the service temperature is limited to freezing point of water, at 0 °C. The main issue with cold water is that it cannot be piped vertically to significant depth (past 2500m) without heating the water significantly (du Plessis, Scott, Moorcraft, 2018).

Most industrial air conditioning applications of refrigerants are capable of maintaining the liquid phase state far below 0 °C (ASHRAE, 1997). This dissertation primarily investigates the practical use of low-pressure, chilled organic propylene glycol, which has a freezing point of -68 °C, in a closed circuit as the source of cooling.

Given that a deep and hot mine will need to be considered safe and productive, a cost-effective cooling system is desired in order for the mining operation to be considered sustainable. For underground mines at northern latitudes, cooling applied to the intake fresh air is only required 3 to 4 months of the year (e.g. June, July, August). During the rest of the year, the ambient atmospheric conditions could be harnessed for use at a later time. Storing the cooling potential from the winter months is what this new design is all about.

A new design for a closed circuit refrigerant bulk air cooling system employing propylene glycol as the refrigerant is presented as the main design topic of this dissertation. The basis of this sustainable design uses very cold ambient air which is circulated around galvanized steel refrigerant reservoir tanks. The propylene glycol reservoir tanks are arranged in a concrete walled pit, or tank farm, excavated in bedrock. During the coldest months, the tank farm will be exposed to the open air. As the seasons change the tank farm will be covered with insulation to maintain the maximum cooling potential for use during the warmest months of the year. A thermodynamic ventilation model is developed in Ventsim© to estimate the cooling of the reservoir tanks from the frigid ambient atmosphere.

2.2 Renewable Cooling Power for Ramp Mines

The current market trend in profitable mining operations involves continued mining activity of a viable mineral deposit which was initially developed and extracted in an open pit. Due to the scale of this type of operation, a popular alternative from the surface mining perspective is to use very large haul trucks bringing ore up a long ramp system which daylights in the open pit (Howes, 2010). These types of ramp mining operations use an underground access drift which is driven into the most stable strata surrounding the open pit. This mining arrangement is the proposed application for bulk air cooling via ice accumulation reservoir tunnels. Since many underground mines are accessed through large open pits, the theorized ice accumulation reservoir arrangement would work successfully in northern Nevada, or any mining operation that experiences cold winters.

Using compressed air and water, snow is blown, during freezing conditions across porous snow fences arranged in an array perpendicular to the airflow in the galleries. Commercial high-pressure snow gun nozzles used at ski resorts to broadcast artificially made snow are the type being specified for this renewable air-cooling system.

Snowmaking is a heat exchange process. A thermodynamic ventilation model is developed in Ventsim© to estimate both the cooling potential capacity of the proposed ice accumulation reservoirs and the heat exchange occurring during the snowmaking process. Seasonal variations of the intake air temperatures are estimated using conditions similar to those experienced at open pit operations on the Carlin trend. The simulated seasonal low and high wet bulb and dry bulb temperatures are input to the Ventsim© thermal flywheel effect solution module.

3. Introduction

For an underground mine's atmosphere to be a safe, healthy and ultimately a highly productive workplace is a challenge in our current economic environment. Financial viability of a mine depends strongly on the conceptual, prefeasibility, and feasibility studies undertaken. Ongoing input into these projects provided by ventilation engineers is equally important thereby ensuring a revolving scope was developed with continuation of requirements needed as design alternatives and changes while mining methodologies are investigated.

The heat load in underground mines largely depend on the mining depth (e.g. geothermal gradient), the rock thermal properties (e.g. conductivity, diffusivity), the mining method employed, equipment fleet (e.g. diesel, electrical) and other site specific characteristics. Some examples and basic fundamentals of heat sources and heat sinks are given to illustrate their influence and relationship as commonly encountered in underground mining operations. Also provided is general ventilation and cooling design procedures for new and existing deep and hot underground mines.

A method of improving our working environment is by making use of emerging new technology advancements and the willingness of the mining industry to adopt these new technologies and absorb changes to improve productivity while reducing production costs The atmosphere in an underground mine differs from that on surface in the sense that people have to operate in confined spaces, always surrounded by ore/rock and moving equipment. The available fresh and uncontaminated air has limitations in heat adsorption, dust removal and fumes dilution. The quantity of fresh air demanded depends on the combined ventilation and cooling methodology adopted.

Different cooling systems are employed around the world to allow effective production activities for deep and hot mines. These systems support mitigations of different environmentally or economically driven overloaded heat conditions and the available strategies to tackle the same condition. These strategies, with relevant examples include:

- Spot cooling – the air conditioner in the lunchroom, with up to 1000 ton of cooling capacity;
- Bulk air cooling - sub-level district production or development heat mitigation, with installed cooling plant of 3-5 MW;
- Personal cooling – vehicle cooling systems, and hydration PPE.

In most methods, the main source of potential cooling energy comes from cold water. The cold water can come from ice (stowed or transported), in situ reservoirs or refrigerated water chillers. Although underground refrigeration plants have better positional efficiency (closer to where the cooling is actually needed) than surface plants, they have the following disadvantages when compared with surface plants:

- High condensing temperatures as a result of limited airflow quantities in confined spaces underground;
- Underground air with relatively high wet bulb temperatures of eviscerated

return air be used for condenser heat rejection;

- Water quality is inferior to that used on surface, which contributes to quicker service water fowling;
- Supervision, maintenance and cleaning are onerous, which shortens the lifespan of the equipment.

The intent of this dissertation is to thoroughly review currently employed and proposed subsurface cooling systems appropriately scaled for modern mechanized mining. Each system will be properly evaluated, and new methods are described to offer cost effective alternatives to bulk air cooling supported by traditional high-pressure surface refrigerant plants.

In order for deep deposits to be mined at increasing depths, mechanical cooling systems used to maintain an acceptable underground climate may become increasingly complex and expensive. As relatively hot mineral deposits are being developed to considerable depth, the issue of mitigating heat will require significant cooling capacity in some cases. Establishment of more financially sound and practical solutions for heat mitigation will also require forward thinking to apply simple innovations than have been successfully adopted in other industrial applications.

4. Defining Requirements for Cooling

Besides government regulations in respect to air volume and air quality requirements, the conditions that define the cooling capacity required to maintain an acceptably safe and healthy working environment should be evaluated from the perspective of sustainability as well. When profitability and the bottom line are the primary corporate concerns, the work force's ability to enhance these two indexes through increased productivity is thoroughly dampened. Operating with sustainability also means reflecting the value of the work force's wellbeing in the adopted approaches to the mining method and processes.

When industry truly values the health and safety of every underground worker, we state without a doubt the intention that productivity lies ultimately with the most valuable asset a mining company can engender: the first–person workforce that enables efficient production and development of the targeted orebodies. The ethics behind sustainability can thusly engender ownership never before experienced in industrial mining operations. Stakeholders could reap benefits in the long-term due to the perceived value of the employee by the operator.

High-rise office buildings are designed around the central concept that occupant comfort directly leads to employee productivity. This concept has been largely overlooked by the mining industry, primarily due to dated design priorities and methodologies. A new focus should be embraced in all sectors of mining to put the worker's comfort and experience in the forefront. When employees are valued, at a very temporal level, the level of worker dedication can flourish without hindrance. This means that mundane occupations become enjoyable and employee retention rates will soar. A mining company that embraces this mentality will profit immeasurably due to low-level ownership of all vitally important tasks.

4.1 Ventilation Design Information

In the ventilation and cooling methodology that would be employed for the design of the new underground mine, three successive phases are generally followed, namely that of the conceptual phase, the pre-feasibility studies, and finally the feasibility phase. Basic information required in all three phases includes: mining horizons and layout, mining method, drill log data, geothermal gradient, mining depth, mine water inflow temperature and inflow rate, haulage design criteria and surface ambient atmospheric conditions. Each of these topics are reviewed in the following sections.

4.2 Mining Horizons and Extent

The proposed extents and vertical horizons of a mining operation will greatly influence the capability of a mine design to effectively mitigate heat generated during the mining processes. The further and deeper a mine extends its boundaries, the actions required to deliver cool air, to reduce the effects of heat induced upon workers in the underground necessarily become more intensive. The scale of a mining operation also brings various issues relating to the handling the requirement of increased airflow. Some of these issues revolve around the elevated construction standards necessary for ventilation controls to reliably bear the applied forces from the ventilation pressure required to deliver large air volumes to deep vertical horizons. Additional precautions must be given to minimize leakage, such as the fortification of ground surrounding locations underground where return air splits come into close proximity to main fresh air sources airways.

An in-depth understanding of different mining operations experiencing similar operating conditions due to layout and design are important, when initially focusing on the ventilation design and planning for the proposed horizontal and vertical layout of the mine. They are important factors relating to the mitigation of the possible added heat loads imposed on the operation. Ultimately to counter the effects experienced, or inferred directly, either by ventilation alone or through a combination of ventilation and refrigeration techniques. This could involve an application of mixed cooling arrangements to achieve the required cooling power.

4.4 Mining Method

Some mining methods will, by necessity, induce more applied heating load than others. For example, an operation that adopts cementation to allow effective ground support where poor conditions mandate extreme measures, will experience more background heating due to the curing of cement than an operation that simply excavates ore and development in a very sound deposit, which is by nature mechanically stable. Some mining methods intentionally allow minimal airflow through old mine workings, to essentially “cool” air from direct contact with old workings during passage through lesser accessed production districts by passing that airflow among cooler stopes which historically have been mostly phased out of production. Oftentimes, these strategies have failed when a stope springs a leak and becomes a significant source of moisture in the fresh air, effectively lowering the cooling power capacity of the fresh air.

Optimally, old workings will be effectively sealed off from active production districts to simplify ventilation requirements. Minimizing the ventilation footprint will further reduce operating capital by directing available airflow through active workings exclusively. This will also reduce the effects of unknown contaminants from fouling the fresh air supply.

4.4 Drill Log Data

During preliminary exploration of an ore body, intensive drilling programs are conducted in order to define the three-dimensional extents of the targeted ore body. Many different considerations are placed upon the core drilling program. Most of these considerations revolve around the economic valuation of the mineral deposit being considered for mass excavation. The entire mining process will be developed around the economic feasibility of the extents of the mineralized zone. The drilling programs primarily are concerned with mineral valuation.

During the conceptual phase of an exploratory drilling program, thermal analysis of the core samples can be mandated to be performed in the field. Alternately, down the hole temperature sensors can be prescribed for the drilling apparatus. This would alleviate any potential user error during transcribing measured temperatures from core samples. The main benefit from having down the hole temperature sensors is that temperatures can be read directly at the depth of the operating apparatus. This means that no temperature is lost or gained during the extraction of core from the drill shaft.

Temperature sensors need to be calibrated regularly, as drilling is a very mechanically hazardous environment. Sensors and sensor systems are bound to break down under such adverse conditions. Care should be given to ensure that core data gathered from drilling programs be rigorously evaluated and calibrated against regionally assigned exploration drilling programs.

4.5 Geothermal Gradient

Considerable amounts of research have been performed to quantify the intercontinental effects of geothermal influences globally. These influences have been mapped extensively and have been reported by Texas A&M, during ongoing research reports. Several geologic locations around the world experience higher than normal geothermal gradients, but these are well documented. However, anomalies do exist so it is up to the mine operator to verify potential needs for future bulk air conditioning.

Care of analysis should be given to thoroughly understand localized heating effects within the earth's crust. The addition of heat sensor data to an exploratory drilling program is rather inexpensive, compared with the overall mobilization and operation of an anticipated exploratory surface drilling program. In any region where geothermal heat is a possibility of becoming a considerable factor in a mine's heat load, thermal logging of drill data should be considered required information.

During excavation, the operator should log as-built tunnel temperatures as progressively deeper levels are developed in the mine. This will give feedback data to make corrections to the assumed geothermal gradient. Climatic modeling should be revised, and the overall ventilation forecast model should be adjusted. Modeling results could indicate that there will be a change in the anticipated heat load induced by the mine workings.

Temperature surveying should be conducted on 2-week periods from sample drill holes, near level intersections and close to large production districts. Thermal surveying should be conducted using 3-m or 10-foot deep, 1-inch diameter drill holes drilled perpendicular to the main axis of the excavated mining drift. The surveying instrument will be a sensitive resister-type thermistor in a temperature tolerant and highly heat conductive capsule suspended within a tripod-like frame, presumably to suspend the temperature sensor equilaterally in the surveying drill holes. Each hole's temperature sensor should be connected to 15-feet of protected lead network cable, capable of withstanding numerous bi-weekly sampling observations. These temperature sensor cables should be carefully identified and marked with obvious signage to designate the importance of the drill hole location, so that the area be kept free of additional ground support, shotcrete or cementation. The loop of cable lead should be pulled tight to the rib and tethered, preferably, to the bearing plate of a nearby ground support bolt or anchored to some other arrangement specifically installed to provide shelter for the rock temperature sampling holes during the prescribed thermal survey duration.

During surveying activities, observations should be directed towards changes in heat flux from rock to the mine air. Not only should thermal readings be logged, but additional psychrometric observations should be noted at the time of logging survey activities. Thermal images of the strata surrounding the survey holes should be recorded along with images throughout the associated levels. Comprehensive thermal images should be collected during ramp and level access development of any mining district that demonstrates virgin rock temperatures in excess of 32 °C. Visual catalogues with a spectrum of pictures and thermal imaging during mining life will assist decision makers when the timing is appropriate to scale back ventilation requirements based upon lowering heat load from strata.

In the most practical sense, the heat load from the strata in which a deep and hot mine is excavated will develop more influence when airflow velocities are minimized. This velocity region is mostly laminar flow and allows eddies in the airflow that experience localized recirculation and subsequent overheating from exposure to the young mine workings. In practice, the mine operator would mandate minimum allowable airflow velocities in districts where hot mine rock exists to mitigate potentially unsafe working conditions downstream.

4.6 Mining Depth

In practice, mineral deposits get warmer the deeper the operation proceeds. This is to say that the longer a mine remains in production, the deeper the vertical extents of the ore body are exploited. The deeper any mine invades the earth crust; the greater will be the expected heat load due to geothermal influences. Certain factors affect mine ventilation more than others. Depth of the mining operation specifically affects the influence of auto compression.

Eventually the depth of a mine cannot overcome the effects of the combined mass of the total air column for the supplied fresh air. This effect of auto-compression has been found to increase the temperature of air supply to an underground mine by 4-½ °C per thousand meters. Eventually the effects of auto-compression cannot be overturned. From this point forward, primary surface air conditioning supplied by a surface refrigeration plant will be required to provide a healthy and safe work environment underground.

4.7 Mine Inflow Water

Hot geothermal water flowing into a mining excavation will seriously raise the wet bulb temperature of fresh air being supplied to the mining operation. Minimizing the effects and interaction of water and air should become a primary consideration for ventilation engineers around the world.

Containment and redirection of water flowing into an underground mine will greatly reduce the potential for saturation of the fresh air supply. Additionally, keeping hot water separated from direct contact with fresh air will keep fresh air cooler until it reaches mining district where cooling power, i.e. coolth, becomes required.

4.8 Haulage Design Criteria

Often times the biggest culprit for additive heat loading in the underground environment revolve around haulage methods. Length of hauling ramps and size of the haulage fleet will adversely affect fresh air underground. The process of re-mucking significantly impinges a production level's available ventilation capacity due to the heat added. Dedicated fresh air splits for secondary ore handling can help alleviate heat induced within the miner's environment. Care needs to be given during planning phases to ensure that air delivered downstream is not eviscerated or fouled by upstream mining equipment that irreparably contaminate the source of fresh airflow.

The design of effective ventilation systems will preclude potential air fowling at the source. Haulage programs need to revolve around clean and cool air delivery to the actual working districts. Alternative methods for ore and waste rock haulage should anticipate additive heat loads, reducing unnecessary heat wherever possible. Making the most out of electric equipment will greatly reduce the heat load applied to the fresh air supply. Battery electric equipment will especially reduce potential for added heat and always reduce the addition of moisture to the fresh air underground.

4.9 Surface Ambient Atmospheric Conditions

The real issue here is that during warmer climatic periods, i.e. summer months, the air source is relatively warmer. Optimal ambient air wet bulb temperature at the primary ventilation intake source should not exceed 23° C

(75° F) for highly mechanized underground mines. Once the consideration for depth is factored in, this would ideally be reduced by 2.5° C (36.5° F)/ 1,000-m (3,281-feet) of mean operational horizon. Further reductions of the atmospheric wet bulb temperature will be required to maintain an acceptably safe work environment until the point where air conditioning is required. These further reductions primarily consist of mining equipment. Smaller, more efficient operations will realize these reductions later down the development timeline than massive corporate operations. Smaller operations can switch to maintenance mode exclusively during summer months, utilizing the cold air of winter to facilitate production friendly air supply conditions. Larger operations that extend to considerable depth will most certainly encounter the need for bulk air cooling during warm atmospheric conditions after the mine operation has reached the point of positive return on investment and sustained economic viability.

5. Ventilation Standards

Significant air power is required to maintain required pressures in key locations when all available districts are operational. Vane axial fan installations capable of developing 2.0 kPa of pressure could be required as booster fans for each production or development district. Each fan could be controlled in a ventilation-on-demand (VOD) network, operating only when mining activities warrant ventilation to be supplied to an individual district. This reduces the overall power impact of the operation, ultimately reducing capital costs for electrical substation installations to adequately manage the current supply necessary to keep all possible combinations of simultaneously operating production districts energized continuously. Additionally, operating costs are reduced since a VOD system will operate a district's booster fan only if mining activities are actually occurring in the district.

The cooling requirements could mandate the installation of a surface ammonia refrigeration plant complete with the storage of hot and cold mine service water for underground use. It is also typically necessary to install a surface bulk air cooling facility, which cools ventilating air going to the underground workings. The surface bulk air cooler usually applies primary cooling power. Other cooling arrangements make use of various combinations of primary surface and distributed bulk air and/or spot coolers as needed during the progression of the mining horizon. Oftentimes, spot chilling is required to periodically cool mining equipment during tunnel bore or shaft development.

The traditional approach to a bulk air cooler is a direct contact, two-stage counter flow spray chamber. Total amount of service water circulated averages 470 liters per second for systems currently being specified by major mining ventilation consultants. The cold water from the chillers is sprayed upwardly in the first stage (closest to the shaft), at right angle to the intake airflow. The water collects in a sump and it is pumped to a second stage (closer to the fans), where the water is again sprayed in a similar fashion as the first stage. The water is then returned to the water chillers following collection behind the hot water dam.

The alternative to the traditionally immense installed footprint of a surface refrigeration plant and the potential ammonia quantities involved, and the application for mine airflow, (no ammonia can go underground, either in service water or in the mine air) could optimally be a reverse running heat pump using small, incremental volumes of the total stored cold glycol reservoir capacity as the heat sink for day to day mine air refrigeration needs.

Special regulatory considerations for ammonia or Freon based refrigerants, including yearly renewed operating permits for each surface plant installation can be disregarded if an intrinsically healthy and safe refrigerant is employed for bulk air-cooling needs. Additional advantages that intrinsically safe mining service fluids provide include the means to distribute the fluids throughout the underground without chance of hazardous contamination events due to potential refrigerant leakage.

The cooling duty of a surface bulk air cooler is heavily dependent on the ambient wet bulb temperature. Because of the daily wet bulb temperature variation in many parts of the world, use can be made of a cold thermal harvesting and storage facilities amounting to massive heat exchange reservoirs. The unused chilled refrigerant is stored away from solar radiation and warm ambient atmospheric periods, for use by the main production shifts during adverse climatic conditions, as needed. Potential discussion includes the control philosophy used to maximize the cooling output, as well as addressing the boundary atmospheric thermal processes that must be overcome to maintain acceptable refrigerant service temperature.

5.1 Integrated Cooling Optimization

In many underground metal mines, the air volumes which need to be delivered to the production stopes, development headings and throughout the mine are usually determined according to diesel exhaust dilution considerations of 0.063 m^3/s/kW (100 cfm/bhp). However, in deep and hot underground mines the actual heat load would determine the quantity of air that must be supplied by the fans (and hence the fan motor input power required), which ultimately leads to the cooling power required to maintain acceptable working conditions. The difference between the intake air temperature (T_d, T_w) minus the heat sink or addition (as air travels along vertical and horizontal airways) and the reject air temperature before the exhaust shaft will determine the amount of cooling that is needed in order to provide adequate work conditions underground. It is necessary for this reason to ascertain the cooling arrangement of the mine and to use this layout as the basis for an optimization model, once the underground pumping systems supporting bulk air cooling requirements have been established. This optimization model should be used to determine the most cost-effective times of refrigeration usage and corresponding intake/reject temperatures for air and service refrigerant.

Determination of the correct size fan for auxiliary and main ventilation systems vary by pressure duty and will factor heavily in the amount of cooling power the fresh air can deliver. This is a gross oversimplification in that a fan must be able to withstand the rigors of the installed environment and applied conditions due to the mining operation. Considerable wear metrics should be applied to return air booster fan blade sets acquired for stope fans versus development section fans. The design criteria for fan use should include the variations amongst installed duty versus operational pressure, which is nonetheless implied by the fact that the ratio of relative hub to blade tip diameter will usually determine whether a fan will be assigned to a long development drift or a production district at a draw point, for example.

Adoption of exhaust network style ventilation systems at the early onset of a project maintain limited heat additions during the course of the project due to the fact that no additional fan heat is added to the mine’s fresh air supply. Although additional air power will be required to overcome unexpected leakage problems experienced during actual mining operations, the cost savings of surface fan installations versus underground fan installations more than offsets the operating expenses involved in the exhaust ventilation network adoption. It is the interaction of these parameters and the related costs associated with each that have to be optimized by developing a predictive simulation algorithm, using active control metrics (such as airflow temperatures, airflow quantity, water flow rates).

Development of administrative and engineering controls will aid significantly in the optimization of the stored refrigerant storage temperature. Creating additional maintenance tasks for cooling plant employees, which basically involves blanketing the fresh air service refrigerant use piping circuits, during seasonal atmospheric temperature variation periods will help maintain cooling reservoir temperatures at the cold end of the relative human experience of the temperature spectrum.

5.2 Diesel Equipment Considerations

Under certain circumstances, diesel equipment generates approximately 3 times more heat as electric or battery-powered mining equipment. As a result, diesel equipment requires at least 30% more air volume than equivalently sized battery electric equipment, as has been shown in recent professional studies. The main thing is that diesel particulate matter is carcinogenic and has other ill effects on equipment and other installations within the mining infrastructure. Serious amounts of faith have been placed in diesel equipment, primarily because this type of equipment has a huge horsepower to productive output ratio. An inordinate amount of infrastructure needs to be added just to accommodate diesel equipment. This infrastructure includes fuel bays, extensive maintenance bays, and excessive cross-sectional areas for tunnels and raises throughout the entire mining plan. Much of the desired airflow in a mine needs to be dedicated to the diffusion of diesel fumes.

Often times, the mine design is compromised due to the accommodation of diesel equipment. Many different considerations are in place here, primarily the oversized design of tunnels and drifts within the mine. Delivering diesel fuel to the underground fuel bays is a huge consideration in operations planning. Acquisition of diesel fuel requires an inordinate amount of equipment and manpower just to get that fuel to the underground. The presence of diesel equipment in underground mining operations requires continual testing of the air quality in the underground atmosphere. As long as workers are exposed to diesel particulate matter, the air should be tested in a qualified laboratory.

Oversized ramps need to be designed within production districts just to accommodate the operation of diesel equipment. As the diesel paradigm has progressed in underground mining, operators have accepted the need for larger cross-sectional dimensioned stope access and muck re-handling bays, due to huge machine sizes and elevated airflow requirements imposed by diesel mining equipment. If smaller sized equipment were applied in larger numbers of mining sections, within any given district, the implications could be immeasurable. The lessening of the equipment heat load impact will be decreased significantly, leading to smaller cross-sectional area access drifts, resulting in lower excavation operating costs.

The sustainable approach to mine design will embrace a lower tons per month production rate. This will accommodate smaller development and production equipment, meaning smaller scale drifts, tunnels, shafts and raises, resulting in lower capital costs to initiate expected mining operations.

Smaller scale equipment could mean slightly higher cost per ton, but this higher cost will ultimately be offset by higher retention rates of employees which means better productivity. in the long run, the shift to smaller scale operations can yield longer, more fruitful dividends for investors. The human aspect of small-scale mining adoption should realize more sustainability and long-term fortitude in the local economies that rely upon mining operations for employment.

The adaptation of diesel equipment underground requires a policy of acceptance to higher noise levels by decibel and sound pressure levels. The acceptance of higher sound pressure levels means that district employees will have to endure long periods of elevated noise. This condition is counterproductive to an effective and efficient mining operation. The long-term health effects of higher noise levels are truly destructive and have far reaching implications. Miners that are continually exposed to excessive sound pressure levels in confined spaces are desensitized to hazardous situations both at work and in the civilian world. Extreme noise exposure leads to annoyance, disturbs sleep and causes daytime sleepiness, increases the occurrence of hypertension and cardiovascular disease, and impairs cognitive performance.

Oftentimes decisions are made based upon familiar and usually dated design paradigms, driven primary by financial indices that ignore health and safety. Adoption of new technology requires forward thinking that challenges accepted operational practices and the vanguard harboring conventional ideas. An entire change in types of haulage trucks and the infrastructure required to support those trucks would be required. Supply lines of equipment and change of maintenance contracts will need to be considered. Maintenance workers would need retraining to support the different types of mining equipment. The adoption of an electric equipment fleet would require more electricians to install the required infrastructure. Since diesel fuel and engine oil would not be required, the continual supply line is removed from the financial equation and logistics chain of resupply. This also means that the continual transportation and logistics for storage of those consumables goes away. This reduces the hazard of fires and explosions since those fuel sources are removed from the underground workplace and transportation via container or pipeline.

5.3 Alternative Mining Equipment

As battery technology continues to advance, electric and battery-powered equipment might be the future of underground mining operations. Battery technology is advancing rapidly, bringing the industry faster charging times with longer operating ranges to heavy equipment. Manufacturers are currently embracing the advancements in battery support by developing heavy-duty loaders with extended tramming capabilities and larger haul trucks. These changes are just a reflection of the automobile industry's shift towards clean energy implementation. Reduced fuel consumption demands may force the fossil fuel industry to become more environmentally friendly as the economy shifts toward the electric vehicle future. . I interpret this as an inevitable progression towards global sustainability. Electricity has been historically under supplied and overpriced, globally speaking. Electrical utilities have a veritable strangle hold on consumers and industrial customers are no exception. Bulk pricing for industrial customers is traditionally lower than tiered rates imposed upon the majority of household electrical consumers. However, mining companies are typically required to purchase on-site transformers, switching equipment and even the high-voltage transmission network of towers and power lines. These infrastructure investment costs can take over 20 years to financially realize the true net present value of the negotiated bulk kilowatt-hour pricing. Production of electricity also needs to be ramped up to meet the higher demand imposed by our theoretical all-electric mine of the future.

Making the switch to an all or mostly electric vehicle fleet will not be an easy task, since most mechanics have been trained on diesel equipment. Electricians will need to be qualified by various manufacturer’s factory representatives and existing mechanics will need to master new skill sets to service and maintain battery electric vehicles.

5.4 Fugitive Dust and Fumes Removal

The production of dust and fumes by mining operations is a necessary evil. Drilling, blasting, loading and haulage activities liberate quantities of dust and fumes that have numerous negative health and safety consequences. Procedurally speaking, these hazards can be largely reduced and sometimes eliminated through judicious use of water sprays or blanketing.

Roadway development and maintenance is another main source of fugitive dust. Incorporation of roadway conditioning agents, such as lignin, can result in lower roadway maintenance activities and dust. This will help reduce fugitive dust from main traveled ways at the source, and reduces the amount of water that needs to be applied to the roadway to allay the dust. Lower water usage on ramps and at load out or remucking bays means less plumbing, lowering operating costs and onerous workforce maintenance requirements.

Maintaining minimum airflow velocities is necessary to ensure removal of respirable dusts that will remain suspended in the airmass if the flow is very low. When the airmass has become completely stagnant and remains stationary for an extended period, extremely small particles will settle out of the air. However, if the airmass moves along the airways, that mass of air can collect more and more respirable dust sized particles which makes that dust-laden mass of air harmful to both humans and mining equipment.

6. Air Quality Considerations

In order to ensure the health and safety of the underground workforce, the quality of air delivered to the workplace is vitally important. Sufficient airflow also needs to be delivered to remove waste heat, noxious fumes and fugitive dust that will adversely affect the performance of mining equipment. Both workers and equipment will suffer from poor performance due to prolonged exposure to relatively hot working environments. Workers will experience loss of concentration creating various dangerous situations when exposed to excessive heat that could easily be avoided when the same workers are alert and focused on the task at hand. Mining equipment will experience core system failures and a shortened mechanical lifespan in high thermal loading environments.

6.1 Equipment Heat Load

Equipment heat load may be quantified through time dependent calculations. In practice, however, any piece of equipment in the underground is given a utilization factor which is multiplied by the equivalent mechanical power expressed in kilowatts. All equipment locations are specified as a function of the distance from the beginning of an airway branch. For diesel equipment, moisture content of the fuel or water vapor added to the fuel/air mixture prior to combustion must also be provided to the calculation. The age of an airway based upon the timing of excavation in the mining horizon will be given so that heat flow, as a balanced energy relationship, may be determined between the rock and the diesel heat load delivered by the mining equipment.

Ultimately it is the airflow coursing through the mining entries that picks up the heat delivered either by the rock mass through which the airways have been excavated or by the mining equipment. Since the cooling capacity of humid air is less efficient than that of dry air under the same dry bulb temperature conditions, significant amounts of air must be moved through the mine in order to balance the heat transfer equation, thereby keeping the environment acceptable for underground human workers. Mechanically forced airflow is the normal means by which an underground mine is ventilated. The more mechanical energy applied to solve the terse environmental situation equates to more operating capital and lower returns to the mine operator, shareholders or investors.

6.2 General Heat Load Sources

Stationary heat loads include pumps, rock breakers and crushers, and transformers/power load centers or even welders. Another type of spot heat load is the auxiliary fan attached to a long length of semi rigid ducting or booster fan installed in a bulkhead. Some of the heat generated by the fan is transferred to the surrounding environment through the conduction mechanisms while the majority of the heat generated by the fan motor and blade tip interaction with the airflow is transferred to said airflow coursing past the fan blades through convection. This fan derived heat load is given directly to the airflow which the fan is applying dynamic pressure courtesy of the rotating blades. The sum of heat given to the airflow is a function of the pressure applied to the air. That heat is then dissipated as the air courses through the mine ventilation network of airways. The energy dissipated in the airflow is primarily loss through molecular level excitement of nitrogen and oxygen.

Linear heat load sources include conveyor belts that are transporting hot ore out of the mine. Additional linear heat sources may include hot water piping which is removing rejected service water from a bulk air cooler. Optimally these hot water pipes would be placed in return shaft thereby eliminating that heat from the mine as air is exhausted up the return air raise. Very high voltage electric lines are also potential sources of linear heat load. This is only the case for transmission level voltages. As long as the mine ventilation network is designed correctly, these types of linear heat sources can be all but negated.

Perhaps the most inconspicuous and potentially abundant heat effect can come from hot inflow water. As hot water seeps into a mine, the air directly in contact with the water will heat up significantly due to the enthalpy of the hot water. It takes a long while for this water to cool down and during that time the air in contact with the water continues to heat up. Mitigation of heat generated by hot ground water can be complex. Ditches that gather this hot inflow water should be covered to keep the airflow from contacting the relatively hot ditch water. Sumps where hot water is accumulated should also be covered for this very same reason.

7. Mine Air Conditioning Systems and Refrigeration Plants

By far the most common approach used to cool the underground mining environment is through the use of appropriate amounts of fresh air. The excavated openings in any underground mine can transfer heat to the mine air for a long period of time. The industry standard practice involves excessive amounts of air volumes to remove fumes, dust and waste heat generated in the highly mechanized mining operations supported by diesel equipment. Small scale operations do not experience these types of drawbacks, mostly because they do not employ large scale mechanized equipment.

However, fresh air can only supply so much power for cooling purposes. This is very true and more problematic as a mining operation pushes the horizons of development and production extents deeper. The main culprit now is not necessarily the high virgin rock temperature or even the hot inflow of groundwater, but the effects of auto-compression as air descends into a deep and hot mine. Ultimately the effects of auto-compression cannot be overturned through the application of more fresh air. From this point forward, additional bulk air cooling needs to be employed to ensure a productive, safe and healthy working environment underground.

7.1 Theoretical Background

There are many transient phenomena that are known to produce a cooling effect, varying from endothermic chemical reactions to the sublimation of solid carbon dioxide (dry ice). Where a continuous cooling effect is required, then a means must be employed by which a supply of mechanical, electrical or thermal energy is utilized to remove heat from some source, and to transport it to a thermal sink where it can be rejected. If the primary objective is to cool the source, then the device is known as a refrigerator. If, however, the desired effect is to heat the sink, then it is called a heat pump. In fact, both effects occur simultaneously. Hence, a domestic refrigerator cools the interior of the container but heats the air in the kitchen.

Of the several devices that have been developed to achieve a continuous refrigeration or heat pump effect, the most common is based on the vapor compression cycle. This may be used on small units such as air conditioning equipment fitted to automobiles or for very large scale cooling of mine workings where many megawatts of heat require to be transferred. In this section, we shall examine the basic principles of the vapor compression cycle, how rates of heat exchange may be calculated, and the essential components of a refrigeration plant (McPherson, 2009).

7.1.1 Principles of the Vapor Compression Cycle

When a liquid boils, it does so at constant temperature provided that the applied pressure remains fixed. The heat added is utilized in increasing the internal kinetic energy of the molecules until they can no longer remain in the liquid phase but burst free to form a vapor or gas. If, however, the applied pressure is raised to a higher value, then additional heat is required to vaporize the liquid and the boiling temperature will increase. The liquid may be vaporized either by increasing the temperature or decreasing the pressure. Similarly, condensation from vapor to liquid may occur either by decreasing the temperature or increasing the pressure.

The change in physical appearance of a fluid on crossing the vapor pressure line is quite distinct, liquid to gas or vice versa. However, there is a critical pressure-temperature coordinate beyond which the change of phase is gradual rather than sudden and there is no clearly defined moment of evaporation or condensation. This is known as the critical point.

Although the vapor pressure curve appears as a single line on the pressure-temperature diagram, it takes a finite amount of time and energy exchange to cross that line. During this time, part of the fluid will be liquid and the remainder will be vapor. This is the situation that exists inside a boiling kettle. When a liquid boils at a given value of applied pressure it will extract heat from the surroundings or other available medium. If the vapor thus produced is then transported to a new location and compressed to a higher pressure, then it can be condensed at a correspondingly higher temperature, yielding up its heat of condensation to the new surroundings or any cooling medium that may be supplied. This is the basic principle underlying the vapor compression refrigeration cycle (McPherson, 2009).

7.1.2 Main Components of the Vapor Compression Cycle

There are four essential components of hardware in a vapor compression refrigeration unit, as shown in Figure 1. The evaporator is a heat exchanger, typically of the shell-and-tube configuration in mining refrigeration plant. In the larger units, the refrigerant liquid is on the outside of the tubes while the medium to be cooled (for example, water, brine or glycol) passes through the tubes. Smaller units employed for direct cooling of an airstream are sometimes called "direct evaporators" and contain the refrigerant within the tubes while the air passes over their outer surface (McPherson, 1993).

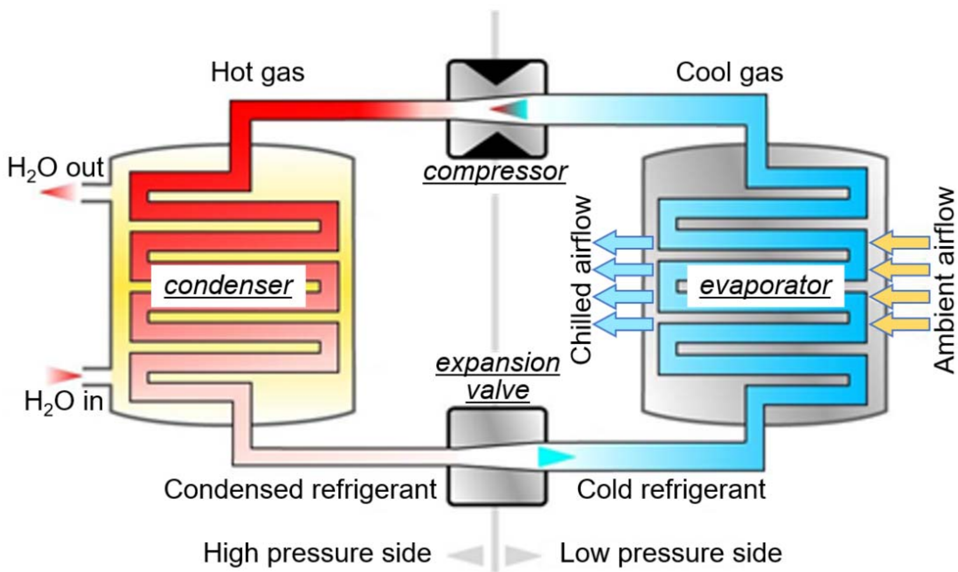

Figure 1: Main components of the vapor compression cycle.

Within the evaporator, the refrigerant pressure is maintained at a relatively low level and boils at a correspondingly low temperature. The heat required to maintain the boiling is extracted from the gas or liquid passing on the other side of the tube walls. Hence, that gas or liquid is cooled. The refrigerant, now vaporized, collects at the top of the evaporator and is allowed to gain a few degrees of superheat to ensure full vaporization before it passes on the compressor. Except for direct evaporators, it may be necessary to insulate the external surface of the evaporator in order to prevent excessive heat gain from the ambient atmosphere.

The compressor is the device where mechanical work is input to the system. Reciprocating, screw or centrifugal compressors are all employed. The latter are favored for the larger units and where the required pressure ratio remains constant. However, the development of large diameter screw compressors allows a good efficiency to be maintained under conditions of variable cooling load. (Baker-Duly, 1989). Multi-stage compressors are employed to give high differentials of pressure and, hence, large temperature differences between the evaporator and condenser. Electric motors are normally employed to drive the compressors on mine refrigeration units although internal combustion engines may be used on surface or as standby units. The duty of a refrigeration plant can be modified by changing the speed of the compressor. The flow of vapor through the compressor and, hence, rate of heat transfer can also be controlled by inlet guide vanes.

The refrigerant vapor leaves the compressor and passes into the condenser at a relatively high pressure and temperature. The condenser itself may be of similar construction to the evaporator, that is, a shell-and-tube heat exchanger. Heat is removed from the refrigerant by air, water or some other fluid medium to the extent that the refrigerant cools and condenses back to a liquid. As the pressure is high, this occurs at a relatively high temperature. The latent heat of condensation is removed by the cooling fluid for subsequent rejection in a cooling tower or other type of separate heat exchanger. As the vapor compression cycle is a closed system (ignoring heat losses or gains from the surrounding atmosphere), the rate at which heat is removed from the refrigerant in the condenser must equal the combined rates of heat addition in the evaporator and work provided by the compressor.

The condensed refrigerant passes from the condenser to the fourth and final component of the cycle. This is the expansion valve whose purpose is simply to reduce the pressure of the refrigerant back to evaporator conditions. An expansion valve may be a simple orifice plate or can be controlled by a float valve. At the exit from the expansion valve, the liquid is at low pressure and has a correspondingly low boiling temperature. Provided that the pipework is insulated, the latent heat for boiling can come only from the liquid refrigerant itself. Hence, the temperature of the refrigerant drops rapidly as it passes from the expansion valve to the evaporator where it enters as a mixture of liquid and vapor, thus closing the cycle (McPherson, 2009).

7.1.3 Performance of a Refrigeration Cycle

Electrical motors or heat engines are devices that convert one form of energy into another. Their efficiency may, therefore, be defined as an energy output/input ratio. However, in the case of refrigerators or heat pumps, the purpose is to remove heat from a given source and to reject it at a higher temperature to a receiving sink. A different measure of performance is required.

Figure 2 shows the temperature-entropy diagram for the ideal (frictionless) Carnot cycle to which an actual vapor compression cycle can aspire but never attain. We may follow the ideal cycle by commencing at position 1, the entry of refrigerant vapor to the compressor. The ideal compression process is isentropic. The compressed refrigerant vapor enters the condenser at position 2 and, in the ideal condenser, passes through to position 3 with neither a pressure drop nor a fall in temperature. This assumes frictionless flow and perfect heat transfer. The ideal expansion valve allows an isentropic fall in pressure and temperature to position 4, the entrance to the evaporator. The cycle closes via frictionless flow and perfect heat transfer in the evaporator.

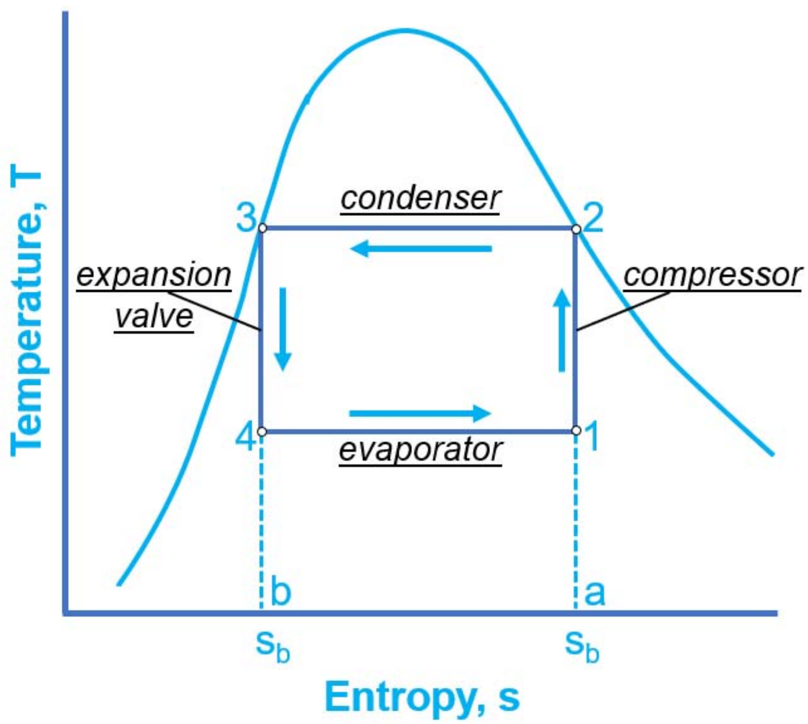

Figure 2: Temperature-Entropy Diagram for an Ideal Vapor Compression Cycle (Carnot Cycle)

In order to quantify the ideal Carnot cycle, we apply the steady-flow energy equation. The kinetic and potential energy terms are small and, in any event, cancel out in a closed cycle. Using the numbered station points from Figure 2, the steady-flow energy equation gives:

compressor:	W_{12}	=	$H_2 - H_1$	J/kg	(7.1.3.1)
condenser:	q_{23}	=	$H_3 - H_2$	J/kg	(7.1.3.2)
expansion valve:	0	=	$H_4 - H_3$	J/kg	(7.1.3.3)
evaporator:	q_{41}	=	$H_1 - H_4$	J/kg	(7.1.3.4)
cycle summation:	$W_{12} + q_{23} + q_{41}$		= 0	J/kg	(7.1.3.5)

where:

W_{12} = mechanical energy added by the compressor

q_{23} = heat exchange in the condenser (negative, heat leaving the refrigerant)

q_{41} = heat added to the refrigerant in the evaporator

H = enthalpy

The measure of performance of a refrigeration cycle is known as the Coefficient of Performance, COP, and is defined as:

$$COP = \frac{Usefulcoolingeffect(evaporatorheattransfer)}{work\ input\ from\ the\ compressor} = \frac{q_{41}}{W_{12}} \quad (7.1.3.6)$$

Using equation (7.1.3.5), this may be reformed as:

$$COP = \frac{q_{41}}{-q_{23}-q_{41}} \quad (7.1.3.7)$$

Recalling that the area under a process line on a Ts diagram represents heat, the terms in equation (7.1.3.7) may be related to Figure 2 for the Carnot cycle:

q_{41} = Area 41ab

$-q_{23}$ = Area 23ba

And $-q_{23}$ $-q_{41}$ = Area 1234 (since q_{23} is numerically negative)

Hence, W_{12} = Area 1234 and equation (7.1.3.7) becomes

$$Carnot\ COP = \frac{Area\ 41\text{ab}}{Area\ 1234} = \frac{T_1(s_a - s_b)}{(T_2 - T_1)(s_a - s_b)}$$

$$= \frac{T_1}{(T_2-T_1)}\ or\ \frac{T_4}{(T_3-T_4)} \quad (7.1.3.8)$$

Since $T_1 = T_4$ and $T_2 = T_3$

The ideal or Carnot coefficient of performance is therefore given as the ratio:

$$Carnot\ COP = \frac{Evaporatortemperature(absolute)}{Condenser\ temperature - Evaporator\ temperature} \quad (7.1.3.9)$$

The performance of a refrigeration unit may be enhanced beyond that illustrated in the example. For large units, it may be necessary to employ two or more stages of compression in order to achieve the desired difference in temperature between evaporator and condenser. In that case, it is usual to employ the same number of expansion valves as stages of compression. A fraction of the refrigerant is vaporized on passing through an expansion valve. That fraction can be read from the corresponding point on the pressure-enthalpy diagram or calculated from the isobaric enthalpies at the saturated liquid and saturated vapor curves. This "flash gas" may be separated out and piped to the corresponding intermediate point between compressor stages. This is known as interstage cooling or, simply, intercooling and reduces the total mass of refrigerant that passes through all stages of compression. The result is to reduce the required compressor power and/or increase the useful refrigerating effect.

In some units, the hot liquid refrigerant leaving the condenser is partially cooled by a secondary cooling circuit. This subcooling reduces the fraction of flash gas produced at the downstream side of expansion valves and gives a small increase in the performance of the plant. The coefficient of performance as defined by equation (7.1.3.6) takes into account the isentropic efficiency of the compressor. However, it does not cater for the efficiency of the motor or other device that drives the compressor. The W_{12} in equation (7.1.3.6) may be replaced by the power fed to the compressor unit to give a practical coefficient of performance. Since the compressor is not the only device that consumes energy in a refrigeration unit, water pumps or fans that promote flow of the cooled airflow at the evaporator and the cooling refrigerant at the condenser. Overall coefficient of performance may then be defined as:

$$Overall\ COP\ = \frac{\text{Heat transfer in the evaporator}}{Total\ energy\ consumption\ of\ the\ refrigeration\ unit} \qquad (7.1.3.10)$$

Care should, therefore, be taken that any quoted values of COP are interpreted in the correct manner (McPherson, 2009).

7.2 Underground Mining Air Cooling System Components

A direct evaporator, or “spot cooler”, is a simple application of a refrigeration unit providing cool air to a hot working underground mining environment. The evaporator of the refrigeration unit takes the form of copper or cupronickel tubular coils located within an air duct. The refrigerant passes through the inside of the evaporator tubes and cools the air flowing along the duct. The heat from the condenser is rejected directly to the return air. This system has the advantage that the cooling effect produced by the refrigeration unit is utilized directly and immediately at the place where cooling is required. There is no loss of efficiency introduced by an intervening water reticulation system between the evaporator and working area. Similarly, heat rejection from the condenser is direct and immediate. The spot cooler is merely an industrial version of a domestic air conditioning unit where heat is rejected directly to the outside atmosphere.

Unfortunately, the spot cooler has a major disadvantage that limits its application in subsurface ventilation systems. The air emerging from the end of the duct will be at a reduced temperature when the refrigeration unit is operating.

Although this is the desired effect, a consequence will be that the flow of strata heat into the heading will increase due to the lowered air temperature. More heat is added as the air returns over the condenser. The net effect is that the return air leaving the area has a greater enthalpy (plus elevated temperature and humidity) than would be the case if the refrigeration unit were not operating. The increase in enthalpy is the sum of the additional strata heat and the energy taken by the compressor. The use of spot coolers is restricted by the availability of return air and the debilitating effect on psychrometric conditions within local return airways.

There are three ways of alleviating the situation. First, the condenser could take the form of a shell and tube heat exchanger and be cooled by a water circuit. The hot water can then be piped away and recirculated through a heat exchanger in a main return airway. Secondly, the refrigeration unit itself may be located away from the working area and water that has been chilled by the evaporator piped to a heat exchanger in the workings. Thirdly, the first two arrangements may be combined, offering positional efficiencies. The refrigeration plant is sited in an outby location to provide chilled water for a number of work areas. The chilled water flows through thermally insulated pipes to heat exchangers in the faces, stopes or headings and returns to the plant via uninsulated pipes. Some of the chilled water may be used for dust suppression purposes in which case additional make-up water must be supplied to the plant. Hot water from the condenser is recirculated through heat exchangers that are located in a main return airway. If that return airway is to remain open for persons to travel, either for routine purposes or as an emergency escapeway, then the psychrometric conditions must remain physiologically acceptable. Again, this provides a limit on the degree of heat rejection and, hence, size of refrigeration plant that can be utilized as a district cooler. If, however, a return route can be dedicated fully to heat rejection, then physiological acceptability limits may be exceeded. In this case, the dedicated return or "dirty pipe", as it is sometimes called, must be made inaccessible to inadvertent entry by personnel. Inspection or maintenance can be carried out either when the plant is shut down or by persons wearing protective clothing. It may be necessary to seek exemption from national or state legislation in order to utilize a "dirty pipe" arrangement (McPherson, 2009).

For mines that have a widespread heat problem, the economies of scale and the need for flexibility indicate a requirement for large centralized cooling facilities. Banks of individual refrigeration units, each producing a typical 3.5 MW of cooling capacity, may be assembled to give a total duty which might exceed 100 MW for a large and deep metal mine. The "coolth" is normally distributed via chilled water lines to provide any required combination of bulk air cooling, face or stope air cooling and chilled service water.

Until the mid-nineteen seventies, centralized plant tended to be located underground in excavated refrigeration chambers close to shaft bottoms. All of the mine return air could then be utilized for heat rejection. In South Africa, it was common for large cooling towers to be situated in, or adjacent to, the upcast shaft bottoms. Chilled water from the centralized underground plant could be transmitted to other levels. However, at elevations greater than some 500 m below the plant, water pressures in the pipe ranges become excessive. This can be counteracted either by pressure reducing valves (adjustable orifices) or by employing water to water heat exchangers and secondary, low pressure, cold water circuits. Unfortunately, there are difficulties associated with both of these types of device. Pressure reducing valves necessitate the employment of high duty pumps to raise the heated water back to the plant elevation. Maintaining the high pressure water in a closed circuit by means of water to water heat exchangers balances the pressure heads in the supply and return shaft ranges. However, the intermediate water to water heat exchangers produce an additional loss of heat transfer efficiency between the work areas and the refrigeration plant. Furthermore, they are a further source of potential corrosion and fouling of internal tubes.

In the mid 'seventies a number of factors coincided to promote a trend towards the location of centralized refrigeration plant at the surface of deep and/or hot mines. First, there was a significant drop in the wet bulb temperatures at which mining workforces would be expected to work. Cut-off wet bulb temperatures have been reduced from 32°C to 28°C with an expectation of further improvements to 27°C or less. Secondly, the combination of greater depths of workings and more intensive mechanization produced higher heat loads to be handled by the mine environmental control system. These factors combined to give very significant increases in the required cooling capacities of mine refrigeration plant, to the extent that untenable and uneconomic quantities of return air would be required for heat rejection. There was no choice but to locate the larger new plant on surface where heat rejection is relatively straightforward. Thirdly, the problem of high pressures developing in the shaft pipes was combatted by the development of energy recovery devices including water turbines (McPherson, 2009).

7.2.1 Heat Exchangers

In general, a heat exchanger may be defined as a device that facilitates the transfer of thermal energy from one solid or fluid system to another. In subsurface air conditioning systems, there are two classifications of heat exchanger in common use, both involving heat transfer between fluids. An indirect heat exchanger transfers heat across a solid medium that separates the two fluids, with no direct contact between the fluids. Examples include:

- the shell and tube evaporators and condensers of refrigeration units
- shell and tube water to water heat exchangers employed to transfer heat between water systems of differing pressure and/or water quality
- tubular coil heat exchangers to transfer heat from air to water

As the term implies, direct heat exchangers involve direct contact between the two fluids. Cooling towers and other types of spray chambers fall into this category. The objective may be to reject heat from the water to the air as in a conventional cooling tower. Conversely, a spray chamber supplied with chilled water provides a means of cooling an airstream. The higher efficiency of heat transfer associated with direct heat exchangers caused a distinct trend away from tube coil air coolers during the nineteen eighties. Good performance of large horizontal spray chambers for bulk air cooling promoted the further development of compact and enclosed spray chambers for more localized use. In this section we shall examine the essential structure and operating principles of both indirect and direct forms of heat exchanger (McPherson, 2009).

7.2.2 Indirect Heat Exchangers

A shell and tube heat exchanger may contain over 200 tubes. In a counter-flow heat exchanger, the fluids inside and outside the tubes move in opposite directions, maximizing the total heat transfer. The water to water heat exchanger may be sacrificed in the interest of compactness. In an air to water indirect heat exchanger, a bank of tubes carrying chilled water is located within an air duct. The tubes are often inclined to the direction of airflow to improve the efficiency of the unit and to control the movement of condensate. The two important features of a heat exchanger are that a good efficiency of heat transfer is obtained and that the pressure drops suffered by both fluid streams should remain within acceptable limits. Heat transfer is facilitated by choosing a tube material that has a high thermal conductivity and is also resistant to corrosion and the build-up of scale deposits within the tubes. Chemical additives can be used to control such fouling of the tubes. Copper tubes are commonly employed for air to water heat exchangers. For water to water heat exchangers and in the evaporator and condensers of refrigeration units, cupronickel and stainless steel are more resistant to corrosion. Even titanium may be used within evaporators and condensers. If tubes are not maintained in a clean condition then the efficiency of the unit can fall dramatically. Periodic manual brushing of the tubes is time-consuming and may be replaced by a variety of automatic tube cleaning devices including reverse flushing with brush inserts or ultrasonic vibration. Air to water tube coils are subject to caking by dust deposits in mine atmospheres. This may be handled by periodic cleaning with a high pressure water jet. Alternatively, sprays may be located permanently upstream from the coils. In humid atmospheres, the coils may be made self-cleaning by arranging them into horizontal banks with air passing upwards over the tubes. The droplets of condensate fall back through the coils giving a continuous and oscillating cleaning action on the outer surfaces of the tubes.

A second major factor that controls the duty of a heat exchanger is the effective area available for thermal transfer. Spiral fins welded to the tubes may be used. Metal plates welded between consecutive and partially flattened tubes have also been used (Mücke, 1984; Weuthen, 1975). It is important that such means of area enlargement should have good thermal contact with the tubes and that they are oriented such that they present minimum resistance to flow over the tubes. In evaporators and condensers, the tube surfaces may be knurled or sintered. In addition to enhancing the surface area, this assists in the promotion of boiling or condensation (McPherson, 2009).

7.2.2.1 Performance Calculations for Indirect Heat Exchangers

At equilibrium, the heat gained by one fluid in a heat exchanger must equal the heat lost by the other fluid. Hence, taking the example of an air to water heat exchanger, we can express the rate of heat transfer to be

$$q = m_w C_w \Delta t_w = m_a \Delta S \quad \text{W} \qquad (7.2.2.1)$$

where m_w = mass flow of water (kg/s)

C_w = specific heat of water (4.187 kJ/(kg °C))

Δt_w = rise in temperature of the water (°C)

m_a = mass flow of air (kg/s)

ΔS = fall in sigma heat of the air (J/kg)

As each of the factors in equation (7.2.2.1) can be calculated easily from measured temperatures and flowrates, either the water or the air may be used to determine the rate of heat transfer, q. As measurements on the water circuit can normally be made more accurately than those on the airflow, the former are preferred for a determination of heat transfer. If condensation occurs on the outside of the coils then the third part of equation 7.2.2.1 is slightly in error as it does not take into account the heat removed from the system by the condensate. However, this is usually small and may be neglected.

Another way of expressing the heat transfer is in terms of overall heat transfer coefficient, U, (W/m^2·°C) between the coils and adjacent fluid boundary layers, and the difference between the mean temperatures of the air and the water, (t_{ma} - t_{mw}), giving

$$q = UA(t_{ma} - t_{mw}) \text{ W} \qquad (7.2.2.2)$$

where A = area available for heat transfer (m^2)

As the temperatures of both the air and water streams are likely to vary in a logarithmic rather than a linear fashion through the heat exchanger, it is more accurate to employ logarithmic mean temperature difference in equation (7.2.2.2), giving

$$q = \frac{UA(\Delta t_1 - \Delta t_2)}{ln(\Delta t_1 - \Delta t_2)} \quad \text{W} \qquad (7.2.2.3)$$

where ln indicates natural logarithm and Δt_1 and Δt_2 are differences between fluid temperatures at each end of the heat exchanger.

The *UA* product is usually quoted as a measure of the effectiveness of an indirect heat exchanger. A performance check should be carried out at monthly or three monthly intervals in order to determine any deterioration in the *UA* caused by corrosion, scaling, or other forms of deposition on the tube surfaces.

The *UA* of a clean coil may lie between 10 and 25 kW/°C depending upon the design of the heat exchanger and the configuration of fluid flows. Records should be kept of the periodic performance tests on each heat exchanger. Significant reductions in *UA* values indicate the need for cleaning or replacement of the tubes.

Although *UA* values are normally determined by measurement, they may also be defined by the following equation:

$$\frac{1}{UA} = \frac{1}{h_i A_i} + \frac{1}{h_{fi} A_i} + \frac{x}{k_t A_m} + \frac{1}{h_o A_o} + \frac{1}{h_{fo} A_o} \ \text{°C/W} \qquad (7.2.2.4)$$

where

h = heat transfer coefficients (W/(m^2°C)

A = area available for heat transfer (m^2)

x = thickness of tube walls (m)

	k_t	=	thermal conductivity of tube material (W/(m°C)
and subscripts	i	=	inside surface of tubes
	o	=	outer surface of tubes
	m	=	mean of inner and outer surfaces

h_{fi} and h_{fo} are the heat transfer coefficients associated with fouling (scale deposits and dust/debris) on the inside and outside surfaces of the tubes respectively. On a clean tube there are no such deposits; h_{fi} and h_{fo} are both then infinite.

Radiation terms have been left out of equation (7.2.2.4) as these are normally small in a heat exchanger. They may, however, become significant in situations such as an uninsulated pipe suspended in an airway.

Equation (7.2.2.4) can be further simplified for practical application. First, the term $x / (k_t A_m)$ is very small compared with the others. Secondly, the terms involving fouling of the tubes are often combined and attributed to the inside surface only, giving

$$\frac{1}{UA} = \frac{1}{h_i A_i} + \frac{1}{h_f A_i} + \frac{1}{h_o A_o} \text{ °C/W} \qquad (7.2.2.5)$$

As fouling of the tubes occurs, h_f will decrease causing the UA value also to fall. Whillier (1982) quotes a typical value of some 3 kW/(m^2·°C) for h_f in a mine refrigeration plant. For turbulent flow inside smooth tubes, the heat transfer coefficient can be determined from the Colburn equation:

$$h_i = 0.023 \frac{k}{d} Re^{0.8} Pr^{0.4} \text{ W/(m}^2\text{·°C)} \qquad (7.2.2.6)$$

where	k	=	thermal conductivity of fluid (W/(m^2°C)

	d	=	internal diameter of tube (m)
	Re	=	Reynolds number = $\rho\ u\ \mu$ (dimensionless)
	ρ	=	fluid density (kg/m^3)
	u	=	fluid velocity (m/s)
	μ	=	dynamic viscosity (Ns/m^2)
	Pr	=	Prandtl number = $(C_p\mu)/k$ (dimensionless, 0.7 for air)
and	C_p	=	Specific heat at constant pressure (J/(kg°C))

The values of h_o for the outer surfaces of the tubes vary widely according to geometry and the configuration of tubes. For turbulent cross flow of air over tubular surfaces, McAdams (1954) gives:

for a single tube:

$$h_o\ =\ 0.24\frac{k_a}{d_o}Re^{0.6}\ \text{W/(m}^2\cdot{}^\circ\text{C)} \qquad (7.2.2.7)$$

for staggered tubes in a bank (chiller car):

$$h_o\ =\ 0.29\frac{k_a}{d_o}Re^{0.6}\ \text{W/(m}^2\cdot{}^\circ\text{C)} \qquad (7.2.2.8)$$

where	k_a	=	thermal conductivity of air (W/(m^2°C)
	d_o	=	outer diameter of tube (m)

The Reynolds' Numbers for the equations (7.2.2.7) and (7.2.2.8) are determined on the basis of the maximum velocity of the air as it flows between the tubes. The maximum airflow velocity traveling through cooling tubes depends intimately on the spacing of downstream tube sets. Careful consideration should be given to maintaining ventilating air flow velocities such that a sufficient factor of safety is built in that will help eliminate fouling due to dirty mine air. The selection of cooling coils is facilitated greatly by tables and graphs provided by manufacturers (McPherson, 2009).

7.2.3 Direct Heat Exchangers

In direct heat exchangers, air is brought into contact with water surfaces. The purpose may be to cool water from the condensers of a refrigeration plant. In this case the hot water is sprayed into a cooling tower and descends as a shower of droplets through an ascending airstream. Heat is transferred from the water droplets to the air by a combination of convection (sensible heat) and evaporation (latent heat). The cooled water that collects at the base of the cooling tower is then returned to the condenser.

Alternatively, the objective may be to cool the air. In this case, chilled water is sprayed into a vertical or horizontal spray chamber. Provided that the airflow enters with a wet bulb temperature that is higher than the temperature of the water, then heat will be transferred from the air to the water by a combination of convection and condensation.

Although there are significant differences between the designs of cooling towers and spray coolers, there are several common factors that influence the amount and efficiency of heat exchange:

a) water mass flowrate
b) supply temperature of water
c) air mass flowrate
d) psychrometric condition of the air at inlet

e) duration and intimacy of contact between the air and the water droplets.

Factor e) depends upon physical design of the heat exchanger, as follows:

i. the relative velocity between the air and water droplets
ii. the size and concentration of water droplets - governed by the flow and pressure of the supply water, the type and configuration of spray nozzles, and the presence of packing within the heat exchanger.

The traditional use of direct heat exchangers in mine air conditioning systems has been for cooling towers either underground or on surface. Tube coil heat exchangers with closed circuit water systems have been used extensively for air cooling in or close to mine workings. However, the greater efficiency of direct heat exchangers led to the development of large permanent spray chambers for bulk air cooling. Furthermore, through the 1980s, smaller portable spray chambers (swamp coolers) began to be employed for local cooling (McPherson, 2009).

7.2.3.1 Cooling Towers

First, let us examine the essential features of cooling towers. Hot water from refrigeration plant condensers is sprayed into the cooling tower and moves downward in counterflow to the rising air current. The purpose of the packing is to distribute the water and airflow uniformly over the cross section and to maximize both the time and total area of contact between the air and water surfaces. The packing may take the form of simple splash bars or riffles arranged in staggered rows, egg-crate geometries or wavy (film-type) surfaces located in vertical configurations. The materials used for packing may be treated fir or redwood timber, galvanized steel, metals with plastic coatings and injection molded PVC or polypropylene. Concrete is used primarily for casings, structural reinforcements and water sumps or dams. Air velocities through counterflow packed cooling towers lie typically in the range 1.5 to 3.6 m/s.

In underground cooling towers, the packing is often eliminated completely or takes the form of one or two screens arranged horizontally across the tower. Such heat exchangers are essentially vertical spray chambers. Other means of maximizing contact time are then employed. These include designs that introduce a swirl into the air at entry, and directing the sprays upward rather than downward. Again, in underground installations, airflow is induced through the cooling towers by the mine ventilating pressure or by booster fans in return airways rather than by fans connected directly to the tower. The pressure drop through underground cooling towers may be further reduced by replacing the mist eliminator screens with an enlarged cross-sectional area; the lower air velocity in this zone decreases the carry-over of water droplets. The optimum air velocity in open spray towers lies in the range 4 to 6 m/s with a maximum of some 8 m/s. Water loadings should not be greater than (16 l/s)/ m^2 of cross-sectional area (Stroh, 1982).

Cooling towers of the type used for mine air conditioning are typically 10 to 20 m in height and some 3 to 8 m in diameter, depending upon the rate at which heat is to be exchanged. Heat loads may be as high as 30 MW.

Natural draft cooling towers do not have fans but rely upon air flow induction by the action of the sprays, or by density difference between the outside atmosphere and the hot moist air within the tower. The hyperbola shaped cooling towers employed commonly for the high heat loads of power stations are of this type and may be over 150 m high in order to accentuate the chimney effect. The air leaving a cooling tower is usually saturated. This often results in the formation of a fog plume in the surface atmosphere. The environmental effects of such a plume should be considered carefully and may influence the siting of a surface cooling tower. In large installations with unacceptable fog plumes, part of the hot condenser water may be cooled within a finned tube indirect heat exchanger. This involves sensible heat exchange only and reduces the humidity of the air leaving the cooling tower. However, such an arrangement detracts from the overall efficiency of heat transfer. In a direct exchange cooling tower, some water is lost continuously from the circuit both by evaporation and by drift (or carry-over) of small droplets. The evaporation loss approximates some one percent for each 7°C of water cooling and drift loss is usually less than 0.2 percent of the water circulation rate (ASHRAE, 1988). However, evaporation can result in a rapid escalation in the concentration of dissolved solids and other impurities leading to scaling, corrosion and sedimentation within the system. In order to limit the buildup of such impurities, some water is continuously removed from the system (bleedoff or blowdown). The bleedoff rate is controlled by monitoring the quality of the water but may be of the order of one percent of the circulation rate. The combined losses from evaporation, drift and bleedoff are made up by adding clean water to the circuit. Further protection of metal components and, particularly the tubes of condensers is obtained by administering anticorrosion compounds. These generally take the form of chromates, phosphates or polyphosphonates of zinc, and promote the formation of a protective film on metal surfaces. Some of these compounds are toxic and precautions may be necessary against accidental release into natural drainage systems. Biocides such as chlorine are also added on a periodic basis to control the growth of algae and other organic slimes (McPherson, 2009).

7.2.3.2 Chilled water spray chambers

If the water supplied to a direct contact heat exchanger is at a temperature below that of the wet bulb temperature of the air, then cooling and dehumidification of the air is achieved. Chilled water spray chambers fall into two categories with respect to size. First, the larger installations are constructed at fixed sites for bulk cooling of main airflows. Secondly, portable spray chambers for localized use within working areas have many advantages over the more traditional tube coil (indirect) stope or face coolers. We shall consider each of these two applications in turn. For bulk air cooling, spray chambers may be designed in vertical or horizontal configuration. Indeed, if the cooling tower shown on Figure 18.13 were supplied with chilled water, then it would act equally well as a vertical spray air cooler. Such designs may be employed either on surface or underground for bulk cooling of intake air and may have heat transfer duties up to 20 MW. Horizontal spray chambers have more limited maximum capacities of some 3.5 MW. They are, however, more convenient for underground use in that existing airways may be utilized without additional excavation. Figure 18.14 illustrates a single stage horizontal spray chamber. The sprays may be directed against or across the airflow. The nozzles can be distributed over the cross section as shown in the sketch or, alternatively, located at the sides or near the base of the chamber. Although the position of the nozzles appears not to be critical, it is important that both the sprays and the airflow are distributed uniformly over the cross section. The spray density should lie within the range 2 to 5 l/s for each square meter of cross sectional area (Bluhm, 1983). The area of liquid/air interface and efficiency of heat exchange increase for smaller sizes of droplets. However, very small droplets result in excessive carry-over or necessitate highly constrictive mist eliminators. Furthermore, higher water pressures and, therefore, pumping costs are required to produce fine sprays. In practice, droplet diameters of some 0.5 mm and water pressures in the range 150 to 300 kPa give satisfactory results in horizontal spray chambers (Reuther, 1988). At positions fairly close to the nozzles, the relative directions of the air and water droplets may be counterflow or crossflow, dependent upon the orientation of the nozzles. However, aerodynamic drag rapidly converts the spray to parallel flow, particularly for the smaller droplets. In order to regain the higher efficiency of counterflow heat exchange, the spray chamber may be divided into two or three stages so that the air leaves the chamber at the position of the coldest sprays. Chilled water should be supplied at as low a temperature as practicable but, in any event, not higher than 12°C. An additional sump at each end assists in balancing the pumping duties.

If the surrounding strata are unfractured and unaffected by water, then the spray chamber may utilize the full cross section of a bypass airway. If, however, the rock must be protected against the effects of water, then concrete lining or prefabricated sections may be employed to contain the spray chamber. In cases where the strata is very sensitive to water (such as evaporite strata) then it is advisable to protect the rock surfaces for 50 to 100 m downstream from the spray chamber.

The cross-sectional area of the spray chamber should be chosen to give a preferred air velocity of some 4 to 6 m/s, but not more than 7 m/s. Higher air velocities will reduce the efficiency of heat exchange and can result in excessive pressure drops in the airflow.

In addition to cooling and dehumidifying the air, spray coolers can also reduce dust concentrations. However, the buildup of dust particles in the recirculating water system may cause fouling of the pipes and other heat exchangers. This may require filters or sedimentation zones to be included in the design.

Internal packing can also be employed to improve the efficiency of horizontal spray chambers (Stroh, 1980). This can increase the air frictional pressure drop across the cooler. However, the water supply pressure (gauge) may be as low as 30 kPa since the spray nozzles can be replaced by low resistance dribbler bars.

In order to extend the applicability of direct spray coolers, enclosed and portable units have been developed (Thimons, 1980; Ramsden, 1984; Reuther, 1988). These may be mounted on wheels or sleds and are often referred to as spray mesh coolers. In order to maintain the design to acceptable dimensions for portable application, the water loading may be much higher than open spray chambers and it becomes even more important to maximize the area and time of contact between the air and water. This occurs in three stages. First, the air passes through the lower mesh of plastic or knitted stainless steel. Secondly, the airflow is directed through the upward pointing and finely divided sprays. The final stage of cooling occurs within the upper mesh which also acts as a demister. The distribution of droplets of water falling from the upper to the lower mesh may be assisted by installing drip fins. These also help to prevent water running down the walls (Heller, 1982). Between the two meshes, heat exchange occurs by a combination of counterflow, crossflow and parallel flow. Another type of portable spray cooler employs film packing and crossflow heat exchange (Reuther, 1988).

The dry bulb temperature of air can be reduced by passing it through a spray chamber supplied with unchilled water. The device is then known as an evaporative cooler. No heat is removed from the air. Hence, if the water is supplied at wet bulb temperature, then the exhaust air may attain that same wet bulb temperature while the moisture content will have increased. Evaporative coolers have an application for surface structures in hot dry climates but are seldom used in underground mines. They have been employed for very localized effects in hot evaporite mines. However, the reduced dry bulb temperature encourages enhanced heat flow from the strata which, when combined with the raised moisture content, reduces the cooling power of the air downstream from the cooled area (McPherson, 1993).

7.2.3.3 Performance Calculations for Direct Heat Exchangers

A common theoretical analysis may be applied to direct heat exchangers irrespective of the direction of heat transfer. The results of such analyses apply equally well to cooling towers and chilled water spray chambers. In order to avoid unnecessary repetition, we will conduct the following analysis on the assumption of a cooling tower. Water recycles continuously through the condenser of a refrigeration plant (where it gains heat) and the cooling tower where it rejects that heat to the atmosphere. The first observation is that if we ignore the small heat losses from interconnecting pipes and the equally small effects of make-up water, then, at steady state, the heat rejected in the cooling tower must be equal to the heat gained in the condenser. This leads to the initially surprising statement that the rate of heat rejection in the cooling tower depends only upon the heat load imposed by the condenser and not at all upon the design of the cooling tower. However, if the cooling tower is inefficient in transferring heat from the water to the air, then the temperature of the water throughout the complete circuit will rise until balance is attained between heat gain in the condenser and heat rejection in the cooling tower. This would be unfortunate as the coefficient of performance of the refrigeration plant deteriorates as the condenser temperature increases (Section 7.1.3). Figure 3 illustrates the decrease in temperature of the water as it falls through the cooling tower and the corresponding increase in the wet bulb temperature of the ascending air. Figure 3 also illustrates the meaning of two terms that are commonly employed:

The $range$ is the change in temperature of the water

$$range = t_{w,in} - t_{w,out} \text{ °C} \qquad (7.2.3.1)$$

while the $approach$ is the difference between the temperatures of the water outflow and the wet bulb temperature of the air inflow:

$$approach = t_{w,out} - t_{a,in} \text{ °C} \qquad (7.2.3.2)$$

where	*t*	=	temperature (°C)
and subscripts	*w*	=	liquid water
	a	=	air (wet bulb)
	in	=	inflow
	out	=	outflow

Manufacturers will usually accept requests for approach values down to 2°C.

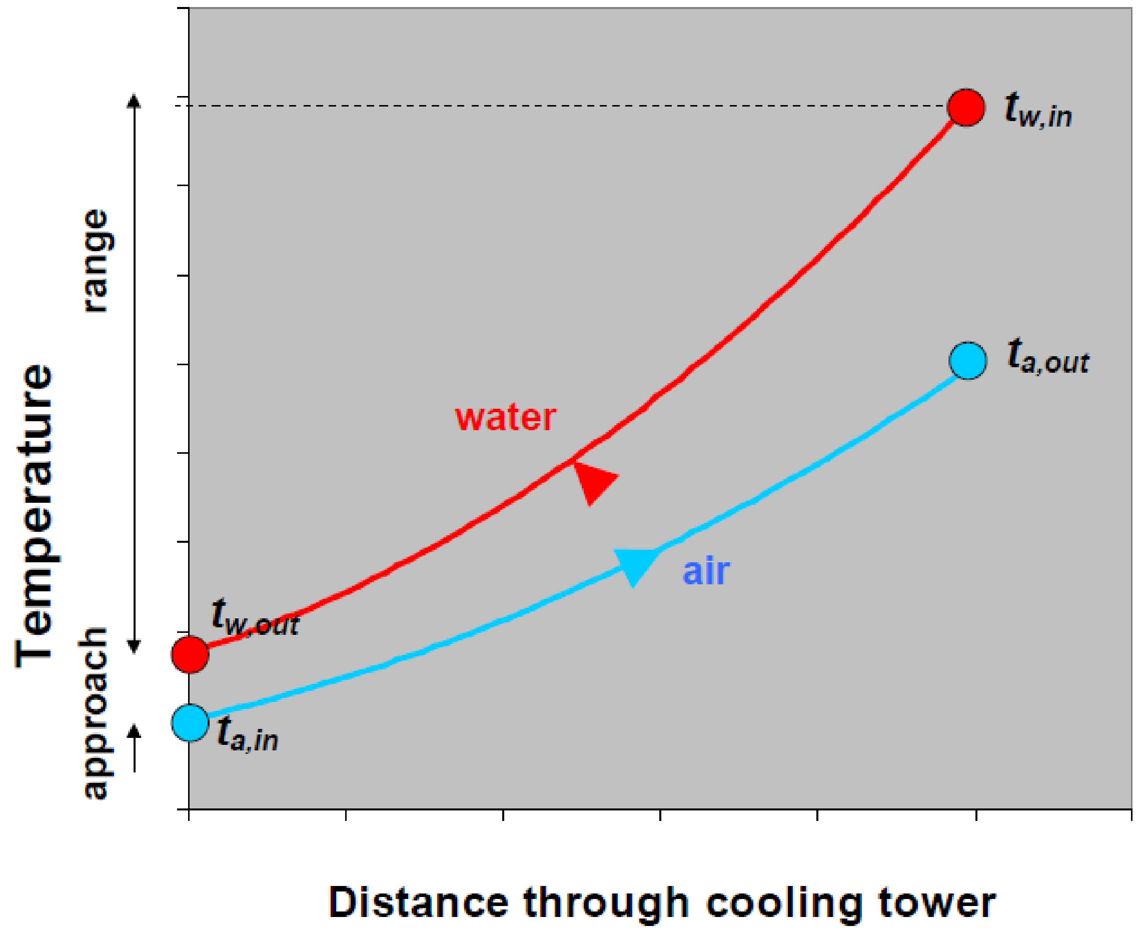

Figure 3: Variation of water temperature, t_w, and wet bulb temperature of the air, t_a, through a cooling tower (McPherson, 2009).

The quantitative analysis of the cooling tower commences by writing down the balance that must exist between rates of heat gained by the air and heat lost from the water:

$$m_a(S_{out} - S_{in}) = m_w C_w(t_{w,in} - t_{w,out})\ \mathrm{W} \qquad (7.2.3.3)$$

where m = mass flow (kg/s)

S = sigma heat of air (J/kg)

and C_w = specific heat of water (4.187 kJ/(kg °C))

This is, in fact, an approximation as evaporation changes the value of m_w within the tower. However, the error does not normally exceed 4 percent and may be neglected for practical purposes.

As in so many cases of assessing performance, it is useful to imagine the unattainable perfect cooling tower. In such a device, the two curves on Figure 3 would coincide and, in particular, the water would leave at inlet air wet bulb temperature while the air would leave at the temperature of the incoming water, that is:

$$t_{w,out} = t_{a,in} \tag{7.2.3.4}$$

and

$$t_{a,out} = t_{w,in} \tag{7.2.3.5}$$

The concept of a perfect cooling tower allows us to devise efficiencies of heat transfer for both the water and the air streams:

water efficiency

$$\eta_w = \frac{actual\ heat\ lost\ from\ the\ water}{theoretical\ maximum\ heat\ that\ could\ be\ lost\ from\ the\ water}$$

$$= \frac{m_w C_w (t_{w,in} - t_{w,out})}{m_w C_w (t_{w,in} - t_{a,in})} = \frac{(t_{w,in} - t_{w,out})}{(t_{w,in} - t_{a,in})} = \frac{range}{range + approach} \tag{7.2.3.6}$$

Similarly, air efficiency (See Figure 3)

$$\eta_a = \frac{actual\ heat\ gained\ by\ the\ air}{theoretical\ maximum\ heat\ that\ could\ be\ gained\ by\ the\ air}$$

$$= \frac{m_a (S_{out} - S_{in})}{m_a (S_{w,in} - S_{in})} = \frac{(S_{out} - S_{in})}{(S_{w,in} - S_{in})} \tag{7.2.3.7}$$

where *Sw,in* = sigma heat of saturated air at a temperature equal to that of the inlet water, J/kg. (The term "thermal capacity" is sometimes employed where we have used "theoretical maximum heat".)

Although the water and air efficiencies are useful indicators of the efficacy of heat transfer for each of the two fluids, neither gives any clue to the overall quality of design for the complete cooling tower. For example, if the water flow were low giving relatively few small droplets falling through a large airflow, then the water efficiency would be very high. However, the air would be used to only a small fraction of its thermal capacity and, hence, the air efficiency and overall heat transfer would be low.

To examine this problem let us consider, again, perfect heat transfer in a cooling tower. Then,

maximum thermal capacity of water = $m_w C_w (t_{w,in} - t_{a,in})$ J

and maximum thermal capacity of airstream = $m_a(S_{w,in} - S_{in})$ J

The ratio of these thermal capacities defines the tower capacity factor, *R*

$$R = \frac{m_w}{m_a} C_w \frac{(t_{w,in} - t_{a,in})}{(S_{w,in} - S_{in})} \text{ (dimensionless)} \qquad (7.2.3.8)$$

The liquid to gas ratio, m_w/m_a normally lies within the range 0.4 to 2.0.

The theoretical concept of tower capacity factor ignores the practical reality that in a real cooling tower the rate of heat loss from the water must equal the rate of heat gain by the air. It may be defined in words as follows:

'If both of the given fluid streams were used to their maximum thermal capacity, then R would be Watts lost by the water for each Watt gained by the air.'

An important observation here is that *R* depends only upon the flowrates and the inlet conditions of the water and air. It is completely independent of the construction of the cooling tower. Notice also that we have been quite arbitrary in choosing to define *R* as the ratio of water thermal capacity divided by air thermal capacity, rather than the other way round. The values of tower capacity factor vary from 0.5 to 2.

The tower capacity factor is also related to the ratio of air and water efficiencies.

From equations (7.2.3.7 and 7.2.3.8)

$$\frac{\eta_a}{\eta_w} = \frac{(S_{out} - S_{in})}{(S_{w,in} - S_{in})} \frac{(t_{w,in} - t_{w,out})}{(t_{w,in} - t_{a,in})}$$

and substituting for

$(S_{out} - S_{in}) = \frac{m_w}{m_a} C_w (t_{w,in} - t_{w,out})$ from equation (7.2.3.4) gives

$$\frac{\eta_a}{\eta_w} = \frac{m_w}{m_a} C_w \frac{(t_{w,in} - t_{a,in})}{(S_{w,in} - S_{in})}$$

Since this is identical to equation (7.2.3.8), then tower capacity factor

$$R = \frac{\eta_a}{\eta_w} \qquad (7.2.3.9)$$

indicating that the ratio of air and water efficiencies is also independent of the design of the cooling tower or spray chamber. The rate of heat transfer, air and water efficiencies, and the tower capacity factor are all dependent on inlet temperatures. It is, therefore, somewhat misleading to quote a single value of cooling duty to characterize a heat exchanger (McPherson, 2009).

7.2.4 Water Distribution Systems

A significant item in the design and economic analysis of mine air conditioning systems is the choice of piping that carries water between the refrigeration plant and heat exchangers or mining equipment. There are, essentially, two matters of importance. First, the size of the pipe should be selected carefully. If it is too small for the given flowrate, then the frictional pressure drops and pumping costs will be high. On the other hand, if too large a pipe is chosen the costs of purchase and insulation will be high while the larger surface area and low velocity will exacerbate unwanted heat transfer with the surroundings.

This brings us to the second consideration, the thermal properties of the pipe material and the need for additional insulation. We shall discuss each of these matters in turn (McPherson, 1993).

7.2.4.1 Pipe Sizing

The first step in determining the diameters of the various pipes that comprise a water network is to assess the flowrates that are to be carried in each branch. The cooling duty, q, of a heat exchanger is given as

$$q = m_w C_w \left(t_{w,out} - t_{w,in}\right) \text{ W} \tag{7.2.4.1}$$

where m_w = water flowrate (kg/s)

C_w = specific heat of liquid water (4.187 kJ/(kg·°C))

$t_{w,in}$ = inlet water temperature (°C)

$t_{w,out}$ = outlet water temperature (°C)

The heat transferred is dependent equally upon the water flowrate and the temperature rise of the water through the unit. The latter, in turn, is governed by the construction of the heat exchanger and the supply temperature of the water.

Calculations of the type included in Section 7.2.2 allow flowrates to be assessed. For service water lines, the flowrates must also satisfy the machine requirements for dust suppression or hydraulic power (McPherson, 1993).

Having established the water flowrate, the actual sizing of a pipe becomes a combination of simple analysis and practical considerations. Taking into account capital, operating and installation costs, van Vuuren (1975) suggested optimum water velocities of 1.8 to 2.0 m/s for 4000 kPa pipes and 2.0 to 2.2 m/s for 7000 kPa pipes. A common rule of thumb is to employ 2 m/s for an initial exercise in pipe sizing (McPherson, 2009). For practical calculations, water density remains constant at 1000 kg/m^3.

The frictional pressure drop, p, along the pipe may then be determined from the Chezy Darcy relationship:

$$p = \frac{4fL\rho_w u^2}{2d} \text{ Pa} \qquad (7.2.4.2)$$

where f = coefficient of friction (dimensionless)

L = length of pipe (m), typically unity to yield p/m

ρ_w = water density (kg/m^3)

u = water velocity (m/s)

d = pipe diameter (m)

Manufacturers usually provide charts for their pipes relating frictional pressure losses to pipe diameter and flowrate. Plastic pipes have a coefficient of friction averaging about 0.0032. The pressure loss that can be tolerated depends upon the pumping cost function which is proportional to the product pQ

(McPherson, 1993), and the pressure required at the end of the pipeline. If the pumping costs are shown to be high, then consideration should be given to increasing the pipe diameter, reducing the velocity, decreasing the outlet pressure or a combination of these considerations.

Pressure losses are also incurred at bends or pipe fittings. Again, manufacturer-specific data can be employed to determine such losses. However, for mine water systems, it is common to cater for bends and fittings by simply adding ten percent to the computed pressure drop.

Pipe diameters determined through this procedure should be rounded up to the next highest standard size. Consideration should be given to any increases in water flow that may be required in the future. Furthermore, pipe ranges that might be used for firefighting should be sized to give adequate flow and pressure at the hydrants. The sizes of pipes that are to be installed within existing airways or shafts may also be constrained by the space available (McPherson, 2009).

7.2.4.2 Pipe Insulation

The performance of heat exchangers is dependent upon the temperature of the supply water. It is, therefore, important that heat gain along chilled water pipelines is minimized. This is normally accomplished by providing thermal insulation on those pipes. One exception is where the pipeline traverses or intersects an intake airway which may require air cooling. This situation may allow partial or total insulation omission.

In addition to having a low thermal conductivity, the insulating materials for chilled water pipes in mines should conform to several other criteria:

- The insulation should provide a barrier against the ingress of water that condenses on the outer surfaces. A porous and permeable insulation that becomes waterlogged will be much more conductive to heat. Furthermore, water that reaches the surface of metal pipes will cause problems of corrosion. The required vapor barrier may be achieved either by covering the insulation with an impermeable sheath or by using an insulating material that is, itself, non-permeable. An example is cellular glass in which the small air pockets are isolated from each other.
- The insulation or outside sheath should have sufficient mechanical strength to withstand the rigors of transport and utilization in mine environments. Insulation on shaft pipelines must be able to withstand impact from falling objects.
- The flammability of insulating materials and the toxicity of gases that they may produce when heated in a mine fire is of great importance. Polyurethane foams have been employed widely in the past. However, they emit carbon monoxide and, perhaps, cyanide vapors at temperatures that may be reached in mine fires. Phenolic foams in which phenols are bound into a resin base are safer in that they have a higher ignition temperature, and a much lower rate of flame spread (Rose, 1989).
- The cost of purchase and ease of installation of insulating materials or pre-insulated piping should also be taken into account.

A common practice has been to apply insulating materials to pipes on the mine site - either on the surface or after the pipework has been installed in its underground location. The application of foam insulators may be carried out by injecting the foam within a PVC vapor barrier jacket installed over spacers on the outside of the pipe. Pre-cast semicircular sections of cellular glass or other rigid insulators may be bound on to the pipes with adhesives or an outer sealing material. Expanded polystyrene granules and fiberglass have also been used widely (Arkle, 1985; Ramsden, 1985). The thickness of applied insulators varies from 25 to 40 mm.

The continued development of thermoplastics has allowed the manufacture of pipes that combine mechanical strength with good thermal insulating properties. These may consist of concentric and impermeable cylinders with the annulus containing a cellular infill (McPherson, 2009).

7.2.4.3 Energy and Temperature Changes Within Water Systems

Fluid frictional effects influence temperature changes within water distribution systems. The steady state flow equation will be used to assess energy within a piping network , as follows

$$\frac{{u_1}^2 - {u_2}^2}{2} + (Z_1 - Z_2)g + W_{12} = \int_1^2 V dP + F_{12} = (H_2 - H_1) - q_{12} \text{ J/kg} \qquad (7.2.4.3)$$

where u = velocity (m/s)

Z = height above datum (m)

g = gravitational acceleration (m/s^2)

W = work input (J/kg)

V = specific volume of fluid (m^3/kg)

F = work done against friction (J/kg)

H = enthalpy (J/kg)

q = heat added from surroundings (J/kg)

Enthalpy is defined in its basic form equation

$$H = PV + U \tag{7.2.4.4}$$

where U = internal energy (J/kg)

and assuming water to be incompressible, V will be a constant. By substituting equation (7.2.4.4) into (7.2.4.3), the right hand side becomes

$$V(P_2 - P_1) + F_{12} = P_2V - P_1V + U_2 - U_1 - q_{12}$$

or

$$F_{12} = U_2 - U_1 - q_{12} \text{ J/kg} \tag{7.2.4.5}$$

Incorporating the specific heat of water into the work terms, we get

$$(U_2 - U_1) = C_w(T_2 - T_1) \text{ J/kg} \tag{7.2.4.6}$$

Incorporating the frictional pressure drop, *p*, the equation now becomes

$$p = \rho_w F_{12} = \rho_w(C_w(T_2 - T_1) - q_{12}) \text{ Pa} \tag{7.2.4.7}$$

where ρ_w = water density (kg/m^3)

The energy balance equation (7.2.4.3) in this case has adiabatic flow, q_{12} = 0, and the increase in water temperature along a pipeline becomes

$$(T_2 - T_1) = \frac{p}{\rho_w C_w} \text{ °C} \tag{7.2.4.8}$$

The term $1/\rho_w C_w$ is known as the Joule-Thompson coefficient with a standard value of 1/(1000 x 4187) = 2.39e^{-7} °C/Pa for water.

The adiabatic rise in temperature along a water pipe is shown by equation (7.2.4.8) to be directly proportional to the frictional pressure drop and is independent of changes in elevation. The frictional pressure drop, p, may occur by viscous or turbulent action within the length of the pipe or by shock loss across a valve or other obstruction.

For flow through a water pump or turbine, we can apply the left and right sides of equation (7.2.4.3). Since kinetic energy and elevation difference the device are both negligible, equation (7.2.4.3) becomes

$$W_{12} = (H_2 - H_1) - q_{12}$$

$$= V(P_2 - P_1) + (U_2 - U_1) - q_{12}$$

$$= \frac{(P_2 - P_1)}{\rho_w} + C_w(T_2 - T_1) - q_{12} \text{ J/kg} \qquad (7.2.4.9)$$

With negligible heat exchange across the casing of the pump or turbine, we may assume adiabatic flow (q_{12} = 0) giving the temperature rise as

$$(T_2 - T_1) = {\left\{W_{12} - \frac{(P_2 - P_1)}{\rho_w}\right\}}\Big/{C_w} \text{ °C} \qquad (7.2.4.10)$$

While W_{12} is the total work applied to a pump impeller, the term $(P_2 - P_1)/\rho_w$ represents the output of useful mechanical energy. The difference between the two indicates the degradation of some of the input power to thermal energy and produces a measurable temperature rise. In a turbine, it is the other way round with $(P_1 - P_2)/\rho_w$ representing the work input and $-W_{12}$ being the output work.

The actual work output for a pump is then given by

$$W_{12}\,\eta = {(P_2 - P_1)}/{\rho_w} \text{ J/kg} \qquad (7.2.4.11)$$

and, for a turbine, the actual work output is

$$W_{12} \;=\; {}^{(P_2 - P_1)\eta}\!/_{\rho_w} \text{ J/kg} \qquad (7.2.4.12)$$

where η = efficiency of the device

Substituting for W_{12} in equation (7.2.4.10) gives the temperature rise <u>across a pump:</u>

$$(T_2 - T_1) \;=\; \frac{(P_2 - P_1)}{C_w \rho_w}\left(\frac{1}{\eta} - 1\right) \text{ °C} \qquad (7.2.4.13)$$

and <u>across a water turbine:</u>

$$(T_2 - T_1) \;=\; \frac{(P_2 - P_1)}{C_w \rho_w}(\eta - 1) \text{ °C} \qquad (7.2.4.14)$$

In these analyses, it has been assumed that water is incompressible. In fact, the slight compressibility of water does give it a small isentropic temperature change with respect to pressure (Whillier, 1967). This is given approximately as

$$\Delta t/_{\Delta P} \;=\; (0.759t \;-\; 0.2)e^{-6} \text{ °C/kPa} \qquad (7.2.4.15)$$

where t = initial temperature (°C)

This effect may be neglected for most practical purposes. However, if equations (7.2.4.13) or (7.2.4.14) are transposed in order to determine the efficiency of the device from temperature observations, then the measured temperature rise should be corrected according to equation (7.2.4.15) (negatively for a pump and positively for a turbine) (McPherson, 1993).

7.2.4.4 Heat Exchange Across the Walls of Pipes and Ducts

When a fluid flowing through a pipe or duct is at a temperature different to that of the ambient air, then heat exchange will occur across the walls of the pipe and any insulating material that surrounds it. The previous section's analysis of indirect heat exchangers correlates strongly with heat transfer mechanisms that exist for pipes and ducts.

Figure 3 illustrates an insulated pipe transferring a fluid with temperature t_{in} while the temperature of the outside air is t_{out}.

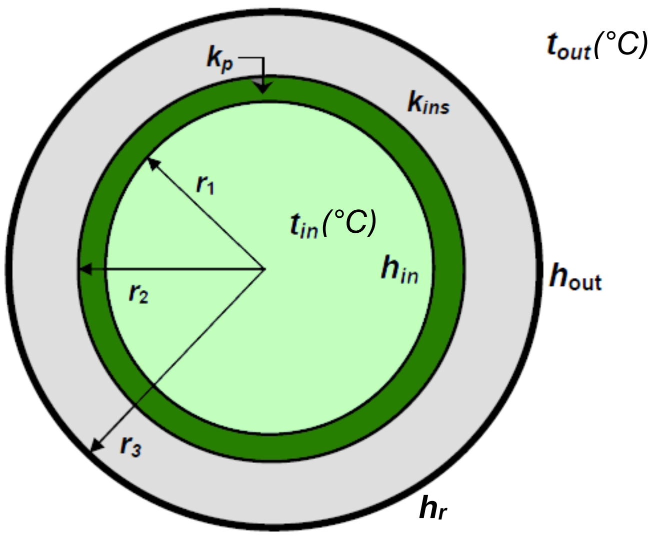

Figure 4: Heat transfer across an insulated pipe or duct.

For a relatively short length of pipe over which neither t_{in} nor t_{out} vary significantly allows the heat transfer to be expressed by:

$$q = UA(t_{in} - t_{out}) \text{ W} \qquad \text{(see equation 7.2.2.2)}$$

The *UA* value is given by

$$\frac{1}{UA} = \frac{1}{h_{in}A_{in}} + \frac{r_2 - r_1}{k_p A_{12}} + \frac{r_3 - r_2}{k_{ins} A_{23}} + \frac{1}{(h_{out} + 0.95 h_r) A_{out}} \text{ °C/W} \qquad (7.2.4.1)$$

where h_{in} = heat transfer coefficient of inner surface (W/(m^2°C)

h_{out} = heat transfer coefficient of outer surface (W/(m^2°C)

h_r = radiative heat transfer coefficient at outer surface (W/(m^2°C)

r = radii (m)

k_p = thermal conductivity of pipe (W/(m°C)

k_{ins} = thermal conductivity of insulation (W/(m°C)

A = cross sectional area of heat transfer (m^2)

0.95 = assumed airflow emissivity and view factor, (Whillier, 1982)

The radiative heat transfer coefficient at the outer insulation surface will become numerically negative when the ventilating airflow temperature is below the temperature of the refrigerant fluid running through the pipeline.

The heat transfer coefficients may be estimated from the following relationships which take into account the variations of fluid viscosity and thermal conductivity with respect to temperature.

<u>Air inside a duct</u>

The Colburn equation (7.2.2.5) gives the heat transfer coefficient for turbulent flow inside smooth tubes. For air, the Prandtl Number, P_r, remains essentially constant at 0.7 over a wide range of temperatures and pressures (McPherson, 1993). Further analysis of the Colburn equation yields

$$h_{in}(air) = 3.169\frac{(\rho_a u_a)^{0.8}}{d^{0.2}}(1 + 9.4e^{-4}t_{in} - 6.49e^{-6}{t_{in}}^2) \text{ W/(m}^2\text{°C)} \quad (7.2.4.2)$$

where ρ_a = duct airflow density (kg/m^3)

u_a = duct airflow velocity (m/s)

d = internal duct diameter (m)

Changing the Colburn equation to compensate for air density allows equation (7.2.2.9) to be used for compressed air pipes as well as ventilation ducts.

<u>Water inside a pipe</u>

A similar Colburn equation analysis for water inside a pipe yields

$$h_{in}(water) = (1430 + 20.9t_{in})\frac{{u_w}^{0.8}}{d^{0.2}} \text{ W/(m}^2\text{°C)} \qquad (7.2.4.3)$$

where u_w = water velocity (m/s)

In this case, the near constant value of water density allows it to be eliminated as a variable. Since viscosity of water varies significantly in the range 0 to 60°C, the effect of temperature should not be ignored in equation (7.2.4.3).

<u>Air outside a pipe</u>

The heat transfer coefficient of the airflow moving over a pipeline is derived using a similar analysis of equation (7.2.2.5)

$$h_{out}(air) = (4.24 + 0.0015t_{out})\frac{(\rho_a u_a)^{0.6}}{d^{0.4}} \text{ W/(m}^2\text{°C)} \qquad (7.2.4.4)$$

<u>Radiative heat transfer coefficient</u>

This can be calculated from the Stefan-Boltzman equation using the measured dry bulb temperature of the surrounding air, yielding

$$h_r = 22.68e^{-8}(273.15 + t_{out})^3 \text{ W/(m}^2\text{°C)} \qquad (7.2.4.5)$$

Over long lengths of pipe or ducting the inner and outer temperatures, t_{in} and t_{out}, will exhibit nonlinear changes. In this case the logarithmic mean temperature difference should be employed when calculating heat transferred by the pipeline:

$$q = UA\frac{(\Delta t_1 - \Delta t_2)}{ln\left({\Delta t_1}/{\Delta t_2}\right)} \text{ W/(m}^2\text{°C)} \qquad (7.2.4.6)$$

where Δt_1 and Δt_2 are the values of the temperature difference (t_{in} - t_{out}) at the two ends of the pipe and *ln* is natural logarithm.

The techniques described in this section can be incorporated into mine climate simulation software in order to take into account heat transfers between pipes or ducts and the surrounding airflow. If the fluid inside the pipe moves in the same direction as the ventilating airstream, then the heat transfers and corresponding temperature changes can be computed sequentially along each incremental length of simulated airway. In the case of the piped fluid and the ventilating airstream moving in opposite directions, then an iterative procedure becomes necessary to compute the equilibrium condition.

7.3 Design Methodologies

Commercially available high efficiency refrigeration systems use ammonia as the cooling medium due to its long lifespan, small construction footprint and relatively inexpensive operation properties. Furthermore, mechanical engineers have embraced the widespread practice of employing ammonia refrigerant for closed-circuit air-conditioning system designs for well over 60 years through ongoing research by the American Society of Heating, Refrigeration and Air-Conditioning Engineers (ASHRAE, 1997).

South Africa and Australia mining regulatory agencies have approved the use of ammonia for surface refrigeration plants as long as stringent guidelines are followed thoroughly. The adoption of ammonia for refrigerant requires the mining operation to provide extensively detailed lists of protocols and procedures to be followed during operation, maintenance and emergency action plans of the ammonia supplied compressors powering the surface refrigeration plants. These guidelines ensure no ammonia will be allowed to enter any underground workings, either in the supplied airflow or water sources. Special considerations must be given to environmentally responsible containment and disposal of spent refrigerant. Additional plans must be detailed to observe the preservation of watersheds and sensitive natural landscapes.

7.3.1 Centralized vs. Distributed Cooling Strategies

Bulk air cooling for mining has traditionally been accomplished using evaporative cooling. Lowering the temperature of the intake airflow also requires saturation of that air when evaporative cooling is employed, in regions that typically experience moderate to high levels of relative humidity. Requiring a surface cooling plant to supply cold service water to the underground is taxing on the system and adds levels of complexity not usually necessary.

Monetarily speaking, centralized bulk air cooling systems are better. Logistically speaking however, distributed cooling systems are more effective. When you take into account the piping and extra pumping required, plus the associated cost of construction in the underground environment, a network of distributed coolers becomes prohibitive for large footprint operations. In reality, an operational trade-off exists wherein a combination of centralized and distributed cooling coexist.

Self-contained cooling systems, with remote heat exchangers, are more attractive since the piping and pumps are not required to connect these to a centralized cooling system. The initial capital cost for these self-contained coolers are more than a distributed system however the cost of a full-blown installation is virtually eliminated, and the system can be relocated as needed.

An accurate estimation of the mine’s heat load is the first and most important step in sizing any bulk air-cooling system. An intimate understanding of the anticipated mining production schedule, along with detailed drilling records that include thermal logging of exploratory core drillings are requisite information for correctly estimating the ultimate heat load of any mine.

In the majority of large scale mine cooling systems, there are usually three sets of heat transfer involved:

1. transfer of heat from the work areas to the evaporators of the refrigeration units
2. transfer of heat from the evaporators to the condensers in the refrigeration units (the vapor compression cycle)
3. transfer of heat from the condensers to the free atmosphere on surface.

There exist tremendous variations in the duty, complexity and efficiency of the hardware involved in these three phases, dependent upon the severity and dispersion of the heat problem in the mine.

7.3.2 Energy Recovery Devices

The trend towards siting main refrigeration plant on the surface of mines accelerated during the 1980's. This was caused in large part by the utilization of energy recovery devices, particularly water turbines. Prior to that time, the provision of chilled water at the surface had three major drawbacks.

First, it caused high water pressures at shaft bottoms which necessitated a choice between high pressure heat exchangers and associated pipework or, alternatively, to pass the water through pressure reducing valves. The latter choice not only resulted in high operating costs of pumping to return the water to surface, but also converted the potential energy of the water to thermal energy, giving a rise in temperature and eroding the cooling capacity of the chilled water.

Energy recovery devices address each of these problems and divide into two major groups. First, water turbines or hydraulic motors employ the potential energy of shaft water lines to drive electrical generators or other devices. Secondly, hydrolift systems utilize the weight of descending chilled water to help raise heated return water back to surface. We shall discuss each of these systems in turn.

7.3.2.1 Water Turbines

Shaft bottom turbines provide:

- work output that may be used to drive pumps, generators or any other mechanical device; this work may provide part of the energy required to raise return water back to surface;
- reduced temperature of the subsurface supply of chilled water, and hence, savings in refrigeration costs;
- a low pressure water system underground.

Two types of turbines are in use. Figure 5 illustrates an impulse turbine, commonly known as a Pelton Wheel. In this device, the pressure of the supply water is used to produce kinetic energy by means of one or more nozzles. The high velocity jets are directed at cups attached to the periphery of a rotating wheel. Inside the casing of the device, the jets operate at ambient atmospheric pressure. Hence, the water leaves at zero gauge pressure. Control of the mechanical output may be achieved by a needle valve in the nozzle which changes the water flowrate. Alternatively, if the flow is to be maintained, deflector plates may be used to direct part of the jets away from the cups.

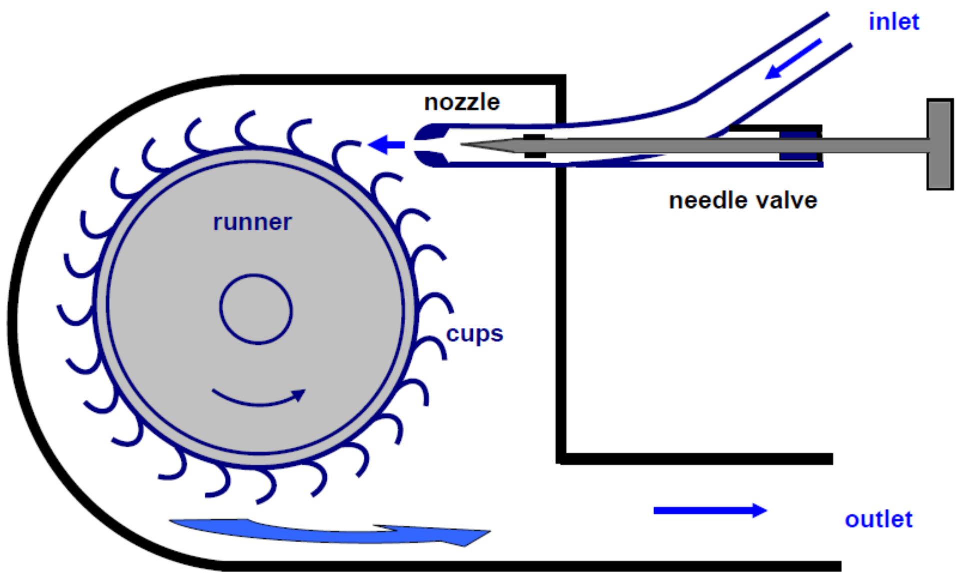

Figure 5: Illustration of a Pelton Wheel (McPherson, 2009).

The advantages of a Pelton Wheel are that it is simple and rugged in construction, reliable and may reach efficiencies of over 80 percent. The speed control is effective and no high pressure seals are required on the casing.

The second type of water turbine is the reaction device and is often referred to as a Francis or Kaplan turbine. This is essentially a centrifugal runner (Figure 10.2) with the impeller designed to operate in reverse and incorporating guide vanes to minimize shock losses. Indeed, a reversed centrifugal pump may be used as a reaction turbine although at a considerably reduced efficiency. Control of the device is by valves located upstream and/or downstream. Unlike the Pelton Wheel, a reaction turbine operates in a "flooded" mode giving rise to its primary advantage, i.e. the water pressure at exit can be maintained above the ambient air pressure and, hence, may be utilized further downstream to overcome pipe losses, provide the required pressure at spray chambers or to activate further hydraulic devices. Pelton Wheels give better efficiencies at the higher duties, typically 2 MW. The Francis turbines are better suited for lower differential pressure duties.

In addition to shaft bottom stations, water turbines may be used for more local applications. For example, if the water pressure available at a spray chamber exceeds that required at the spray nozzles, then a turbine can be sited in the water supply line and used to power local pumps or fans. This is particularly advantageous for multi-stage spray chambers (Ramsden, 1985).

7.3.2.2 Hydrolift Systems

The principle of operation of a hydrolift system is illustrated by Figure 18.21. The device is sometimes also known as a hydrochamber or hydrotransformer. The chamber is excavated or constructed underground and is alternately filled from opposite ends with chilled water delivered from surface, then with hot water returned from the mine. Let us assume that the chamber is initially filled with warm water. Both of the automated valves A are opened and valves B are closed. The pump at the surface cold water dam causes chilled water to flow down the shaft pipe and into the chamber. This, in turn, forces the hot water to exit the chamber and ascend the return shaft pipe.

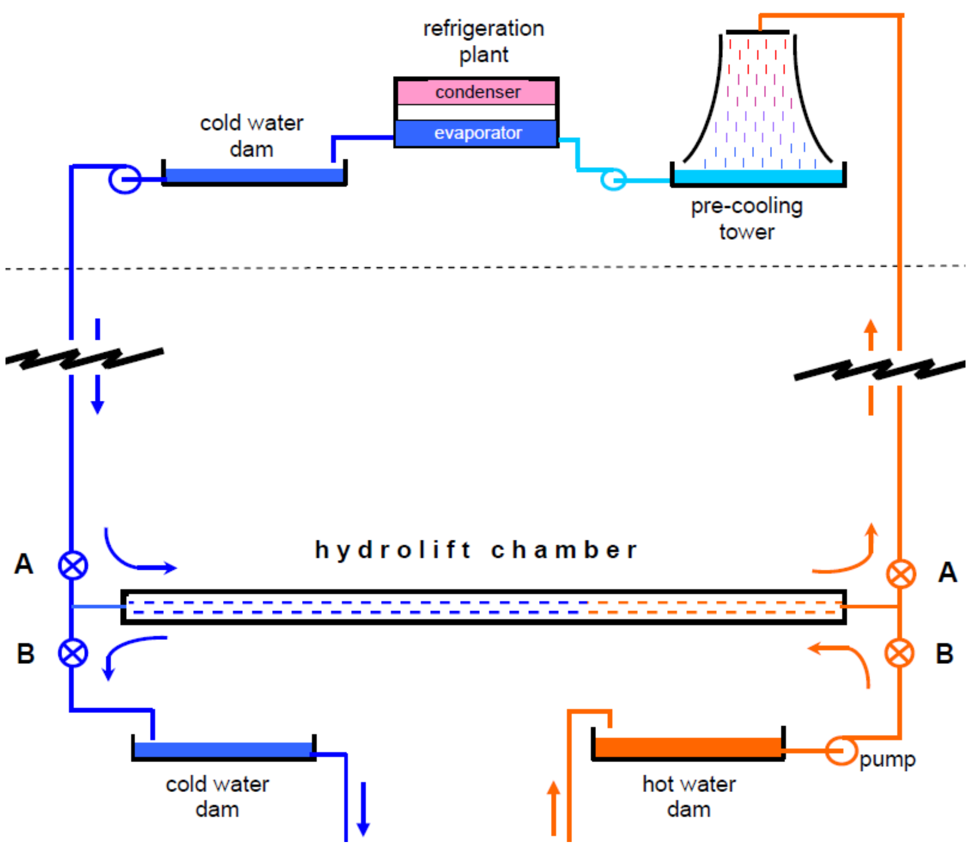

Figure 6: Operating principle of a hydrolift system (McPherson, 2009).

As the two columns of water are nearly balanced, the duty of the pump is simply to overcome pipe friction. When the chamber is filled with chilled water, valves A are closed and valves B are opened. The underground hot water dam pump then forces the hot return water into the chamber, expelling the chilled water to the underground cold water dam. The cyclic nature of the system can be negated by having three hydrolift chambers with the sets of valves phased to give a continuous flow into and out of the water dams. The size of chambers and water dams should be determined on the basis of the cooling requirements of the mine. An inherent disadvantage of the hydrolift system is that the rate of chilled water flow must be equal to that of the heated return water. It is, therefore, advisable that the water dams should be sized to accommodate several hours supply. A loss of efficiency occurs because of heat exchange with the walls of the chamber and due to mixing and thermal transfer at the hot and cold interface within the chamber. The latter may be minimized by inclining the chamber such that the hot water end is at a higher elevation.

7.3.3 Cooling Design Procedure Stages

The initial question is how much heat could be removed by applied fresh air and how much would be removed by mechanical cooling systems. The following list describe the stages of the design procedure for a subsurface air conditioning system.

- Determine the expected heat load for the entire mine and also each district, level or zone where heat would be excessive.
- Determine the heat removal capacities of the district, level or zone airflows. If this is greater than the corresponding heat loads for

individual sections of the mine, then the heat can be removed entirely by ventilation and there is no need to consider a cooling system.

- Determine the heat to be removed by cooling as the difference between the heat load and the heat removal capacity of the air. Iterative studies should also be conducted to optimize between ventilation and air conditioning (Anderson, 1986).
- These investigations will establish the required distribution of air cooling devices. If this is limited to a few localized areas, then the feasibility of employing spot or district coolers should be investigated. However, if the heat problem is more widespread, then centralized refrigeration plant should be evaluated.
- Evaluate alternative locations of refrigerating plant and the feasibility of using energy recovery devices.
- Establish refrigeration plant operating duty by totaling heat exchanging capacities and allowing for line losses.
- Estimate evaporator and condenser temperatures on the basis of the desired temperature of the cooled medium and the heat rejection facilities respectively.
- Determine the required flowrates of chilled water to estimate piping sizes and pumping duties.

None of these steps may be begun until the ventilation system is completely quantified, balanced and accurately simulated. This would necessitate a comprehensive ventilation and climatic survey of the mine.

7.4 Sustainability Considerations

Many factors contribute to the core fundamentals of sustainability. Cultural responsibility to sustainability and maintaining the environment in a safe and healthy condition lends credibility to mining operations with extensive mineral reserves that could potentially lead to strategic economic viability. Positioning a mine operation with lower capital expenditure and lower operating expenses will provide long-term economic sustainability through uncertain economic times. Innovative use of the environment and responsible care of natural resources available at the mine site will inevitably lead to a sustainable mine.

Regulations must be reformed to allow the use of ammonia for Canadian or US mining operations. The idea of replacement by continual recirculation of low-grade refrigerant vs. the use of a regenerative coolant is uneconomic.

7.5 Revolutionary Cooling System Designs

Harvesting energy during favorable natural conditions is the core concept of sustainable energy system designs. Using the cold of wintertime to cool down refrigerant in the most cost-effective method possible, and storing the chilled refrigerant until summertime. Alignment with ideas and the pursuit of effective sustainable energy plans will save millions of dollars in both capital and operating expenses, while reducing GHG emissions.

By definition, the application of energy efficient ventilation to this arrangement will need to consume the least amount of energy possible. Slow moving airflow directed around the propylene glycol storage tanks will provide the maximum availability for negative heat exchange between the cold air mass and the significantly warmer tanks of propylene glycol mixture. In order to maintain low airflow velocities, low pressure fans are being specified for this cooling system type.

8. Propylene Glycol Storage Reservoir

A new design for a closed refrigerant bulk air cooling system employing propylene glycol as the refrigerant is presented as the main design topic of this dissertation. Given that a deep and hot mine will need to be considered safe and productive, a cost-effective cooling system is desired in order for the mining operation to be considered sustainable. For underground mines at northern latitudes, cooling applied to fresh air is only required 3 to 4 months of the year. During the rest of the year, the ambient atmospheric conditions could be harnessed for use at a later time. Storing the cooling potential during the winter months is what this new design is all about.

The basis of this sustainable design uses very cold ambient air which is circulated around galvanized steel refrigerant reservoir tanks. The propylene glycol reservoir tanks are arranged in a concrete walled pit, or tank farm, excavated in bedrock. During the coldest months, the tank farm will be exposed to the open air. As the seasons change the tank farm will be covered with insulation to maintain the maximum cooling potential for use during the warmest months of the year.

The most difficult part of the construction phase is the tunneling of a subsurface conditioned airway from the bulk air cooler to the operating vertical shaft. This was done without disruption of the hoisting of the workforce and material or skipping of ore in the shaft.

The tank farm will be constructed in close proximity to the fresh air decline, near the main intake shaft. The chilled propylene glycol is circulated through a closed cooling system using heat exchanger plates to directly cool fresh air as it passes over the heat exchanger plates. Multiple tanks are housed in the tank farm and only one tank is employed at a time. Pressurized supply and return refrigerant tanks and all circulation plumbing infrastructure will be completely insulated. In this way the stored cooling potential will be maximized and not diluted with spent refrigerant.

8.1 Site Design

The majority of fresh air delivered underground through the production shaft typically passes through a decline tunnel, or plenum, as depicted in Figure 7, which intersects the fresh air shaft between 50 and 75 meters below the shaft collar. The cross-sectional area of the fresh air decline drift closely approximates the effective cross sectional area of the fresh air shaft. The fresh air shaft is outfitted with piping and conveyance for workers that must be kept warm in the sub-freezing winter atmospheric conditions.

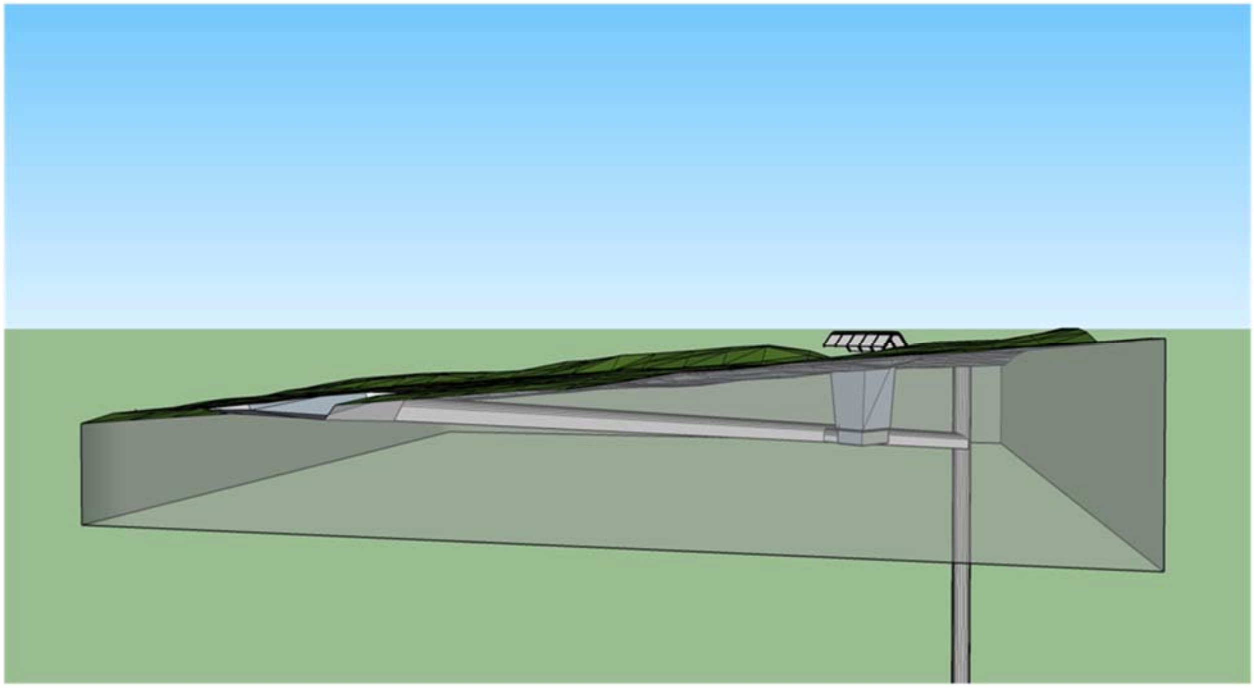

Figure 7: Site plan of Propylene glycol Reservoir with Fresh Air Decline and Shaft

Most importantly, the upper section of the shaft must be kept above freezing to avoid cracking and subsequent caving failure of the shaft infrastructure surrounding vital collar installations. In order to supply significant amounts of fresh air required by modern highly mechanized mines, during winter, fresh air must be heated prior to entering the fresh air shaft. The location of the bulk air heating and cooling infrastructure (e.g. direct heaters and cooling heat exchangers) are constructed in the fresh air decline leading to the intake shaft.

8.1.1 Tank Storage Pit Design Details

The excavated pit where the tank storage is located houses multiple tanks and various infrastructures necessary to supply cold propylene glycol to the cooling circuits as shown in Figure 8. Some of the required equipment include pressurized tanks for supply of cold propylene glycol and receiving propylene glycol that has passed through the closed heat exchanger plates, pumping circuitry, thermostats, automation controls, manifolds and valves. Piping will be sufficiently insulated to minimize heat exchange within the tank storage pit and between the tanks and heat exchangers located in service tunnels.

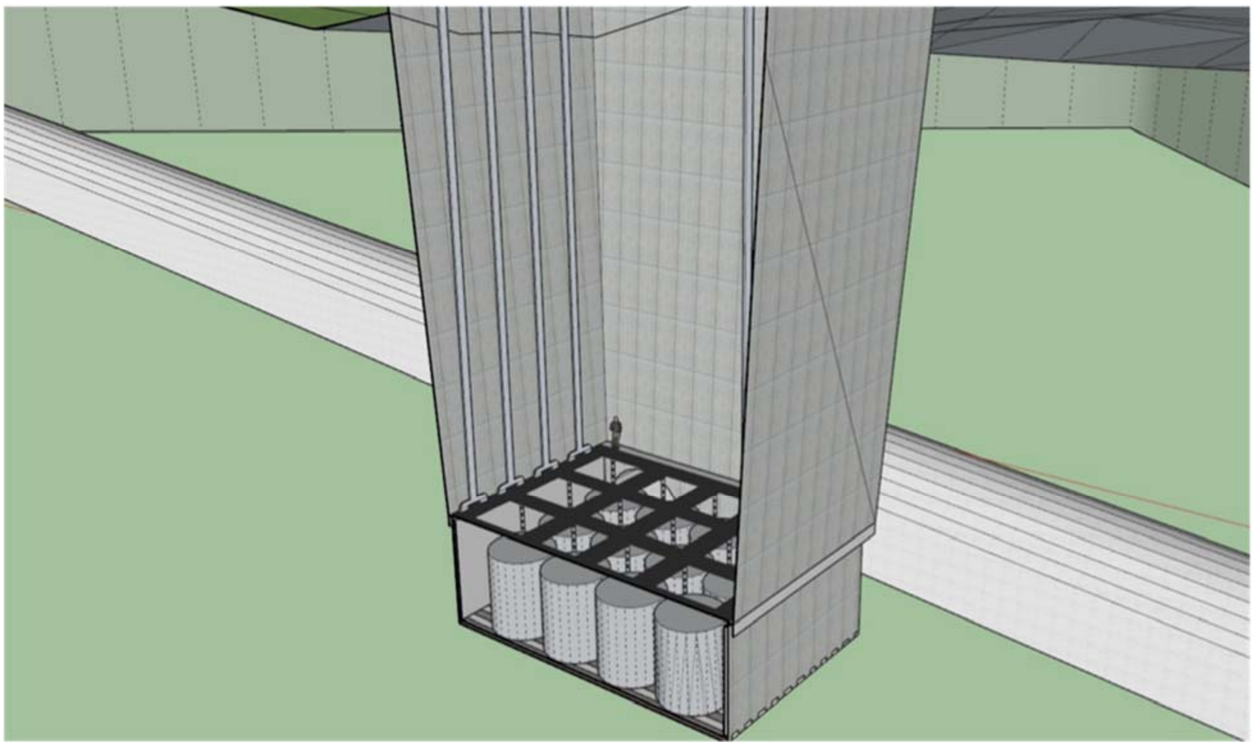

Figure 8: Cutaway detail of Propylene glycol Reservoir Storage pit and walls in relation to fresh air decline.

The entire tank storage pit will be covered by expansive shade structures on the surface, as depicted in Figure 9. Every effort should be given to keep direct sunlight from affecting the temperature of the reservoir tanks. Multiple layers of shade cloth will be installed on the south facing side of the pit. The inner shade cloth will be pulled down to near the finished ground level, well outside the concrete pit walls. A removable waterproof cover, erected under the shade cloth, will cover the entire tank storage pit to maintain a dry pit.

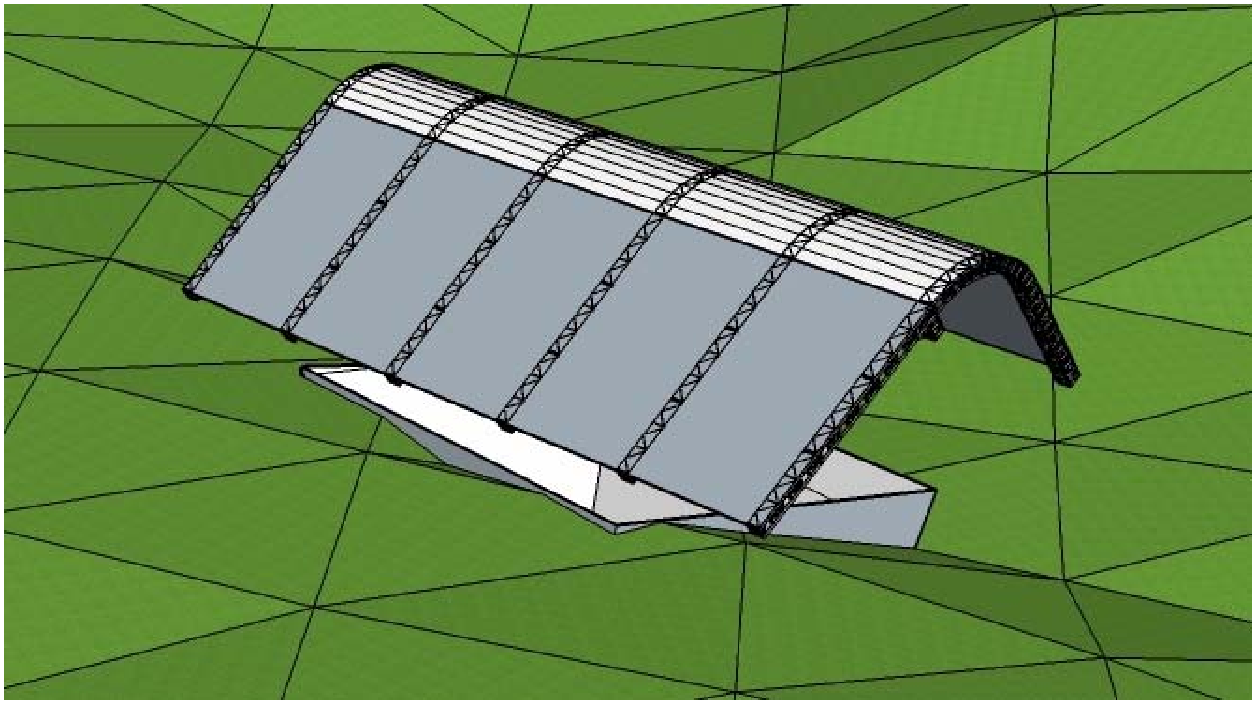

Figure 9: Shade structure covering reservoir pit.

The pit bottom will consist of compacted roadbed gravel with French drains under the gravel leading to a sub-level sump to provide safe capture of rainfall during construction or unexpected leaks of the glycol/water mixture during operation and maintenance. Above the compacted roadbed gravel, cast-in-place concrete piers will run the entire length of the pit, as shown in Figure 10. Reservoir tanks will sit on the concrete piers to allow cold air to circulate completely around the tank bottoms. In the open spaces among tank bottoms, between the concrete beams, multiply bonded layers of brattice will be installed with reinforced openings at key locations to help circulate cold air among and under the tanks during periods of refrigerant cooling.

Figure 10: Cutaway diagram of Propylene Glycol Storage Reservoir with man standing between cast-in-place concrete piers for scale reference.

Additional covering along the tops of the reservoir tanks will provide a boundary layer for the ventilation of cold air circulating the propylene glycol reservoirs. The upper tank farm cover will be constructed of multiple layers of an impervious layer, similar to brattice used for temporary ventilation structures. The brattice material will be connected to the underside of a super structure that will serve as support of the warm season insulation layer. The upper ventilation boundary cloths will be sufficiently bound together to maintain a relatively airtight layer.

8.1.2 Reservoir Control and Maintenance

As cooling demand comes online, each tank will be brought into service sequentially. Manifold valves for propylene glycol supply and return will be controlled by automated software. The monitoring and control architecture will be connected to a Human Machine Interface (HMI) that will provide both active control and real-time feedback of the pumping and thermistor networks. Override of the automation software will include an integrated set of recorded profiles to allow the operator fine tuning of the refrigerant supply.

Remote thermistor arrays will be installed in each reservoir tank to monitor differential propylene glycol temperatures. The thermistor feedback will provide data to the control logic to determine the sequencing of valve activations. Since the need for cooling will not be required continually, the control logic will need to incorporate feedback from atmospheric monitoring stations. Spent refrigerant monitoring will provide temperature and pressure feedback as indices to the control logic. Similarly, these two indices will be gathered from the supply side to help balance out the logical control system.

Maintenance of the tank farm will include application of insulation as the ambient temperature warms beyond the cooling capacity. Insulation would also be applied after the reservoir tanks have reached an acceptable chilled temperature. The insulative layer would lay directly on a maintenance platform depicted in Figure 11. Inversely, as the seasonal climate changes to primarily cold the insulation will be removed and stored in safe keeping. Having the tanks open to the atmosphere will allow maximum cooling potential during the winter months.

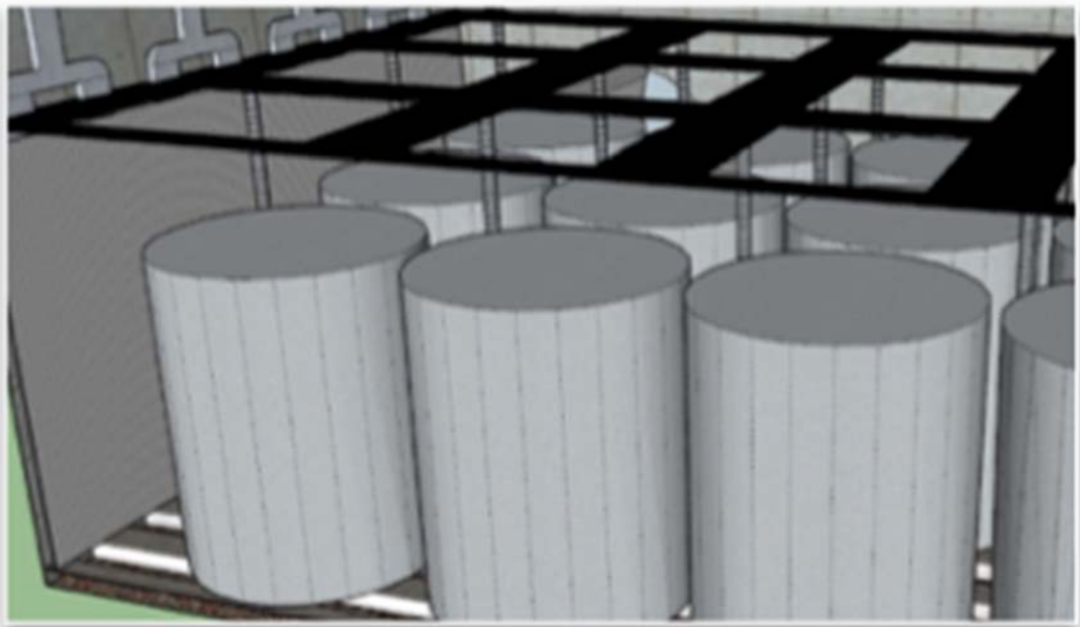

Figure 11: Detail cutaway of Propylene glycol Storage Reservoir pit showing tanks resting on concrete piers with maintenance platform suspended above tanks on steel posts and galvanized exhaust plenum with exhaust ducting connections.

The reservoir tanks are assumed to experience brief periods of temperature rise and falls, along with temperature stasis, at the boundary layer. These temperature variations are not consistent due to daily changes in ambient atmospheric conditions. Additionally, variations in tank temperatures are assumed as the warmed refrigerant becomes chilled due to the negative heat exchange with the pit walls. In the larger picture, the tanks should get colder and these temperature variations of the propylene glycol will become smaller and shorter-lived the longer the cold snaps last. Initially, the theory is that within two months of low temperatures averaging at or below -15° C (5° F) the reservoir tanks will have reached this average. Selective cooling sessions will allow the mean reservoir temperature to reach -20° C (-4° F), which is the target reservoir low maintenance temperature.

Procedures for regular inspection of piping for leaks will need to be formalized. Monitoring of the sump level and temperature below the propylene glycol storage reservoir will aid in detection of leaks and eventual piping network failures. Additional maintenance of pumping circuits will need to be performed during periods when the cooling system is inoperative. Standard operating procedures should not be so rigid that opportunities for continual improvement are lost. Moreover, onerous maintenance should be periodically evaluated by an independent contractor to ensure that new technologies or methodologies may be integrated seamlessly.

Special regular maintenance tasks will be required in order to keep the specified heat exchanger plate arrangement, see example in Figure 12, in top operating condition. First, cleaning of the plates will need to be performed annually so that dust or other airborne constituents don’t hinder the exceptional heat exchange capacity of the clean stainless-steel nature of the plate heat exchangers. Secondly, containment fencing surrounding the plate heat exchangers will need to be routinely cleaned of airborne debris such as plastic bags or leaves that regularly foul the fresh air supply.

8.1.3 Heat Exchanger Discussion

Based on discussions with industry leading professionals concerning specification of highly efficient air conditioning heat exchange systems, design alternatives favor the use of plate heat exchangers. These systems are typically designed, and project managed during the build-out phase by industrial contracting mechanical engineering firms specializing in customized design-build HVAC systems, along with systems considered ancillary to the specified HVAC systems. Figure 12 shows an example gasketed plate heat exchanger array.

Figure 12: Example: Gasketed Plate Heat Exchanger array.

8.1.4 Advantages and Disadvantages of Plate Heat Exchangers

Advantages:

- Plate heat exchangers are the most efficient design style, allowing for maximum heat transfer between the refrigerant and the warm air being cooled down

- Evaporative coolers require less maintenance than closed circuit cooling heat exchange system components
- Tube and fin heat exchangers require less maintenance cleaning than plate heat exchangers
- Plate heat exchangers pick up less moisture from the atmospheric airflow than tube and fin style
- Tube and fin heat exchangers add less airflow resistance than plate heat exchanger arrangements.

Disadvantages:

- Evaporative coolers saturate the intake airflow. A prime consideration when the intake must descend more than 1500 meters, since the compression of water vapor in the air (auto-compression) is the main source of natural air heating in deep mines.
- Closed circuit heat exchange system components exposed to atmospheric air must be cleaned of dust and debris as part of regularly scheduled maintenance to maintain cooling system efficiency
- Plate heat exchangers add the highest resistance to the intake airflow.

8.1.5 Development of Proof of Concept Models

Scaled models provide insights and show weaknesses through pilot plant implementations. Development of dry run lab experiments will show how different components react at very low temperatures. Much can be learned through the fine tuning of these small scale experiments. Control logic can be developed as the requisite piping network and various valve solenoids are put to the test.

Alternative design concept arrangement evaluations should be an ongoing process during the development of the proof of concept models. Computer models should be simulated and kept up to date with the current development of alternative concept configurations. These models will help guide experimental procedures and lead to a more cohesive development during inception of the proof of concepts.

8.1.6 Avenues to Advance Heat Exchanger Development

Industry partners should be sought out to fund research of this advanced heat exchanger development including mining operations with refrigeration requirements. Mechanical engineering consultants and HVAC contractors along with refrigeration manufacturers should also be approached to assist in research funding. Government funding for research could come from sources such as the Center for Disease Control-National Institute for Occupational Safety and Health (CDC-NIOSH), National Renewable Energy Laboratories, or the Department of Energy (DOE). Lastly, manufacturers of propylene glycol could also support research for this groundbreaking research in renewable energy.

9. Estimation of Required Storage Reservoir

Many special considerations must be taken into account when determining the required refrigerant reservoir size for any hot and or deep mining operation. Geographical location, elevation, production rate and seasonal atmospheric temperature variations will account for much of the primary accountable consideration that play into sizing a fresh air refrigeration system for a mine of any significant size. Many variables must be estimated or assumed to aid in the sizing of an appropriate heat exchange system.

Basically, each pass of the chilled refrigerant through the cooling system reduces the overall system capacity. The underlying assumption of the proposed stored chilled refrigerant system, that warm airflow passing over the heat exchangers will reduce the temperature of the intake air by 15° C for a corresponding assumed rise in the refrigerant temperature of 2.5° C.

The volume of refrigerant to accomplish this corresponding temperature drop is roughly equivalent to the ratio of mass to heat capacity for either the airflow or the refrigerant. This is to say that the mass of air is taken as roughly 1.2 kg/m^3 and the mass of the propylene water solution is roughly 1004.3 kg/m^3 and also the ratio of heat capacities is about 3.54 with air over the propylene/water refrigerant solution. The combined heat exchange potential based upon the mass/heat capacity relationship shows that a ratio of over 1:2,960 exists between each kilogram of stored glycol refrigerant to the fresh air cooled during the refrigeration process.

Two design parameters must be established before a system can be properly estimated: (1) expected refrigerant throughput temperature drop to achieve baseline cooling performance, and (2) expected operating hours. These two variables will determine the sizing for refrigerant reservoir capacity, which will be demonstrated as an empirical engineering exercise. Each of these items will be discussed in the following sections.

9.1 Determination of Refrigerant Requirement

A stored refrigerant can presumably preform multiple service operations without appreciable loss of potential thermal energy during its life of service. This means that when a refrigerant liquid goes from -2.5 °C to 0.0 °C during a heat exchange process, an equivalent amount of potential thermal energy will be transferred as when the liquid transforms from 12.5 °C to 15.0 °C. This idea is a central assumption to the capacity analysis for the heat exchanger storage reservoir. Assuming the refrigerant can be chilled down to -4.5 °C remaining viable up to 2.5 °C, the intake airflow can be chilled down to say 3.0 °C, yielding 7 heat exchanging passes through the heat exchanger arrays.

9.2 Expected hours of operation

In very many design locales, the need for bulk air cooling is not perpetual but seasonally and even varies during daily operations. Sometimes a mine can operate fully with a minimal cooling application, while other times the same operation struggles to maintain acceptable temperature conditions underground. Taking a clear advantage of these regular background climatic variations can directly reduce cooling needs by simply operating a mine at peak capacity only during cooler seasonal atmospheric temperatures. Extended infrastructure development and rigorous cooling system maintenance activities can be scheduled during the warmest months in order to reduce the heat load applied by mining activities that require the maximum heavy equipment employment.

Every mining location with expected cooling needs should have surface atmospheric conditions monitored hourly for successive years prior to requiring cooling applications. This atmospheric monitoring will aide operators in development of acceptable operating procedures, based upon hourly operational expectations for the air-cooling system. A statistical model of expected low and high daily wet and dry bulb temperatures should be developed from recorded atmospheric monitoring station observations. The longer the data available for the model the better. Factoring in historical daily high and low readings will help improve the general statistical atmospheric temperature model.

The main output of the statistical atmospheric temperature model will be the 97.5% mean wet bulb temperatures (ASHRAE, 1997) bracketing acceptable working conditions. This refers to the upper and lower temperature design limits that comprise 97.5% of all yearly hours. These are the recognized limits for developing heating or cooling systems, as established in the United States by ASHRAE for human occupation and industrial or commercial activities.

This means that a heating or cooling system will normally be designed to accommodate 97.5% of temperatures experienced during a representative year.

Mechanical engineers developing heating and cooling duties for large buildings use the same design principle. Designing a heating system to successfully heat a structure to 22° C when the atmospheric temperature is -35° C may benefit the occupants for only two days every five years. Designing systems capable of providing a 57° C (-35° C to 22° C) temperature gain for the intake air requires a much larger burner and intake air capacity than say a system capable of providing a 47° C gain at maximum capacity.

The expected return on performance is only expected to be an advantage for several working hours in any given year, at the expense of an overrated heating system. The overdesigned system will still need to operate at a higher output requirement, even under favorable atmospheric conditions, during all times of heating or cooling system operation. This results in much higher capital and operating costs during the life of the mining operation.

9.3 Propylene Glycol Storage Reservoir Estimation

The theoretical mine design used for the calculation exercise has ventilation demand psychrometric parameters as defined in Table 1, corresponding to the 95th percentile of historical summer atmospheric conditions for Sudbury, Ontario. Inlet and outlet airflow wet bulb temperatures, along with the barometric pressure, are the design parameters that are used to determine the heat transfer (ASHRAE, 1997) (using Sigma Heat, the heat transfer capacity expressed in kJ/kg (kilojoules per kilogram)) required to lower the design air mass to the target intake fresh air temperature. Two equations presented below can be used to determine the required cooling duty using design atmospheric parameters.

Table 1: Airflow psychrometric design conditions

Barometric Pressure (kPa)	Airflow Density (kg/m³)	Airflow Quantity (m³/s)	Air Mass flow (kg/s)	Inlet Wet Bulb Temperature (°C)	Outlet Wet Bulb Temperature (°C)
101.575	1.187	469.72	557.56	18.0	3.0

Sigma heat, from psychrometric data:

$$S = \frac{\left(\left(1000(2502.5-(2.386T_W))*\left(0.622*\frac{610.6e^{\frac{17.27T_W}{237.3+T_W}}}{1000P_B-610.6e^{\frac{17.27T_W}{237.3+T_W}}}\right)\right)+(1005T_W)\right)}{1000} \tag{9.3.1}$$

where S = Sigma Heat, kJ/kg

T_W = Air Mass Wet Bulb Temperature, °C

P_B = Barometric Pressure, kPa

Cooling duty, from calculated Sigma heats, using air mass flow:

$$q = m_a(S_{in} - S_{out}) = 557.56(14.68 - 49.81) = -19{,}558.78 \tag{9.3.2}$$

where q = Cooling Duty, kW (kJ/s)

m_a = Air Mass Flow, (kg/s)

S_{in} = Inlet Air Sigma Heat, (kJ/kg)

S_{out} = Outlet Air Sigma Heat, (kJ/kg)

The second calculation indicates that 19,559 kW would be required to cool the requisite 469.72 m³/s from 18.0 °C to 3.0 °C wet bulb temperature. The accepted industry lowest fresh air wet bulb temperature to eliminate the chance of concrete failure of shaft collar support structure is 3.0 °C (Fava, Millar, Anderson, Schafrik, O'Connor, Allen, 2012).

The theoretical propylene glycol storage reservoir is designed with 12, 4-meter diameter by 8-meter deep tanks, yielding a reservoir total 1206.37 m^3, or 1,211,559 kg propylene glycol. As previously stated, the heat exchange rate of 1:2,960 per kg exists between the propylene glycol ($C_3H_8O_2$) and modeled atmospheric air for each 15.0 °C of air temperature change in the airflow per hour. Assuming the reservoir propylene glycol has 7 heat exchange cycles, the operating hours that 18.0 °C air would be chilled to 3.0 °C is determined with the following calculation:

$$\frac{1{,}211{,}559\ kg\ C_3H_8O_2\ x\ 2{,}960\,\frac{kg\ air}{kg\ C_3H_8O_2\ \cdot cycle}\ x\ 7\ cycles}{557.56\,\frac{kg\ air}{s}\ x\ 3600\,\frac{s}{hr}} = 5{,}002.65\ hours$$

Given a deep and hot shaft serviced mine would see fresh air wet bulb temperatures exceeding 18.0 °C approximately 5% of the time, the estimated 5,002.65 operating hours might just completely provide the required cooling duty without supplemental refrigeration systems.

10. Evaluation of Mine Cooling Systems

The concept for the propylene glycol cooling system was born during a survey conducted while on site at a mine in Ontario which was evaluating two different types of cooling systems to supplement the existing renewable mine air cooling system (Acuna and Lowndes, 2013). The mine was in the process of advancing the depth horizon of development operations when the capacity (Twort, Lowndes, Pickering, 2009) of the existing mine air cooling system was expected to be overcome by thermal conditions encountered during development mining activities. An evaporative air cooling system was in process of being constructed but would not be ready until the following summer. The mining operation therefore decided to lease temporary supplemental air cooling which was to be provided through a mechanical refrigeration system.

Prior to the commissioning of the temporary air cooling system, a climatic survey of the existing mine ventilation network was conducted down to the point where the supplemental air cooling would be mixed with fresh intake airflow that had been cooled by the renewable mine air cooling system. Following the commissioning of the temporary air cooling system, the same fresh air network was surveyed to the mixing point. The following summer the same climatic survey was conducted following the supplemental evaporative air cooling system commissioning. It is important to note that the atmospheric conditions were not exactly the same during each climatic survey, but barometric pressure and temperatures (dry bulb and wet bulb) were very similar.

10.1 Climatic Survey Ventilation Network

During each of the three climatic surveys conducted in the supplemental cooling intake airflow network, the same air path was followed to the aforementioned mixing point. Fresh air from the open atmosphere courses into an access ramp, acting as a plenum, into the main intake shaft. The shaft descends over 2100 meters and connects to an underground ramp. Fresh airflow joins this ramp from upper mine workings that get fresh air which passes through the renewable air cooling area. This air path is described with physical properties of the 19 ventilation network branches as listed in Appendix A.

The air branch network was measured and stations marked by the client's surveying team before the climatic surveys began to ensure precision. The climatic surveys were conducted using a TSI Alnor RVA501 anemometer, a Vaisala HM 40 R/H Temp Probe and a Druck DPI740 precision barometer. Each piece of survey equipment was within the National Institute of Standards and Technology (NIST) traceable calibration certification period of 2 years, therefore considered accurate for scientific observations.

In order to determine the cooling capacity of the fresh airflow, three branch properties of the thermal network listed in Appendix A are used to calculate heat added to (or subtracted from) the airflow passing through the network. These three branch properties are virgin rock temperature (VRT, °C), geothermal temperature step change interval (Geo. Step, m/°C) and age (in days) since the mine entry was excavated. The remaining physical air branch properties table of Appendix A describe the geometry of the ventilation network.

10.2 Climatic Survey and Derived Data

During each of the three climatic surveys, airflow parameters which consist of dry bulb and wet bulb temperatures (°C) along with barometric pressure (kPa) and airflow velocity (m/s) were measured at the same location in each of the 19 air branches. Airflow quantity (m^3/s) was calculated by multiplying the cross-sectional area (m^2, see Appendix A) of the air branch at the observation location by the recorded velocity.

Climatic data from the three surveyed air cooling arrangements was used to simulate cooling capacity of the fresh intake airflow. The available cooling capacity of air at a survey location is estimated by calculating Sigma heat (S, kJ/kg - equation (9.3.1)) using the wet bulb temperature (t_w, °C) and barometric pressure (P_B, kPa). The wet bulb temperature plays the more significant role when determining Sigma heat of the airflow. Data gathered and calculated from each of the three climatic surveys in shown in Appendix A.

10.3 Evaluation of Climatic Survey Data

To assist performance evaluation of the two mine air cooling systems, two graphs were developed to show the magnitude of change in observed wet bulb temperature (t_w, °C) and calculated Sigma heat (S, kJ/kg see equation (9.3.1)) along the climatic survey pathway as a function of climatic survey pathway. Figure 13 shows the derived Sigma heat parameter for the no cooling, evaporative cooling, and mechanical cooling configurations. These graphs follow the climatic survey path listed in order from left to right, with the survey station labeled along the x-axis.

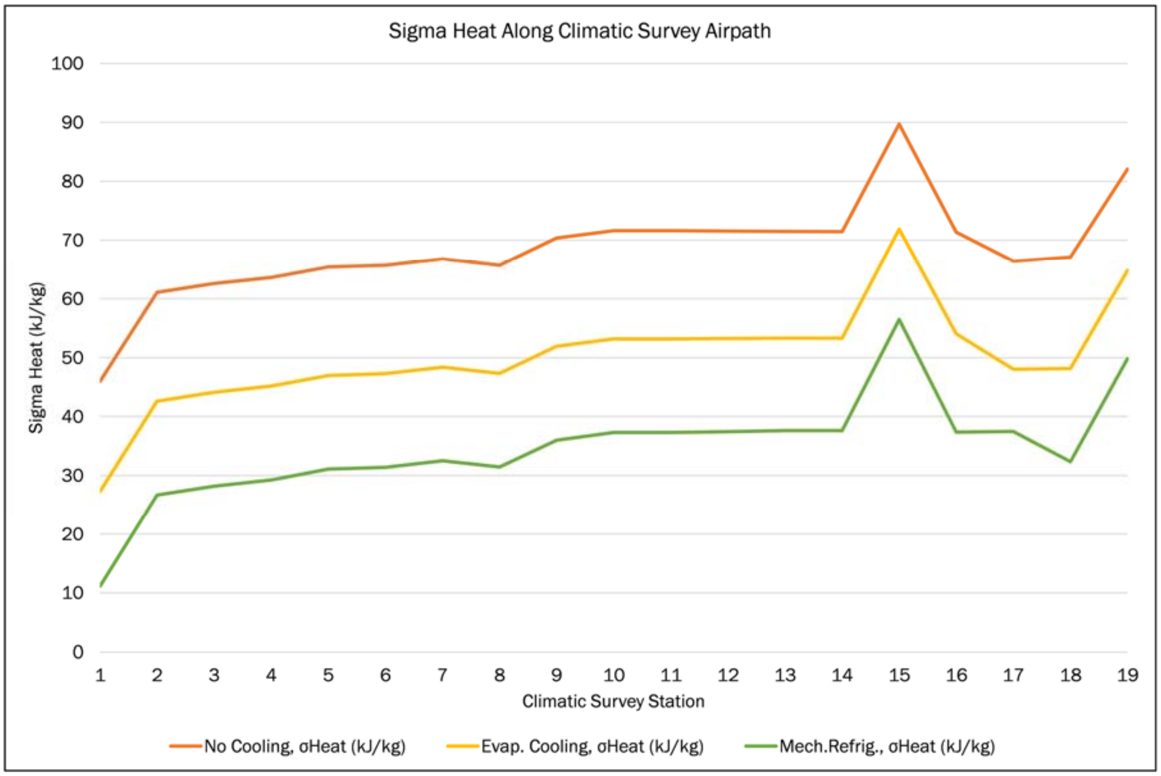

Figure 13: Calculated Sigma heat from climatic survey data.

The graph shows a direct correlation between the cumulative airpath length and the Sigma heat of the intake airflow, as the fresh air mass flow descends into a deep and hot underground mine. Using the concept of Sigma heat, thermal additions or losses from an airstream can readily be quantified from psychrometric observations (McPherson, 1993). Spikes in Sigma heat along a climatic survey network path easily identify heat sources or sinks.

Hence, lower relative Sigma heat values have a greater cooling capacity, compared to an air mass with higher wet. Therefore, it makes good business sense to provide the lowest reasonably achievable Sigma heat when delivering fresh airflow to provide maximum dilution potential of heat contamination in the underground environment.

11. Modeling the Storage Reservoir Chill-down Process

Proper determination of boundary conditions for the tank storage pit is a challenge in itself. The representation of heat exchange amongst the cold winter air mass and the steel tanks, which serve as the storage reservoir, is a complex time dependent ventilation modeling exercise. Understanding the physical nature of cold airflow circulating smooth walled steel tanks filled with propylene glycol is surely no easy or straight forward exercise. The ventilation model (see Figure 14) for this exercise was developed in Ventsim© Design 5, using the thermal flywheel effect simulation style, and is depicted in Figure 15 in the winter "recharge" mode. An additional summer "coolth" mode is modeled later once the heat exchanger system design is known.

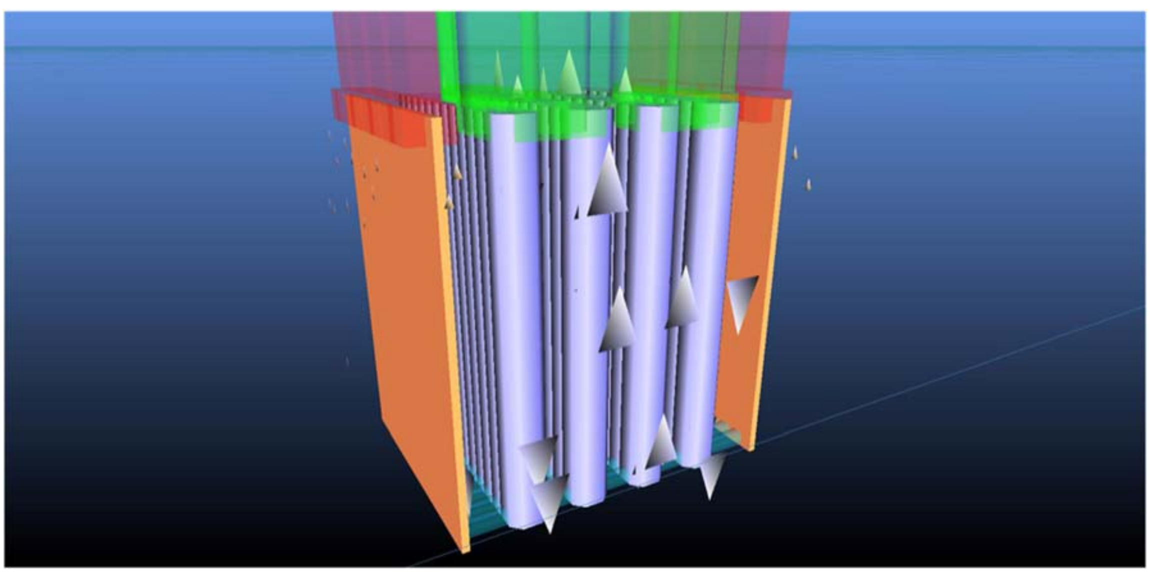

Figure 14: Thermal ventilation model of Propylene Glycol Reservoir Storage facility.

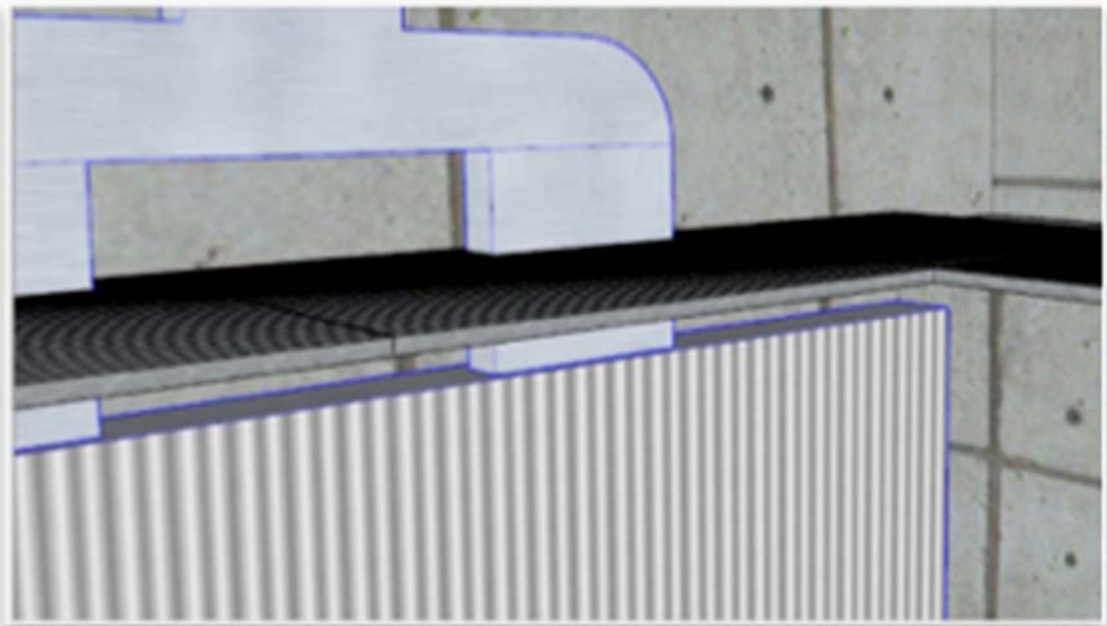

Figure 15: Exhaust ducting detail, showing plenum connections below maintenance decking.

11.1 Model Physical Layout

Equivalent areas are used to determine representative airway cross-sectional areas within the reservoir pit. These areas are determined by the physical layout of the storage reservoir tanks in the finished pit and the diameter of the tanks. Since air cannot flow through the tanks, the remaining area in the pit can be reduced into 48 equivalently sized vertical airways designated as thermal mixing intake airways. These serve to represent the winter cycle heat exchange boundaries as the mass of cold air removes heat from the propylene glycol storage tanks while airflow circulates around the reservoir tanks.

The underlying assumption of the entire ventilation modeling exercise is that warm atmospheric air flows down into the pit due to the natural ventilation pressure (NVP) and circulates in the pit, mixing with air directly in contact with the tanks before circulating underneath the tanks. Air is exhausted up the plenum space on the pit ends from under the reservoir tanks, into manifolds leading to vertical ducting and flows upward to the atmospheric sink at the surface. It is assumed that exhaust fans are connected to the end of each pit ventilation exhaust duct pathway to generate the required pressure. This exhausting, negative pressure airflow arrangement will not directly add heat to the reservoir storage environment.

Intake airways are designated as fresh air and connect directly to the atmosphere as shown in Figure 16. Fresh airways are divided into 24 equivalent branches with a cross sectional area of 11 square feet each and subject to daily temperature variations, specified through the thermal flywheel conditions of the simulation application.

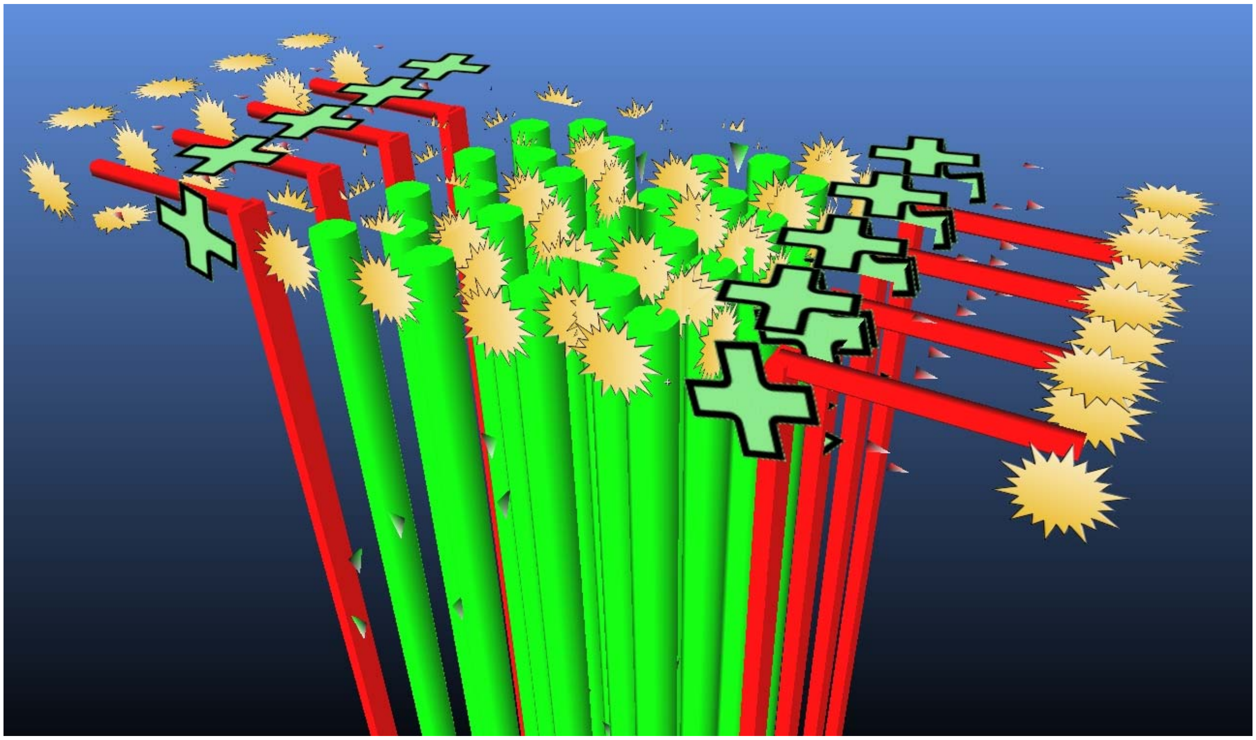

Figure 16: Fresh and Exhaust Fan Surface Branches

Two levels of mixing within the pit amongst the reservoir storage tanks are defined. These two areas are segregated into 114 horizontal above, and 48 vertical airways laterally surrounding the steel tanks. Figure 17 shows the upper horizontal airways with a cross sectional area of 5.5 square feet and are multiply interconnected to the fresh air branches, which serve as the atmospheric heat sink connections. The fresh air mixing branches are assigned thermal properties of dry air. The 48 vertical airways surrounding the tanks are assigned the thermal characteristics of anodized steel. These 48 airways represent the interface between seasonally cold winter air and warm propylene glycol and are assigned a cross sectional area of 5.5 square feet.

Additional thermal mixing happens within the equivalent airflow areas below the tanks, within the area between the concrete piers. This type of heat transfer involves thermal energy exchange among reservoir tanks, glycol in the tanks, concrete piers upon which the tanks rest and the airflow passing between the tanks and concrete piers.

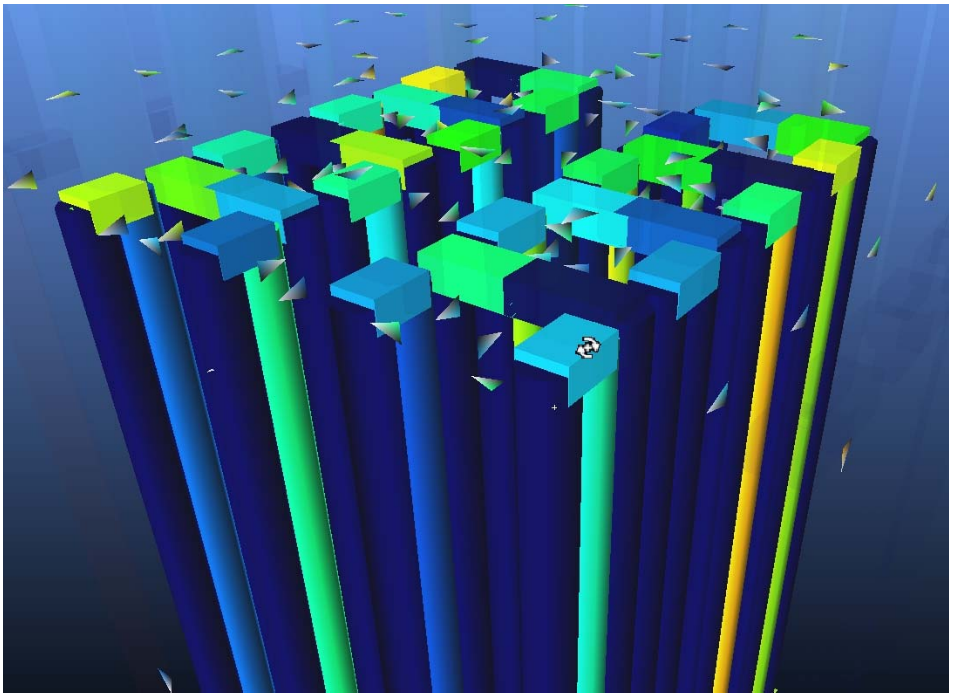

Figure 17: Horizontal Upper Mixing and Vertical In-Pit Mixing Branches displaying predicted wet bulb temperatures.

Twelve parallel airways, shown in Figure 18, divided into five equivalent branches, are defined as the airways below the tanks. Each of these 12 airways have a cross sectional area of 4 square feet and are assigned two different sets of thermal coefficients, one for the side contacting the reservoir tanks and the other three contacting the concrete piers. This discretization represents a simplified modeling condition, since a truly complex interaction is actually happening here with a porous floor of compact gravel surrounding the French drains in the bottom of the reservoir pit.

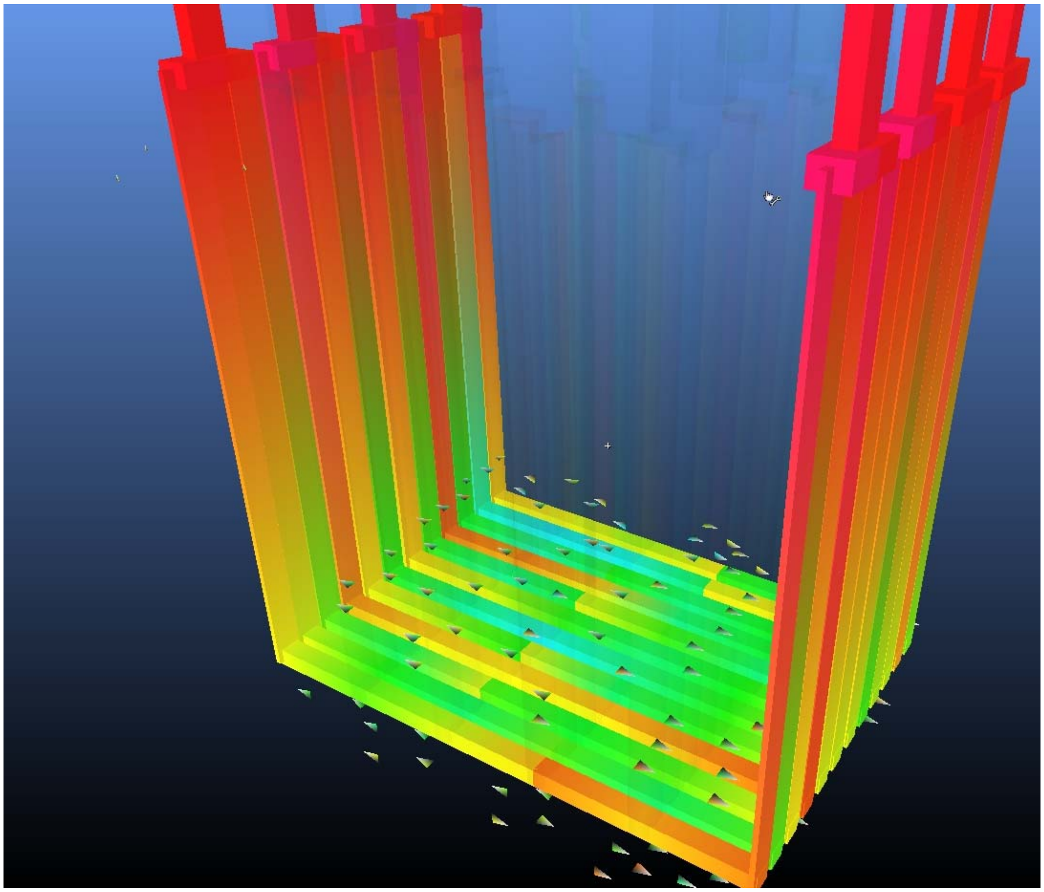

Figure 18: Horizontal Sub-Level and Vertical Equivalent Plenum End Panel Branches

The lower horizontal airways connect directly to 12 equivalent area airways, each with a cross sectional area of 1.5 square feet in which air flows up along the walls on each end of the reservoir pit. These airway branches have corrugated anodized steel on one side and concrete on the other. Once again, a simplified model condition is representing a more complex interaction of the airflow passing over the cast in place concrete pit walls and steel boundary of the pit walls plenum.

Modeling shows that the velocity of the airflow is the main component of heat exchange capacity between surfaces directly contacting the airflow. If the airflow velocity is too low, laminar flow patterns can form and density separations will inhibit effective heat transfer from the glycol in the reservoir tanks to the airflow potentially stalling and reversing airflow in branches or causing localized recirculation. However, should velocity of the airflow become too high, the cold air mass will not allow appropriate heat exchange to the circulating cold air mass from the warmer anodized steel reservoir tanks.

11.2 Thermophysical Properties of Model Elements

In order to determine heat exchange amongst the different elements of the thermal model, thermodynamic properties for each material type need to be defined for all model elements of the cooling system. Air is the main constituent to facilitate the heat transfer process of the propylene glycol during the cooling of the refrigerant reservoir. However, the air has the lowest density component in the system.

This means that a large mass of air will be required to chill the tanks of glycol down to the target low storage temperature. Since air is in direct contact with all other model elements, density, specific heat, thermal conductivity and thermal diffusivity are defined for each interface between the different model element types. These thermal coefficients are shown in Table 2 and assigned to each respective model element in the Ventsim© model.

Table 2: Thermal coefficients for model elements

Thermophysical Properties for Materials in Reservoir Cooling Model					
	Units	Air	Anodized Steel	Concrete	Propylene Glycol Mixture
Density	lb/ft^3	0.0797	150	144	66.7
Specific Heat	$BTU/(lb_m \cdot °F)$	0.24028	0.12	0.18	0.85
Thermal Conductivity	$BTU/(h \cdot ft \cdot °F)$	0.01407	26	0.17	0.18
Thermal Diffusivity	ft^2/hr	0.73471	1.44444	0.00656	0.00317

Furthermore, the Gibson aging function is used in determining the quantity of heat flux (positive for heating and negative for cooling) between model elements. The complexity of the ventilation model could become substantial if simplification measures are not applied. Each model element has therefore been given the minimum age possible, to invoke the maximum heat exchange possible between all model elements.

11.3 Baseline vent model description

Due to the nature of the low-pressure ventilation system being recommended in the described cooling arrangement, care has been given to maintain the intended direction of airflow in the model, especially surrounding the reservoir tanks. Once boundary conditions have been defined for the physical model, assumed time steps describe the atmospheric conditions for one week's time with linear temperature changes. At the end of each time step the residual heat exchange from the pit mixing branches are used as data input for the next time step. During each subsequent time step, the gradual lowering temperature of the seasonal atmospheric condition is represented as a new boundary condition for the fresh air entering the heat exchange simulation.

11.4 Discussion

Extensive modeling work was needed by the initial versions of the storage reservoir chill-down process model. Simulations of the firsthand models did not return results that would be congruous with what one would know from estimation by time in the field. Real world experience would dictate that micro-mixing climates are developing pressure differential air flows as the colder air will sink and the warmer air surrounding the tanks rises.

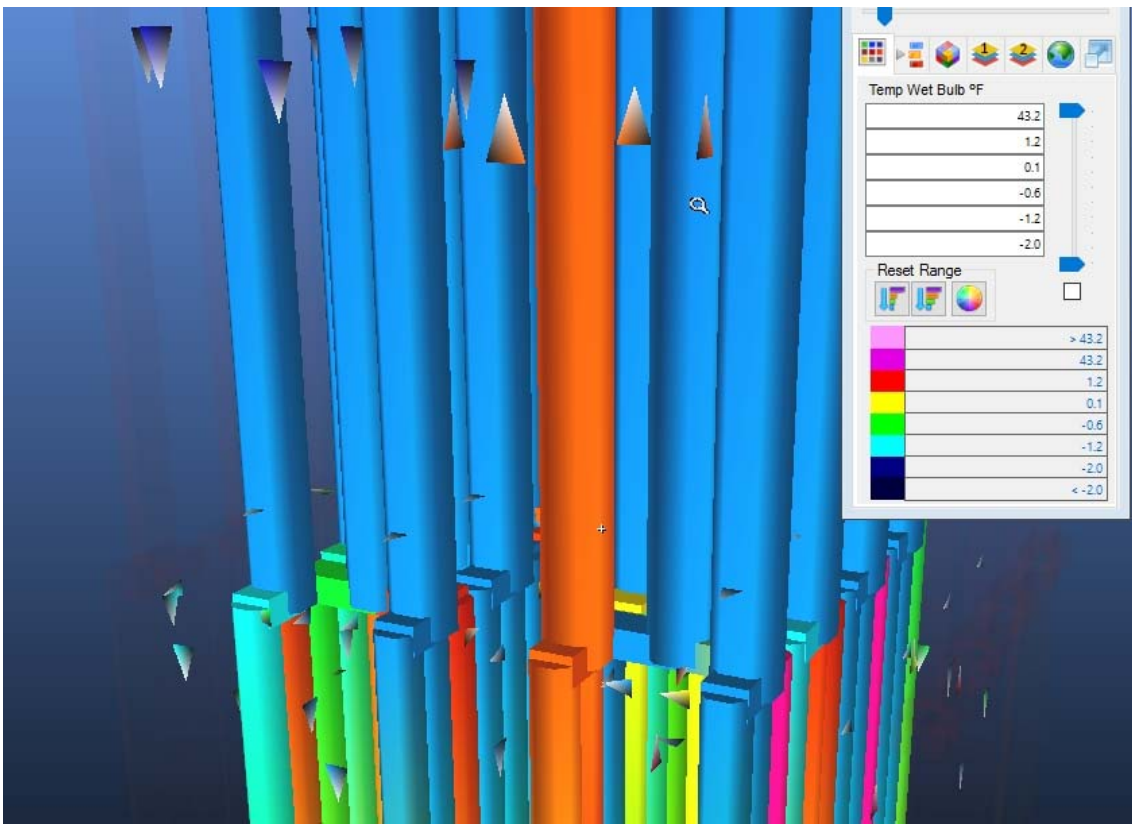

Figure 19: Problematic Ventsim© thermal model displaying wet bulb temperatures, higher temperature fresh air column in foreground; arrows show reversed airflows

Modeling this freezing environment is an extremely complex scenario. As an airway crosses the boundary into a freezing condition, the resistance will drop significantly. What's really unusual but at the same time interesting is the fact that I can set the airways from and to node assignments, lock the direction of the airflows, and the software will just continue to reset the model network and airflow directions before the airway crosses the freezing boundary condition (see Figure 19). Due to the low-pressure nature of the model conditions some airways tend to have an affinity to reverse airflow direction, which is indicative of three different things.

1) There is inadequate resistance added to the network; the resistance values will vary as storage tank temperatures change. There is currently no method to vary airway resistance with the change in temperature.
2) Heat rising off of the tanks initially is driving a recirculation process with air mixing inside of the pit; this is a very complex simulation scenario and most likely not an intended result of the Ventsim©'s solution algorithms.
3) Some questionable results are given by the ventilation software because of the compressible flow issue with Ventsim© not correctly resolving natural ventilation pressures.

Apparently, events of this nature are trying to show that the temperature can drive some airflow reversals rather easily when low velocity conditions exist. This sets up possible conditions for some serious recirculation.

Presently, it is difficult to analyze the boundary airflow conditions reliably for each of the evaluation time frames using models initially developed in Ventsim©. To assist with analysis, another cooling model was developed in VNet and this model was by nature incompressible flow. The predefined airflow directions remain in the ascribed from/to arrangement. This is much easier to generate a preliminary airflow network as boundary conditions for the thermal model when airway directions are easily described. Perhaps the most accurate method would be to generate several different temperature scenarios and define which airways are allowed to reverse.

There is a considerable infrastructure cost of constructing a pit, which complies with the recommendations listed in Section 8. However, this cost is negligible when compared to the cost of gaining access to a shaft below the collar. A construction crew will already be working on the fresh air decline at shaft access, carefully working around the collar. For this reason, it makes practical sense to simply add construction tasks so that the project incurs no additional mobilization costs or second contractor fees.

11.5 Future Work

Supplying cold glycol harvested on the surface to underground cooling systems is a potential source of immense savings for mines that currently send cold water to hot underground mine workings. Investigation of practical, operable air cooling systems for underground mining should include maximum transfer distance, both laterally and vertically, for chilled propylene glycol transport via low pressure piping networks. Piping should be selected to render the minimum resistance while maintaining thermal shielding.

Considerable capital and operating expense is typically dedicated to coolant piping insulation. If there was one way to eliminate this necessity for insulation of the piping networks, the costs to develop and install this efficient cooling system could be quickly recovered, as it's quite well known that insulating piping networks typically costs 3 times what the piping capital costs, just in labor (Bluhm, Moreby, von Glehn, & Pascoe, 2014). Perhaps selecting a newly innovative piping material could make use of innovative recycled composites. Modeling the piping network will determine empirical values into how far the coolant can maintain effectiveness, which is to say, how much cooling energy can be supplied for a wide range of spot cooler locations.

Investigation of low-temperature polymer concretes used in cryogenics to increase reservoir storage time potential. Ultimately, additional simulations will need to be conducted. Careful estimation of the thermal flywheel effect for the given location will need to be considered during the course of these simulations.

12. Conclusion

Sigma heat is used (section 9.3) to determine the cooling duty required of an air cooling system to deliver cold dry air to a deep and hot underground mine metal for the 95th percentile summer atmospheric condition at the site of the climatic survey. Over 19 MW cooling power would be required to cool the requisite airflow to the lowest acceptable wet bulb temperature. Conservative estimation of a theoretical, renewable air cooling plant delivering a wet bulb temperature of 3.0°C (from 18.0°C atmospheric air) fresh air was determined to provide nearly 5,000 operating hours. Since the 3 summer months are nearly

2,200 hours total, less than half of the assumed 7 propylene glycol reservoir heat exchange cycles could be required to provide that 19 MW cooling.

The conceptual propylene glycol refrigeration system can generate over 19 MW for over 5000 hours, yielding over 97.8 GWh of electrical equivalent. According to the United States Environmental Protection Agency (EPA, 2021), 1 kWh is equivalent to 7.09e-4 metric tons CO_2 gas. This renewable cooling system could offset 69,342 tonnes CO_2 annually.

Climatic surveys described in Section 10 show the significant value of mechanical versus evaporative air cooling systems since colder air can be delivered to deeper vertical horizons using cooler, drier airflow. Sigma heat is calculated using wet bulb temperature and barometric pressure measured is used for each climatic survey station to describe the cooling potential Any location along the survey path. Using the concept of Sigma heat, thermal additions or losses from an airstream can readily be quantified from psychrometric observations (McPherson, 1993). Spikes in Sigma heat along a climatic survey network path easily identify heat sources or sinks.

The use of an inert refrigerant, with an extremely low freezing point, allows storage of coolth harvested during winter to be used during the summer months. Due to the non-toxic physical and chemical makeup of propylene glycol, it can safely be used in and around the fresh air supply for mining or other subsurface industrial applications since no harm can be rendered to workers that rely upon the continuous supply of clean, healthy air to provide a safe working environment. Since propylene glycol ($C_3H_8O_2$) can be chilled to a reliable operating temperature of -20 °C (50% $C_3H_8O_2$ / 50% H_2O blend), this will allow the chilled refrigerant to be transferred much greater distances than, for example the transfer of ice into a deep and hot underground mine working environment. Due to the viscous lubricating nature of propylene glycol in a relatively high concentration mixture blend with water, piping infrastructure and pumps will last longer compared to cold water systems. Resistance of the refrigerant fluid moving through the piping network will be lower due to the viscous nature of the propylene glycol mixture, attributing to lower induced heat of the refrigerant and lower required pumping energies. Transfer of super chilled refrigerant down to deep levels of a mine will provide opportunity to develop energy recovery systems that generate electricity to pump warmed refrigerant back up to a storage reservoir installation near the surface.

Significant energy savings coupled to substantial financial benefits can be achieved through the use of renewable energy generated from natural sources. Substantial capital and operating expenses are removed from the construction costs of a typical mechanical refrigeration system relying upon high duty industrial components of the mechanical vapor compression cycle. By taking high pressure multistage screw compressors out of the equation, a majority of the electrical expenses for the refrigeration installation would be removed from the annual operating budget. Since heat rejection of heated refrigerant gas from condensing heat exchangers is taken out of the equation, there is no need to have high pressure infrastructure, including piping and valves to accommodate heat removal tasks arising from hot refrigerant gas from a traditional mechanical vapor compression cycle system. In fact, the only high pressure portion of the piping network relates to a standing vertical column of cold or warmed refrigerant passing through a deep mine shaft. The high pressure induced by the inbound cold refrigerant would be it alleviated by energy recovery systems installed at the deep shaft levels.

As previously mentioned, the omission of the refrigerant condensing circuit eliminates the necessity for heat rejection of the refrigerating fluid. This removes the substantial cost of an underground cooling tower or spray chamber to facilitate low pressure heat rejection for a water based system or a compressed refrigerant gas through high pressure condensing heat exchangers. Either way heat rejection costs are removed from the overall air cooling system budget.

The cost of a high-pressure mechanical surface refrigeration plant to effectively cool an underground mine can be significant when considering all-in operating expenses and the potential to purchase off-setting carbon tax credits to provide the additional electrical generation required to power an industrial mechanical air cooling system. The development of low-pressure refrigeration systems deserves studious research and pilot plant development to bring this renewable energy technology to market.

Development of cost-effective monitoring and control systems capable of achieving the lowest possible storage temperature of the glycol reservoir will be a major deciding factor in the implementation of the proposed low-pressure refrigerant system described in this dissertation.

In practice, the plant operator would monitor the air mass wet bulb globe temperature invoking higher operating fan pressures when mixing temperatures exceed agreed upon optimal heat exchange conditions. Monitoring freezing temperature variations within the tank farm will be key in determining timing for fan control procedures. Alerting the plant operator will be instrumental in defining these procedural instructions.

Chilling the propylene glycol below minus 20 °C means that the refrigerant will maintain its cooling power much longer than chilled water. Delivering the cooling power in a distributed piping network, using thermally efficient piping material, will greatly improve the positional efficiency of distributed air cooling systems for deep and hot underground mines. Low pressure piping networks are much less expensive to acquire, install, operate and maintain than high pressure versions. Innovative use of the plate heat exchanging system can allow winter air to be warmed before passing through the burners of air heaters. By circulating warm propylene glycol through the heat exchangers, the mine intake airflow could be raised just above freezing which will dramatically reduce the amount of natural gas or propane required to heat the airflow to 6 °C. The effect of winter's wind chill will also greatly enhance the refrigerant chilling process.

13. Ice Accumulation Reservoirs

The current market trend in profitable mining operations involves continued mining activity below a viable mineral deposit which was initially developed with an open pit. Due to the scale of this type of operation, a popular current trend from the surface mining perspective is to use very large haul trucks bringing ore up a long ramp system which daylights in the open pit. These types of ramp mining operations use an underground access drift which is driven into the most stable strata surrounding the open pit. This mining arrangement is the proposed application for bulk air cooling via ice accumulation reservoirs. Since many underground mines are accessed through large open pits, the following ice accumulation gallery arrangement would work successfully in northern Nevada, or any mining operations that experience very cold winters. Triple gallery snow storage reservoirs constructed in bedrock, adjacent to the underground access tunnels, to maintain sufficiently cool environment until the heat of summer.

During the beginning of the hot climate months, fresh air will be drawn across the accumulated ice and snow cooling the intake air before it reaches the underground fresh air supply. Each gallery has efficient drainage and sub level pumping to allow water recovery. Lower level cold water reservoirs are lined with hydrophobic geo-liner to keep water from seeping into the main open pit.

This type of ice generation system would preferably be excavated into the sound and extremely stable high-wall of an open pit. Preference would be given, for the construction area, to be in close proximity to the ramp system accessing the underground below. In order to continually verify structural integrity, the host pit wall stability, and the snow accumulation gallery footprint, monitoring wells will be drilled into the strata surrounding the galleries and main access tunnel.

Additionally, groundwater monitoring and seepage drainpipes would be drilled horizontally below the cold-water bulk air cooling service water reservoir.

13.1 Geo-Mechanical Considerations

Detailed slow slip analysis needs to be conducted in the immediate vicinity of the planned site with numerous core drill data in the immediate area where the ice accumulation galleries are to be excavated. Thorough rock mechanics analysis needs to be performed to determine all possible failure planes in the construction zone. Careful attention will be given during the core logging so that localized weakness planes and failure zones can be accurately identified. This careful analysis will reveal if required structural load-bearing exists to store proposed ice banks for 5 months until the ice would be used for cooling.

Construction of the underground ice reservoir will require diligence in planning and care during excavation. Selection of the site where the ramp system is driven will be extremely important if this type of system is to be employed. Open pit high wall in which the construction will be excavated needs to be seismically sound and proven to be devoid of significant failure joints, weakness planes or ground water draws that will decrease the geological structure rating. In other words, finding the most attractive site, rock mechanically speaking, will be of significant importance during the planning. This geo-mechanical consideration, and many others, must be weighed judiciously concerning all other site parameters.

Maintaining the integrity of the reservoir liner during installation is of extremely high importance. Floors of the reservoir should be reinforced concrete slabs substantial enough to withstand extreme freeze/thaw conditions. A starting recommendation would use two pours of concrete. The first pour is 18-inch thick concrete poured over a 2-foot by 2-foot lattice of low-grade welded ½-inch rebar.

The second pour should be at least 9-inch thick with hog fence panels laid in mid-pour. Walls of the reservoir should be sprayed with shotcrete as the minimum. Preferably, the walls would be finished concrete or pre-cast arched tunnel sections. Walls and reservoir bottom should be lined with a waterproof sealing material, impregnated with polyurethane. A cast-in-place reinforced concrete dam will be constructed at the reservoirs low point. Additional sumps should be driven down grade of the reservoir galleries to ensure any melt water from the reservoirs be captured before allowing overflow into mine workings.

13.2 Ice Accumulation Gallery Arrangements

Triple gallery entries would be driven into the pit wall adjacent to the underground ramp entry. These three galleries would be only be accessible to the surface via the main access tunnel ramp. The entire ice storage site should have sufficient water storage capacity in a lower sump to accommodate 50% more water mass than the predicted mass of stored ice.

This additional amount should account for seasonal freeze-thaw that represents “conditioning” of the cooling mass from heavy snow to 99% solid ice. This lower sump will be excavated well below the elevation of the ice accumulation galleries, and will serve as the annual reservoir for service water to blow snow and thusly create ice banks. The main sump should have course filtration circuits with the ability to sample water, monitor and allow maintenance of water quality thereby restoring the nucleation agent concentration to optimum levels before returning water to the snowmaking nozzle circuit reservoirs.

Regulators with air locked bulkheads are installed on either end of each gallery to maintain the control airflow velocities during snow and ice accumulation. The regulators will close completely to isolate the snow deposits during conditioning and storage phases while opening completely during the renewable cooling system usage. The lower bulkhead in each gallery should be equipped with a vehicle door to allow scheduled seasonal maintenance activities.

13.3 Snow Fence Arrangements

Considerable research has been conducted in the area of snow fence development by agricultural engineers at Purdue University’s Cooperative Extension Service. The basis for much of the modern design concepts of snow and wind control has been provided by Dr. F. H. Theakston at the University of Guelph in Canada. Snow fence arrays have been implemented in northern latitude areas prone to significant winter precipitation. Fence height and airflow velocity play the major roles in the eventual geometry of the snow deposited downwind of a snow fence.

When winds predominantly blow in certain directions, snow can be transported over long distances making hazardous drifting conditions for roadway traffic. Fence rows provide protected snow free regions on the downstream aspect of installed fence rows, especially surrounding highways that experience prevailing windy surface conditions.

Figure 20 shows solid and porous fence influences on the deposition of snow adjacent to a constructed fence, assuming constant airflow velocity. Selecting a 20% porous fence fabric should allow the majority of the snow to drift to a length of five times the fence height and almost touch the fence itself.

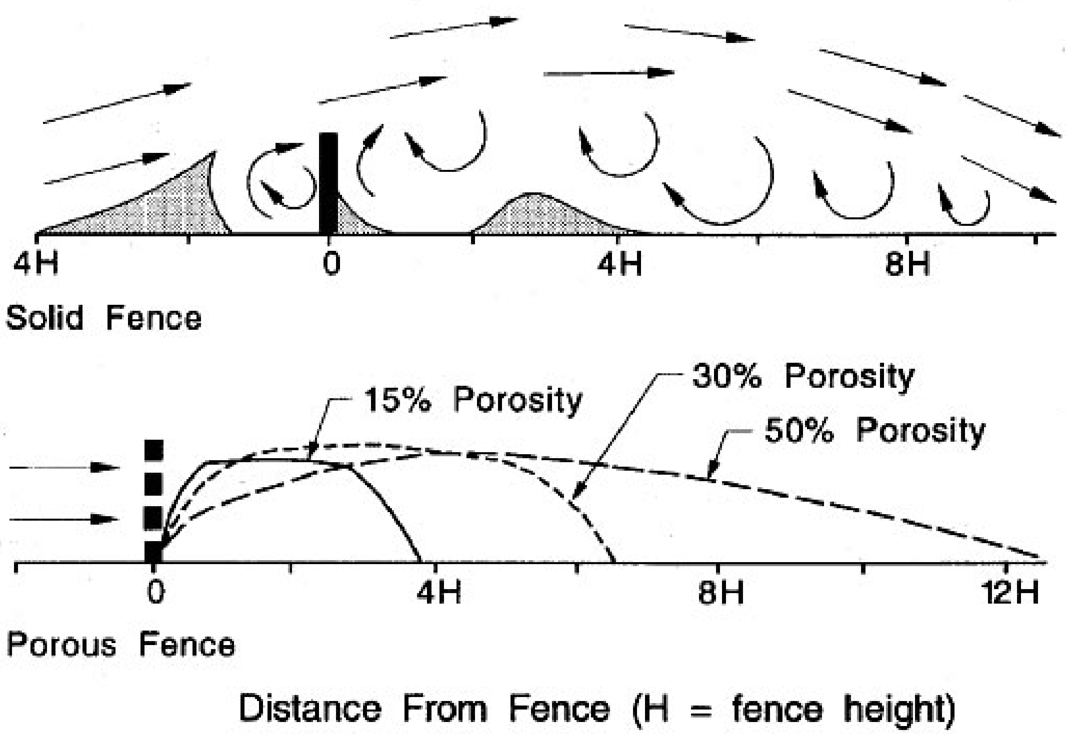

Figure 20: Snow fence porosity research findings.

Figure 21 shows snow drifted in front of a solid fence, which is what will happen once the snow curb is built up on the downwind side of a porous fence. Assuming the fence fabric selected previously, the eventual ice bank would be 6 times the height of the fence fabric. An 8 foot high fence would therefore develop a 48 foot long ice bank.

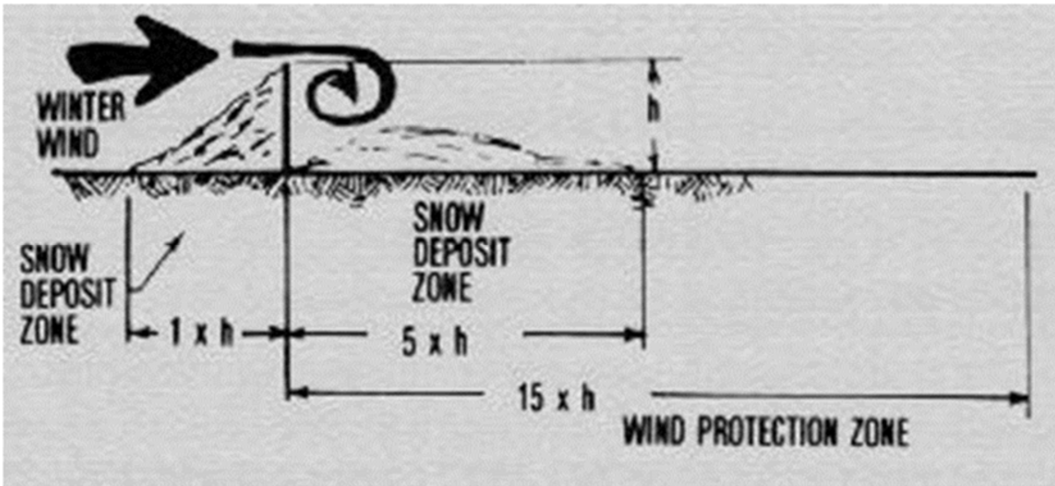

Figure 21: Snow deposition geometry in relation to solid fence height

Using compressed air and water, snow is blown, during freezing conditions across snow fences arranged in an array perpendicular to the airflow. Each fence will be 8 feet high, extending to 5 feet from each rib, to allow safe passage around each ice bank, with the spacing of 50 feet between fences. 15 rows of fences, equally spaced, will be arranged in each 1,013 foot long gallery with over 200 feet dedicated to the lower regulator/water dam arrangement. An iterative modeling process was conducted in Ventsim© to determine optimum fence spacing in relation to the snowmaking nozzle arrays.

Figure 22: High-pressure commercial snow gun nozzle.

Installed 15-feet upstream of each snow fence, will be an array of snow gun nozzles aligned perpendicular to the gallery's long axis. Commercial high-pressure snow gun nozzles used at ski resorts to broadcast artificially made snow is the type being specified for this application (White, 2019). The nozzles will be mounted on tripods to allow fine tuning of the snow blowing process. Water supplied to the nozzles will use low-cost, high temperature snow nucleation agents in the supplied water to maximize the snow making potential of the supplied water with a wider range of applicable deposition temperatures.

13.4 Snowmaking Heat Exchange Process

Snowmaking is a heat exchange process. Heat is removed from snowmaking water by evaporative and convective cooling and released into the surrounding environment. This heat creates a micro-climate inside the snowmaking plume that is very different from ambient conditions. Understanding this process can lead to practical benefits to the snowmaker. There are many variables that affect snowmaking. Three of the most important variables are wet bulb temperature, nucleation temperature and droplet size. Water can be cooled well below 0° C (32° F) and still stay a liquid unless it is nucleated. (SMI Snowmakers, 2012).

13.5 Wet Bulb Temperature

The temperature of a water droplet exiting a snow gun is typically between 1.1° C and 6.7° C (34° F and 44° F). Once a water droplet passes the nozzle and is released into the air, its temperature falls rapidly due to expansive and convective cooling and evaporative effects (White, 2019). The droplet's temperature will continue to fall until equilibrium is reached. This is the wet bulb temperature and it is as important as dry bulb (ambient) temperature in predicting snowmaking success. For example, snowmaking temperatures at -2.2° C (28° F) and 10% humidity are equivalent to those at -6.7° C (20° F) and 90% humidity.

13.6 Nucleation Temperature

Once the wet bulb temperature is known, there must be a way to predict whether water droplets will actually freeze at that temperature. Ice is the result of a liquid (water) becoming a solid (ice) by an event called nucleation (Lui, 2012). A water droplet must first reach its nucleation temperature to freeze. There are two types of nucleation, homogeneous nucleation and heterogeneous nucleation. Homogeneous nucleation occurs in pure water with no contact with any other foreign substance or surface. With homogeneous nucleation, the conversion of the liquid state to solid state is done by either lowering temperatures or by changes in pressure. However, the primary influence on the conversion of water to ice or ice to water is temperature.

In homogeneous nucleation, the nucleation begins when a very small volume of water molecules reaches the solid state. This small mass of water molecules is called the embryo and becomes the basis for further growth until all of the water is converted. The growth process is controlled by the rate of removal of the latent heat being released. Molecules are attaching and detaching from the embryo at roughly equal and very rapid rates.

As more molecules attach to the embryo, energy is released causing the temperature of the attached molecules to be lower than the temperature of the unattached molecules. The growth rate continues until all the molecules are attached. At this point, you have the solid state (ice). The nucleation event (freezing) for pure water will take place as low as minus 40° C or (- 40° F). This is mostly likely to occur in laboratory experiments or high in the upper regions of the atmosphere (upper troposphere).

The heterogeneous nucleation process is when ice forms at temperatures above minus 40° C (- 40° F) due to the presence of a foreign material in the water. This foreign material acts as the embryo and grows more rapidly than embryos of pure water (White, A. 2019). The location on which an ice embryo is formed is called an ice-nucleating site. As with homogeneous nucleation, heterogeneous nucleation is governed by two major factors: (1) the free energy change involved in forming the embryo, and 2) the dynamic of fluctuating embryo growth. In heterogeneous nucleation, the configuration and energy of interaction at the nucleating site become the dominating influence in the conversion of water to ice. Artificial snowmaking involves the process of heterogeneous nucleation.

There are many materials and substances which can act as nucleating agents, each promotes freezing at a specific temperature or nucleation temperature. These nucleating agents are generally categorized as high-temperature (i.e., silver iodide, dry ice and ice nucleating proteins) or low-temperature (i.e., calcium, magnesium, dust and silt) nucleates. It is the low-temperature nucleators that are found in large numbers in untreated snowmaking water. The ideal nucleation temperature of snowmaking water is between -9 °C and -7 °C (15 °F and 20 °F) .

There is an energy interaction between the ice-nucleating site in the water with the surface. This causes the water droplets to freeze very near to 0 °C (32 °F). In snowmaking it is the nucleator having the highest nucleation temperature that determines when a water droplet will freeze. As a water droplet cools, heat energy is released into the atmosphere at a rate of one calorie per gram of water. As it freezes into an ice crystal, the water droplet will release additional energy at a rate of 80 calories per gram of water. This quick release of energy raises the water droplet temperature to 32 °F, where it will remain while freezing continues. This is one reason why we are accustomed to thinking that water freezes at 0° C

(32 °F). To be precise, the water will continue to freeze as long as it remains at or below 0° C (32 °F), but only after it has first cooled to its nucleation temperature. Any excess energy will be dissipated into the atmosphere.

13.7 Droplet Size vs. Nucleation Reagent Mixing

Since the distribution of various nucleators in a given volume of water is totally random, the size of the water droplet or the number of high-temperature nucleators has a significant effect on the temperature at which freezing occurs (nucleation temperature). In natural water, as the size of the water droplet decrease, the likelihood that the droplet will contain a high-temperature nucleator also decreases. Conversely, larger water droplets stand a better chance of containing high-temperature nucleators. The optimum situation for snowmakers is one where each and every droplet of water passing through the snow gun nozzle contains at least one high-temperature nucleator and where each droplet freezes in the plume (SMI Snowmakers, 2012). It is assumed that the lower reservoirs dedicated to the snowmaking process have sufficient mixing with high-temperature nucleators reagents prior to the reservoir water being pumped into the snowmaking nozzles.

The relationship between the variables of nucleation temperature and droplet size is summarized in two statistically valid conclusions. Firstly, a 50% increase in the droplet size results in a 0.5 °C (1 °F) increase in nucleation temperature. Secondly, a 50% decrease in droplet size results in a three-degree Fahrenheit decrease in nucleation temperature. These conclusions are based on an average droplet size can be counter-productive to promoting high-temperature nucleation, unless enough high-temperature nucleators are present to compensate.

Looking at the relationship between droplet size and evaporation, research in cloud seeding shows that:

- These conclusions further point out the undesirable results from using very small droplets, especially in areas where water loss is a critical issue;
- Relating droplets size to nucleation temperature, it is possible to increase snowmaking production and efficiency by using high-temperature nucleators together with larger water droplets;
- This frequently not only allows increased water flow, but also reduces evaporation and yields more snow on the ground;
- In fact, studies indicate that a 20% increase in water flow can increase snow volume up to 40% if droplet size and nucleation temperature is optimized (SMI Snowmakers, 2012).

Resultant droplet size can reliably the attending through judicious control of feed water pressure and feed air pressure. There is no way to ensure that each droplet will contain at least one high temperature nuclear agent reagent, other than ensuring the mixture is well agitated. In order to ensure adequate mixing are of the snowmaking feedwater sump, several centrifugal pumps should be employed throughout water management procedure supporting the snowmaking process. In the best case scenario one pump will be used when any reagent is added to the reservoir mix. Additionally, one pump should be used aerate and agitate the water mixture being supplied to the snowmaking nozzles.

13.8 Modeling Cooling Capacity from Ice Accumulation Reservoirs

A thermodynamic ventilation model is developed in Ventsim© to estimate the cooling potential capacity of the proposed ice accumulation reservoirs. Ventsim© was never designed to simulate the physical phenomena of snowmaking or ice melting. Prudent modeling will take into account the energies created, i.e. stored, or used using simplistic energy balance equations. Ventsim© will however account for heat sources and sinks added to a mine ventilation network. Seasonal variations of the intake air temperatures are estimated using conditions similar to those experienced at open pit operations on the Carlin trend. The simulated seasonal low and high wet bulb and dry bulb temperatures are input to the Ventsim© thermal flywheel effect solution module.

In order to simulate the snow making process, the latent heat of fusion as a heating source needs to be estimated. Each snowmaking nozzle array will therefore be assigned a small heating source. In order to simulate the potential cooling power from the ice melting process, the latent heat of melting must be applied to the ventilation model as heat sinks in each ice accumulation gallery as the respective ice stopes melt when exposed to the warm fresh air supply.

13.8.1 Modeling Latent Heat of Snowmaking

In order to adequately model this snowmaking process, as developed by an individual snow blowing nozzle, the latent heat of fusion must be quantified. The latent heat of fusion is the heat generated when water goes from the liquid to the solid phase. Ventsim© (the ventilation simulation software employed for this thesis) has no way of automatically understanding the snow making process, thermodynamically speaking. Therefore, the small heat source for each snow blowing nozzle array is added to each ice accumulation gallery during the snow making process.

13.8.2 Determination of Latent Heat of Fusion

Latent heat due to the moisture in air can be calculated with the following equation:

$$h_l = q\ \rho\ h_{\mathrm{we}}\ dw_{\mathrm{kg}} \tag{13.8.1}$$

where: h_l = latent heat (kW)

q = air volume flow (m^3/s); 12.9 m^3/s

ρ = density of air (1.186 kg/m^3)

h_{we} = latent heat of vaporization of water (2465.56 kJ/kg)

dw_{kg} = humidity ratio difference (kg water/kg dry air), estimated from Mollier's Chart, see Figure 23, at 0.0025

Given the optimal conditions for snow genesis, at 12.9 m^3/s airflow:

Latent heat = (12.9)(1.186)(2465.56)(0.0025) = 94.3 kW

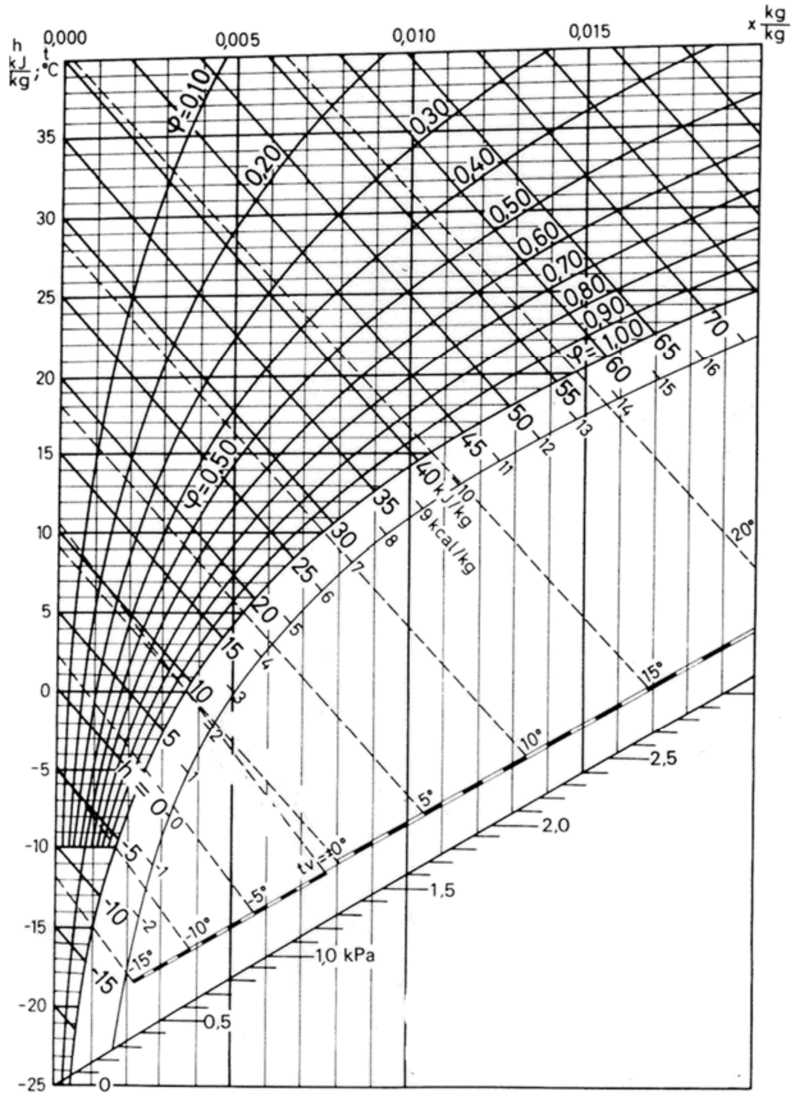

Figure 23: Mollier's Chart

13.8.3 Modeling Latent Heat of Melting Ice

In order to adequately model the ice melting process, as delivered to the ventilation network, the latent heat of melting must be quantified. The mass of ice curb each gallery can easily be calculated using the volumetric relationship yielding the volume by solving for the product of the length (50 ft., or 15.2 m) times the height (8 ft., or 2.4 m) times the width (13 ft., or 4.0 m) which has been reduced by 5 ft. (1.5 m) on each side to allow safe passage by system audit personnel and maintenance crews. The resultant curb volume of 146 m^3 for each ice curb is then multiplied by 15 ice curbs per gallery, yields 2,189 m^3 of ice per gallery. Since ice has a specific weight of 1000 kg/m^3, each ice curb has an estimated mass of 2,188,800 kg of ice initially before ice melting begins, theoretically speaking.

Calculation of the potential cooling energy provided in each ice accumulation Gallery is based upon the mass of ice in the Gallery multiplied by the latent heat of melting. The latent heat of melting is 334 kilojoules (kJ) per kilogram (kg), the resultant cooling power available is therefore 334 kJ/kg times the estimated mass of ice which is 2,188,800 kg, would potentially generate 731.06 GW of cooling power. This is not a reasonable assumption. A more realistic and practical assumption would assume the outer inch, or 2.5 centimeters, of ice which is intimately involved with the cooling process due to constant exposure to the ventilating airflow, at any given time-step during the modeling exercise.

Two sides on the length and width of each ice curb, plus the ice curb top is exposed to the warm ventilating airflow during the cooling phase of this proposed mine air conditioning system. Assuming a one inch thickness for the melting ice interface with the ventilating air flow, 134 ft^3 of ice can be allocated for cooling recruitment by each ice curb in every ice accumulation of gallery. This means a total of 15 ice curbs times 3.8 cubic meters of ice per accumulation gallery yields

57 m^3 of ice contributing to the cooling system per gallery. This ultimately yields 19.2 kW of cooling power per gallery when the ice curbs are exposed to the warm, fresh air to which the cooling power, or coolth, is being applied. This ultimately yields 855 kW of cooling power applied to the ventilation network on a continual basis, once employed until all the ice melts.

13.8.4 Model Development

The theoretical mine is described in the following modeling example with physical dimensions and layout as previously described in the text. The model is drawn in AutoCAD to define the layout of the 3D network of airway branches and, as far as the calculation of natural ventilation pressure is concerned, elevation coordinates for each airway branch junction. The physical model layout is given various attributes that makes the manipulation of model elements more efficient and the workflow of ventilation simulation more fluid. Different types of airways are grouped into layers to aid in property modifications, airway classifications or characteristics and subsequent thermal analysis. The model layout is then exported in the DXF format to facilitate import and generation of a blank ventilation model in Ventsim©.

Once the initial model has been imported, the network branches are assigned characteristics, the most important of which involve connection to the open atmosphere. Care is given when determining the assumed airflow direction by defining each branch’s respective from and to junctions. Appropriate resistances are also assumed, based upon recommendations from historical survey data on similarly sized airway branches are given before initially simulating the ventilation network. The model assumes connection to the atmosphere at the top of the pit access ramp.

Preliminary ventilation controls are defined to assign the airflow regime for each galley, assessing pressure contributions along each network air pathway. Regulators are given a set of resistance positions that will generate resistances of varying intensities. These resistances are assigned to regulators for the respective ice accumulation gallery, depending on the life cycle of stored ice. Connection to the intake air side of the ice accumulation galleries at the main ramp is given a different type of control, specifically a well-constructed vehicle airlock with integrated regulator. Below each gallery's dam is positioned a well-constructed vehicle door, also with an integrated regulator.

13.8.5 Model Assessment

Figures 25 through 36, describe the air volumes and temperature characteristics for each of the initial snow formation steps. Firstly, each airflow regime is described for each of the three initial snow deposition sequences. Next, airflow temperatures are quantified for each of three distinct snowmaking phases: 1) beginning snowmaking process, 2) midway through the accumulation of the respective galleries' temperature responses and 3) once the respective gallery has been effectively filled with snow for the initial ice conditioning phase of the respective gallery. Figure 24 shows model airflow designations for each gallery and the main ramp before snowmaking begins.

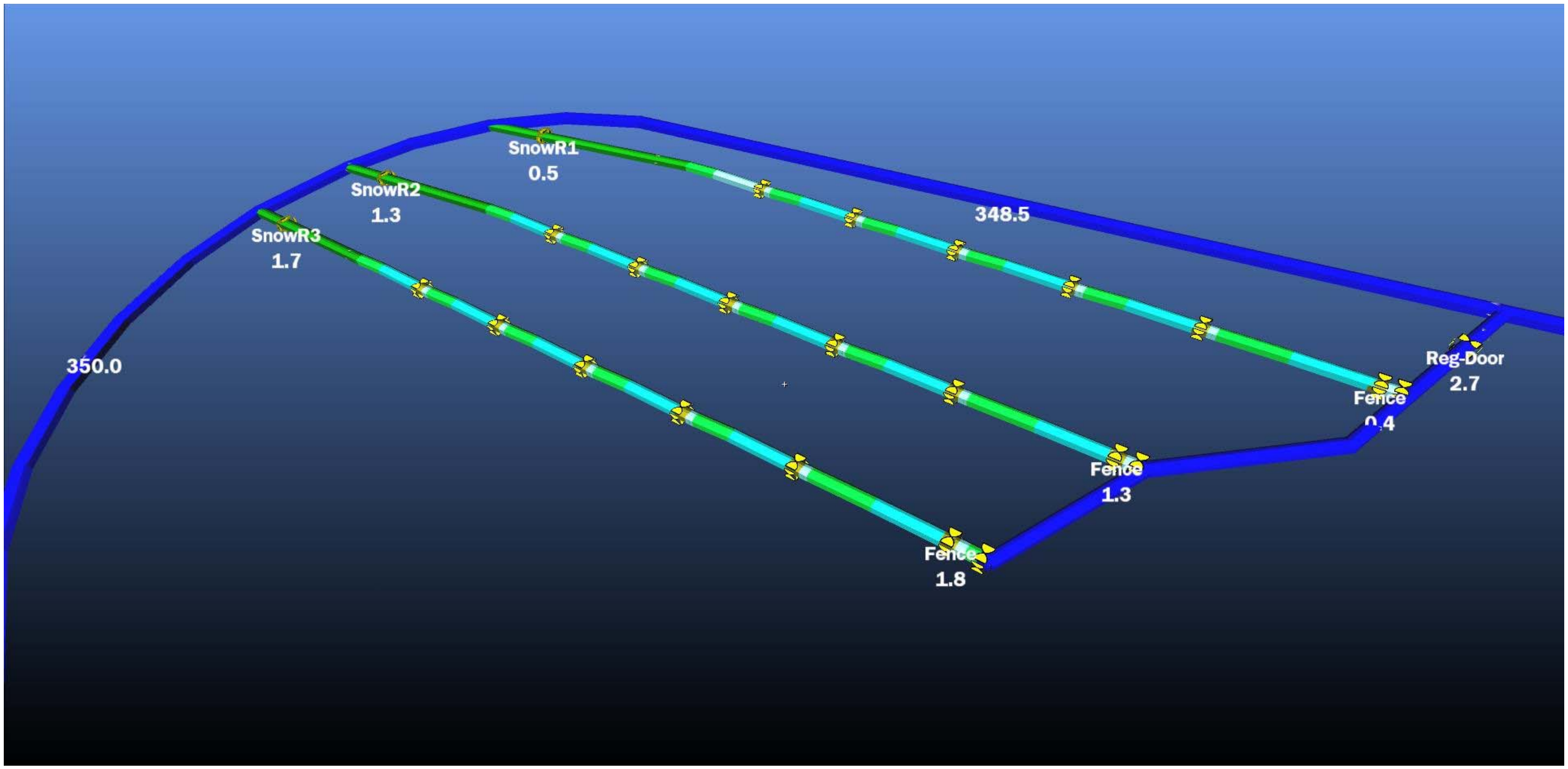

Figure 24: Ventsim© model of ice accumulation galleries with no snowmaking or bulk air cooling; airflow quantities shown in m³/s.

Figure 25 shows model airflow estimations for airflow quantities of each gallery and the main ramp following snowmaking, which begins in gallery #1.

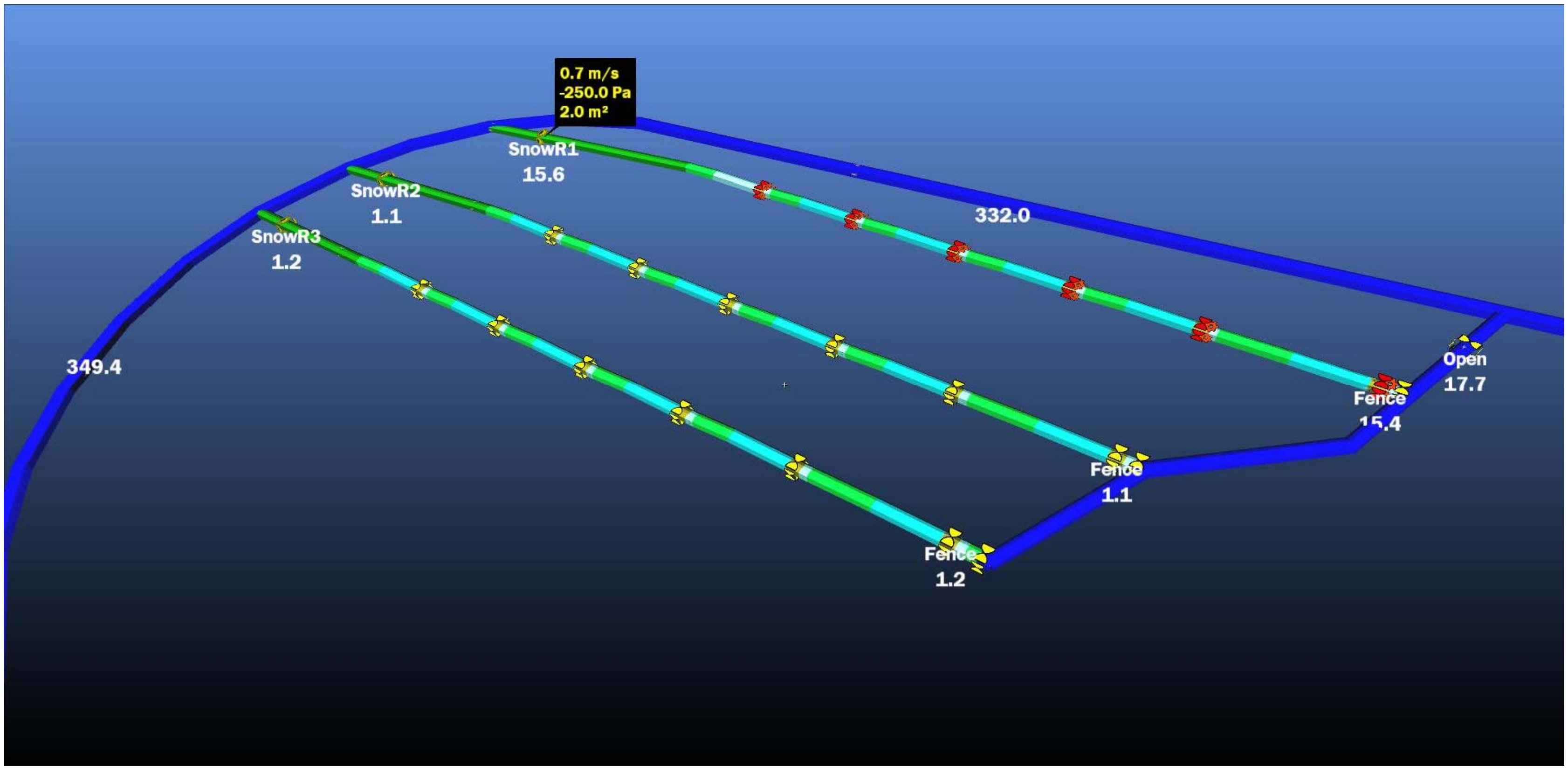

Figure 25: Ventsim© model of ice accumulation gallery #1 when snowmaking begins; no accumulated snowbanks; airflow quantities shown in m³/s.

Figure 26 shows temperatures, both wet bulb and dry bulb in °C for the ice accumulation galleries when gallery

#1 begins the initial snowmaking phase. Figure 26 shows gallery #1 when snow has accumulated halfway during initial snowmaking phase. In the next modeling phase, gallery #1 is full of snow and gallery #2 is getting the initial application of snow. During all subsequent phases, snow placed previously has conditioned becoming ice after a few weeks. The previously emplaced snow reduces in volume by up to 50% during any conditioning phase, which has a minimum conditioning time of three weeks.

Snow will continue to be blown in place while conditions are favorable following the initial snow blowing procedure. Subsequent “lifts” of ice occur after emplacement of new snow, adding to and following snow conditioning of prior snowmaking cycle time steps.

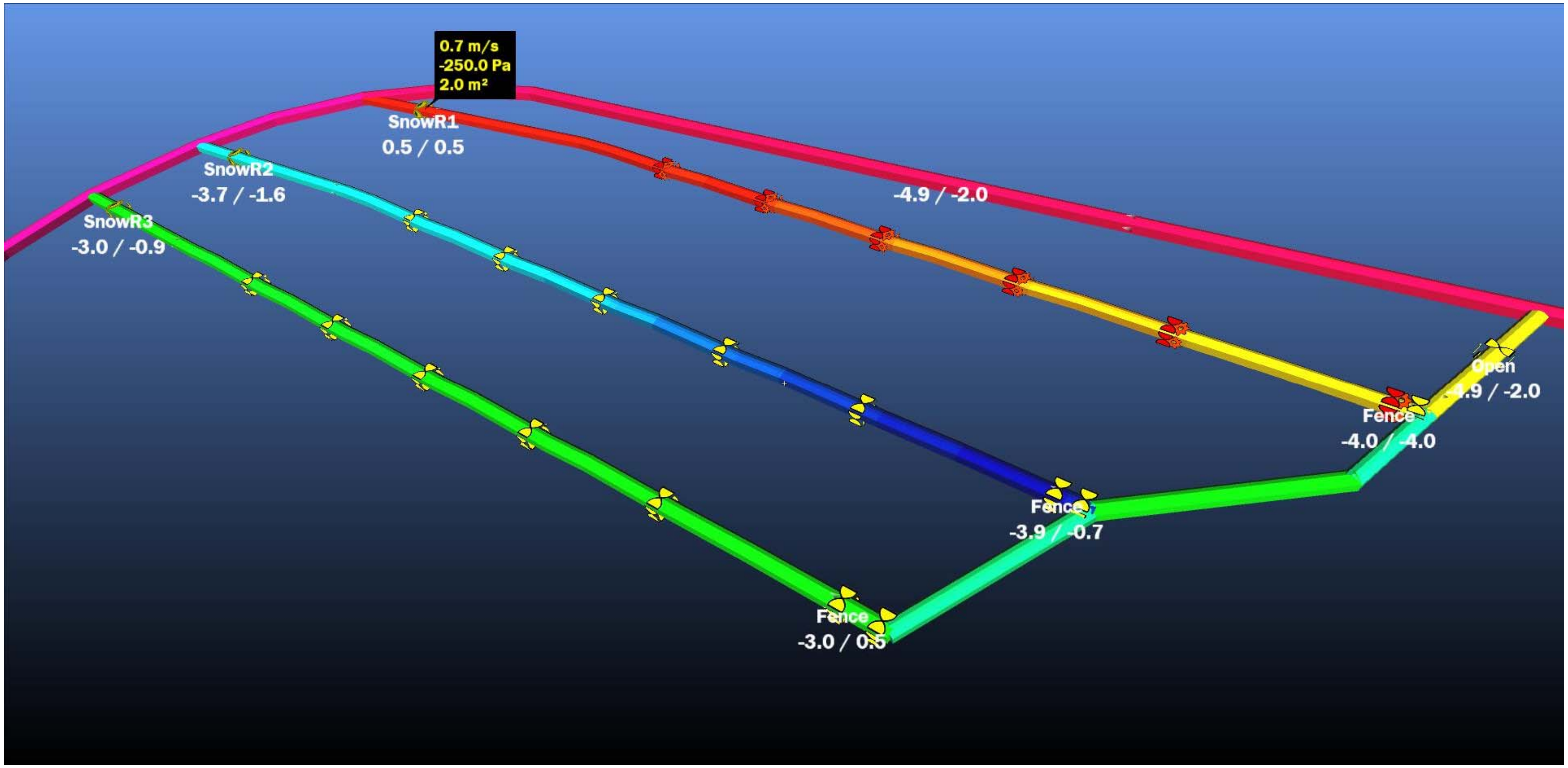

Figure 26: Ventsim© model of ice accumulation gallery #1 when snowmaking begins; wet bulb/dry bulb temperatures shown in °C.

Figure 27 shows model airflow estimations for air volumes of each gallery and the main ramp following snowmaking begins in gallery #2.

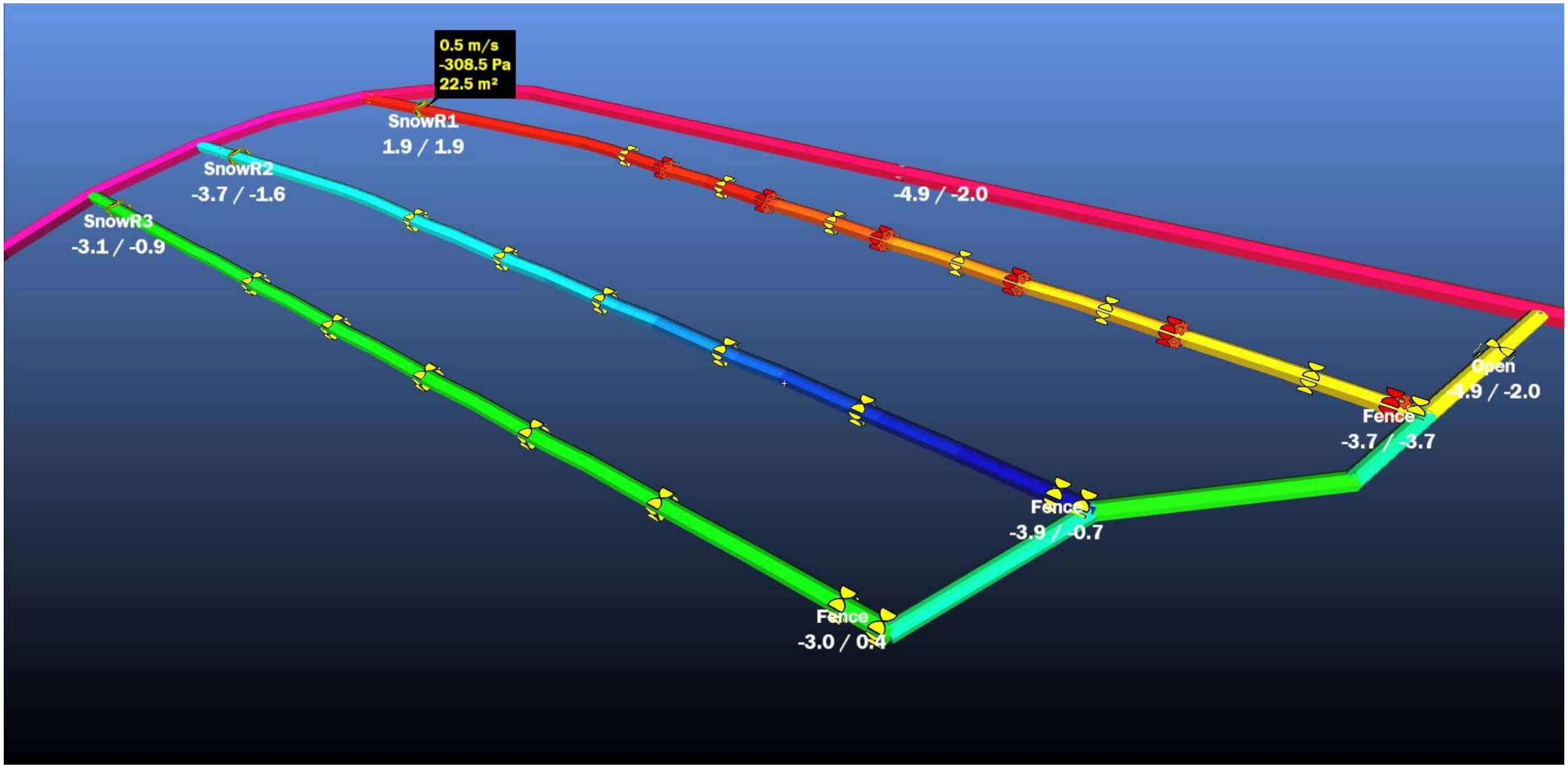

Figure 27: Ventsim© model of ice accumulation gallery #1 when snow has accumulated halfway during initial snowmaking phase; wet bulb/dry bulb temperatures shown in °C.

Figure 28 shows temperatures, both wet bulb and dry bulb in °C for the ice accumulation galleries when gallery #2 begins the initial snowmaking phase. Figure 29 shows gallery #2 when snow has accumulated halfway during the initial snowmaking phase. In the next modeling phase, gallery #1 is full of snow and gallery #2 is getting the initial application of snow.

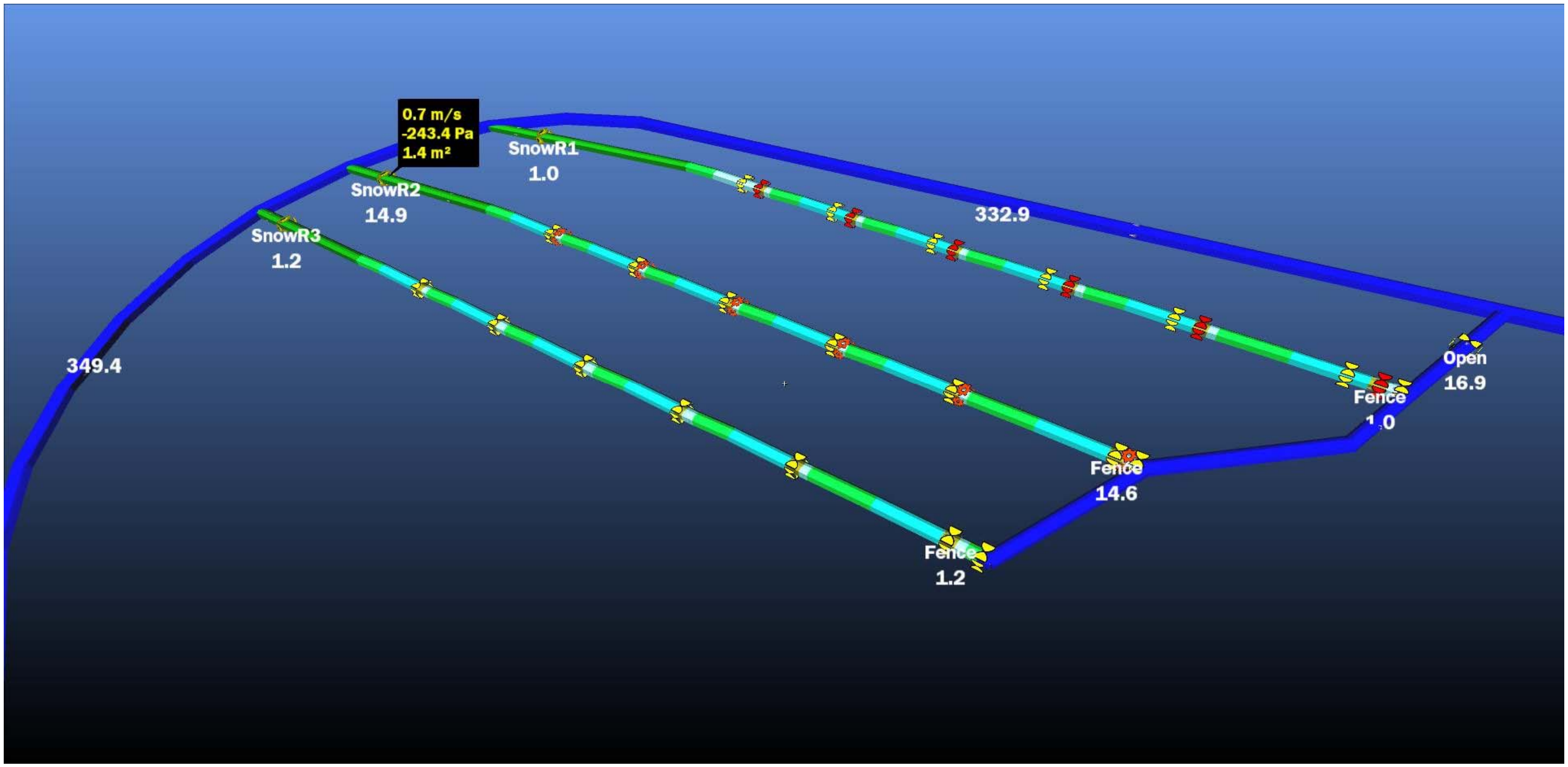

Figure 28: Ventsim© model of ice accumulation gallery #2 during initial snowmaking phase; gallery 1 in initial conditioning phase; airflow quantities shown in m³/s.

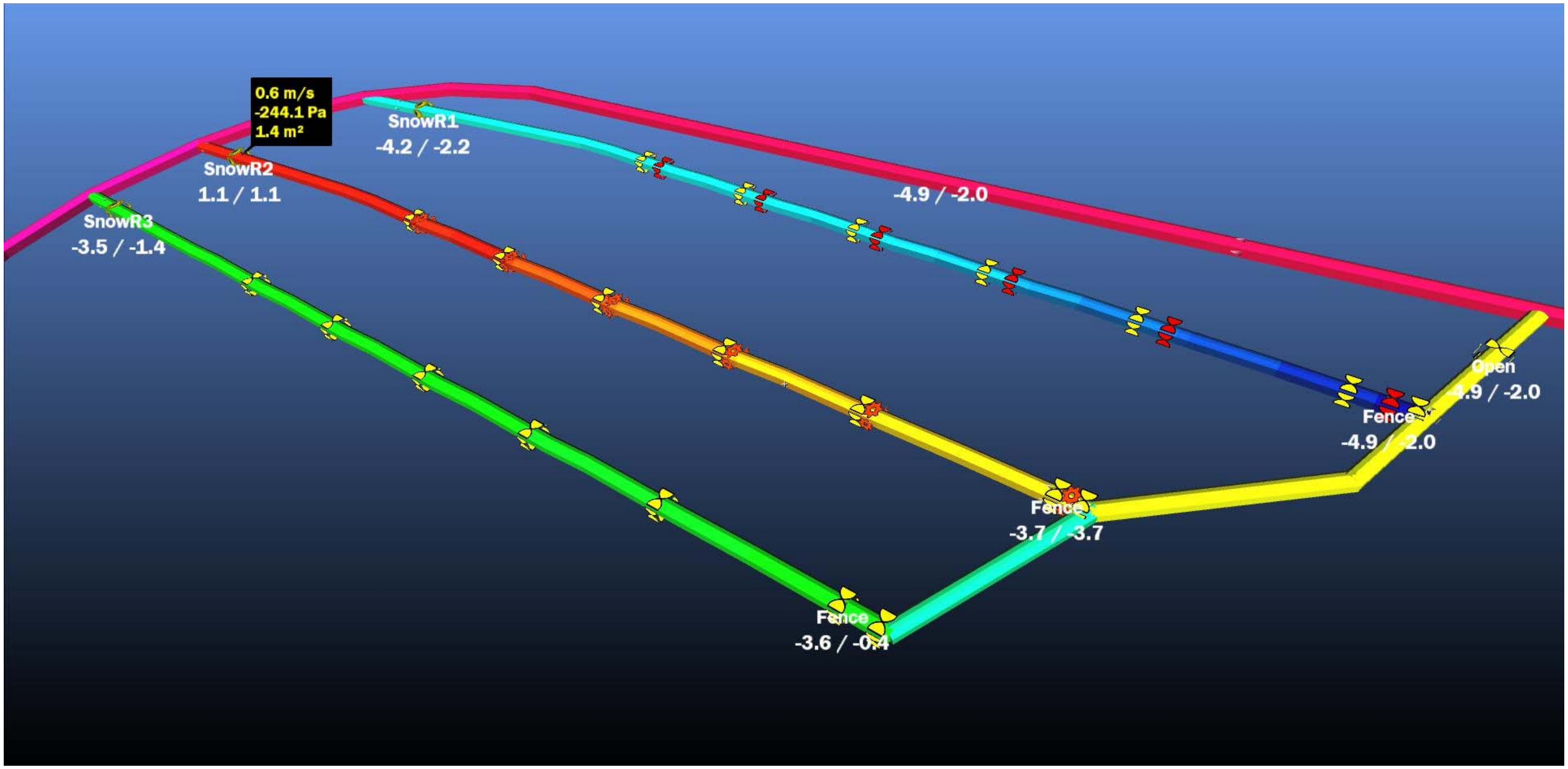

Figure 29: Ventsim© model of ice accumulation gallery #2 during initial snowmaking phase; gallery 1 in initial conditioning phase; wet bulb/dry bulb temperatures shown in °C.

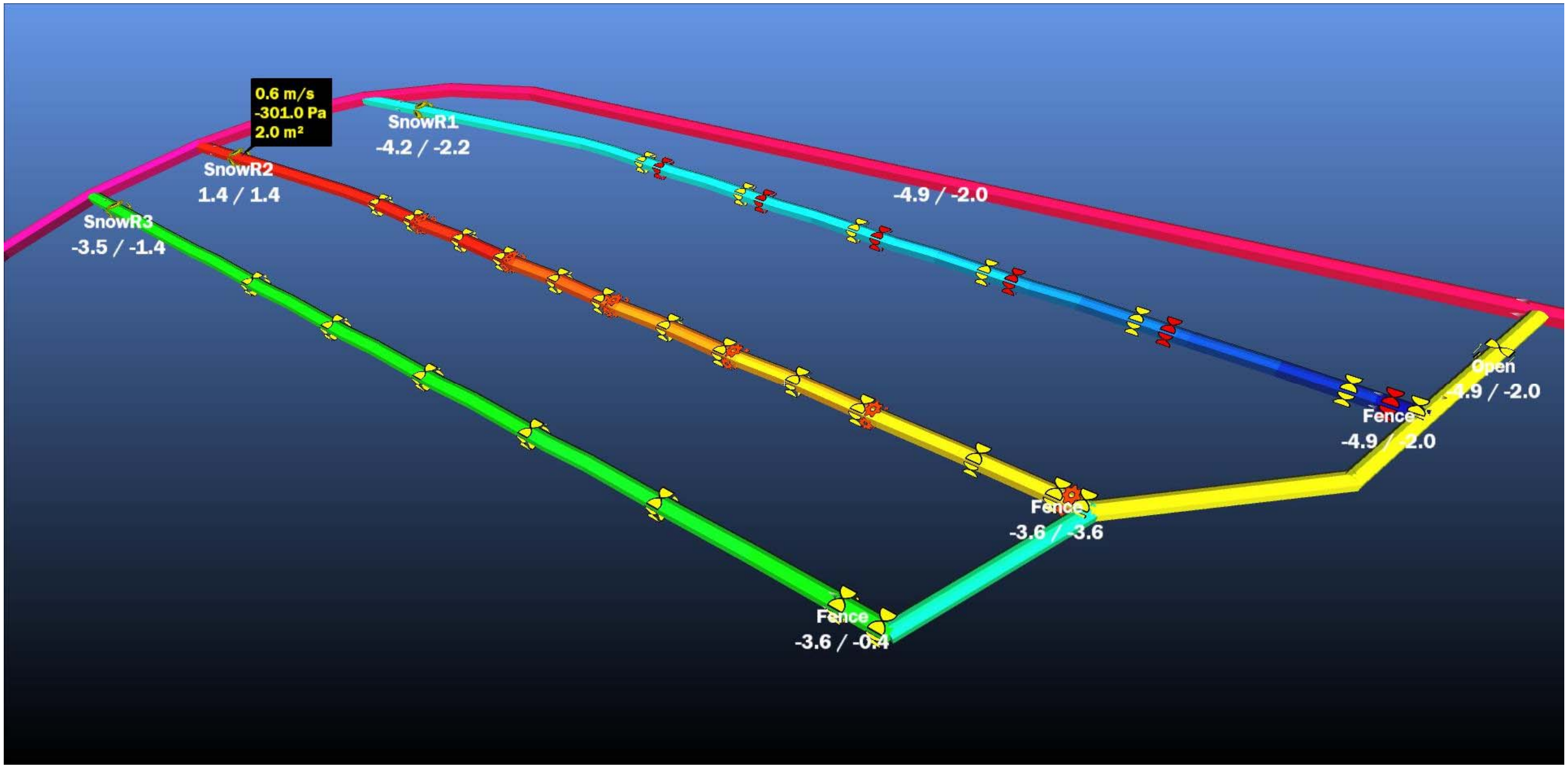

Figure 30: Ventsim© model of ice accumulation gallery #2 during snowmaking with snow accumulated halfway; gallery 1 in initial conditioning phase; wet bulb/dry bulb temperatures shown in °C.

Figure 30 shows temperatures, both wet bulb and dry bulb in °C for the ice accumulation galleries when gallery #2 completes the initial snowmaking phase, beginning the first conditioning phase. Gallery #1 and #2 are now conditioning towards a more solid ice composition, balancing energy between the mass of snow and the mass of rock in direct contact with the snow. In the next modeling phase, gallery #1 and #2 are full of snow and gallery #3 is getting the initial application of snow.

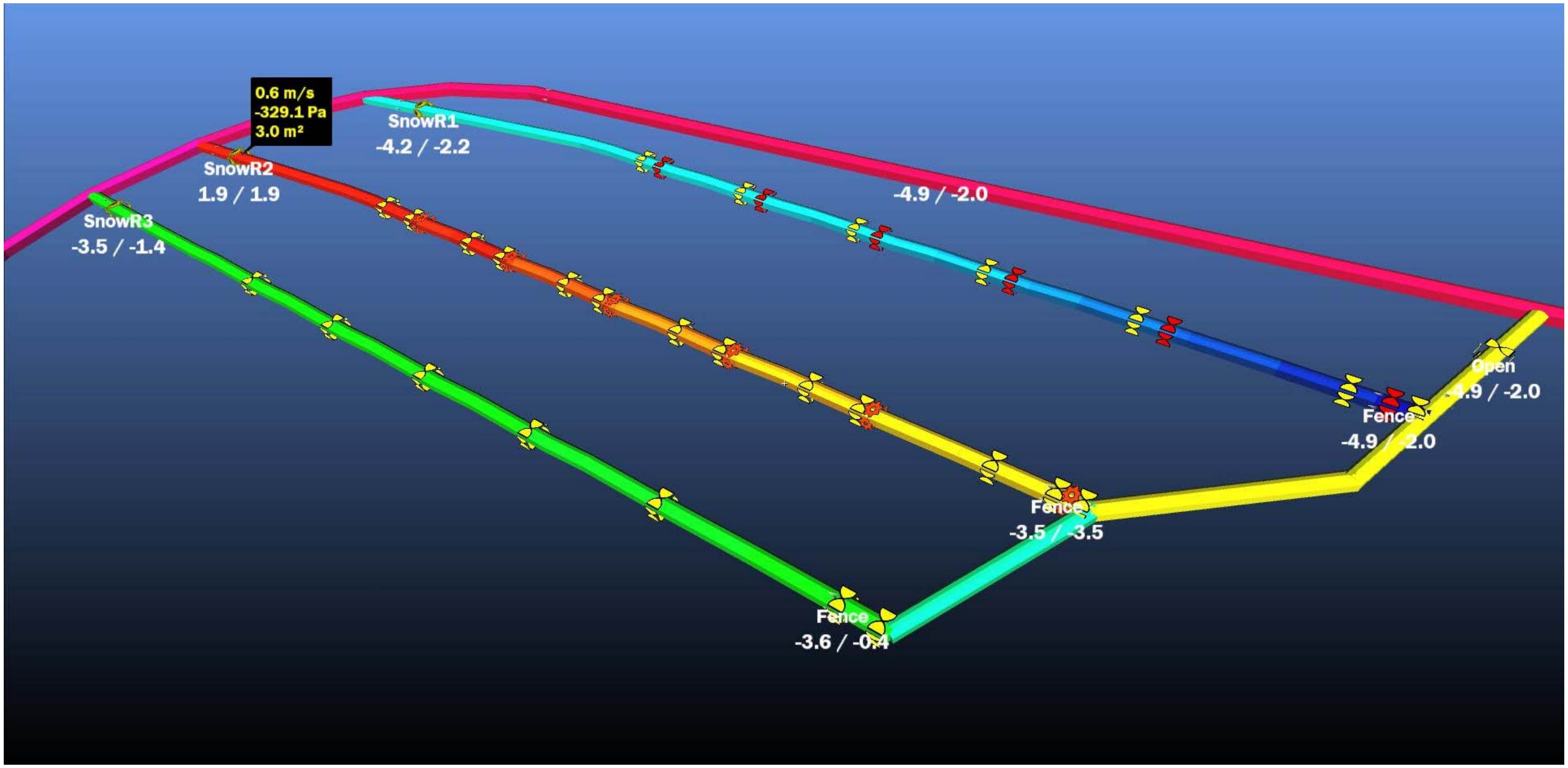

Figure 31: Ventsim© model of ice accumulation gallery #2 when snow has fully accumulated in gallery 2; gallery 1 in initial conditioning phase; wet bulb/dry bulb temperatures shown in °C.

Figure 32 shows model airflow estimations for air volumes of each gallery and the main ramp following snowmaking which begins in gallery #3. Figure 33 shows temperatures, both wet bulb and dry bulb in °C for the ice accumulation galleries when gallery #3 begins the initial snowmaking phase. Figure 34 shows gallery #3 when snow has accumulated halfway during the initial snowmaking phase. Figure 35 shows temperatures, both wet bulb and dry bulb in °C for the ice accumulation galleries when gallery #2 completes the initial snowmaking phase, beginning the first conditioning phase.

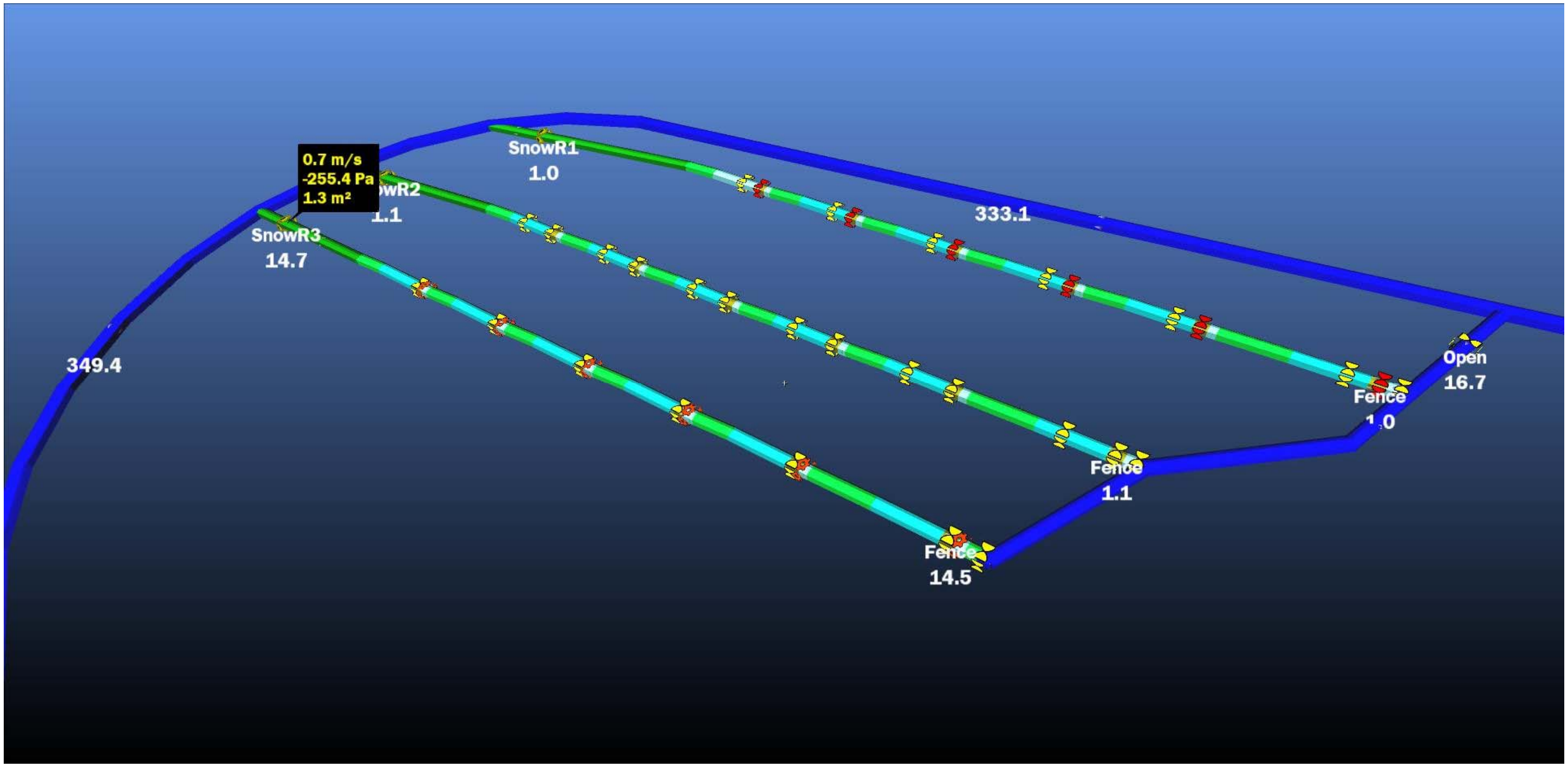

Figure 32: Ventsim© model of ice accumulation gallery #3 when snowmaking begins; gallery #1 and #2 in initial conditioning phase; airflow quantities shown in m³/s.

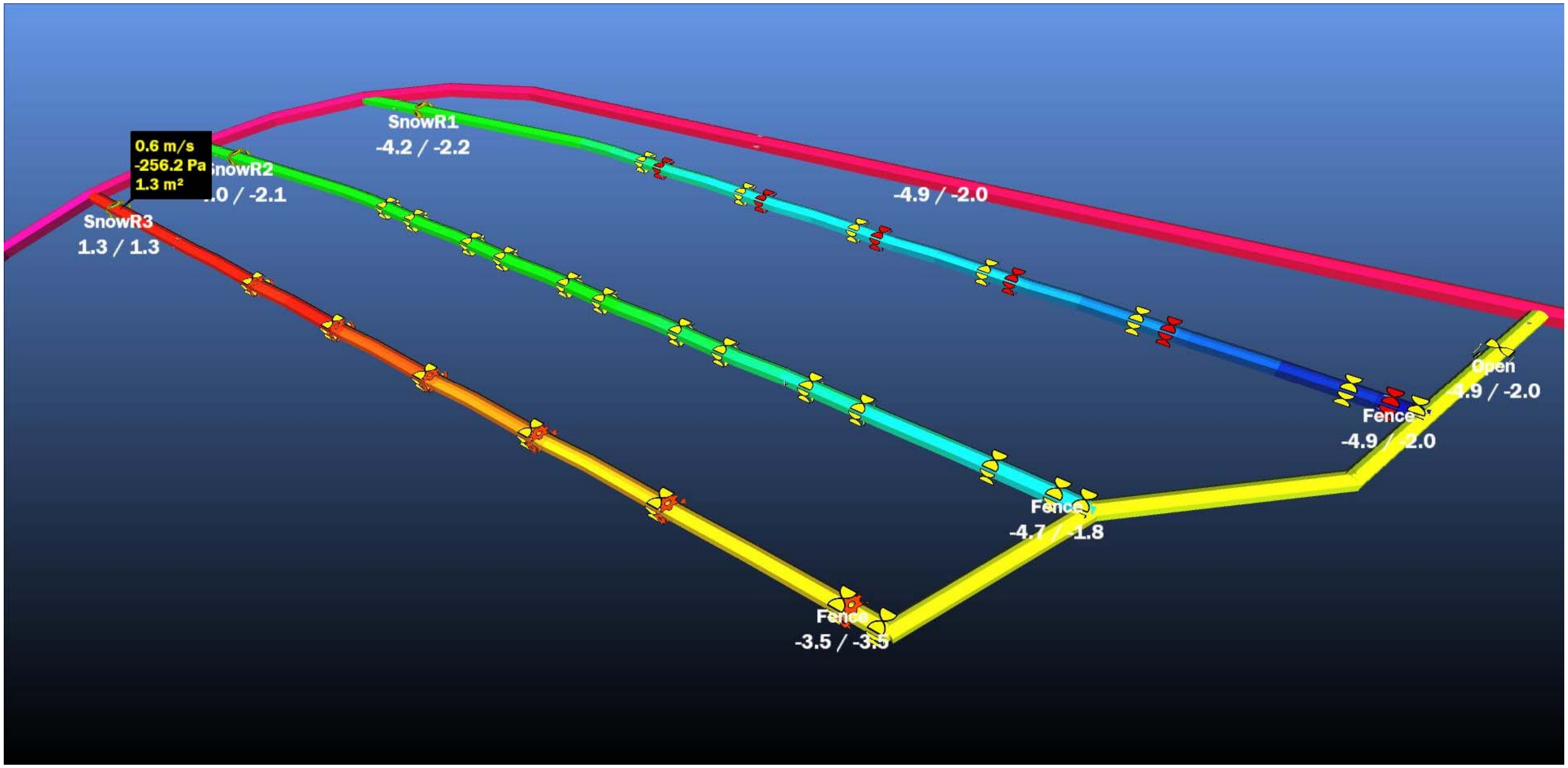

Figure 33: Ventsim© model of ice accumulation gallery #3 when snowmaking begins; gallery #1 and #2 in initial conditioning phase; wet bulb/dry bulb temperatures shown in °C.

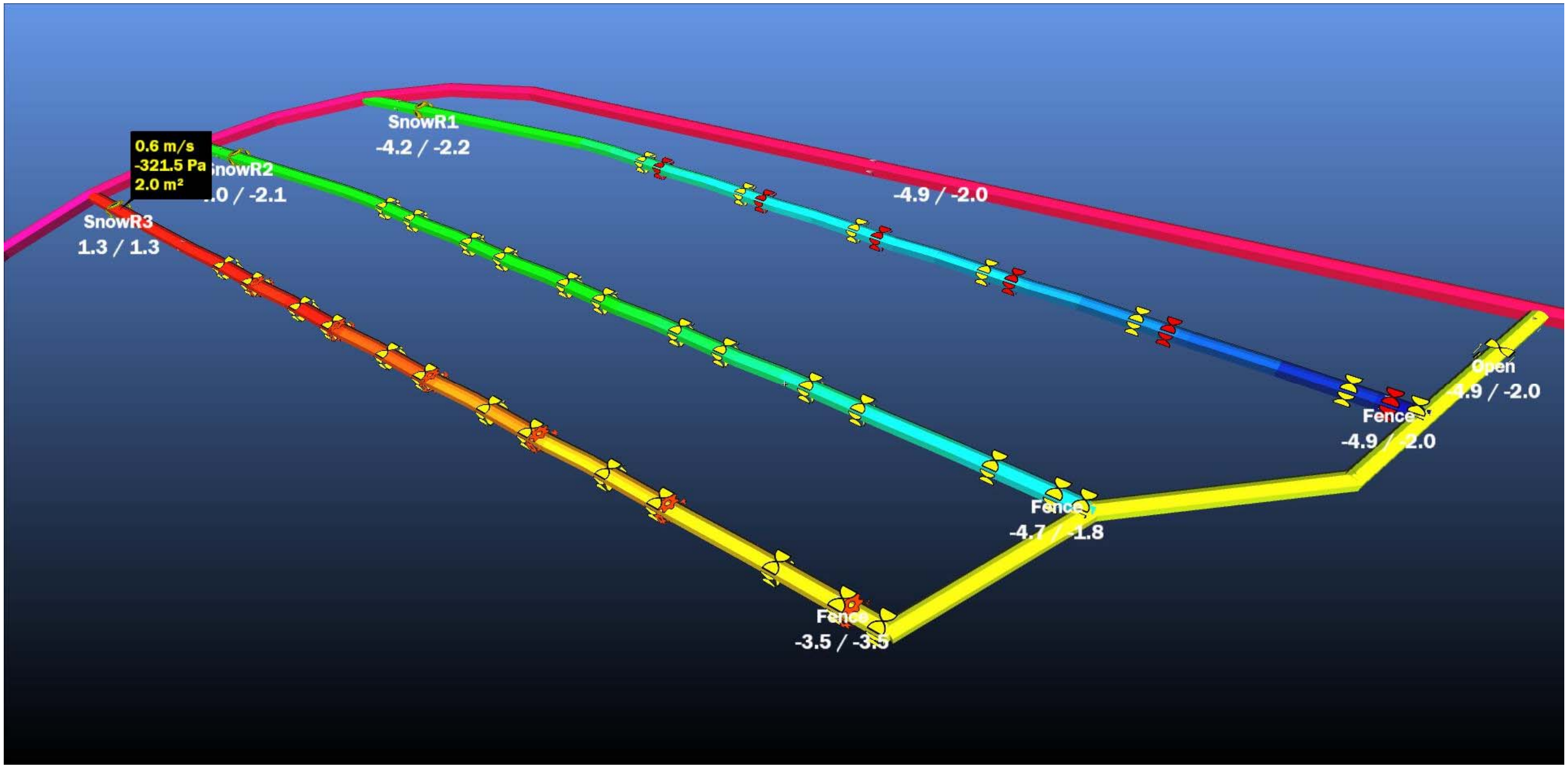

Figure 34: Ventsim© model of ice accumulation galleries when snow has accumulated halfway in gallery #3; gallery #1 and #2 in initial conditioning phase; wet bulb/dry bulb temperatures shown in °C.

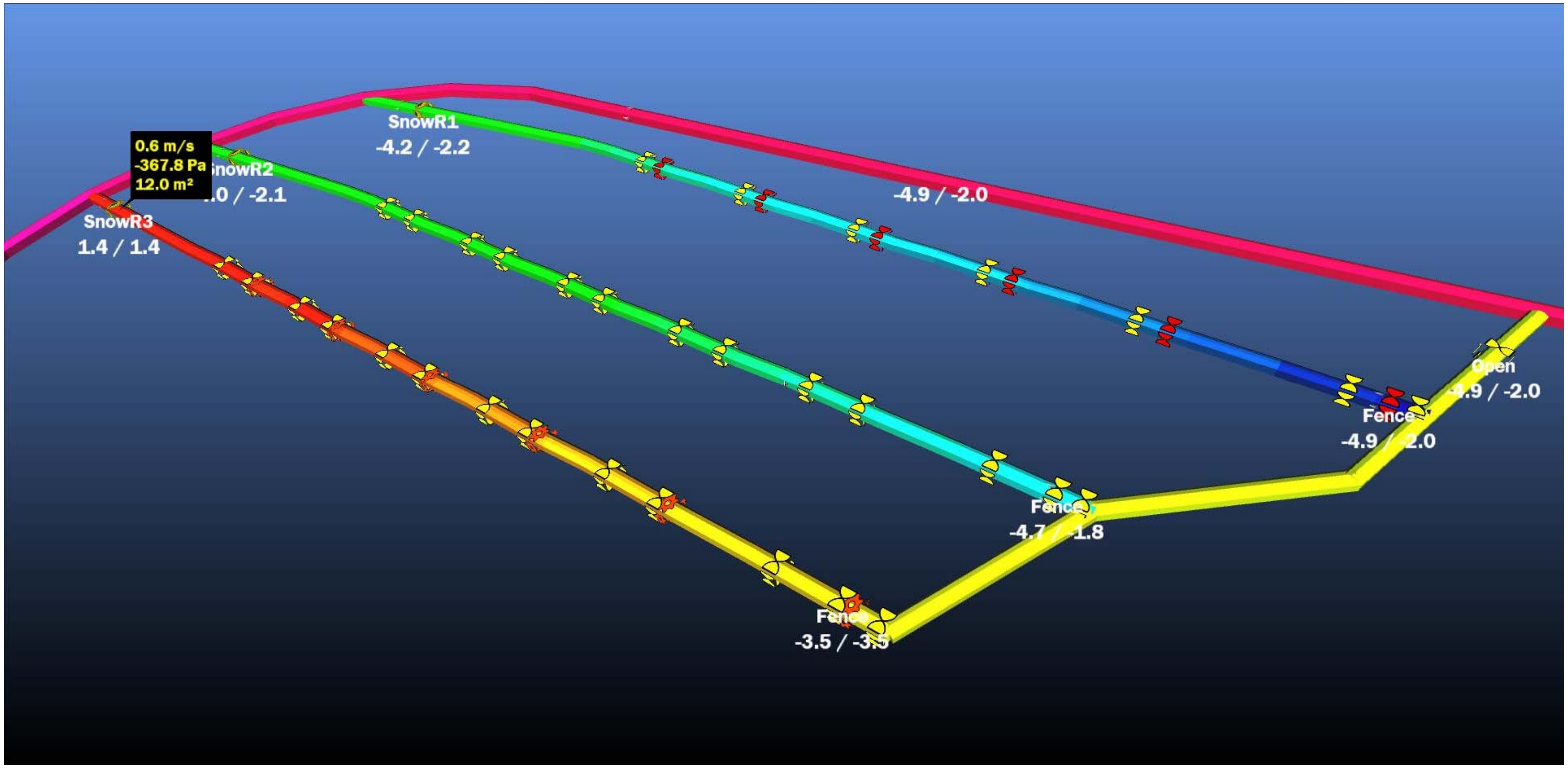

Figure 35: Ventsim© model of ice accumulation galleries when snow has fully accumulated in gallery #3; gallery #1 and #2 in initial conditioning phase; wet bulb/dry bulb temperatures shown in °C.

13.8.6 Using the stored ice to cool mine intake air

When seasonally warm intake air of nearly 60 m^3/s is passed over the three ice accumulation galleries, the wet bulb and dry bulb temperatures in the ramp are depressed by 2 °C and 4 °C (5 °F and 9 °F), respectively, as shown in Figure 36. Almost 20 m^3/s with gallery airflow average velocity pf 0.6 m/s will pass through each gallery during the cooling phase, as specified by each galleries' regulator. Individually, each gallery injects airflow below freezing onto the ramp where mixing occurs in the turbulent ramp air.

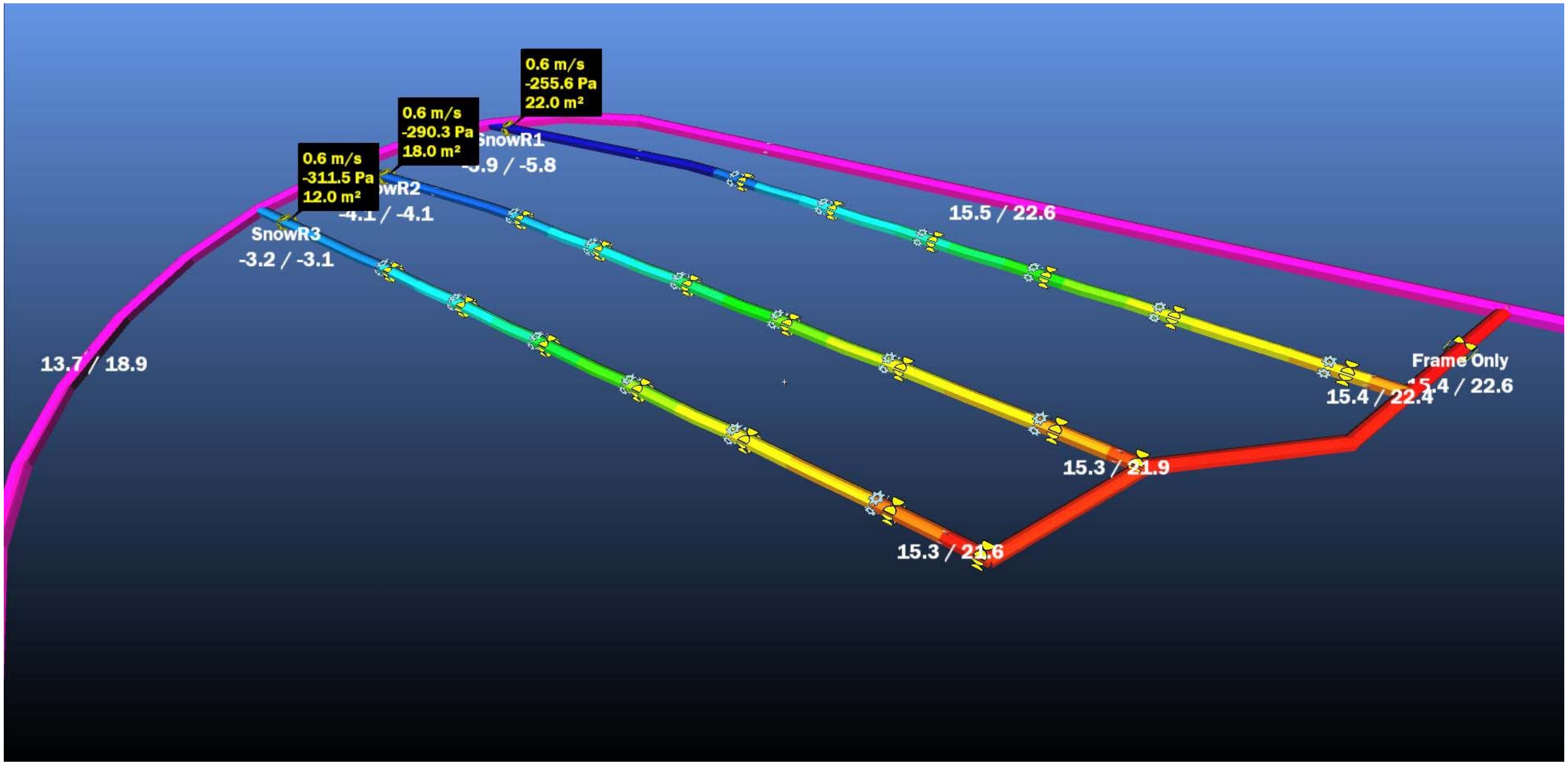

Figure 36: Ventsim© model of ice accumulation galleries when stowed ice is used for bulk air cooling; wet bulb/dry bulb temperatures shown in °C.

14. Conclusions and Future Work

Both innovative air cooling systems described in this dissertation will help underground mines reduce the operational carbon footprint by replacing electrical power with renewable cooling energy. The conceptual propylene glycol refrigeration system can generate over 19 MW for over 5000 hours, yielding over 97.8 GWh of electrical equivalent. The ice accumulation reservoirs supplying 855 kW of cooling power continuously over the same period (5000+ hours) would yield over 4.2 GWh. According to the United States Environmental Protection Agency (EPA, 2021), 1 kWh is equivalent to 7.09e-4 metric tons CO_2 gas. The renewable cooling systems could offset 69,342 and 3,031 tonnes CO_2 annually.

14.1 Low Pressure Organic Air Conditioning System

The use of an inert refrigerant, with an extremely low freezing point, allows storage of coolth harvested during winter to be used during the summer months. Due to the non-toxic physical and chemical makeup of propylene glycol, it can safely be used in and around the fresh air supply for mining or other subsurface industrial applications since no harm can be rendered to workers that rely upon the continuous supply of clean, healthy air to provide a safe working environment.

Sigma heat is used (section 9.3) to determine the cooling duty required of an air cooling system to deliver cold dry air to a deep and hot underground mine metal for the 95th percentile summer atmospheric condition at the site of the climatic survey. Over 19 MW cooling power would be required to cool the requisite airflow to the lowest acceptable wet bulb temperature. Conservative estimation of a theoretical, renewable air cooling plant delivering a wet bulb temperature of 3.0°C (from 18.0°C atmospheric air) fresh air was determined to provide nearly 5,000 operating hours. Since the 3 summer months are nearly 2,200 hours total, less than half of the assumed 7 propylene glycol reservoir heat exchange cycles could be required to provide that 19 MW cooling.

Climatic surveys described in Section 10 show the significant value of mechanical versus evaporative air cooling systems since colder air can be delivered to deeper vertical horizons using cooler, drier airflow. Sigma heat calculated using wet bulb temperature and barometric pressure measured is used for each climatic survey station to describe the cooling potential at every location along the survey path. Using the concept of Sigma heat, thermal additions or losses from an airstream can readily be quantified from psychrometric observations (McPherson, 1993). Spikes in Sigma heat along a climatic survey network path easily identify heat sources or sinks.

The use of an inert intrinsically safe refrigerant, with an extremely low freezing point, allows storage of coolth harvested during winter to be used during the summer months. Due to the non-toxic physical and chemical makeup of propylene glycol, it can safely be used in and around the fresh air supply for mining or other subsurface industrial applications since no harm can be rendered to workers that rely upon the continuous supply of clean, healthy air to provide a safe working environment. Since propylene glycol ($C_3H_8O_2$) can be chilled to a reliable operating temperature of -20 °C (50% $C_3H_8O_2$ / 50% H_2O blend), this will allow the chilled refrigerant to be transferred much greater distances than, for example the transfer of ice into a deep and hot underground mine working environment. Due to the viscous lubricating nature of propylene glycol in a relatively high concentration mixture blend with water, piping infrastructure and pumps will last longer compared to cold water systems. Resistance of the refrigerant fluid moving through the piping network will be lower due to the viscous nature of the propylene glycol mixture, attributing to lower induced heat of the refrigerant and lower required pumping energies. Transfer of super chilled refrigerant down to deep levels of a mine will provide opportunity to develop energy recovery systems that generate electricity to pump warmed refrigerant back up to a storage reservoir installation near the surface.

Significant energy savings coupled to substantial financial benefits can be achieved through the use of renewable energy generated from natural sources. Substantial capital and operating expenses are removed from the construction costs of a typical mechanical refrigeration system relying upon high duty industrial components of the mechanical vapor compression cycle. By taking high pressure multistage screw compressors out of the equation, a majority of the electrical expenses for the refrigeration installation would be removed from the annual operating budget. Since heat rejection of heated refrigerant gas from condensing heat exchangers is taken out of the equation, there is no need to have high pressure infrastructure, including piping and valves to accommodate heat removal tasks arising from hot refrigerant gas from a traditional mechanical vapor compression cycle system. In fact, the only high pressure portion of the piping network relates to a standing vertical column of cold or warmed refrigerant passing through a deep mine shaft. The high pressure induced by the inbound cold refrigerant would be it alleviated by energy recovery systems installed at the deep shaft levels.

As previously mentioned, the omission of the refrigerant condensing circuit eliminates the necessity for heat rejection of the refrigerating fluid. This removes the substantial cost of an underground cooling tower or spray chamber to facilitate low pressure heat rejection for a water based system or a compressed refrigerant gas through high pressure condensing heat exchangers. Either way heat rejection costs are removed from the overall air cooling system budget

The cost of a high-pressure mechanical surface refrigeration plant to effectively cool an underground mine can be significant when considering all-in operating expenses and the potential to purchase off-setting carbon tax credits to provide the additional electrical generation required to power an industrial mechanical air cooling system. The development of low-pressure refrigeration systems deserves studious research and pilot plant development to bring this renewable energy technology to market.

Development of cost-effective monitoring and control systems capable of achieving the lowest possible storage temperature of the glycol reservoir will be a major deciding factor in the implementation of the proposed low-pressure refrigerant system described in this dissertation.

In practice, the plant operator would monitor the air mass wet bulb globe temperature invoking higher operating fan pressures when mixing temperatures exceed agreed upon optimal heat exchange conditions. Monitoring freezing temperature variations within the tank farm will be key in determining timing for fan control procedures. Alerting the plant operator will be instrumental in defining these procedural instructions.

Chilling the propylene glycol below minus 20 °C means that the refrigerant will maintain its cooling power much longer than chilled water. Delivering the cooling power in a distributed piping network, using thermally efficient piping material, will greatly improve the positional efficiency of distributed air cooling systems for deep and hot underground mines. Low pressure piping networks are much less expensive to acquire, install, operate and maintain than high pressure versions. Innovative use of the plate heat exchanging system can allow winter air to be warmed before passing through the burners of air heaters. By circulating warm propylene glycol through the heat exchangers, the mine intake airflow could be raised just above freezing which will dramatically reduce the amount of natural gas or propane required to heat the airflow to 6 °C. The effect of winter's wind chill will also greatly enhance the refrigerant chilling process.

14.1.1 Future Work

Supplying cold glycol harvested on the surface to underground cooling systems is a potential source of immense savings for mines that currently send cold water to hot underground mine workings. Investigation of practical, operable air cooling systems for underground mining should include maximum transfer distance, both laterally and vertically, for chilled propylene glycol transport via low pressure piping networks. Piping should be selected to render the minimum resistance while maintaining thermal shielding.

Considerable capital and operating expense is typically dedicated to coolant piping insulation. If there was one way to eliminate this necessity for insulation of the piping networks, the costs to develop and install this efficient cooling system could be quickly recovered, as it's quite well known that insulating piping networks typically costs 3 times what the piping capital costs, just in labor (Bluhm, Moreby, von Glehn, & Pascoe, 2014). Perhaps selecting a newly innovative piping material could make use of innovative recycled composites. Modeling the piping network will determine empirical values into how far the coolant can maintain effectiveness, which is to say, how much cooling energy can be supplied for a wide range of spot cooler locations.

Investigation of low-temperature polymer concretes used in cryogenics to increase reservoir storage time potential. Ultimately, additional simulations will need to be conducted. Careful estimation of the thermal flywheel effect for the given location will need to be considered during the course of these simulations.

14.2 Ice Accumulation Galleries

The ice accumulation reservoirs supplying 855 kW of cooling power continuously over the same period (5000+ hours) as the low pressure organic air conditioning system would yield over 4.2 GWh electric equivalent. According to the United States Environmental Protection Agency (EPA, 2021), 1 kWh is equivalent to 7.09e-4 metric tons CO_2 gas. This renewable cooling system could offset 3,031 tonnes CO_2 annually.

Lowering the intake airflow requirement down the ramp will significantly improve the performance of the ice accumulation galleries contribution into the overall capacity of the mine air conditioning system. Sensitivity analyses should be conducted to determine optimum airflow regimes for given atmospheric conditions of relative humidity, temperature and barometric pressure. Additional analyses should be conducted to determine optimum gallery length, cross sectional area, grade, orientation, trajectory and total number of galleries simulated for this sustainable mine air conditioning system.

Investigation of practical, operable air cooling systems for underground mining should include maximum transfer distance, both laterally and vertically, for air cooled from the ice accumulation galleries. Development of renewable energy air cooling systems for hot underground mines will ultimately benefit any operation that can take advantage of this seasonably available energy resource. Correct sizing of the air cooling system will determine the success of this type of air conditioning system. Supplying ice harvested near the surface to underground air cooling systems is a potential source of immense savings for mines that would require bulk cooling of the intake airflow of the identified mining scenario.

14.2.1 Future Work

Ultimately, additional model simulations would need to be conducted. Careful estimation of the thermal flywheel effect for the given location will need to be considered during the course of these simulations. Snowmaking sensitivity analyses should also be conducted to determine optimal nozzle types, flow rates and temperature domains for all possible snowmaking conditions. Additional analyses should be conducted to determine optimum underground psychrometric conditions including wet bulb temperature and airflow velocity. Intrinsically safe nucleation agents should also be evaluated by ongoing testing of spray water for total dissolved solids. Careful chemical evaluation of the interaction between the resident dust in the water and nucleation agents should also be considered when modeling the snow making process.

15. Contributions to Knowledge

Both innovative air cooling systems described in this dissertation will help underground mines reduce the operational carbon footprint by replacing electrical power with renewable cooling energy. Many factors contribute to the core fundamentals of sustainability. Cultural responsibility to sustainability and maintaining the environment in a safe and healthy condition lends credibility to mining operations with extensive mineral reserves that could potentially lead to strategic economic viability. Positioning a mine operation with lower capital expenditure and lower operating expenses will provide long-term economic sustainability through uncertain economic times. Innovative use of the environment and responsible care of natural resources available at the mine site will inevitably lead to a sustainable mine. Sustainable cooling systems could reduce or eliminate the need for mechanical cooling if installed with favorable conditions. Successful installations will prioritize environmental management to favor long time span usage of sustainable cooling systems.

15.1 Innovative Site Designs

Employ renewable energy to harvest and store coolth for deep mines in northern latitudes. Using the cold of wintertime to cool down refrigerant in the most cost-effective method possible, and storing the chilled refrigerant until summertime. Alignment with ideas and the pursuit of effective sustainable energy plans will save millions of dollars in both capital and operating expenses while reducing GHG emissions.

The ability to effectively use renewable energy sources in large part revolve around the ability to store that energy for use later. Planning for sustainable cooling potential requires protected space to successfully maintain chilled refrigerant in storage, at the lowest achievable temperature, until needed during summer. Stored refrigerant should be judiciously cared for, safely kept from the ill effects of heat, in order to remain useful for bulk air-cooling.

15.2 Low Pressure Organic Air Conditioning System

Cold dry air delivers greater air cooling capacity much further, vertically speaking, than saturated cool air chilled by evaporative cooling systems. This is the main attraction from dehumidified cold air that has been refrigerated with mechanical air cooling systems. Development of a renewable mine air cooling system that mimics the benefits of mechanically refrigerated air flow is certainly viable, given the field observations from the comparative climatic survey.

Overall reduction in energy consumption due to the low pressure nature of the closed loop air conditioning system will limit the mine’s carbon footprint. The use of an intrinsically safe organic refrigerant, with an extremely low freezing point, allows storage of coolth harvested from the winter to be used during the summer months. Due to the non-toxic physical and chemical makeup of propylene glycol, it can safely be used in and around the fresh air supply for mining or other subsurface industrial applications since no harm can be rendered to workers that rely upon the continuous supply of clean, healthy air to provide a safe working environment.

The conceptual propylene glycol refrigeration system can generate over 19 MW for over 5000 hours, yielding over 97.8 GWh of electrical equivalent. According to the United States Environmental Protection Agency (EPA, 2021), 1 kWh is equivalent to 7.09e-4 metric tons CO_2 gas. This renewable cooling system could offset 69,342 tonnes CO_2 annually.

Chilling the propylene glycol below minus 20 °C means that the refrigerant will maintain its cooling power much longer than chilled water. Delivering the cooling power in a distributed piping network, using thermally efficient piping material, will greatly improve the positional efficiency of distributed air cooling systems for deep and hot underground mines. Low pressure piping networks are much less expensive to acquire, install, operate and maintain than high pressure versions. Innovative use of the plate heat exchanging system can allow winter air to be warmed before passing through the burners of air heaters. By circulating warm propylene glycol through the heat exchangers, the mine intake airflow could be raised just above freezing which will dramatically reduce the amount of natural gas or propane required to heat the airflow to 6 °C. The effect of winter's wind chill will also greatly enhance the refrigerant chilling process.

15.3 Ice Accumulation Galleries for Ramp Mines

Building miniature glaciers underground will cool ramp intake airflow coming from an open pit to help large operations as they advance the mining horizon underground. Snow is produced under favorable atmospheric conditions using commercial snow making equipment typically found at ski resorts. Regulators with air locks would be installed on either end of each gallery to maintain minimum velocities during snow and ice accumulation. Using compressed air and water, snow is blown, during near-freezing conditions across snow fences arranged in an array aligned with the airflow. Snow fences are employed to maximize the snow deposition potential.

The ice accumulation reservoirs supplying 855 kW of cooling power continuously over the same period (5000+ hours) as the low pressure organic air conditioning system would yield over 4.2 GWh electric equivalent. According to the United States Environmental Protection Agency (EPA, 2021), 1 kWh is equivalent to 7.09e-4 metric tons CO_2 gas. This renewable cooling system could offset 3,031 tonnes CO_2 annually.

The system will use wastewater from the mine and recycle water during operation as the ice melts into storage sumps. Snow water quality will need to be monitored and maintained. Nucleation reagents allow for warmer snowmaking conditions that can extend seasonal usefulness especially at higher altitudes. Nucleation agents will need to be added to the reservoir water and sufficiently mixed before spraying application.

Additional geotechnical measures will be necessary to ensure pit portal integrity due to the addition of the stowed ice reservoirs. In order to maintain the highest level of safety, both surface and underground, continual monitoring of ground conditions will be maintained during the operation and maintenance of the renewable cooling ice storage facility.

References

Acuna, E., Lowndes, I.S. (2013). A review of primary mine ventilation system optimization. (confidential client report)

Anderson, J., Longson, I. (1986). The optimization of ventilation and refrigeration in British coal mines. The Mining Engineer. Vol. 146, pp 115-120.

Anderson, R.E., von Glehn F.H., Wilson, R.W. (2011). Improving the efficiency of mine ventilation and cooling systems through active controls. (confidential client report)

Arkle, K. et al (1985). Use of thermal insulation materials in mines. Journal of Mine Ventilation Society of South Africa. Vol. 38, No.4, April, pp 43-45.

AMAP (Arctic Monitoring & Assessment Programme) (2019). Arctic Ocean Acidification Assessment 2018: Summary for Policy-Makers. https://www.amap.no/documents/download/3296/inline , accessed 10-2-2020.

ASHRAE (1988). Handbook on Equipment. Ch. 20. Cooling towers. American Society of Heating, Refrigerating and Air Conditioning Engineers.

ASHRAE Handbook-Fundamentals (1997) American Society of Heating, Refrigerating and Air-conditioning Engineers.

Baker-Duly, C. et al (1988). Design of a large flexible underground refrigeration installation. 4th Int. Mine Ventilation Congress, Brisbane, Australia, pp 443-449.

Bao, L., Wang, J., Wang, J., & Yu, Z. (2017). The heat recovery technologies of mine waste heat sources. (confidential client report)

Basner, M., Babisch, W., Davis, A., Brink, M., Clark, C., Janssen, S., Stansfeld, S. (2014). Auditory and non-auditory effects of noise on health. Retrieved from: https://www.ncbi.nlm.nih.gov/pmc/articles/PMC3988259/, accessed 10-3-2020.

Bluhm, S.J. (1980). Predicting performance of spray chambers for cooling air. Heating, Refrigeration and Air Conditioning, S. Africa, pp 27-39.

Bluhm, S.J. (1981). Performance of direct contact heat exchangers. Journal of Mine Ventilation Society of South Africa. Vol. 34, Aug. and Sept., Nos. 8 and 9.

Bluhm, S.J. (1983). Spot cooling of air in direct contact heat exchangers. Report of Environmental Engineering Lab. Chamber of Mines Research Organization, South Africa.

Bluhm, S., Moreby, R., von Glehn, F., & Pascoe, C. (2014). Life-of-Mine

Ventilation and Refrigeration. The Journal of The Southern African Institute of Mining and Metallurgy, 114.

Bluhm, S., von Glehn, F., & Smit, H. (2003). Important Basics of Mine Ventilation and Cooling, Planning; Managing the Basics Conference.

Brake, D.J. (2009). Performance and Acceptance Testing of Mine Refrigeration Plants. (confidential client report)

Burrows, J. (1982). Refrigeration - theory and operation. Environmental engineering in S. African mines. Chapter 23. Published by Cape and Transvaal Printers (Pty), Cape Town, South Africa.

Butterworth, M.D., Sheer, T.J. (2011). Ejector Refrigeration Systems for Chilled Water Using High Pressure Water as the Motive Fluid.

Carpenter, K.E., Roghanchi, P., & Kocsis, K.C. (2015). Investigating the Importance of Climatic Monitoring and Modeling in Deep and Hot US Underground Mines. 15th North American Mine Ventilation Symposium.

Department of Industry and Resources. (1997). Management and Prevention of Heat Stress. Retrieved from: https://www.dmp.wa.gov.au/Documents/Safety/MSH_G_ManagementAndPreventionOfHeatStress.pdf, accessed 1-22-2019.

Del Castillo, D.O., T Baard, T., Pieters, A. (2009). Maximizing the Output of a Surface Bulk Air Cooling Installation on a South African Mine.

deRuiter, H. et al (1989). Geothermal heat recovery at Lac Minerals Ltd., Macassa Division. 91st CIMM Annual General Meeting. May, Quebec, Canada.

du Plessis, J.J., D Scott, D., Moorcraft, H.E.S. (2018). Modern Cooling Strategies for Ultra-Deep Hydropower Mines. (confidential client report)

EPA (2021). United States Environmental Protection Agency https://www.epa.gov/energy/greenhouse-gases-equivalencies-calculator-calculations-and-references, accessed 4-22-2021.

Fava, L., Millar, D., Anderson, B., Schafrik, S., O'Connor, D., Allen, C. (2012). Modeling of the Natural Heat Exchange Area at Creighton Mine for Operational Decision Support, 14th U.S./North American Mine Ventilation Symposium.

Gebler, W.F. et al (1988). The design and evaluation of a large direct-contact ice-air cooler for Vaal Reefs Gold Mine. 4th Int. Mine Ventilation Congress, Brisbane, Australia, pp 425-432.

Goss, M., Swain, D.L., Abatzoglou, J.T., Sarhadi, A., Kolden, C.A., Williams A.P., Diffenbaugh, N.S. (2020). Climate change is increasing the likelihood of extreme autumn wildfire conditions across California. https://iopscience.iop.org/article/10.1088/1748-9326/ab83a7/pdf, accessed 10-2-2020.

Hall A.E. (1985). The use of controlled recirculation ventilation to conserve energy. 2nd U.S. Mine Ventilation Symposium, Reno, NV, pp. 207-215.

Hall, A.E. et al (1988). The use of controlled recirculation to reduce heating costs in Canada. 4th Int. Mine Ventilation Congress, Brisbane, Australia, pp 301-307.

Hall, A.E. et al (1989). Controlled recirculation investigation at Central Canada Potash Division of Noranda Minerals, Inc. 4th U.S. Mine Ventilation Symposium, Berkeley, CA, pp 226-233.

Hancock, W. (1926). Local air-conditioning underground by means of refrigeration. Transactions of the Institute of Mining Engineers. London, United Kingdom, Vol. 72, pp 342-366.

Hanna, E.G., Kjellstrom, T., Bennett, C., Dear, K. (2011). Climate change and rising heat: population health implications for working people in Australia. Asia Pacific Journal of Public Health 23:14S–26S

Hardcastle, S.G., Kocsis, C.K. (2002) ‘The ventilation challenge – a Canadian perspective on maintaining a good working environment in deep mines’, Proceedings of the ACG Deep Mining Symposium, Perth, Western Australia, November, pp.4–9.

Hartman, H.L., Mutmansky, J.M. (2002). Introductory Mining Engineering. 2nd ed., John Wiley and Sons, Inc., New York, NY

Hartman, H.L., Mutmansky, J.M., Ramani, R., Wang Y.J. (1997) Mine Ventilation and Air Conditioning. 3rd ed., John Wiley and Sons, Inc., New York, NY

Heller, K. et al (1982). Development of a high performance, low maintenance, in-line water spray cooler for mines. 1st US Mine Ventilation Symposium, Tuscaloosa, AL.

Hemp, R. (1967). The performance of a spray-filled counterflow cooling tower, Journal of Mine Ventilation Society of South Africa. Vol. 25, pp 159-173.

Hemp, R. (1972). Contribution to the design of underground cooling towers by A. Whillier. Journal of Mine Ventilation Society of South Africa. Vol. 25, No.6, June, pp 85-93.

Hemp, R. (1982). Environmental engineering in South African mines, Chapter 22. Sources of heat in mines, pp 569-612. Cape and Transvaal Printers (Pty), Cape

Town, South Africa.

Hemp, R. (1988). A 29 MW ice system for mine cooling. 4th Int. Mine Ventilation Congress, Brisbane, Australia, pp 415-423.

Howes, M.J. (2010). Ventilation and cooling design for long declines. (confidential client report)

Howes, M.J., Hortin, K. (2009). Surface cooling at Kid Creek Mine. (confidential client report)

ISO 7243 (1989) Hot environments - estimation of the heat stress on working man, based on the WBGT-index (Wet Bulb Globe Temperature)

Johnson, O.S. (2000). Thermo- and Psychrometric properties of intake air passing through fragmented strata. (confidential client report)

Kjellstrom T, Lemke B, Hyatt O, Otto M (2014) Climate change and occupational health: a South African perspective. South African Medical Journal, 104(8):586

Kocsis, C.K., Hardcastle, S.G., Keen, B. (2008). A heat study and the modelling of future climatic conditions at Vale Inco's Coleman/McCreedy East Mine. (confidential client report)

Kocsis, K., & Hardcastle, S. (2010). Prediction and analysis of the underground climatic conditions and their cause in deep mechanized Canadian metal mines. (confidential client report)

Kocsis, C.K., Danko, G. (2019). Assessing, Modeling, and Cooling Underground Workings in Deep and Hot Mines. Capacity Building Report for the National Institute for Occupational Safety and Health (NIOSH).

Kurnia, J.C., Sasmito, A.P., & Mujumdar, A.S. (2014). Simulation of a novel intermittent ventilation system for underground mines. Tunneling and Underground Space Technology, 206-215.

Liu, X. (2012). "What processes control ice nucleation and its impact on ice-containing clouds?" (PDF). Pacific Northwest National Laboratory, accessed 10-26-2019.

Maizza, V., & Maizza, A. (2001). Unconventional working Fluids in organic Rankine-cycles for waste energy recovery systems. Applied Thermal Energy, 381-390.

Marx, W., von Glehn F.H., Wilson, R.W. (2012). Design of energy efficient mine ventilation and cooling systems. (confidential client report)

McAdams, W.H. (1954). Heat transmission, 3rd. ed. McGraw-Hill, New York, NY

McPherson, M.J. (1984). Mine ventilation planning in the 1980s. International Journal of Mining Engineering, 185-227.

McPherson, M.J., & Robinson, G. (1980). Barometric survey of shafts at Boulby Mine. Transactions of the Institution of Mining and Metallurgy (89A).

McPherson, M.J. (1993). Subsurface Ventilation and Environmental Engineering. Mine Ventilation Services, Inc., 1st. ed., Lafayette, CA

McPherson, M.J. (2009). Subsurface Ventilation Engineering. Mine Ventilation Services, Inc., 3rd. ed., Fresno, CA

Mine Safety and Health Administration (MSHA), (2012). Heat Stress in Mining. Retrieved from https://www.msha.gov/sites/default/files/Alerts and Hazards/Heat Stress.pdf, accessed 10-26-2019.

Moore, D.T. (1985). Geothermal air heating in a southwestern Wyoming trona mine. 2nd U.S. Mine Ventilation Symposium, Reno, NV, pp 561-570.

Mücke, G. and Uhlig, H. (1984). Performance of finned coil and water spray coolers. 3rd Int. Mine Ventilation Congress, Harrogate, United Kingdom, pp 231-237.

MVS (1990). Investigation of geothermal air heating for General Chemical's Green River soda ash operations. Mine Ventilation Services, Inc. (confidential client report)

Nevada Bureau of Mines and Geology (n.d.). Retrieved from Renewable Energy in Nevada: https://gisweb.unr.edu/RenewableEnergy/, accessed 10-3-2020.

Office of Energy Efficiency & Renewable Energy (2017). 5 Things You Should Know about Geothermal Heat Pumps. Retrieved from energy.gov: https://www.energy.gov/eere/articles/5-things-you-should-know-about-geothermal-heat-pumps, accessed 10-3-2020.

Ramsden, R. and Bluhm, S.J. (1984). Air cooling equipment used in South African gold mines. 3rd Int. Mine Ventilation Congress, Harrogate, United Kingdom, pp 243-251.

Ramsden, R. and Bluhm, S. (1985). Energy recovery turbines for use with underground air coolers. 2nd U.S. Mine Ventilation Symposium, Reno, Nevada, pp 571-580.

Ramsden, R. (1985). Insulation used on chilled water pipes in South African gold mines. Journal of Mine Ventilation Society of South Africa. Vol. 38, No.5, May, pp

49-54.

Ramsden, R., Allen, C., Millar, D., Guse, T. (2014). The use of natural cooling to delay and reduce refrigeration requirements. The Mine Ventilation Society of South Africa.

Ramsden, R., Branch, A.A.R., Wilson, R.W. (2010). Factors influencing the choice of cooling and refrigeration systems for mines. (confidential client report)

Reuther, E.U. et al (1988). Optimization of spray coolers for cooling deep coal mines. 4th Int. Mine Ventilation Congress, Brisbane, pp 451-458.

Robinson, G., Weller, R.C and McPherson, M.J. (1981). Underground environmental planning at Boulby Mine, Cleveland Potash Ltd. Trans. Inst. of Mining and Metallurgy (U.K.), July. Reprinted in the Journal of Mine Ventilation Society of South Africa. Vol. 35, No.9, Sept. 1982, pp 73-88.

Roghanchi, P., & Kocsis, K. C. (2018). Quantifying the thermal damping effect in underground vertical shafts using the nonlinear autoregressive with external input (NARX) algorithm. International Journal of Mining Science and Technology, 29(2).

Roghanchi P (2017) Managing and controlling the thermal environment in underground metal mines. Doctoral Dissertation, University of Nevada, Reno, NV.

Rose, H. (1989). Personality Profile. Journal of Mine Ventilation Society of South Africa. Vol. 42, No.6, June, pp 110-113.

Saeidi, N., Fava, L., Allen, C. (2017). Towards Improving the Performance of Creighton Mine’s Natural Heat Exchange Area, Proceedings of the 3rd World Congress on Mechanical, Chemical, and Material Engineering (MCM'17).

Schafrik, S. (2001). The use of packed sphere modelling for airflow and heat exchange analysis in broken or fragmented rock, Ph.D. Thesis: Faculty of Graduate Studies Laurentian University, Canada.

Schlotte, W., Walasiak, J. (2011). Planning of air cooling systems in mines and tunnels. (confidential client report)

Sheer, T.J. et al (1984). Research into the use of ice for cooling deep mines. 3rd Int. Mine Ventilation Congress, Harrogate, United Kingdom, pp 277-282.

Shone, R.D.C. and Sheer, T.J. (1988). An overview of research into the use of ice for cooling deep mines. 4th Int. Mine Ventilation Congress, Brisbane, Australia, pp 407-413.

Simon, C.A. (2020). Alternative Energy: Political, Economic, and Social

Feasibility. The Rowman and Littlefield Publishing Group, London, United Kingdom.

SMI Smowmakers (2012), https://www.snowmakers.com/snowmaking-advanced.html, accessed 10-2-2020.

Stachulak, J. (1989). Ventilation Strategy and Unique Air Conditioning at Inco Limited. 4th U.S. Mine Ventilation Symposium, Berkeley, CA, pp 3-9.

Stroh, R.M. (1980). Refrigeration practice on Anglo American gold mines. Mine Ventilation Soc. of S. Africa Symposium on Refrigeration and Air Conditioning. Cape and Transvaal Printers (Pty), Cape Town, South Africa.

Stroh, R.M. (1982). Environmental engineering in South African mines. Cape and Transvaal Printers (Pty), Cape Town, South Africa.

Song X,Wang S, Hu Y, Yue M, Zhang T, Liu Y, Tian J, Shang K (2017) Impact of ambient temperature on morbidity and mortality: an overview of reviews. Sci Total Environ 586:241–254.

Sylvestre, M. J.-G. (1999). Heating and Ventilation Study of Inco's Creighton Mine. M.S. thesis: Department of Mining and Metallurgical Engineering, McGill University.

Thimons, E.D. et al (1980). Water spray vent. tube cooler for hot stopes. US Bureau of Mines Technology Progress Report TPR 107.

Trewin, B., Baddour, O. (2018). Global indicators for monitoring climate change, changing levels of risk, and the attribution of extreme climate events. Eleventh meeting of the Research Dialogue: Science for Transformation [United Nations Climate Change] https://unfccc.int/sites/default/files/resource/3.7WMO_Trewinposter.pdf, accessed 10-3-2020.

Twort, C.T., Lowndes, I.S., Pickering, S.J. (2009). Novel approach to the energy analysis of mine cooling strategies. (confidential client report)

United Nations Framework Convention on Climate Change (UNFCCC) (2015). Decision 1/CP.21 - Adoption of the Paris Agreement https://unfccc.int/resource/docs/2015/cop21/eng/10a01.pdf, accessed 10-3-2020.

Van der Walt, J. (1984). Cooling the world's coldest mine. Journal of Mine Ventilation Society of South Africa. Vol. 37, No. 12, Dec., pp 138-141.

Van Vuuren, S.P.J. (1975). The optimization of pipe sizes in a refrigeration system. Journal of Mine Ventilation Society of South Africa. Vol. 28, No. 6, pp.

86-90.

Webber-Youngman, R.C.W. (2009). An integrated approach towards the optimization of ventilation, air cooling and pumping requirements for hot mines.

Weuthen, P. (1975). Air coolers in mines with moist and warm climatic conditions. 1st Int. Mine Ventilation Congress, Johannesburg, South Africa, pp 299-303.

Whillier, A. (1967). Pump efficiency determination from temperature measurements. South African Mechanical Engineer, Oct., pp 153-160.

Whillier, A. (1977). Predicting the performance of forced draught cooling towers. Journal of Mine Ventilation Society of South Africa. Vol. 30, No. 1, Jan., pp 2-25.

Whillier, A. (1982). Heat transfer: Environmental engineering in South African mines. Cape and Transvaal Printers (Pty), Cape Town, South Africa.

White, A. (2019). "How Artificial Snow Was Invented". Smithsonian, https://www.smithsonianmag.com/arts-culture/how-artificial-snow-was-invented-180973334/, accessed 10-2-2020

Wilson, R.W., Pieters, A. (2008). Design and construction of a surface air cooling and refrigeration installation at a South African mine. (confidential client report)

Xie, H., Tang, H., & Liao, Y.-H. (2009). Time series prediction based on NARX neural networks: An advanced approach. 2009 International Conference on Machine Learning and Cybernetics, (pp. 1275-1279)

Appendix A: Climatic Data

Air Branch Survey Properties

Branch #	Length (m)	Area (m^2)	Perimeter (m)	Depth (m)	VRT (°C)	Geo. Step (m/°C)	Age (days)	Description
1	164	41.9	23.00	0	7.0	63	7300	FA Plenum
2	1568	41.9	23.00	18	7.0	63	7300	No 1 Shaft FA
3	151	41.9	23.00	1586	28.6	58	7262	5400L No 1 FA
4	107	41.9	23.00	1737	30.6	58	7232	5900L No 1 FA
5	183	41.9	23.00	1844	33.7	55	7198	6200L No 1 FA
6	30	41.9	23.00	2027	34.1	55	7190	6950L No 1 FA
7	71	41.9	23.00	2057	34.8	55	7170	Sump No 1 FA
8	27	22.0	18.50	2057	34.2	55	7170	6850L Access
9	25	22.0	18.50	2057	34.2	55	1762	6850L 1
10	31	22.0	18.50	2057	34.2	55	1754	6850L 2
11	20	22.0	18.50	2057	34.2	55	1752	6850L 3
12	94	22.0	18.50	2057	34.2	55	1740	6850L 4
13	105	22.0	18.50	2057	34.2	55	1720	6850L 5
14	29	22.0	18.50	2057	34.2	55	1736	6850L 4r1
15	140	22.0	18.50	2057	34.2	55	1700	6850L 4r2
16	259	22.0	18.50	2057	34.2	55	1600	6850L 3r1
17	105	22.0	18.50	2128	35.4	55	1540	Shaft bottom ramp
18	210	22.0	18.50	2088	34.8	55	1540	FA xfr BAC
19	950	22.0	18.50	2057	34.2	55	1480	Ramp 6850-5 to 7350

Climatic Survey and Derived Data

	No Cooling					Evaporative Cooling					Mechanical Cooling				
Branch #	Dry Bulb (°C)	Wet Bulb (°C)	Pressure (kPa)	Quantity (m^3/s)	Sigma Heat (kJ/kg)	Dry Bulb (°C)	Wet Bulb (°C)	Pressure (kPa)	Quantity (m^3/s)	Sigma Heat (kJ/kg)	Dry Bulb (°C)	Wet Bulb (°C)	Pressure (kPa)	Quantity (m^3/s)	Sigma Heat (kJ/kg)
1	19.0	16.6	101.000	408.66	45.98	19.6	17.4	100.974	397.26	27.30	18.8	17.1	101.008	390.27	11.14
2	19.1	16.7	101.196	408.66	61.09	9.2	9.2	101.179	399.29	42.62	4.3	1.0	101.214	393.54	26.67
3	32.1	23.2	117.129	386.38	62.58	23.4	17.0	117.883	373.92	44.11	17.9	10.3	118.435	366.29	28.17
4	33.3	23.9	118.760	260.92	63.62	24.7	17.7	119.599	257.52	45.17	19.2	11.1	120.211	255.44	29.24
5	34.1	24.3	120.060	207.16	65.41	25.6	18.2	120.953	204.72	46.97	20.1	11.7	121.603	203.22	31.11
6	35.5	25.1	122.382	176.29	65.7	27.1	19.1	123.368	171.81	47.30	21.6	12.7	124.085	169.06	31.40
7	35.7	25.2	122.771	176.29	66.78	27.4	19.3	123.773	172.90	48.39	21.8	12.9	124.502	170.83	32.52
8	35.7	25.2	122.771	35.49	65.69	27.4	19.3	123.773	34.85	47.32	21.8	12.9	124.502	34.46	31.46
9	35.5	25.2	122.770	34.89	70.37	27.3	19.3	123.772	34.37	51.92	21.8	12.9	124.501	34.05	36.00
10	40.0	26.5	122.769	34.28	71.62	31.8	20.9	123.771	33.56	53.19	26.2	14.9	124.500	33.11	37.29
11	41.1	26.9	122.768	49.60	71.60	32.9	21.4	123.77	49.17	53.19	27.4	15.5	124.499	48.91	37.31
12	40.9	26.9	122.767	39.65	71.55	32.8	21.4	123.769	39.16	53.23	27.3	15.5	124.498	38.86	37.44
13	40.3	26.9	122.763	32.18	71.48	32.4	21.4	123.765	31.86	53.30	26.9	15.5	124.494	31.67	37.62
14	40.3	26.9	122.763	7.47	71.46	32.4	21.4	123.765	7.30	53.30	26.9	15.5	124.494	7.19	37.64
15	39.8	26.8	122.763	7.47	89.69	32.2	21.4	123.765	7.37	71.88	26.9	15.6	124.494	7.31	56.47
16	40.9	26.9	122.767	9.95	71.36	32.8	21.4	123.769	9.83	54.06	27.3	15.5	124.498	9.76	37.38
17	34.7	25.6	123.699	176.29	66.41	26.9	19.7	124.737	171.81	48.03	21.3	13.4	125.493	169.06	37.45
18	34.0	25.4	123.069	184.94	67.11	26.3	19.6	124.088	181.39	48.16	20.7	13.2	124.829	179.21	32.35
19	39.5	26.8	122.760	34.85	82.04	31.9	21.4	123.762	34.22	64.80	26.6	15.6	124.491	33.84	49.83

Appendix B: No cooling simulation results

Results Table - FA Plenum

Row	Distance (m)	Dry Bulb (°C)	Wet Bulb (°C)	Pressure (kPa)	Sigma Heat (kJ/kg)	Density (kg/m³)	Humidity (%)	VRT (°C)	MST (°C)
1	0	19.00	16.60	101.000	45.83	1.196	78.73	7.0	32.67
2	10	19.01	16.60	101.012	45.84	1.197	78.71	7.0	32.67
3	20	19.02	16.61	101.024	45.85	1.197	78.68	7.0	32.67
4	30	19.02	16.61	101.036	45.86	1.197	78.66	7.0	32.67
5	40	19.03	16.62	101.048	45.87	1.197	78.63	7.1	32.67
6	50	19.04	16.62	101.060	45.88	1.197	78.61	7.1	32.68
7	60	19.05	16.63	101.072	45.89	1.197	78.58	7.1	32.68
8	70	19.05	16.63	101.084	45.90	1.197	78.56	7.1	32.68
9	80	19.06	16.63	101.096	45.90	1.197	78.53	7.1	32.68
10	90	19.07	16.64	101.108	45.91	1.198	78.51	7.2	32.68
11	100	19.08	16.64	101.120	45.92	1.198	78.48	7.2	32.69
12	110	19.08	16.65	101.132	45.93	1.198	78.46	7.2	32.69
13	120	19.09	16.65	101.144	45.94	1.198	78.43	7.2	32.69
14	130	19.10	16.66	101.156	45.95	1.198	78.41	7.2	32.69
15	140	19.11	16.66	101.167	45.96	1.198	78.38	7.2	32.69
16	150	19.12	16.67	101.179	45.97	1.198	78.36	7.3	32.69
17	160	19.12	16.67	101.191	45.98	1.198	78.33	7.3	32.70
18	164	19.13	16.67	101.196	45.98	1.198	78.32	7.3	32.70
19	Strata heat totals: sensible heat = -23.63 kW, latent heat = 9.16 kW								
20	Other heat totals: sensible heat = 0.00 kW, latent heat = 0.00 kW								
21	Metabolic rate = 200 W/m², Skin temperature limit value = 34.98 °C								

Results Table - No 1 Shaft FA

Row	Distance (m)	Dry Bulb (°C)	Wet Bulb (°C)	Pressure (kPa)	Sigma Heat (kJ/kg)	Density (kg/m³)	Humidity (%)	VRT (°C)	MST (°C)
1	0	19.13	16.67	101.196	45.98	1.198	78.28	7.0	32.71
2	10	19.22	16.71	101.290	46.07	1.199	77.94	7.2	32.73
3	20	19.31	16.76	101.385	46.17	1.200	77.60	7.3	32.75
4	30	19.40	16.80	101.479	46.26	1.201	77.26	7.5	32.77
5	40	19.49	16.84	101.574	46.36	1.201	76.92	7.6	32.78
6	50	19.58	16.89	101.669	46.45	1.202	76.59	7.8	32.80
7	60	19.66	16.93	101.764	46.55	1.203	76.26	8.0	32.82
8	70	19.75	16.97	101.859	46.64	1.204	75.93	8.1	32.83
9	80	19.84	17.02	101.954	46.74	1.204	75.60	8.3	32.85
10	90	19.93	17.06	102.049	46.83	1.205	75.28	8.4	32.87
11	100	20.02	17.10	102.144	46.93	1.206	74.95	8.6	32.88
12	110	20.11	17.14	102.239	47.03	1.207	74.63	8.8	32.90
13	120	20.19	17.19	102.335	47.12	1.207	74.32	8.9	32.91
14	130	20.28	17.23	102.430	47.22	1.208	74.00	9.1	32.92
15	140	20.37	17.27	102.526	47.31	1.209	73.69	9.2	32.94
16	150	20.46	17.32	102.621	47.41	1.210	73.38	9.4	32.95
17	160	20.55	17.36	102.717	47.50	1.211	73.07	9.5	32.97
18	170	20.63	17.40	102.813	47.60	1.211	72.77	9.7	32.98
19	180	20.72	17.44	102.909	47.70	1.212	72.46	9.9	32.99
20	190	20.81	17.49	103.005	47.79	1.213	72.16	10.0	33.01
21	200	20.90	17.53	103.101	47.89	1.214	71.86	10.2	33.02
22	210	20.98	17.57	103.197	47.98	1.214	71.56	10.3	33.03
23	220	21.07	17.62	103.293	48.08	1.215	71.27	10.5	33.04
24	230	21.16	17.66	103.390	48.17	1.216	70.98	10.7	33.05
25	240	21.25	17.70	103.486	48.27	1.217	70.69	10.8	33.07
26	250	21.33	17.74	103.583	48.37	1.217	70.40	11.0	33.08
27	260	21.42	17.79	103.679	48.46	1.218	70.11	11.1	33.09
28	270	21.51	17.83	103.776	48.56	1.219	69.83	11.3	33.10
29	280	21.59	17.87	103.873	48.65	1.220	69.54	11.4	33.11
30	290	21.68	17.92	103.970	48.75	1.221	69.26	11.6	33.12
31	300	21.77	17.96	104.067	48.84	1.221	68.99	11.8	33.13
32	310	21.85	18.00	104.164	48.94	1.222	68.71	11.9	33.14
33	320	21.94	18.04	104.261	49.04	1.223	68.43	12.1	33.15
34	330	22.03	18.09	104.358	49.13	1.224	68.16	12.2	33.16
35	340	22.11	18.13	104.455	49.23	1.224	67.89	12.4	33.17
36	350	22.20	18.17	104.553	49.32	1.225	67.62	12.6	33.19
37	360	22.28	18.21	104.650	49.42	1.226	67.36	12.7	33.20
38	370	22.37	18.26	104.748	49.52	1.227	67.09	12.9	33.21
39	380	22.46	18.30	104.846	49.61	1.228	66.83	13.0	33.22
40	390	22.54	18.34	104.944	49.71	1.228	66.57	13.2	33.22
41	400	22.63	18.38	105.041	49.80	1.229	66.31	13.4	33.23
42	410	22.71	18.43	105.139	49.90	1.230	66.05	13.5	33.24
43	420	22.80	18.47	105.238	49.99	1.231	65.79	13.7	33.25
44	430	22.88	18.51	105.336	50.09	1.231	65.54	13.8	33.26
45	440	22.97	18.55	105.434	50.19	1.232	65.29	14.0	33.27
46	450	23.05	18.60	105.532	50.28	1.233	65.04	14.1	33.28
47	460	23.14	18.64	105.631	50.38	1.234	64.79	14.3	33.29
48	470	23.23	18.68	105.729	50.47	1.235	64.54	14.5	33.30
49	480	23.31	18.72	105.828	50.57	1.235	64.29	14.6	33.31
50	490	23.40	18.77	105.927	50.67	1.236	64.05	14.8	33.32
51	500	23.48	18.81	106.025	50.76	1.237	63.81	14.9	33.33
52	510	23.56	18.85	106.124	50.86	1.238	63.57	15.1	33.34

Results Table - No 1 Shaft FA

Row	Distance (m)	Dry Bulb (°C)	Wet Bulb (°C)	Pressure (kPa)	Sigma Heat (kJ/kg)	Density (kg/m³)	Humidity (%)	VRT (°C)	MST (°C)
53	520	23.65	18.89	106.223	50.95	1.239	63.33	15.3	33.34
54	530	23.73	18.93	106.322	51.05	1.239	63.09	15.4	33.35
55	540	23.82	18.98	106.422	51.15	1.240	62.86	15.6	33.36
56	550	23.90	19.02	106.521	51.24	1.241	62.62	15.7	33.37
57	560	23.99	19.06	106.620	51.34	1.242	62.39	15.9	33.38
58	570	24.07	19.10	106.720	51.44	1.243	62.16	16.1	33.39
59	580	24.16	19.15	106.819	51.53	1.243	61.93	16.2	33.40
60	590	24.24	19.19	106.919	51.63	1.244	61.70	16.4	33.40
61	600	24.32	19.23	107.019	51.72	1.245	61.48	16.5	33.41
62	610	24.41	19.27	107.119	51.82	1.246	61.25	16.7	33.42
63	620	24.49	19.31	107.219	51.92	1.247	61.03	16.8	33.43
64	630	24.58	19.36	107.319	52.01	1.247	60.81	17.0	33.44
65	640	24.66	19.40	107.419	52.11	1.248	60.59	17.2	33.44
66	650	24.74	19.44	107.519	52.20	1.249	60.37	17.3	33.45
67	660	24.83	19.48	107.619	52.30	1.250	60.15	17.5	33.46
68	670	24.91	19.52	107.720	52.40	1.251	59.93	17.6	33.47
69	680	24.99	19.57	107.820	52.49	1.252	59.72	17.8	33.48
70	690	25.08	19.61	107.921	52.59	1.252	59.50	17.9	33.48
71	700	25.16	19.65	108.021	52.69	1.253	59.29	18.1	33.49
72	710	25.24	19.69	108.122	52.78	1.254	59.08	18.3	33.50
73	720	25.33	19.73	108.223	52.88	1.255	58.87	18.4	33.51
74	730	25.41	19.78	108.324	52.97	1.256	58.67	18.6	33.52
75	740	25.49	19.82	108.425	53.07	1.256	58.46	18.8	33.52
76	750	25.58	19.86	108.526	53.17	1.257	58.25	18.9	33.53
77	760	25.66	19.90	108.627	53.26	1.258	58.05	19.1	33.54
78	770	25.74	19.94	108.729	53.36	1.259	57.85	19.2	33.55
79	780	25.82	19.99	108.830	53.46	1.260	57.65	19.4	33.55
80	790	25.91	20.03	108.932	53.55	1.261	57.45	19.5	33.56
81	800	25.99	20.07	109.033	53.65	1.261	57.25	19.7	33.57
82	810	26.07	20.11	109.135	53.75	1.262	57.05	19.9	33.58
83	820	26.15	20.15	109.237	53.84	1.263	56.86	20.0	33.58
84	830	26.24	20.19	109.339	53.94	1.264	56.66	20.2	33.59
85	840	26.32	20.24	109.441	54.04	1.265	56.47	20.3	33.60
86	850	26.40	20.28	109.543	54.13	1.265	56.28	20.5	33.61
87	860	26.48	20.32	109.645	54.23	1.266	56.08	20.6	33.61
88	870	26.57	20.36	109.747	54.32	1.267	55.89	20.8	33.62
89	880	26.65	20.40	109.850	54.42	1.268	55.71	21.0	33.63
90	890	26.73	20.44	109.952	54.52	1.269	55.52	21.1	33.64
91	900	26.81	20.49	110.055	54.61	1.270	55.33	21.3	33.64
92	910	26.89	20.53	110.158	54.71	1.270	55.15	21.4	33.65
93	920	26.98	20.57	110.260	54.81	1.271	54.96	21.6	33.66
94	930	27.06	20.61	110.363	54.90	1.272	54.78	21.8	33.67
95	940	27.14	20.65	110.466	55.00	1.273	54.60	21.9	33.67
96	950	27.22	20.69	110.569	55.10	1.274	54.42	22.1	33.68
97	960	27.30	20.74	110.672	55.19	1.275	54.24	22.2	33.69
98	970	27.38	20.78	110.776	55.29	1.275	54.06	22.4	33.69
99	980	27.46	20.82	110.879	55.39	1.276	53.88	22.6	33.70
100	990	27.55	20.86	110.982	55.48	1.277	53.71	22.7	33.71
101	1000	27.63	20.90	111.086	55.58	1.278	53.53	22.9	33.72
102	1010	27.71	20.94	111.190	55.68	1.279	53.36	23.0	33.73
103	1020	27.79	20.99	111.293	55.77	1.280	53.19	23.2	33.73
104	1030	27.87	21.03	111.397	55.87	1.281	53.01	23.4	33.74

Results Table - No 1 Shaft FA

Row	Distance (m)	Dry Bulb (°C)	Wet Bulb (°C)	Pressure (kPa)	Sigma Heat (kJ/kg)	Density (kg/m³)	Humidity (%)	VRT (°C)	MST (°C)
105	1040	27.95	21.07	111.501	55.97	1.281	52.84	23.5	33.75
106	1050	28.03	21.11	111.605	56.06	1.282	52.67	23.7	33.75
107	1060	28.11	21.15	111.709	56.16	1.283	52.50	23.8	33.76
108	1070	28.19	21.19	111.814	56.26	1.284	52.34	24.0	33.77
109	1080	28.27	21.23	111.918	56.35	1.285	52.17	24.1	33.78
110	1090	28.35	21.28	112.022	56.45	1.286	52.00	24.3	33.78
111	1100	28.43	21.32	112.127	56.55	1.286	51.84	24.5	33.79
112	1110	28.51	21.36	112.231	56.65	1.287	51.68	24.6	33.80
113	1120	28.59	21.40	112.336	56.74	1.288	51.51	24.8	33.81
114	1130	28.68	21.44	112.441	56.84	1.289	51.35	24.9	33.81
115	1140	28.76	21.48	112.546	56.94	1.290	51.19	25.1	33.82
116	1150	28.84	21.52	112.651	57.03	1.291	51.03	25.3	33.83
117	1160	28.92	21.56	112.756	57.13	1.292	50.87	25.4	33.84
118	1170	29.00	21.61	112.861	57.23	1.292	50.71	25.6	33.84
119	1180	29.08	21.65	112.966	57.32	1.293	50.56	25.7	33.85
120	1190	29.16	21.69	113.072	57.42	1.294	50.40	25.9	33.86
121	1200	29.24	21.73	113.177	57.52	1.295	50.25	26.1	33.87
122	1210	29.32	21.77	113.283	57.61	1.296	50.09	26.2	33.87
123	1220	29.39	21.81	113.389	57.71	1.297	49.94	26.4	33.88
124	1230	29.47	21.85	113.494	57.81	1.298	49.79	26.5	33.89
125	1240	29.55	21.89	113.600	57.90	1.299	49.64	26.7	33.89
126	1250	29.63	21.93	113.706	58.00	1.299	49.48	26.8	33.90
127	1260	29.71	21.98	113.812	58.10	1.300	49.33	27.0	33.91
128	1270	29.79	22.02	113.919	58.20	1.301	49.19	27.2	33.92
129	1280	29.87	22.06	114.025	58.29	1.302	49.04	27.3	33.92
130	1290	29.95	22.10	114.131	58.39	1.303	48.89	27.5	33.93
131	1300	30.03	22.14	114.238	58.49	1.304	48.74	27.6	33.94
132	1310	30.11	22.18	114.344	58.58	1.305	48.60	27.8	33.95
133	1320	30.19	22.22	114.451	58.68	1.305	48.45	27.9	33.95
134	1330	30.27	22.26	114.558	58.78	1.306	48.31	28.1	33.96
135	1340	30.35	22.30	114.665	58.88	1.307	48.17	28.3	33.97
136	1350	30.43	22.35	114.772	58.97	1.308	48.03	28.4	33.98
137	1360	30.50	22.39	114.879	59.07	1.309	47.88	28.6	33.98
138	1370	30.58	22.43	114.986	59.17	1.310	47.74	28.8	33.99
139	1380	30.66	22.47	115.093	59.26	1.311	47.60	28.9	34.00
140	1390	30.74	22.51	115.201	59.36	1.312	47.47	29.1	34.01
141	1400	30.82	22.55	115.308	59.46	1.312	47.33	29.2	34.01
142	1410	30.90	22.59	115.416	59.56	1.313	47.19	29.4	34.02
143	1420	30.98	22.63	115.523	59.65	1.314	47.05	29.5	34.03
144	1430	31.05	22.67	115.631	59.75	1.315	46.92	29.7	34.04
145	1440	31.13	22.71	115.739	59.85	1.316	46.78	29.9	34.04
146	1450	31.21	22.75	115.847	59.95	1.317	46.65	30.0	34.05
147	1460	31.29	22.80	115.955	60.04	1.318	46.52	30.2	34.06
148	1470	31.37	22.84	116.063	60.14	1.319	46.38	30.3	34.06
149	1480	31.45	22.88	116.172	60.24	1.320	46.25	30.5	34.07
150	1490	31.52	22.92	116.280	60.33	1.320	46.12	30.6	34.08
151	1500	31.60	22.96	116.388	60.43	1.321	45.99	30.8	34.09
152	1510	31.68	23.00	116.497	60.53	1.322	45.86	31.0	34.10
153	1520	31.76	23.04	116.606	60.63	1.323	45.73	31.1	34.10
154	1530	31.84	23.08	116.714	60.72	1.324	45.60	31.3	34.11
155	1540	31.91	23.12	116.823	60.82	1.325	45.47	31.4	34.12
156	1550	31.99	23.16	116.932	60.92	1.326	45.35	31.6	34.13

Results Table - No 1 Shaft FA

Row	Distance (m)	Dry Bulb (°C)	Wet Bulb (°C)	Pressure (kPa)	Sigma Heat (kJ/kg)	Density (kg/m³)	Humidity (%)	VRT (°C)	MST (°C)
157	1560	32.07	23.20	117.041	61.02	1.327	45.22	31.8	34.13
158	1568	32.13	23.24	117.129	61.09	1.327	45.12	31.9	34.14
159	Strata heat totals: sensible heat = -1076.54 kW, latent heat = 1008.79 kW								
160	Other heat totals: sensible heat = 0.00 kW, latent heat = 0.00 kW								
161	Metabolic rate = 200 W/m², Skin temperature limit value = 34.98 °C								

Results Table - 5400L No 1 FA

Row	Distance (m)	Dry Bulb (°C)	Wet Bulb (°C)	Pressure (kPa)	Sigma Heat (kJ/kg)	Density (kg/m³)	Humidity (%)	VRT (°C)	MST (°C)
1	0	32.13	23.24	117.129	61.11	1.327	45.15	28.6	34.13
2	10	32.21	23.28	117.236	61.21	1.328	45.03	28.8	34.14
3	20	32.28	23.32	117.344	61.30	1.329	44.90	28.9	34.15
4	30	32.36	23.36	117.451	61.40	1.330	44.78	29.1	34.16
5	40	32.44	23.40	117.559	61.50	1.331	44.66	29.3	34.16
6	50	32.52	23.44	117.666	61.59	1.332	44.53	29.5	34.17
7	60	32.59	23.48	117.774	61.69	1.333	44.41	29.6	34.18
8	70	32.67	23.52	117.882	61.79	1.333	44.29	29.8	34.19
9	80	32.75	23.56	117.990	61.89	1.334	44.17	30.0	34.20
10	90	32.82	23.60	118.098	61.98	1.335	44.05	30.1	34.20
11	100	32.90	23.64	118.206	62.08	1.336	43.93	30.3	34.21
12	110	32.98	23.68	118.315	62.18	1.337	43.81	30.5	34.22
13	120	33.05	23.72	118.423	62.27	1.338	43.69	30.7	34.23
14	130	33.13	23.76	118.532	62.37	1.339	43.58	30.8	34.24
15	140	33.21	23.80	118.640	62.47	1.340	43.46	31.0	34.24
16	151	33.29	23.85	118.760	62.58	1.341	43.33	31.2	34.25
17	Strata heat totals: sensible heat = -155.57 kW, latent heat = 153.14 kW								
18	Other heat totals: sensible heat = 0.00 kW, latent heat = 0.00 kW								
19	Metabolic rate = 200 W/m², Skin temperature limit value = 34.98 °C								

Results Table - 5900L No 1 FA

Row	Distance (m)	Dry Bulb (°C)	Wet Bulb (°C)	Pressure (kPa)	Sigma Heat (kJ/kg)	Density (kg/m³)	Humidity (%)	VRT (°C)	MST (°C)
1	0	33.29	23.85	118.760	62.58	1.340	43.35	30.6	34.32
2	10	33.37	23.89	118.881	62.68	1.342	43.24	30.8	34.33
3	20	33.44	23.93	119.002	62.78	1.343	43.14	30.9	34.34
4	30	33.52	23.97	119.123	62.87	1.344	43.03	31.1	34.35
5	40	33.59	24.01	119.245	62.97	1.345	42.92	31.3	34.35
6	50	33.67	24.06	119.366	63.07	1.346	42.82	31.5	34.36
7	60	33.74	24.10	119.488	63.17	1.347	42.71	31.6	34.37
8	70	33.82	24.14	119.609	63.26	1.348	42.61	31.8	34.38
9	80	33.89	24.18	119.731	63.36	1.349	42.51	32.0	34.39
10	90	33.97	24.22	119.853	63.46	1.350	42.40	32.1	34.40
11	100	34.04	24.26	119.975	63.55	1.351	42.30	32.3	34.40
12	107	34.09	24.29	120.060	63.62	1.352	42.23	32.4	34.41
13	Strata heat totals: sensible heat = -81.66 kW, latent heat = 80.49 kW								
14	Other heat totals: sensible heat = 0.00 kW, latent heat = 0.00 kW								
15	Metabolic rate = 200 W/m², Skin temperature limit value = 34.98 °C								

Results Table - 6200L No 1 FA

Row	Distance (m)	Dry Bulb (°C)	Wet Bulb (°C)	Pressure (kPa)	Sigma Heat (kJ/kg)	Density (kg/m³)	Humidity (%)	VRT (°C)	MST (°C)
1	0	34.09	24.29	120.060	63.62	1.351	42.24	33.7	34.45
2	10	34.16	24.33	120.186	63.72	1.353	42.14	33.9	34.46
3	20	34.24	24.37	120.312	63.81	1.354	42.05	34.1	34.47
4	30	34.31	24.41	120.438	63.91	1.355	41.95	34.3	34.48
5	40	34.39	24.46	120.564	64.01	1.356	41.85	34.4	34.49
6	50	34.46	24.50	120.691	64.11	1.357	41.76	34.6	34.50
7	60	34.54	24.54	120.817	64.20	1.358	41.66	34.8	34.51
8	70	34.61	24.58	120.944	64.30	1.359	41.56	35.0	34.51
9	80	34.69	24.62	121.071	64.40	1.360	41.47	35.1	34.52
10	90	34.76	24.66	121.197	64.50	1.361	41.37	35.3	34.53
11	100	34.83	24.71	121.324	64.60	1.363	41.28	35.5	34.54
12	110	34.91	24.75	121.451	64.69	1.364	41.18	35.7	34.55
13	120	34.98	24.79	121.579	64.79	1.365	41.09	35.9	34.56
14	130	35.06	24.83	121.706	64.89	1.366	41.00	36.1	34.57
15	140	35.13	24.87	121.833	64.99	1.367	40.90	36.3	34.58
16	150	35.21	24.91	121.961	65.08	1.368	40.81	36.4	34.59
17	160	35.28	24.95	122.088	65.18	1.369	40.72	36.6	34.59
18	170	35.35	25.00	122.216	65.28	1.370	40.63	36.8	34.61
19	180	35.43	25.04	122.344	65.38	1.371	40.54	37.0	34.65
20	183	35.45	25.05	122.382	65.41	1.372	40.51	37.0	34.67
21	Strata heat totals: sensible heat = -116.09 kW, latent heat = 117.99 kW								
22	Other heat totals: sensible heat = 0.00 kW, latent heat = 0.00 kW								
23	Metabolic rate = 200 W/m², Skin temperature limit value = 34.98 °C								

Results Table - 6950L No 1 FA

Row	Distance (m)	Dry Bulb (°C)	Wet Bulb (°C)	Pressure (kPa)	Sigma Heat (kJ/kg)	Density (kg/m³)	Humidity (%)	VRT (°C)	MST (°C)
1	0	35.45	25.05	122.382	65.41	1.371	40.51	34.1	34.75
2	10	35.52	25.09	122.512	65.51	1.373	40.42	34.3	34.80
3	20	35.60	25.13	122.641	65.60	1.374	40.34	34.5	34.84
4	30	35.67	25.17	122.771	65.70	1.375	40.25	34.6	34.88
5	Strata heat totals: sensible heat = -17.57 kW, latent heat = 17.48 kW								
6	Other heat totals: sensible heat = 0.00 kW, latent heat = 0.00 kW								
7	Metabolic rate = 200 W/m², Skin temperature limit value = 34.98 °C								

Results Table - Sump No 1 FA

Row	Distance (m)	Dry Bulb (°C)	Wet Bulb (°C)	Pressure (kPa)	Sigma Heat (kJ/kg)	Density (kg/m³)	Humidity (%)	VRT (°C)	MST (°C)
1	0	35.67	25.17	122.771	65.69	1.375	40.23	34.8	34.88
2	10	35.46	25.21	122.901	65.79	1.377	41.16	35.0	34.88
3	20	35.26	25.25	123.031	65.89	1.380	42.08	35.2	34.88
4	30	35.44	25.40	123.162	66.36	1.380	42.13	35.4	35.00
5	40	35.24	25.44	123.292	66.47	1.382	43.03	35.5	35.00
6	50	35.06	25.48	123.423	66.57	1.385	43.93	35.7	35.01
7	60	34.88	25.52	123.554	66.67	1.387	44.81	35.9	35.01
8	71	34.69	25.57	123.699	66.78	1.389	45.77	36.1	35.01
9	Electric heat source at 29 m, sensible heat = 90.00 kW								
10	Strata heat totals: sensible heat = -499.99 kW, latent heat = 505.09 kW								
11	Other heat totals: sensible heat = 90.00 kW, latent heat = 0.00 kW								
12	Metabolic rate = 200 W/m², Skin temperature limit value = 34.98 °C								

Results Table - 6850L Access

Row	Distance (m)	Dry Bulb (°C)	Wet Bulb (°C)	Pressure (kPa)	Sigma Heat (kJ/kg)	Density (kg/m³)	Humidity (%)	VRT (°C)	MST (°C)
1	0	35.67	25.17	122.771	65.69	1.375	40.23	34.2	35.49
2	10	35.62	25.17	122.771	65.69	1.375	40.41	34.2	35.48
3	20	35.57	25.17	122.770	65.69	1.375	40.58	34.2	35.47
4	27	35.54	25.17	122.770	65.69	1.376	40.71	34.2	35.46
5	Strata heat totals: sensible heat = -6.65 kW, latent heat = 6.59 kW								
6	Other heat totals: sensible heat = 0.00 kW, latent heat = 0.00 kW								
7	Metabolic rate = 200 W/m², Skin temperature limit value = 34.98 °C								

Results Table - 6850L 1

Row	Distance (m)	Dry Bulb (°C)	Wet Bulb (°C)	Pressure (kPa)	Sigma Heat (kJ/kg)	Density (kg/m³)	Humidity (%)	VRT (°C)	MST (°C)
1	0	35.54	25.17	122.770	65.69	1.375	40.70	34.2	35.47
2	10	35.49	25.17	122.770	65.69	1.376	40.88	34.2	35.46
3	20	35.44	25.17	122.769	65.69	1.376	41.06	34.2	35.46
4	25	40.03	26.52	122.769	70.37	1.356	32.04	34.2	37.01
5	Electric heat source at 20 m, sensible heat = 225.00 kW								
6	Strata heat totals: sensible heat = -6.03 kW, latent heat = 5.99 kW								
7	Other heat totals: sensible heat = 225.00 kW, latent heat = 0.00 kW								
8	Metabolic rate = 200 W/m², Skin temperature limit value = 34.98 °C								

Results Table - 6850L 2

Row	Distance (m)	Dry Bulb (°C)	Wet Bulb (°C)	Pressure (kPa)	Sigma Heat (kJ/kg)	Density (kg/m³)	Humidity (%)	VRT (°C)	MST (°C)
1	0	40.03	26.52	122.769	70.36	1.356	32.04	34.2	37.03
2	10	40.59	26.70	122.769	71.00	1.353	31.17	34.2	37.22
3	20	40.52	26.70	122.768	70.99	1.354	31.37	34.2	37.21
4	31	41.07	26.87	122.768	71.62	1.351	30.54	34.2	37.40
5	Electric heat source at 1 m, sensible heat = 30.00 kW								
6	Electric heat source at 29 m, sensible heat = 30.00 kW								
7	Strata heat totals: sensible heat = -11.06 kW, latent heat = 9.79 kW								
8	Other heat totals: sensible heat = 60.00 kW, latent heat = 0.00 kW								
9	Metabolic rate = 200 W/m², Skin temperature limit value = 34.98 °C								

Results Table - 6850L 3

Row	Distance (m)	Dry Bulb (°C)	Wet Bulb (°C)	Pressure (kPa)	Sigma Heat (kJ/kg)	Density (kg/m³)	Humidity (%)	VRT (°C)	MST (°C)
1	0	41.07	26.87	122.768	71.61	1.351	30.52	34.2	37.18
2	10	41.00	26.87	122.767	71.61	1.351	30.70	34.2	37.17
3	20	40.93	26.87	122.767	71.60	1.352	30.88	34.2	37.16
4	Strata heat totals: sensible heat = -9.55 kW, latent heat = 8.61 kW								
5	Other heat totals: sensible heat = 0.00 kW, latent heat = 0.00 kW								
6	Metabolic rate = 200 W/m², Skin temperature limit value = 34.98 °C								

Results Table - 6850L 4

Row	Distance (m)	Dry Bulb (°C)	Wet Bulb (°C)	Pressure (kPa)	Sigma Heat (kJ/kg)	Density (kg/m³)	Humidity (%)	VRT (°C)	MST (°C)
1	0	40.93	26.87	122.767	71.62	1.351	30.90	34.2	37.29
2	10	40.86	26.87	122.767	71.61	1.352	31.09	34.2	37.28
3	20	40.78	26.86	122.766	71.60	1.352	31.28	34.2	37.27
4	30	40.71	26.86	122.766	71.59	1.353	31.47	34.2	37.25
5	40	40.63	26.86	122.765	71.59	1.353	31.66	34.2	37.24
6	50	40.56	26.86	122.765	71.58	1.353	31.85	34.2	37.23
7	60	40.49	26.85	122.765	71.57	1.353	32.04	34.2	37.22
8	70	40.42	26.85	122.764	71.56	1.354	32.23	34.2	37.20
9	80	40.35	26.85	122.764	71.56	1.354	32.42	34.2	37.19
10	90	40.28	26.85	122.763	71.55	1.354	32.61	34.2	37.18
11	94	40.25	26.85	122.763	71.55	1.354	32.69	34.2	37.17
12	Strata heat totals: sensible heat = -37.18 kW, latent heat = 33.10 kW								
13	Other heat totals: sensible heat = 0.00 kW, latent heat = 0.00 kW								
14	Metabolic rate = 200 W/m², Skin temperature limit value = 34.98 °C								

Results Table - 6850L 5

Row	Distance (m)	Dry Bulb (°C)	Wet Bulb (°C)	Pressure (kPa)	Sigma Heat (kJ/kg)	Density (kg/m³)	Humidity (%)	VRT (°C)	MST (°C)
1	0	40.25	26.85	122.763	71.56	1.354	32.69	34.2	37.30
2	10	40.17	26.85	122.763	71.56	1.355	32.90	34.2	37.28
3	20	40.10	26.84	122.762	71.55	1.355	33.10	34.2	37.27
4	30	40.02	26.84	122.762	71.54	1.355	33.30	34.2	37.26
5	40	39.95	26.84	122.762	71.53	1.356	33.51	34.2	37.24
6	50	39.88	26.84	122.762	71.52	1.356	33.71	34.2	37.23
7	60	39.80	26.83	122.761	71.51	1.356	33.91	34.2	37.22
8	70	39.73	26.83	122.761	71.51	1.356	34.11	34.2	37.20
9	80	39.66	26.83	122.761	71.50	1.357	34.31	34.2	37.19
10	90	39.59	26.83	122.761	71.49	1.357	34.52	34.2	37.18
11	100	39.52	26.82	122.760	71.48	1.357	34.72	34.2	37.17
12	105	39.48	26.82	122.760	71.48	1.357	34.82	34.2	37.16
13	Strata heat totals: sensible heat = -34.03 kW, latent heat = 30.09 kW								
14	Other heat totals: sensible heat = 0.00 kW, latent heat = 0.00 kW								
15	Metabolic rate = 200 W/m², Skin temperature limit value = 34.98 °C								

Results Table - 6850L 4r1

Row	Distance (m)	Dry Bulb (°C)	Wet Bulb (°C)	Pressure (kPa)	Sigma Heat (kJ/kg)	Density (kg/m³)	Humidity (%)	VRT (°C)	MST (°C)
1	0	40.25	26.85	122.763	71.56	1.354	32.69	34.2	38.04
2	10	40.09	26.84	122.763	71.53	1.355	33.10	34.2	38.00
3	20	39.94	26.83	122.763	71.49	1.356	33.51	34.2	37.97
4	29	39.80	26.82	122.763	71.46	1.356	33.88	34.2	37.95
5	Strata heat totals: sensible heat = -4.66 kW, latent heat = 3.58 kW								
6	Other heat totals: sensible heat = 0.00 kW, latent heat = 0.00 kW								
7	Metabolic rate = 200 W/m², Skin temperature limit value = 34.98 °C								

Results Table - 6850L 4r2

Row	Distance (m)	Dry Bulb (°C)	Wet Bulb (°C)	Pressure (kPa)	Sigma Heat (kJ/kg)	Density (kg/m³)	Humidity (%)	VRT (°C)	MST (°C)
1	0	39.80	26.82	122.763	71.47	1.356	33.87	34.2	37.95
2	10	39.65	26.81	122.763	71.43	1.357	34.28	34.2	37.92
3	20	39.50	26.80	122.763	71.40	1.357	34.68	34.2	37.89
4	30	39.35	26.79	122.763	71.37	1.358	35.08	34.2	37.86
5	40	58.15	31.69	122.763	90.57	1.281	13.72	34.2	43.65
6	50	58.44	31.82	122.763	91.14	1.280	13.65	34.2	43.77
7	60	58.00	31.78	122.763	90.96	1.281	14.05	34.2	43.68
8	70	57.57	31.74	122.763	90.80	1.283	14.45	34.2	43.59
9	80	57.15	31.69	122.763	90.63	1.285	14.86	34.2	43.50
10	90	56.73	31.65	122.763	90.47	1.286	15.27	34.2	43.41
11	100	56.32	31.61	122.763	90.31	1.288	15.69	34.2	43.33
12	110	55.92	31.58	122.763	90.15	1.289	16.11	34.2	43.25
13	120	55.53	31.54	122.763	89.99	1.291	16.54	34.2	43.16
14	130	55.14	31.50	122.763	89.84	1.292	16.97	34.2	43.08
15	140	54.76	31.46	122.763	89.69	1.293	17.40	34.2	43.00
16	Electric heat source at 30 m, sensible heat = 195.00 kW								
17	Electric heat source at 40 m, sensible heat = 7.50 kW								
18	Strata heat totals: sensible heat = -48.57 kW, latent heat = 30.39 kW								
19	Other heat totals: sensible heat = 202.50 kW, latent heat = 0.00 kW								
20	Metabolic rate = 200 W/m², Skin temperature limit value = 34.98 °C								

Results Table - 6850L 3r1

Row	Distance (m)	Dry Bulb (°C)	Wet Bulb (°C)	Pressure (kPa)	Sigma Heat (kJ/kg)	Density (kg/m³)	Humidity (%)	VRT (°C)	MST (°C)
1	0	40.93	26.87	122.767	71.62	1.351	30.90	34.2	38.04
2	10	40.80	26.87	122.783	71.60	1.352	31.23	34.2	38.02
3	20	40.67	26.86	122.799	71.58	1.353	31.56	34.2	38.00
4	30	40.55	26.86	122.815	71.56	1.354	31.89	34.3	37.98
5	40	40.42	26.85	122.830	71.54	1.354	32.21	34.3	37.95
6	50	40.30	26.85	122.846	71.53	1.355	32.54	34.3	37.93
7	60	40.18	26.85	122.862	71.51	1.356	32.87	34.3	37.91
8	70	40.06	26.84	122.878	71.50	1.356	33.20	34.4	37.89
9	80	39.94	26.84	122.894	71.48	1.357	33.52	34.4	37.87
10	90	39.82	26.84	122.910	71.47	1.358	33.85	34.4	37.85
11	100	39.71	26.83	122.926	71.46	1.358	34.17	34.4	37.84
12	110	39.60	26.83	122.942	71.45	1.359	34.49	34.4	37.82
13	120	39.49	26.83	122.958	71.44	1.360	34.81	34.5	37.80
14	130	39.38	26.83	122.974	71.43	1.360	35.13	34.5	37.78
15	140	39.27	26.83	122.990	71.42	1.361	35.45	34.5	37.77
16	150	39.16	26.82	123.006	71.41	1.361	35.77	34.5	37.75
17	160	39.06	26.82	123.022	71.40	1.362	36.08	34.5	37.73
18	170	38.95	26.82	123.038	71.39	1.363	36.40	34.6	37.72
19	180	38.85	26.82	123.053	71.38	1.363	36.71	34.6	37.70
20	190	38.75	26.82	123.069	71.38	1.364	37.03	34.6	37.68
21	200	38.65	26.82	123.085	71.37	1.364	37.34	34.6	37.67
22	210	38.56	26.82	123.101	71.37	1.365	37.65	34.7	37.65
23	220	38.46	26.82	123.117	71.36	1.366	37.96	34.7	37.64
24	230	38.36	26.82	123.133	71.36	1.366	38.26	34.7	37.63
25	240	38.27	26.82	123.150	71.36	1.367	38.57	34.7	37.61
26	250	38.18	26.82	123.166	71.36	1.367	38.87	34.7	37.60
27	259	38.10	26.82	123.180	71.36	1.368	39.14	34.8	37.59
28	Strata heat totals: sensible heat = -42.82 kW, latent heat = 34.89 kW								
29	Other heat totals: sensible heat = 0.00 kW, latent heat = 0.00 kW								
30	Metabolic rate = 200 W/m², Skin temperature limit value = 34.98 °C								

Results Table - Shaft bottom ramp

Row	Distance (m)	Dry Bulb (°C)	Wet Bulb (°C)	Pressure (kPa)	Sigma Heat (kJ/kg)	Density (kg/m³)	Humidity (%)	VRT (°C)	MST (°C)
1	0	34.69	25.57	123.699	66.79	1.389	45.78	35.4	34.66
2	10	34.62	25.55	123.639	66.75	1.389	45.98	35.3	34.64
3	20	34.55	25.54	123.579	66.71	1.388	46.17	35.3	34.61
4	30	34.49	25.52	123.519	66.68	1.388	46.37	35.2	34.59
5	40	34.42	25.50	123.459	66.64	1.388	46.57	35.1	34.56
6	50	34.35	25.49	123.399	66.61	1.387	46.77	35.0	34.54
7	60	34.28	25.47	123.339	66.57	1.387	46.97	35.0	34.52
8	70	34.21	25.45	123.279	66.53	1.386	47.17	34.9	34.49
9	80	34.15	25.44	123.219	66.50	1.386	47.37	34.9	34.48
10	90	34.08	25.42	123.159	66.46	1.386	47.57	34.8	34.48
11	100	34.01	25.40	123.099	66.42	1.385	47.77	34.7	34.47
12	105	33.98	25.39	123.069	66.41	1.385	47.87	34.7	34.47
13	Strata heat totals: sensible heat = -80.47 kW, latent heat = 82.01 kW								
14	Other heat totals: sensible heat = 0.00 kW, latent heat = 0.00 kW								
15	Metabolic rate = 200 W/m², Skin temperature limit value = 34.98 °C								

Results Table – FA xfr BAC

Row	Distance (m)	Dry Bulb (°C)	Wet Bulb (°C)	Pressure (kPa)	Sigma Heat (kJ/kg)	Density (kg/m³)	Humidity (%)	VRT (°C)	MST (°C)
1	0	33.98	25.39	123.069	66.39	1.385	47.85	34.8	34.46
2	10	33.73	25.39	123.060	66.40	1.386	48.92	34.8	34.44
3	20	33.48	25.39	123.051	66.40	1.387	49.98	34.8	34.42
4	30	33.24	25.39	123.042	66.40	1.388	51.03	34.8	34.41
5	40	33.01	25.38	123.034	66.41	1.389	52.07	34.8	34.39
6	50	32.78	25.38	123.025	66.41	1.390	53.09	34.8	34.38
7	60	32.57	25.38	123.016	66.42	1.390	54.10	34.8	34.36
8	70	32.98	25.61	123.489	67.05	1.394	53.40	34.8	34.42
9	80	32.76	25.61	123.480	67.06	1.395	54.40	34.8	34.41
10	90	32.55	25.61	123.471	67.06	1.395	55.39	34.8	34.39
11	100	32.35	25.61	123.463	67.07	1.396	56.37	34.8	34.38
12	110	32.15	25.61	123.454	67.07	1.397	57.33	34.8	34.36
13	120	31.96	25.61	123.445	67.07	1.398	58.28	34.8	34.35
14	130	31.78	25.61	123.436	67.08	1.398	59.21	34.8	34.34
15	140	31.60	25.61	123.427	67.08	1.399	60.13	34.8	34.33
16	150	31.42	25.61	123.418	67.09	1.400	61.03	34.8	34.31
17	160	31.25	25.60	123.410	67.09	1.400	61.92	34.8	34.30
18	170	31.09	25.60	123.401	67.09	1.401	62.79	34.8	34.29
19	180	30.93	25.60	123.392	67.10	1.401	63.65	34.8	34.28
20	190	30.77	25.60	123.383	67.10	1.402	64.50	34.8	34.26
21	200	30.62	25.60	123.374	67.11	1.402	65.32	34.8	34.25
22	210	30.48	25.60	123.365	67.11	1.403	66.14	34.8	34.24
23	Fan/Reg object at 60 m, pressure = 0.482 kPa, sensible heat = 163.08 kW								
24	Strata heat totals: sensible heat = -1076.22 kW, latent heat = 1092.62 kW								
25	Other heat totals: sensible heat = 163.08 kW, latent heat = 0.00 kW								
26	Metabolic rate = 200 W/m², Skin temperature limit value = 34.98 °C								

Results Table - Ramp 6850-5 to 7350

Row	Distance (m)	Dry Bulb (°C)	Wet Bulb (°C)	Pressure (kPa)	Sigma Heat (kJ/kg)	Density (kg/m³)	Humidity (%)	VRT (°C)	MST (°C)
1	0	39.48	26.82	122.760	71.48	1.357	34.82	34.2	37.11
2	10	39.43	26.82	122.781	71.49	1.358	34.99	34.2	37.11
3	20	39.37	26.83	122.803	71.49	1.358	35.16	34.3	37.10
4	30	39.32	26.83	122.824	71.50	1.359	35.34	34.3	37.10
5	40	39.27	26.84	122.845	71.51	1.359	35.51	34.3	37.09
6	50	39.22	26.84	122.866	71.52	1.360	35.68	34.4	37.09
7	60	39.17	26.85	122.888	71.53	1.360	35.85	34.4	37.08
8	70	39.12	26.85	122.909	71.54	1.361	36.02	34.4	37.08
9	80	39.07	26.85	122.930	71.55	1.361	36.19	34.4	37.08
10	90	39.02	26.86	122.952	71.56	1.361	36.37	34.5	37.07
11	100	38.97	26.86	122.973	71.57	1.362	36.53	34.5	37.07
12	110	43.27	28.07	122.994	75.99	1.344	29.17	34.5	38.48
13	120	43.19	28.07	123.015	75.99	1.344	29.35	34.5	38.47
14	130	43.12	28.08	123.036	76.00	1.345	29.53	34.6	38.46
15	140	43.05	28.08	123.057	76.00	1.345	29.72	34.6	38.45
16	150	42.98	28.08	123.079	76.00	1.346	29.90	34.6	38.44
17	160	42.91	28.08	123.100	76.01	1.346	30.08	34.7	38.44
18	170	42.84	28.09	123.121	76.01	1.347	30.26	34.7	38.43
19	180	42.77	28.09	123.142	76.02	1.347	30.45	34.7	38.42
20	190	42.71	28.09	123.163	76.02	1.348	30.63	34.8	38.41
21	200	42.64	28.09	123.184	76.03	1.348	30.81	34.8	38.40
22	210	43.21	28.27	123.205	76.68	1.346	29.97	34.8	38.60
23	220	43.14	28.27	123.226	76.68	1.346	30.16	34.9	38.59
24	230	43.07	28.28	123.247	76.69	1.347	30.34	34.9	38.59
25	240	43.00	28.28	123.268	76.69	1.347	30.52	34.9	38.58
26	250	42.93	28.28	123.290	76.70	1.348	30.70	34.9	38.57
27	260	42.86	28.28	123.311	76.70	1.348	30.88	35.0	38.56
28	270	42.80	28.29	123.332	76.70	1.349	31.07	35.0	38.55
29	280	42.73	28.29	123.353	76.71	1.349	31.25	35.0	38.55
30	290	42.66	28.29	123.374	76.71	1.350	31.43	35.0	38.54
31	300	42.60	28.30	123.395	76.72	1.350	31.61	35.1	38.53
32	310	42.53	28.30	123.416	76.72	1.351	31.79	35.1	38.53
33	320	42.47	28.30	123.438	76.73	1.351	31.97	35.1	38.52
34	330	42.40	28.31	123.459	76.74	1.352	32.15	35.2	38.51
35	340	42.34	28.31	123.480	76.74	1.352	32.33	35.2	38.50
36	350	42.28	28.31	123.501	76.75	1.353	32.51	35.2	38.50
37	360	42.21	28.31	123.522	76.75	1.353	32.69	35.3	38.49
38	370	42.15	28.32	123.544	76.76	1.354	32.87	35.3	38.49
39	380	42.09	28.32	123.565	76.77	1.354	33.04	35.3	38.48
40	390	42.03	28.32	123.586	76.77	1.355	33.22	35.4	38.47
41	400	41.97	28.33	123.607	76.78	1.355	33.40	35.4	38.47
42	410	41.91	28.33	123.629	76.79	1.356	33.58	35.4	38.46
43	420	41.85	28.34	123.650	76.79	1.356	33.76	35.4	38.45
44	430	41.79	28.34	123.671	76.80	1.357	33.93	35.5	38.45
45	440	41.73	28.34	123.692	76.81	1.357	34.11	35.5	38.44
46	450	41.67	28.35	123.714	76.81	1.357	34.29	35.5	38.44
47	460	41.61	28.35	123.735	76.82	1.358	34.46	35.6	38.43
48	470	41.55	28.35	123.756	76.83	1.358	34.64	35.6	38.43
49	480	41.50	28.36	123.777	76.84	1.359	34.81	35.6	38.42
50	490	41.44	28.36	123.799	76.85	1.359	34.99	35.6	38.42
51	500	41.38	28.36	123.820	76.85	1.360	35.16	35.7	38.41
52	510	45.66	29.51	123.841	81.27	1.342	28.20	35.7	39.77

Results Table - Ramp 6850-5 to 7350

Row	Distance (m)	Dry Bulb (°C)	Wet Bulb (°C)	Pressure (kPa)	Sigma Heat (kJ/kg)	Density (kg/m³)	Humidity (%)	VRT (°C)	MST (°C)
53	520	45.59	29.51	123.862	81.27	1.342	28.39	35.7	39.76
54	530	45.51	29.52	123.883	81.27	1.343	28.57	35.8	39.75
55	540	45.43	29.52	123.904	81.27	1.343	28.76	35.8	39.74
56	550	45.35	29.52	123.925	81.27	1.344	28.94	35.8	39.73
57	560	45.27	29.52	123.946	81.27	1.344	29.13	35.9	39.72
58	570	45.20	29.52	123.967	81.28	1.345	29.31	35.9	39.71
59	580	45.12	29.53	123.989	81.28	1.345	29.50	35.9	39.70
60	590	45.05	29.53	124.010	81.28	1.346	29.68	35.9	39.70
61	600	44.97	29.53	124.031	81.28	1.346	29.87	36.0	39.69
62	610	44.90	29.53	124.052	81.29	1.347	30.05	36.0	39.68
63	620	44.82	29.54	124.073	81.29	1.348	30.23	36.0	39.67
64	630	44.75	29.54	124.094	81.29	1.348	30.42	36.1	39.66
65	640	44.68	29.54	124.115	81.30	1.349	30.60	36.1	39.65
66	650	44.61	29.54	124.136	81.30	1.349	30.78	36.1	39.65
67	660	44.53	29.55	124.158	81.30	1.350	30.96	36.1	39.64
68	670	44.46	29.55	124.179	81.31	1.350	31.15	36.2	39.63
69	680	44.39	29.55	124.200	81.31	1.351	31.33	36.2	39.62
70	690	44.32	29.55	124.221	81.31	1.351	31.51	36.2	39.61
71	700	44.25	29.56	124.242	81.32	1.352	31.69	36.3	39.61
72	710	44.19	29.56	124.263	81.32	1.352	31.87	36.3	39.60
73	720	44.12	29.56	124.285	81.33	1.353	32.06	36.3	39.59
74	730	44.05	29.56	124.306	81.33	1.353	32.24	36.4	39.58
75	740	43.98	29.57	124.327	81.34	1.354	32.42	36.4	39.58
76	750	43.92	29.57	124.348	81.34	1.354	32.60	36.4	39.57
77	760	43.85	29.57	124.369	81.35	1.355	32.78	36.4	39.56
78	770	43.79	29.58	124.391	81.35	1.355	32.96	36.5	39.56
79	780	43.72	29.58	124.412	81.36	1.355	33.14	36.5	39.55
80	790	43.66	29.58	124.433	81.36	1.356	33.32	36.5	39.54
81	800	43.59	29.59	124.454	81.37	1.356	33.50	36.6	39.54
82	810	43.53	29.59	124.476	81.38	1.357	33.67	36.6	39.53
83	820	43.47	29.59	124.497	81.38	1.357	33.85	36.6	39.52
84	830	43.41	29.60	124.518	81.39	1.358	34.03	36.6	39.52
85	840	43.34	29.60	124.539	81.40	1.358	34.21	36.7	39.51
86	850	43.28	29.60	124.561	81.40	1.359	34.39	36.7	39.50
87	860	43.22	29.61	124.582	81.41	1.359	34.56	36.7	39.50
88	870	43.16	29.61	124.603	81.42	1.360	34.74	36.8	39.49
89	880	43.10	29.61	124.625	81.42	1.360	34.92	36.8	39.49
90	890	43.04	29.62	124.646	81.43	1.361	35.09	36.8	39.48
91	900	42.98	29.62	124.667	81.44	1.361	35.27	36.9	39.48
92	910	43.48	29.77	124.689	82.01	1.359	34.43	36.9	39.64
93	920	43.42	29.77	124.710	82.02	1.360	34.61	36.9	39.64
94	930	43.36	29.77	124.731	82.02	1.360	34.79	36.9	39.63
95	940	43.30	29.78	124.753	82.03	1.361	34.96	37.0	39.63
96	950	43.24	29.78	124.774	82.04	1.361	35.14	37.0	39.62
97	Electric heat source at 100 m, sensible heat = 209.00 kW								
98	Electric heat source at 200 m, sensible heat = 30.80 kW								
99	Electric heat source at 500 m, sensible heat = 209.00 kW								
100	Electric heat source at 900 m, sensible heat = 26.80 kW								
101	Strata heat totals: sensible heat = -366.47 kW, latent heat = 317.33 kW								
102	Other heat totals: sensible heat = 475.60 kW, latent heat = 0.00 kW								
103	Metabolic rate = 200 W/m², Skin temperature limit value = 34.98 °C								

Appendix C: Evaporative cooling simulation results

Results Table - FA Plenum

Row	Distance (m)	Dry Bulb (°C)	Wet Bulb (°C)	Pressure (kPa)	Sigma Heat (kJ/kg)	Density (kg/m³)	Humidity (%)	VRT (°C)	MST (°C)
1	0	19.60	17.40	100.974	48.17	1.193	80.73	7.0	32.65
2	10	19.61	17.40	100.986	48.18	1.193	80.71	7.0	32.65
3	20	19.62	17.41	100.998	48.19	1.194	80.68	7.0	32.65
4	30	19.62	17.41	101.010	48.20	1.194	80.65	7.0	32.65
5	40	19.63	17.42	101.022	48.21	1.194	80.63	7.1	32.66
6	50	19.64	17.42	101.034	48.22	1.194	80.60	7.1	32.66
7	60	19.65	17.43	101.046	48.22	1.194	80.58	7.1	32.66
8	70	19.65	17.43	101.058	48.23	1.194	80.55	7.1	32.66
9	80	19.66	17.43	101.070	48.24	1.194	80.53	7.1	32.66
10	90	19.67	17.44	101.082	48.25	1.194	80.50	7.2	32.66
11	100	19.68	17.44	101.094	48.26	1.194	80.47	7.2	32.67
12	110	19.68	17.45	101.106	48.27	1.195	80.45	7.2	32.67
13	120	19.69	17.45	101.118	48.28	1.195	80.42	7.2	32.67
14	130	19.70	17.45	101.130	48.28	1.195	80.40	7.2	32.67
15	140	19.71	17.46	101.142	48.29	1.195	80.37	7.2	32.67
16	*150*	*9.24*	*9.24*	*101.161*	*27.28*	*1.243*	*100.00*	*7.3*	*25.99*
17	*160*	*9.25*	*9.25*	*101.174*	*27.29*	*1.243*	*99.94*	*7.3*	*26.00*
18	*164*	*9.25*	*9.25*	*101.179*	*27.30*	*1.243*	*99.92*	*7.3*	*26.00*

19 Spot heat source at 140 m, sensible heat = -8999.00 kW, latent heat = -1000.00 kW
20 Condensation begins at 150 m
21 Strata heat totals: sensible heat = -21.47 kW, latent heat = 7.34 kW
22 Other heat totals: sensible heat = -8999.00 kW, latent heat = -1000.00 kW
23 Metabolic rate = 200 W/m², Skin temperature limit value = 34.98 °C

Results Table - No 1 Shaft FA

Row	Distance (m)	Dry Bulb (°C)	Wet Bulb (°C)	Pressure (kPa)	Sigma Heat (kJ/kg)	Density (kg/m³)	Humidity (%)	VRT (°C)	MST (°C)
1	0	8.49	8.48	101.205	25.61	1.247	99.87	7.0	25.15
2	10	8.59	8.53	101.303	25.71	1.247	99.32	7.2	25.24
3	20	8.68	8.59	101.401	25.81	1.248	98.76	7.3	25.34
4	30	8.78	8.64	101.500	25.90	1.249	98.21	7.5	25.43
5	40	8.88	8.69	101.598	26.00	1.250	97.67	7.6	25.52
6	50	8.97	8.74	101.697	26.10	1.251	97.13	7.8	25.62
7	60	9.07	8.80	101.796	26.20	1.251	96.60	8.0	25.71
8	70	9.17	8.85	101.894	26.29	1.252	96.07	8.1	25.81
9	80	9.26	8.90	101.993	26.39	1.253	95.54	8.3	25.90
10	90	9.36	8.95	102.092	26.49	1.254	95.02	8.4	25.99
11	100	9.45	9.01	102.191	26.58	1.255	94.51	8.6	26.08
12	110	9.55	9.06	102.290	26.68	1.255	94.00	8.8	26.17
13	120	9.65	9.11	102.389	26.78	1.256	93.49	8.9	26.26
14	130	9.74	9.16	102.489	26.88	1.257	92.99	9.1	26.35
15	140	9.84	9.22	102.588	26.97	1.258	92.49	9.2	26.44
16	150	9.93	9.27	102.688	27.07	1.259	91.99	9.4	26.53
17	160	10.03	9.32	102.787	27.17	1.259	91.50	9.5	26.62
18	170	10.12	9.37	102.887	27.26	1.260	91.02	9.7	26.71
19	180	10.22	9.43	102.987	27.36	1.261	90.54	9.9	26.80
20	190	10.32	9.48	103.087	27.46	1.262	90.06	10.0	26.90
21	200	10.41	9.53	103.187	27.56	1.263	89.58	10.2	26.99
22	210	10.51	9.58	103.287	27.65	1.263	89.11	10.3	27.08
23	220	10.60	9.63	103.387	27.75	1.264	88.65	10.5	27.17
24	230	10.70	9.69	103.487	27.85	1.265	88.19	10.7	27.26
25	240	10.79	9.74	103.587	27.95	1.266	87.73	10.8	27.35
26	250	10.88	9.79	103.688	28.04	1.267	87.27	11.0	27.44
27	260	10.98	9.84	103.788	28.14	1.267	86.82	11.1	27.53
28	270	11.07	9.89	103.889	28.24	1.268	86.37	11.3	27.62
29	280	11.17	9.95	103.990	28.33	1.269	85.93	11.4	27.71
30	290	11.26	10.00	104.090	28.43	1.270	85.49	11.6	27.80
31	300	11.36	10.05	104.191	28.53	1.271	85.06	11.8	27.88
32	310	11.45	10.10	104.292	28.63	1.271	84.62	11.9	27.97
33	320	11.55	10.15	104.393	28.72	1.272	84.19	12.1	28.06
34	330	11.64	10.21	104.495	28.82	1.273	83.77	12.2	28.15
35	340	11.73	10.26	104.596	28.92	1.274	83.35	12.4	28.24
36	350	11.83	10.31	104.697	29.02	1.275	82.93	12.6	28.33
37	360	11.92	10.36	104.799	29.11	1.275	82.51	12.7	28.42
38	370	12.01	10.41	104.900	29.21	1.276	82.10	12.9	28.51
39	380	12.11	10.46	105.002	29.31	1.277	81.69	13.0	28.60
40	390	12.20	10.52	105.104	29.41	1.278	81.29	13.2	28.69
41	400	12.30	10.57	105.205	29.50	1.279	80.88	13.4	28.78
42	410	12.39	10.62	105.307	29.60	1.280	80.49	13.5	28.86
43	420	12.48	10.67	105.409	29.70	1.280	80.09	13.7	28.95
44	430	12.58	10.72	105.512	29.80	1.281	79.70	13.8	29.04
45	440	12.67	10.77	105.614	29.89	1.282	79.31	14.0	29.13
46	450	12.76	10.82	105.716	29.99	1.283	78.92	14.1	29.22
47	460	12.85	10.88	105.819	30.09	1.284	78.54	14.3	29.31
48	470	12.95	10.93	105.921	30.19	1.284	78.16	14.5	29.39
49	480	13.04	10.98	106.024	30.28	1.285	77.78	14.6	29.48
50	490	13.13	11.03	106.126	30.38	1.286	77.41	14.8	29.57
51	500	13.23	11.08	106.229	30.48	1.287	77.04	14.9	29.66
52	510	13.32	11.13	106.332	30.58	1.288	76.67	15.1	29.75
53	520	13.41	11.18	106.435	30.67	1.289	76.30	15.3	29.84
54	530	13.50	11.23	106.538	30.77	1.289	75.94	15.4	29.92
55	540	13.60	11.28	106.641	30.87	1.290	75.58	15.6	30.01
56	550	13.69	11.34	106.745	30.97	1.291	75.22	15.7	30.10
57	560	13.78	11.39	106.848	31.07	1.292	74.87	15.9	30.19
58	570	13.87	11.44	106.952	31.16	1.293	74.52	16.1	30.27
59	580	13.96	11.49	107.055	31.26	1.294	74.17	16.2	30.36

Results Table - No 1 Shaft FA

Row	Distance (m)	Dry Bulb (°C)	Wet Bulb (°C)	Pressure (kPa)	Sigma Heat (kJ/kg)	Density (kg/m³)	Humidity (%)	VRT (°C)	MST (°C)
60	590	14.80	12.25	107.180	33.02	1.291	74.13	16.4	31.08
61	600	14.89	12.30	107.284	33.12	1.292	73.79	16.5	31.16
62	610	14.98	12.35	107.389	33.21	1.293	73.45	16.7	31.25
63	620	15.07	12.40	107.494	33.31	1.294	73.12	16.8	31.33
64	630	15.16	12.45	107.599	33.41	1.294	72.78	17.0	31.41
65	640	15.25	12.50	107.704	33.51	1.295	72.45	17.2	31.50
66	650	15.34	12.55	107.809	33.60	1.296	72.12	17.3	31.58
67	660	15.44	12.60	107.914	33.70	1.297	71.80	17.5	31.66
68	670	15.53	12.65	108.019	33.80	1.298	71.47	17.6	31.74
69	680	15.62	12.70	108.124	33.90	1.299	71.15	17.8	31.82
70	690	15.71	12.75	108.230	33.99	1.300	70.83	17.9	31.90
71	700	15.80	12.80	108.336	34.09	1.300	70.52	18.1	31.98
72	710	15.89	12.85	108.441	34.19	1.301	70.20	18.3	32.06
73	720	15.98	12.90	108.547	34.29	1.302	69.89	18.4	32.13
74	730	16.07	12.95	108.653	34.39	1.303	69.58	18.6	32.21
75	740	16.16	13.00	108.759	34.48	1.304	69.27	18.8	32.29
76	750	16.25	13.05	108.865	34.58	1.305	68.97	18.9	32.36
77	760	16.34	13.10	108.971	34.68	1.306	68.67	19.1	32.43
78	770	16.43	13.15	109.077	34.78	1.306	68.37	19.2	32.50
79	780	16.52	13.20	109.184	34.87	1.307	68.07	19.4	32.54
80	790	16.61	13.25	109.290	34.97	1.308	67.77	19.5	32.59
81	800	16.70	13.30	109.397	35.07	1.309	67.48	19.7	32.63
82	810	16.79	13.35	109.503	35.17	1.310	67.19	19.9	32.67
83	820	16.88	13.40	109.610	35.27	1.311	66.90	20.0	32.70
84	830	16.97	13.45	109.717	35.36	1.312	66.61	20.2	32.73
85	840	17.06	13.49	109.824	35.46	1.313	66.33	20.3	32.76
86	850	17.15	13.54	109.931	35.56	1.313	66.04	20.5	32.79
87	860	17.24	13.59	110.038	35.66	1.314	65.76	20.6	32.82
88	870	17.33	13.64	110.145	35.76	1.315	65.48	20.8	32.84
89	880	17.42	13.69	110.252	35.85	1.316	65.21	21.0	32.87
90	890	17.51	13.74	110.360	35.95	1.317	64.93	21.1	32.89
91	900	17.60	13.79	110.467	36.05	1.318	64.66	21.3	32.92
92	910	17.69	13.84	110.575	36.15	1.319	64.39	21.4	32.94
93	920	17.78	13.89	110.683	36.24	1.320	64.12	21.6	32.96
94	930	17.87	13.94	110.791	36.34	1.320	63.85	21.8	32.98
95	940	17.96	13.99	110.899	36.44	1.321	63.59	21.9	33.00
96	950	18.05	14.04	111.007	36.54	1.322	63.32	22.1	33.02
97	960	18.14	14.08	111.115	36.64	1.323	63.06	22.2	33.04
98	970	18.22	14.13	111.223	36.73	1.324	62.80	22.4	33.06
99	980	18.31	14.18	111.331	36.83	1.325	62.54	22.6	33.07
100	990	18.40	14.23	111.440	36.93	1.326	62.29	22.7	33.09
101	1000	18.49	14.28	111.548	37.03	1.327	62.03	22.9	33.11
102	1010	18.58	14.33	111.657	37.13	1.327	61.78	23.0	33.13
103	1020	18.67	14.38	111.766	37.23	1.328	61.53	23.2	33.14
104	1030	18.76	14.43	111.875	37.32	1.329	61.28	23.4	33.16
105	1040	18.85	14.48	111.984	37.42	1.330	61.04	23.5	33.17
106	1050	18.93	14.53	112.093	37.52	1.331	60.79	23.7	33.19
107	1060	19.02	14.57	112.202	37.62	1.332	60.55	23.8	33.20
108	1070	19.11	14.62	112.311	37.72	1.333	60.30	24.0	33.22
109	1080	19.20	14.67	112.420	37.81	1.334	60.06	24.1	33.23
110	1090	19.29	14.72	112.530	37.91	1.335	59.83	24.3	33.24
111	1100	19.37	14.77	112.640	38.01	1.335	59.59	24.5	33.26
112	1110	19.46	14.82	112.749	38.11	1.336	59.35	24.6	33.27
113	1120	19.55	14.87	112.859	38.21	1.337	59.12	24.8	33.28
114	1130	19.64	14.91	112.969	38.31	1.338	58.89	24.9	33.30
115	1140	19.73	14.96	113.079	38.40	1.339	58.66	25.1	33.31
116	1150	19.81	15.01	113.189	38.50	1.340	58.43	25.3	33.32
117	1160	19.90	15.06	113.299	38.60	1.341	58.20	25.4	33.33
118	1170	19.99	15.11	113.409	38.70	1.342	57.98	25.6	33.34

Results Table - No 1 Shaft FA

Row	Distance (m)	Dry Bulb (°C)	Wet Bulb (°C)	Pressure (kPa)	Sigma Heat (kJ/kg)	Density (kg/m³)	Humidity (%)	VRT (°C)	MST (°C)
119	1180	20.08	15.16	113.520	38.80	1.343	57.75	25.7	33.36
120	1190	20.16	15.21	113.630	38.89	1.344	57.53	25.9	33.37
121	1200	20.25	15.25	113.741	38.99	1.344	57.31	26.1	33.38
122	1210	20.34	15.30	113.851	39.09	1.345	57.09	26.2	33.39
123	1220	20.42	15.35	113.962	39.19	1.346	56.87	26.4	33.40
124	1230	20.51	15.40	114.073	39.29	1.347	56.66	26.5	33.41
125	1240	20.60	15.45	114.184	39.39	1.348	56.44	26.7	33.42
126	1250	20.69	15.50	114.295	39.48	1.349	56.23	26.8	33.43
127	1260	20.77	15.54	114.406	39.58	1.350	56.01	27.0	33.44
128	1270	20.86	15.59	114.518	39.68	1.351	55.80	27.2	33.45
129	1280	20.95	15.64	114.629	39.78	1.352	55.59	27.3	33.46
130	1290	21.03	15.69	114.741	39.88	1.353	55.39	27.5	33.47
131	1300	21.12	15.74	114.852	39.98	1.354	55.18	27.6	33.48
132	1310	21.21	15.78	114.964	40.08	1.354	54.98	27.8	33.49
133	1320	21.29	15.83	115.076	40.17	1.355	54.77	27.9	33.50
134	1330	21.38	15.88	115.188	40.27	1.356	54.57	28.1	33.51
135	1340	21.47	15.93	115.300	40.37	1.357	54.37	28.3	33.52
136	1350	21.55	15.98	115.412	40.47	1.358	54.17	28.4	33.53
137	1360	21.64	16.03	115.524	40.57	1.359	53.97	28.6	33.54
138	1370	21.73	16.07	115.637	40.67	1.360	53.77	28.8	33.55
139	1380	21.81	16.12	115.749	40.76	1.361	53.58	28.9	33.56
140	1390	21.90	16.17	115.862	40.86	1.362	53.38	29.1	33.57
141	1400	21.98	16.22	115.974	40.96	1.363	53.19	29.2	33.58
142	1410	22.07	16.26	116.087	41.06	1.364	53.00	29.4	33.59
143	1420	22.16	16.31	116.200	41.16	1.365	52.81	29.5	33.59
144	1430	22.24	16.36	116.313	41.26	1.365	52.62	29.7	33.60
145	1440	22.33	16.41	116.426	41.36	1.366	52.43	29.9	33.61
146	1450	22.41	16.46	116.539	41.45	1.367	52.24	30.0	33.62
147	1460	22.50	16.50	116.652	41.55	1.368	52.05	30.2	33.63
148	1470	22.58	16.55	116.766	41.65	1.369	51.87	30.3	33.64
149	1480	22.67	16.60	116.879	41.75	1.370	51.69	30.5	33.64
150	1490	22.76	16.65	116.993	41.85	1.371	51.50	30.6	33.65
151	1500	22.84	16.69	117.107	41.95	1.372	51.32	30.8	33.66
152	1510	22.93	16.74	117.220	42.05	1.373	51.14	31.0	33.67
153	1520	23.01	16.79	117.334	42.15	1.374	50.96	31.1	33.68
154	1530	23.10	16.84	117.448	42.24	1.375	50.79	31.3	33.68
155	1540	23.18	16.88	117.563	42.34	1.376	50.61	31.4	33.69
156	1550	23.27	16.93	117.677	42.44	1.377	50.43	31.6	33.70
157	1560	23.35	16.98	117.791	42.54	1.378	50.26	31.8	33.71
158	1568	23.42	17.02	117.883	42.62	1.378	50.12	31.9	33.71

159 Condensation begins at 0 m
160 Condensation ends at 10 m
161 Strata heat totals: sensible heat = -519.76 kW, latent heat = 558.08 kW
162 Other heat totals: sensible heat = 0.00 kW, latent heat = 0.00 kW
163 Metabolic rate = 200 W/m², Skin temperature limit value = 34.98 °C

Results Table - 5400L No 1 FA

Row	Distance (m)	Dry Bulb (°C)	Wet Bulb (°C)	Pressure (kPa)	Sigma Heat (kJ/kg)	Density (kg/m³)	Humidity (%)	VRT (°C)	MST (°C)
1	0	23.42	17.02	117.883	42.63	1.378	50.14	28.6	33.70
2	10	23.50	17.07	117.996	42.72	1.379	49.97	28.8	33.71
3	20	23.59	17.11	118.109	42.82	1.380	49.80	28.9	33.72
4	30	23.67	17.16	118.222	42.92	1.381	49.63	29.1	33.72
5	40	23.76	17.21	118.335	43.02	1.382	49.46	29.3	33.73
6	50	23.84	17.26	118.449	43.12	1.383	49.29	29.5	33.74
7	60	23.93	17.30	118.562	43.22	1.384	49.13	29.6	33.75
8	70	24.01	17.35	118.676	43.31	1.385	48.96	29.8	33.75
9	80	24.09	17.40	118.789	43.41	1.386	48.80	30.0	33.76
10	90	24.18	17.44	118.903	43.51	1.387	48.63	30.1	33.77
11	100	24.26	17.49	119.017	43.61	1.388	48.47	30.3	33.77
12	110	24.35	17.54	119.131	43.71	1.389	48.31	30.5	33.78
13	120	24.43	17.58	119.245	43.81	1.390	48.15	30.7	33.79
14	130	24.52	17.63	119.359	43.90	1.390	47.99	30.8	33.79
15	140	24.60	17.68	119.474	44.00	1.391	47.83	31.0	33.80
16	151	24.69	17.73	119.599	44.11	1.392	47.66	31.2	33.81
17	Strata heat totals: sensible heat = -101.03 kW, latent heat = 108.37 kW								
18	Other heat totals: sensible heat = 0.00 kW, latent heat = 0.00 kW								
19	Metabolic rate = 200 W/m², Skin temperature limit value = 34.98 °C								

Results Table - 5900L No 1 FA

Row	Distance (m)	Dry Bulb (°C)	Wet Bulb (°C)	Pressure (kPa)	Sigma Heat (kJ/kg)	Density (kg/m³)	Humidity (%)	VRT (°C)	MST (°C)
1	0	24.69	17.73	119.599	44.11	1.392	47.67	30.6	33.88
2	10	24.77	17.78	119.725	44.21	1.393	47.52	30.8	33.89
3	20	24.86	17.83	119.851	44.31	1.395	47.37	30.9	33.89
4	30	24.94	17.87	119.977	44.41	1.396	47.22	31.1	33.90
5	40	25.02	17.92	120.103	44.51	1.397	47.07	31.3	33.91
6	50	25.11	17.97	120.230	44.61	1.398	46.93	31.5	33.91
7	60	25.19	18.02	120.356	44.71	1.399	46.78	31.6	33.92
8	70	25.27	18.06	120.483	44.81	1.400	46.64	31.8	33.93
9	80	25.36	18.11	120.610	44.90	1.401	46.49	32.0	33.93
10	90	25.44	18.16	120.737	45.00	1.402	46.35	32.1	33.94
11	100	25.52	18.21	120.864	45.10	1.403	46.21	32.3	33.94
12	107	25.58	18.24	120.953	45.17	1.404	46.11	32.4	33.95
13	Strata heat totals: sensible heat = -53.36 kW, latent heat = 59.01 kW								
14	Other heat totals: sensible heat = 0.00 kW, latent heat = 0.00 kW								
15	Metabolic rate = 200 W/m², Skin temperature limit value = 34.98 °C								

Results Table - 6200L No 1 FA

Row	Distance (m)	Dry Bulb (°C)	Wet Bulb (°C)	Pressure (kPa)	Sigma Heat (kJ/kg)	Density (kg/m³)	Humidity (%)	VRT (°C)	MST (°C)
1	0	25.58	18.24	120.953	45.17	1.404	46.11	33.7	34.00
2	10	25.66	18.29	121.084	45.27	1.405	45.97	33.9	34.00
3	20	25.75	18.34	121.215	45.37	1.406	45.83	34.1	34.01
4	30	25.83	18.38	121.346	45.47	1.407	45.69	34.3	34.02
5	40	25.91	18.43	121.478	45.57	1.408	45.56	34.4	34.02
6	50	26.00	18.48	121.609	45.67	1.410	45.42	34.6	34.03
7	60	26.08	18.53	121.741	45.77	1.411	45.28	34.8	34.03
8	70	26.16	18.58	121.872	45.87	1.412	45.15	35.0	34.04
9	80	26.24	18.63	122.004	45.97	1.413	45.02	35.1	34.05
10	90	26.33	18.67	122.136	46.07	1.414	44.88	35.3	34.05
11	100	26.41	18.72	122.268	46.17	1.415	44.75	35.5	34.06
12	110	26.49	18.77	122.400	46.27	1.416	44.62	35.7	34.06
13	120	26.58	18.82	122.532	46.37	1.417	44.49	35.9	34.07
14	130	26.66	18.87	122.665	46.47	1.419	44.36	36.1	34.08
15	140	26.74	18.91	122.797	46.57	1.420	44.23	36.3	34.08
16	150	26.82	18.96	122.930	46.67	1.421	44.10	36.4	34.09
17	160	26.91	19.01	123.062	46.77	1.422	43.97	36.6	34.09
18	170	26.99	19.06	123.195	46.87	1.423	43.85	36.8	34.10
19	180	27.07	19.10	123.328	46.97	1.424	43.72	37.0	34.11
20	183	27.10	19.12	123.368	47.00	1.425	43.68	37.0	34.11
21	Strata heat totals: sensible heat = -74.89 kW, latent heat = 88.24 kW								
22	Other heat totals: sensible heat = 0.00 kW, latent heat = 0.00 kW								
23	Metabolic rate = 200 W/m², Skin temperature limit value = 34.98 °C								

Results Table - 6950L No 1 FA

Row	Distance (m)	Dry Bulb (°C)	Wet Bulb (°C)	Pressure (kPa)	Sigma Heat (kJ/kg)	Density (kg/m³)	Humidity (%)	VRT (°C)	MST (°C)
1	0	27.10	19.12	123.368	47.00	1.424	43.67	34.1	34.14
2	10	27.18	19.17	123.503	47.10	1.426	43.55	34.3	34.15
3	20	27.26	19.22	123.638	47.20	1.427	43.43	34.5	34.16
4	30	27.35	19.26	123.773	47.30	1.428	43.31	34.6	34.16
5	Strata heat totals: sensible heat = -11.31 kW, latent heat = 13.08 kW								
6	Other heat totals: sensible heat = 0.00 kW, latent heat = 0.00 kW								
7	Metabolic rate = 200 W/m², Skin temperature limit value = 34.98 °C								

Results Table - Sump No 1 FA

Row	Distance (m)	Dry Bulb (°C)	Wet Bulb (°C)	Pressure (kPa)	Sigma Heat (kJ/kg)	Density (kg/m³)	Humidity (%)	VRT (°C)	MST (°C)
1	0	27.35	19.26	123.773	47.29	1.428	43.26	34.8	34.16
2	10	27.22	19.31	123.908	47.39	1.430	44.14	35.0	34.15
3	20	27.10	19.36	124.044	47.50	1.432	45.01	35.2	34.13
4	30	27.35	19.54	124.179	47.96	1.433	44.90	35.4	34.14
5	40	27.23	19.58	124.315	48.07	1.435	45.75	35.5	34.13
6	50	27.12	19.63	124.451	48.17	1.437	46.59	35.7	34.12
7	60	27.01	19.68	124.587	48.27	1.439	47.41	35.9	34.10
8	71	26.89	19.73	124.737	48.39	1.441	48.31	36.1	34.09
5	40	27.23	19.58	124.315	48.07	1.435	45.75	35.5	34.13
6	50	27.12	19.63	124.451	48.17	1.437	46.59	35.7	34.12
7	60	27.01	19.68	124.587	48.27	1.439	47.41	35.9	34.10
8	71	26.89	19.73	124.737	48.39	1.441	48.31	36.1	34.09
9	Electric heat source at 29 m, sensible heat = 90.00 kW								
10	Strata heat totals: sensible heat = -376.13 kW, latent heat = 384.52 kW								
9	Other heat totals: sensible heat = 90.00 kW, latent heat = 0.00 kW								
10	Metabolic rate = 200 W/m², Skin temperature limit value = 34.98 °C								

Results Table - 6850L Access

Row	Distance (m)	Dry Bulb (°C)	Wet Bulb (°C)	Pressure (kPa)	Sigma Heat (kJ/kg)	Density (kg/m³)	Humidity (%)	VRT (°C)	MST (°C)
1	0	27.35	19.26	123.773	47.29	1.428	43.26	34.2	34.38
2	10	27.32	19.26	123.773	47.30	1.428	43.41	34.2	34.37
3	20	27.30	19.27	123.772	47.31	1.428	43.55	34.2	34.37
4	27	27.28	19.27	123.772	47.32	1.428	43.65	34.2	34.37
5	Strata heat totals: sensible heat = -3.47 kW, latent heat = 4.91 kW								
5	Other heat totals: sensible heat = 0.00 kW, latent heat = 0.00 kW								
6	Metabolic rate = 200 W/m², Skin temperature limit value = 34.98 °C								

Results Table - 6850L 1

Row	Distance (m)	Dry Bulb (°C)	Wet Bulb (°C)	Pressure (kPa)	Sigma Heat (kJ/kg)	Density (kg/m³)	Humidity (%)	VRT (°C)	MST (°C)
1	0	27.28	19.27	123.772	47.32	1.428	43.66	34.2	34.38
2	10	27.26	19.27	123.772	47.33	1.428	43.80	34.2	34.37
3	20	27.23	19.28	123.771	47.35	1.429	43.94	34.2	34.37
4	25	31.75	20.91	123.771	51.92	1.407	33.90	34.2	34.62
5	Electric heat source at 20 m, sensible heat = 225.00 kW								
6	Strata heat totals: sensible heat = -2.81 kW, latent heat = 4.50 kW								
5	Other heat totals: sensible heat = 225.00 kW, latent heat = 0.00 kW								
6	Metabolic rate = 200 W/m², Skin temperature limit value = 34.98 °C								

Results Table - 6850L 2

Row	Distance (m)	Dry Bulb (°C)	Wet Bulb (°C)	Pressure (kPa)	Sigma Heat (kJ/kg)	Density (kg/m³)	Humidity (%)	VRT (°C)	MST (°C)
1	0	31.75	20.91	123.771	51.91	1.407	33.90	34.2	34.63
2	10	32.33	21.13	123.771	52.55	1.405	32.88	34.2	34.66
3	20	32.29	21.13	123.770	52.55	1.405	33.05	34.2	34.66
4	31	32.87	21.35	123.770	53.19	1.402	32.09	34.2	34.69
5	Electric heat source at 1 m, sensible heat = 30.00 kW								
5	Electric heat source at 29 m, sensible heat = 30.00 kW								
6	Strata heat totals: sensible heat = -6.68 kW, latent heat = 7.56 kW								
7	Other heat totals: sensible heat = 60.00 kW, latent heat = 0.00 kW								
8	Metabolic rate = 200 W/m², Skin temperature limit value = 34.98 °C								

Results Table - 6850L 3

Row	Distance (m)	Dry Bulb (°C)	Wet Bulb (°C)	Pressure (kPa)	Sigma Heat (kJ/kg)	Density (kg/m³)	Humidity (%)	VRT (°C)	MST (°C)
1	0	32.87	21.35	123.770	53.19	1.402	32.06	34.2	34.61
2	10	32.82	21.35	123.769	53.19	1.402	32.22	34.2	34.61
3	20	32.78	21.35	123.769	53.19	1.403	32.38	34.2	34.61
4	Strata heat totals: sensible heat = -6.34 kW, latent heat = 6.79 kW								
4	Other heat totals: sensible heat = 0.00 kW, latent heat = 0.00 kW								
5	Metabolic rate = 200 W/m², Skin temperature limit value = 34.98 °C								

Results Table - 6850L 4

Row	Distance (m)	Dry Bulb (°C)	Wet Bulb (°C)	Pressure (kPa)	Sigma Heat (kJ/kg)	Density (kg/m³)	Humidity (%)	VRT (°C)	MST (°C)
1	0	32.78	21.35	123.769	53.19	1.402	32.37	34.2	34.65
2	10	32.73	21.35	123.769	53.19	1.403	32.54	34.2	34.65
3	20	32.69	21.35	123.768	53.20	1.403	32.71	34.2	34.65
4	30	32.64	21.35	123.768	53.20	1.403	32.87	34.2	34.64
5	40	32.59	21.35	123.767	53.21	1.403	33.04	34.2	34.64
6	50	32.55	21.36	123.767	53.21	1.403	33.21	34.2	34.64
7	60	32.50	21.36	123.767	53.22	1.404	33.37	34.2	34.64
8	70	32.46	21.36	123.766	53.22	1.404	33.54	34.2	34.63
9	80	32.41	21.36	123.766	53.23	1.404	33.71	34.2	34.63
10	90	32.37	21.36	123.765	53.23	1.404	33.87	34.2	34.63
11	94	32.35	21.36	123.765	53.23	1.404	33.94	34.2	34.62
4	30	32.64	21.35	123.768	53.20	1.403	32.87	34.2	34.64
5	40	32.59	21.35	123.767	53.21	1.403	33.04	34.2	34.64
6	50	32.55	21.36	123.767	53.21	1.403	33.21	34.2	34.64
7	60	32.50	21.36	123.767	53.22	1.404	33.37	34.2	34.64
8	70	32.46	21.36	123.766	53.22	1.404	33.54	34.2	34.63
9	80	32.41	21.36	123.766	53.23	1.404	33.71	34.2	34.63
10	90	32.37	21.36	123.765	53.23	1.404	33.87	34.2	34.63
11	94	32.35	21.36	123.765	53.23	1.404	33.94	34.2	34.62
12	Strata heat totals: sensible heat = -23.81 kW, latent heat = 26.12 kW								
13	Other heat totals: sensible heat = 0.00 kW, latent heat = 0.00 kW								
14	Metabolic rate = 200 W/m², Skin temperature limit value = 34.98 °C								

Results Table - 6850L 5

Row	Distance (m)	Dry Bulb (°C)	Wet Bulb (°C)	Pressure (kPa)	Sigma Heat (kJ/kg)	Density (kg/m³)	Humidity (%)	VRT (°C)	MST (°C)
1	0	32.35	21.36	123.765	53.23	1.404	33.94	34.2	34.67
2	10	32.30	21.36	123.765	53.23	1.404	34.11	34.2	34.66
3	20	32.26	21.36	123.764	53.24	1.405	34.28	34.2	34.66
4	30	32.21	21.37	123.764	53.25	1.405	34.46	34.2	34.66
5	40	32.17	21.37	123.764	53.25	1.405	34.63	34.2	34.65
6	50	32.12	21.37	123.764	53.26	1.405	34.80	34.2	34.65
7	60	32.08	21.37	123.763	53.27	1.405	34.97	34.2	34.65
8	70	32.04	21.37	123.763	53.27	1.406	35.14	34.2	34.64
9	80	31.99	21.37	123.763	53.28	1.406	35.32	34.2	34.64
10	90	31.95	21.38	123.763	53.29	1.406	35.49	34.2	34.64
11	100	31.91	21.38	123.762	53.29	1.406	35.66	34.2	34.64
12	105	31.89	21.38	123.762	53.30	1.406	35.74	34.2	34.63
13	Strata heat totals: sensible heat = -21.06 kW, latent heat = 24.00 kW								
14	Other heat totals: sensible heat = 0.00 kW, latent heat = 0.00 kW								
15	Metabolic rate = 200 W/m², Skin temperature limit value = 34.98 °C								

Results Table - 6850L 4r1

Row	Distance (m)	Dry Bulb (°C)	Wet Bulb (°C)	Pressure (kPa)	Sigma Heat (kJ/kg)	Density (kg/m³)	Humidity (%)	VRT (°C)	MST (°C)
1	0	32.35	21.36	123.765	53.23	1.404	33.94	34.2	34.92
2	10	32.28	21.37	123.765	53.25	1.405	34.22	34.2	34.91
3	20	32.22	21.38	123.765	53.28	1.405	34.50	34.2	34.91
4	29	32.16	21.38	123.765	53.30	1.405	34.76	34.2	34.90
5	Strata heat totals: sensible heat = -2.01 kW, latent heat = 2.76 kW								
6	Other heat totals: sensible heat = 0.00 kW, latent heat = 0.00 kW								
7	Metabolic rate = 200 W/m², Skin temperature limit value = 34.98 °C								

Results Table - 6850L 4r2

Row	Distance (m)	Dry Bulb (°C)	Wet Bulb (°C)	Pressure (kPa)	Sigma Heat (kJ/kg)	Density (kg/m³)	Humidity (%)	VRT (°C)	MST (°C)
1	0	32.16	21.38	123.765	53.29	1.405	34.72	34.2	34.90
2	10	32.10	21.39	123.765	53.32	1.405	35.00	34.2	34.90
3	20	32.03	21.40	123.765	53.35	1.406	35.28	34.2	34.90
4	30	31.97	21.41	123.765	53.37	1.406	35.56	34.2	34.89
5	40	50.51	27.20	123.765	72.18	1.325	13.40	34.2	39.91
6	50	50.91	27.37	123.765	72.80	1.324	13.27	34.2	40.06
7	60	50.58	27.34	123.765	72.69	1.325	13.61	34.2	40.00
8	70	50.27	27.31	123.765	72.58	1.326	13.96	34.2	39.93
9	80	49.96	27.27	123.765	72.47	1.327	14.31	34.2	39.86
10	90	49.65	27.24	123.765	72.37	1.328	14.66	34.2	39.79
11	100	49.35	27.21	123.765	72.27	1.330	15.02	34.2	39.73
12	110	49.05	27.18	123.765	72.17	1.331	15.38	34.2	39.66
13	120	48.76	27.16	123.765	72.07	1.332	15.74	34.2	39.60
14	130	48.47	27.13	123.765	71.98	1.333	16.11	34.2	39.54
15	140	48.18	27.10	123.765	71.88	1.334	16.48	34.2	39.48
5	40	50.51	27.20	123.765	72.18	1.325	13.40	34.2	39.91
6	50	50.91	27.37	123.765	72.80	1.324	13.27	34.2	40.06
7	60	50.58	27.34	123.765	72.69	1.325	13.61	34.2	40.00
8	70	50.27	27.31	123.765	72.58	1.326	13.96	34.2	39.93
9	80	49.96	27.27	123.765	72.47	1.327	14.31	34.2	39.86
10	90	49.65	27.24	123.765	72.37	1.328	14.66	34.2	39.79
11	100	49.35	27.21	123.765	72.27	1.330	15.02	34.2	39.73
12	110	49.05	27.18	123.765	72.17	1.331	15.38	34.2	39.66
13	120	48.76	27.16	123.765	72.07	1.332	15.74	34.2	39.60
14	130	48.47	27.13	123.765	71.98	1.333	16.11	34.2	39.54
15	140	48.18	27.10	123.765	71.88	1.334	16.48	34.2	39.48
16	Electric heat source at 30 m, sensible heat = 195.00 kW								
17	Electric heat source at 40 m, sensible heat = 7.50 kW								
18	Strata heat totals: sensible heat = -34.51 kW, latent heat = 24.65 kW								
16	Other heat totals: sensible heat = 202.50 kW, latent heat = 0.00 kW								
17	Metabolic rate = 200 W/m², Skin temperature limit value = 34.98 °C								

Results Table - 6850L 3r1

Row	Distance (m)	Dry Bulb (°C)	Wet Bulb (°C)	Pressure (kPa)	Sigma Heat (kJ/kg)	Density (kg/m³)	Humidity (%)	VRT (°C)	MST (°C)
1	0	32.78	21.35	123.769	53.19	1.402	32.37	34.2	34.90
2	10	32.73	21.36	123.785	53.22	1.403	32.61	34.2	34.90
3	20	32.67	21.37	123.802	53.25	1.403	32.84	34.2	34.90
4	30	32.62	21.38	123.818	53.28	1.404	33.08	34.3	34.89
5	40	32.57	21.39	123.835	53.31	1.404	33.31	34.3	34.89
6	50	32.52	21.40	123.851	53.34	1.405	33.55	34.3	34.89
7	60	32.47	21.42	123.868	53.37	1.405	33.78	34.3	34.88
8	70	32.42	21.43	123.884	53.40	1.405	34.01	34.4	34.88
9	80	32.37	21.44	123.901	53.43	1.406	34.24	34.4	34.88
10	90	32.32	21.45	123.917	53.46	1.406	34.47	34.4	34.87
11	100	32.27	21.46	123.934	53.49	1.406	34.70	34.4	34.87
12	110	32.23	21.48	123.950	53.53	1.407	34.92	34.4	34.87
13	120	32.18	21.49	123.967	53.56	1.407	35.15	34.5	34.87
14	130	32.14	21.50	123.983	53.59	1.408	35.37	34.5	34.86
15	140	32.09	21.51	124.000	53.63	1.408	35.60	34.5	34.86
16	150	32.05	21.52	124.016	53.66	1.408	35.82	34.5	34.86
17	160	32.01	21.54	124.033	53.70	1.409	36.04	34.5	34.86
16	150	32.05	21.52	124.016	53.66	1.408	35.82	34.5	34.86
17	160	32.01	21.54	124.033	53.70	1.409	36.04	34.5	34.86
18	170	31.96	21.55	124.049	53.73	1.409	36.26	34.6	34.85
19	180	31.92	21.56	124.066	53.77	1.409	36.48	34.6	34.85
20	190	31.88	21.58	124.082	53.80	1.410	36.69	34.6	34.85
21	200	31.84	21.59	124.099	53.84	1.410	36.91	34.6	34.85
22	210	31.80	21.60	124.115	53.87	1.410	37.12	34.7	34.84
23	220	31.77	21.62	124.132	53.91	1.411	37.34	34.7	34.84
24	230	31.73	21.63	124.148	53.95	1.411	37.55	34.7	34.84
25	240	31.69	21.64	124.165	53.98	1.411	37.76	34.7	34.84
26	250	31.65	21.66	124.181	54.02	1.412	37.97	34.7	34.83
27	259	31.62	21.67	124.196	54.06	1.412	38.16	34.8	34.83
28	Strata heat totals: sensible heat = -20.36 kW, latent heat = 27.97 kW								
28	Other heat totals: sensible heat = 0.00 kW, latent heat = 0.00 kW								
29	Metabolic rate = 200 W/m², Skin temperature limit value = 34.98 °C								

Results Table - Shaft bottom ramp

Row	Distance (m)	Dry Bulb (°C)	Wet Bulb (°C)	Pressure (kPa)	Sigma Heat (kJ/kg)	Density (kg/m³)	Humidity (%)	VRT (°C)	MST (°C)
1	0	26.89	19.73	124.737	48.38	1.441	48.32	35.4	33.95
2	10	26.83	19.71	124.675	48.35	1.440	48.51	35.3	33.94
3	20	26.77	19.70	124.613	48.32	1.440	48.71	35.3	33.94
4	30	26.72	19.68	124.551	48.28	1.440	48.91	35.2	33.93
5	40	26.66	19.66	124.490	48.25	1.439	49.10	35.1	33.93
6	50	26.60	19.64	124.428	48.21	1.439	49.30	35.0	33.92
7	60	26.54	19.62	124.366	48.18	1.438	49.50	35.0	33.91
8	70	26.49	19.61	124.304	48.15	1.438	49.70	34.9	33.91
9	80	26.43	19.59	124.242	48.11	1.437	49.89	34.9	33.90
10	90	26.37	19.57	124.180	48.08	1.437	50.09	34.8	33.90
11	100	26.32	19.55	124.119	48.05	1.436	50.29	34.7	33.89
12	105	26.29	19.55	124.088	48.03	1.436	50.39	34.7	33.89
13	Strata heat totals: sensible heat = -53.77 kW, latent heat = 62.56 kW								
14	Other heat totals: sensible heat = 0.00 kW, latent heat = 0.00 kW								
15	Metabolic rate = 200 W/m², Skin temperature limit value = 34.98 °C								

Results Table – FA xfr BAC

Row	Distance (m)	Dry Bulb (°C)	Wet Bulb (°C)	Pressure (kPa)	Sigma Heat (kJ/kg)	Density (kg/m³)	Humidity (%)	VRT (°C)	MST (°C)
1	0	26.29	19.55	124.088	48.04	1.436	50.40	34.8	33.88
2	10	26.10	19.55	124.079	48.05	1.437	51.43	34.8	33.86
3	20	25.92	19.55	124.070	48.05	1.438	52.45	34.8	33.84
4	30	25.74	19.55	124.061	48.06	1.438	53.45	34.8	33.82
5	40	25.56	19.55	124.053	48.07	1.439	54.44	34.8	33.79
6	50	25.40	19.55	124.044	48.07	1.440	55.41	34.8	33.77
7	60	25.23	19.55	124.035	48.08	1.440	56.37	34.8	33.75
8	70	25.07	19.55	124.026	48.08	1.441	57.32	34.8	33.73
9	80	24.92	19.55	124.017	48.09	1.441	58.25	34.8	33.71
10	90	24.77	19.55	124.008	48.09	1.442	59.17	34.8	33.69
11	100	24.62	19.55	123.999	48.10	1.443	60.07	34.8	33.67
12	110	24.48	19.55	123.991	48.11	1.443	60.96	34.8	33.66
13	120	24.35	19.55	123.982	48.11	1.444	61.84	34.8	33.64
14	130	24.21	19.56	123.973	48.12	1.444	62.70	34.8	33.62
15	140	24.08	19.56	123.964	48.12	1.445	63.54	34.8	33.60
16	150	23.96	19.56	123.955	48.13	1.445	64.37	34.8	33.58
17	160	23.83	19.56	123.946	48.13	1.445	65.19	34.8	33.56
18	170	23.72	19.56	123.937	48.14	1.446	65.99	34.8	33.55
19	180	23.60	19.56	123.929	48.15	1.446	66.77	34.8	33.53
20	190	23.49	19.56	123.920	48.15	1.447	67.54	34.8	33.51
21	200	23.38	19.56	123.911	48.16	1.447	68.30	34.8	33.50
22	210	23.28	19.56	123.902	48.16	1.447	69.04	34.8	33.48
23	Strata heat totals: sensible heat = -796.17 kW, latent heat = 824.54 kW								
23	Other heat totals: sensible heat = 0.00 kW, latent heat = 0.00 kW								
24	Metabolic rate = 200 W/m², Skin temperature limit value = 34.98 °C								

Results Table - Ramp 6850-5 to 7350

Row	Distance (m)	Dry Bulb (°C)	Wet Bulb (°C)	Pressure (kPa)	Sigma Heat (kJ/kg)	Density (kg/m³)	Humidity (%)	VRT (°C)	MST (°C)
1	0	31.89	21.38	123.762	53.30	1.406	35.72	34.2	34.62
2	10	31.86	21.39	123.784	53.32	1.407	35.87	34.2	34.62
3	20	31.84	21.40	123.806	53.34	1.407	36.01	34.3	34.62
4	30	31.81	21.41	123.828	53.37	1.407	36.15	34.3	34.61
5	40	31.79	21.42	123.850	53.39	1.408	36.29	34.3	34.61
6	50	31.76	21.43	123.872	53.41	1.408	36.43	34.4	34.61
7	60	31.74	21.44	123.894	53.43	1.408	36.57	34.4	34.61
8	70	31.71	21.45	123.917	53.46	1.409	36.71	34.4	34.61
9	80	31.69	21.46	123.939	53.48	1.409	36.85	34.4	34.61
10	90	31.66	21.46	123.961	53.50	1.409	36.99	34.5	34.60
11	100	31.64	21.47	123.983	53.53	1.410	37.13	34.5	34.60
12	110	35.90	22.92	124.005	57.88	1.390	29.34	34.5	34.84
13	120	35.86	22.93	124.027	57.89	1.391	29.50	34.5	34.84
14	130	35.81	22.94	124.048	57.91	1.391	29.66	34.6	34.84
15	140	35.77	22.94	124.070	57.93	1.392	29.82	34.6	34.83
16	150	35.73	22.95	124.092	57.94	1.392	29.97	34.6	34.83
17	160	35.68	22.96	124.114	57.96	1.393	30.13	34.7	34.83
18	170	35.64	22.97	124.136	57.98	1.393	30.29	34.7	34.83
19	180	35.60	22.97	124.157	58.00	1.393	30.45	34.7	34.83
20	190	35.56	22.98	124.179	58.01	1.394	30.61	34.8	34.82
21	200	35.51	22.99	124.201	58.03	1.394	30.77	34.8	34.82
22	210	36.11	23.20	124.223	58.69	1.392	29.87	34.8	34.86
23	220	36.06	23.21	124.245	58.70	1.392	30.03	34.9	34.85
24	230	36.02	23.21	124.267	58.72	1.393	30.19	34.9	34.85
25	240	35.97	23.22	124.288	58.74	1.393	30.34	34.9	34.85
26	250	35.93	23.23	124.310	58.75	1.393	30.50	34.9	34.85
27	260	35.89	23.23	124.332	58.77	1.394	30.66	35.0	34.85
28	270	35.85	23.24	124.354	58.79	1.394	30.82	35.0	34.84
29	280	35.80	23.25	124.376	58.80	1.395	30.97	35.0	34.84
30	290	35.76	23.26	124.398	58.82	1.395	31.13	35.0	34.84
31	300	35.72	23.26	124.420	58.84	1.396	31.29	35.1	34.84
32	310	35.68	23.27	124.442	58.86	1.396	31.44	35.1	34.84
33	320	35.64	23.28	124.463	58.87	1.396	31.60	35.1	34.83
34	330	35.60	23.28	124.485	58.89	1.397	31.76	35.2	34.83
35	340	35.56	23.29	124.507	58.91	1.397	31.91	35.2	34.83
36	350	35.52	23.30	124.529	58.93	1.398	32.07	35.2	34.83
37	360	35.48	23.31	124.551	58.95	1.398	32.22	35.3	34.83
38	370	35.44	23.31	124.573	58.96	1.398	32.38	35.3	34.82
39	380	35.40	23.32	124.595	58.98	1.399	32.53	35.3	34.82
40	390	35.37	23.33	124.617	59.00	1.399	32.68	35.4	34.82
41	400	35.33	23.34	124.639	59.02	1.400	32.84	35.4	34.82
42	410	35.29	23.34	124.661	59.04	1.400	32.99	35.4	34.82
43	420	35.25	23.35	124.683	59.06	1.400	33.14	35.4	34.82
44	430	35.22	23.36	124.705	59.08	1.401	33.29	35.5	34.81
45	440	35.18	23.37	124.727	59.10	1.401	33.45	35.5	34.81
46	450	35.14	23.38	124.749	59.12	1.402	33.60	35.5	34.81
47	460	35.11	23.38	124.771	59.13	1.402	33.75	35.6	34.81
48	470	35.07	23.39	124.793	59.15	1.402	33.90	35.6	34.81
49	480	35.04	23.40	124.815	59.17	1.403	34.05	35.6	34.81
50	490	35.00	23.41	124.837	59.19	1.403	34.20	35.6	34.81
51	500	34.97	23.42	124.859	59.21	1.404	34.35	35.7	34.80
52	510	39.21	24.77	124.880	63.56	1.385	27.33	35.7	35.93
53	520	39.16	24.78	124.902	63.57	1.385	27.49	35.7	35.93
54	530	39.10	24.79	124.924	63.58	1.386	27.65	35.8	35.92
55	540	39.05	24.79	124.946	63.60	1.386	27.82	35.8	35.92
56	550	38.99	24.80	124.967	63.61	1.387	27.98	35.8	35.91
57	560	38.94	24.80	124.989	63.62	1.387	28.15	35.9	35.91
58	570	38.89	24.81	125.011	63.64	1.387	28.31	35.9	35.90
59	580	38.83	24.81	125.032	63.65	1.388	28.47	35.9	35.90

Results Table - Ramp 6850-5 to 7350

Row	Distance (m)	Dry Bulb (°C)	Wet Bulb (°C)	Pressure (kPa)	Sigma Heat (kJ/kg)	Density (kg/m³)	Humidity (%)	VRT (°C)	MST (°C)
60	590	38.78	24.82	125.054	63.66	1.388	28.64	35.9	35.89
61	600	38.73	24.83	125.076	63.68	1.389	28.80	36.0	35.89
62	610	38.68	24.83	125.098	63.69	1.389	28.96	36.0	35.89
63	620	38.63	24.84	125.120	63.71	1.390	29.13	36.0	35.88
64	630	38.58	24.84	125.141	63.72	1.390	29.29	36.1	35.88
65	640	38.52	24.85	125.163	63.74	1.391	29.45	36.1	35.88
66	650	38.47	24.85	125.185	63.75	1.391	29.61	36.1	35.87
67	660	38.43	24.86	125.207	63.77	1.391	29.77	36.1	35.87
68	670	38.38	24.87	125.229	63.78	1.392	29.93	36.2	35.87
69	680	38.33	24.87	125.250	63.80	1.392	30.09	36.2	35.86
70	690	38.28	24.88	125.272	63.81	1.393	30.26	36.2	35.86
71	700	38.23	24.89	125.294	63.83	1.393	30.42	36.3	35.86
72	710	38.18	24.89	125.316	63.84	1.394	30.58	36.3	35.85
73	720	38.14	24.90	125.338	63.86	1.394	30.74	36.3	35.85
74	730	38.09	24.90	125.360	63.87	1.395	30.89	36.4	35.85
75	740	38.04	24.91	125.381	63.89	1.395	31.05	36.4	35.84
76	750	38.00	24.92	125.403	63.90	1.395	31.21	36.4	35.84
77	760	37.95	24.92	125.425	63.92	1.396	31.37	36.4	35.84
78	770	37.90	24.93	125.447	63.94	1.396	31.53	36.5	35.84
79	780	37.86	24.94	125.469	63.95	1.397	31.69	36.5	35.83
80	790	37.81	24.94	125.491	63.97	1.397	31.84	36.5	35.83
81	800	37.77	24.95	125.513	63.99	1.397	32.00	36.6	35.83
82	810	37.73	24.96	125.535	64.00	1.398	32.16	36.6	35.83
83	820	37.68	24.96	125.557	64.02	1.398	32.32	36.6	35.83
84	830	37.64	24.97	125.579	64.04	1.399	32.47	36.6	35.82
85	840	37.60	24.98	125.601	64.05	1.399	32.63	36.7	35.82
86	850	37.55	24.98	125.622	64.07	1.400	32.78	36.7	35.82
87	860	37.51	24.99	125.644	64.09	1.400	32.94	36.7	35.82
88	870	37.47	25.00	125.666	64.10	1.400	33.09	36.8	35.82
89	880	37.43	25.01	125.688	64.12	1.401	33.25	36.8	35.82
90	890	37.39	25.01	125.710	64.14	1.401	33.40	36.8	35.81
91	900	37.35	25.02	125.732	64.16	1.402	33.56	36.9	35.81
92	910	37.86	25.19	125.754	64.73	1.400	32.72	36.9	36.00
93	920	37.81	25.20	125.776	64.75	1.400	32.88	36.9	36.00
94	930	37.77	25.21	125.798	64.76	1.400	33.03	36.9	36.00
95	940	37.73	25.21	125.820	64.78	1.401	33.19	37.0	35.99
96	950	37.69	25.22	125.842	64.80	1.401	33.34	37.0	35.99
97	Electric heat source at 100 m, sensible heat = 209.00 kW								
98	Electric heat source at 200 m, sensible heat = 30.80 kW								
99	Electric heat source at 500 m, sensible heat = 209.00 kW								
100	Electric heat source at 900 m, sensible heat = 26.80 kW								
101	Strata heat totals: sensible heat = -265.75 kW, latent heat = 270.82 kW								
102	Other heat totals: sensible heat = 475.60 kW, latent heat = 0.00 kW								
103	Metabolic rate = 200 W/m², Skin temperature limit value = 34.98 °C								

Appendix E: Mechanical cooling simulation results

Results Table - FA Plenum

Row	Distance (m)	Dry Bulb (°C)	Wet Bulb (°C)	Pressure (kPa)	Sigma Heat (kJ/kg)	Density (kg/m³)	Humidity (%)	VRT (°C)	MST (°C)
1	0	18.80	17.10	101.008	47.29	1.197	84.66	7.0	32.41
2	10	18.81	17.10	101.020	47.30	1.197	84.63	7.0	32.42
3	20	18.82	17.11	101.032	47.31	1.197	84.60	7.0	32.42
4	30	18.82	17.11	101.044	47.32	1.197	84.57	7.0	32.42
5	40	18.83	17.12	101.056	47.32	1.197	84.54	7.1	32.43
6	50	18.84	17.12	101.068	47.33	1.198	84.51	7.1	32.43
7	60	18.85	17.13	101.080	47.34	1.198	84.48	7.1	32.43
8	70	18.86	17.13	101.092	47.35	1.198	84.45	7.1	32.43
9	80	18.86	17.13	101.104	47.36	1.198	84.42	7.1	32.44
10	90	18.87	17.14	101.116	47.37	1.198	84.40	7.2	32.44
11	100	18.88	17.14	101.128	47.38	1.198	84.37	7.2	32.44
12	110	18.89	17.15	101.141	47.39	1.198	84.34	7.2	32.45
13	120	18.90	17.15	101.153	47.39	1.198	84.31	7.2	32.45
14	130	18.90	17.16	101.165	47.40	1.198	84.28	7.2	32.45
15	140	18.91	17.16	101.177	47.41	1.199	84.25	7.2	32.46
16	150	4.26	0.99	101.196	11.12	1.269	53.40	7.3	20.78
17	160	4.27	1.00	101.209	11.14	1.269	53.38	7.3	20.79
18	164	4.28	1.00	101.214	11.14	1.269	53.37	7.3	20.80
19	Spot heat source at 140 m, sensible heat = -6900.00 kW, latent heat = -10000.00 kW								
20	Strata heat totals: sensible heat = -19.27 kW, latent heat = 6.55 kW								
21	Other heat totals: sensible heat = -6900.00 kW, latent heat = -10000.00 kW								
22	Metabolic rate = 200 W/m², Skin temperature limit value = 34.98 °C								

Results Table - No 1 Shaft FA

Row	Distance (m)	Dry Bulb (°C)	Wet Bulb (°C)	Pressure (kPa)	Sigma Heat (kJ/kg)	Density (kg/m³)	Humidity (%)	VRT (°C)	MST (°C)
1	0	4.28	1.00	101.214	11.14	1.269	53.30	7.0	20.69
2	10	4.37	1.06	101.316	11.24	1.270	53.08	7.2	20.78
3	20	4.46	1.13	101.418	11.33	1.271	52.85	7.3	20.87
4	30	4.55	1.19	101.520	11.43	1.271	52.63	7.5	20.95
5	40	4.64	1.25	101.622	11.53	1.272	52.41	7.6	21.04
6	50	4.73	1.31	101.724	11.63	1.273	52.19	7.8	21.13
7	60	4.82	1.38	101.826	11.73	1.274	51.98	8.0	21.22
8	70	4.91	1.44	101.928	11.83	1.275	51.76	8.1	21.31
9	80	5.00	1.50	102.031	11.92	1.276	51.55	8.3	21.39
10	90	5.09	1.56	102.133	12.02	1.277	51.34	8.4	21.48
11	100	5.18	1.62	102.236	12.12	1.278	51.13	8.6	21.57
12	110	5.27	1.69	102.339	12.22	1.278	50.92	8.8	21.66
13	120	5.36	1.75	102.441	12.32	1.279	50.71	8.9	21.74
14	130	5.45	1.81	102.544	12.42	1.280	50.51	9.1	21.83
15	140	5.54	1.87	102.647	12.51	1.281	50.31	9.2	21.92
16	150	5.63	1.93	102.751	12.61	1.282	50.11	9.4	22.01
17	160	5.72	2.00	102.854	12.71	1.283	49.91	9.5	22.09
18	170	5.81	2.06	102.957	12.81	1.284	49.71	9.7	22.18
19	180	5.90	2.12	103.061	12.91	1.285	49.51	9.9	22.27
20	190	5.99	2.18	103.164	13.00	1.285	49.31	10.0	22.36
21	200	6.08	2.24	103.268	13.10	1.286	49.12	10.2	22.44
22	210	6.17	2.31	103.372	13.20	1.287	48.93	10.3	22.53
23	220	6.26	2.37	103.475	13.30	1.288	48.74	10.5	22.62
24	230	6.35	2.43	103.579	13.40	1.289	48.55	10.7	22.70
25	240	6.44	2.49	103.683	13.50	1.290	48.36	10.8	22.79
26	250	6.52	2.55	103.788	13.60	1.291	48.17	11.0	22.88
27	260	6.61	2.61	103.892	13.69	1.292	47.99	11.1	22.97
28	270	6.70	2.67	103.996	13.79	1.292	47.80	11.3	23.05
29	280	6.79	2.74	104.101	13.89	1.293	47.62	11.4	23.14
30	290	6.88	2.80	104.205	13.99	1.294	47.44	11.6	23.23
31	300	6.97	2.86	104.310	14.09	1.295	47.26	11.8	23.31
32	310	7.06	2.92	104.415	14.19	1.296	47.08	11.9	23.40
33	320	7.15	2.98	104.519	14.28	1.297	46.90	12.1	23.49
34	330	7.24	3.04	104.624	14.38	1.298	46.72	12.2	23.57
35	340	7.33	3.10	104.730	14.48	1.299	46.55	12.4	23.66
36	350	7.41	3.16	104.835	14.58	1.300	46.38	12.6	23.74
37	360	7.50	3.23	104.940	14.68	1.300	46.20	12.7	23.83
38	370	7.59	3.29	105.045	14.78	1.301	46.03	12.9	23.92
39	380	7.68	3.35	105.151	14.88	1.302	45.86	13.0	24.00
40	390	7.77	3.41	105.256	14.97	1.303	45.70	13.2	24.09
41	400	7.86	3.47	105.362	15.07	1.304	45.53	13.4	24.17
42	410	7.95	3.53	105.468	15.17	1.305	45.36	13.5	24.26
43	420	8.03	3.59	105.574	15.27	1.306	45.20	13.7	24.35
44	430	8.12	3.65	105.680	15.37	1.307	45.03	13.8	24.43
45	440	8.21	3.71	105.786	15.47	1.308	44.87	14.0	24.52
46	450	8.30	3.77	105.892	15.57	1.308	44.71	14.1	24.60
47	460	8.39	3.83	105.998	15.66	1.309	44.55	14.3	24.69
48	470	8.48	3.89	106.105	15.76	1.310	44.39	14.5	24.78
49	480	8.56	3.95	106.211	15.86	1.311	44.23	14.6	24.86
50	490	8.65	4.01	106.318	15.96	1.312	44.08	14.8	24.95
51	500	8.74	4.07	106.425	16.06	1.313	43.92	14.9	25.03
52	510	8.83	4.13	106.531	16.16	1.314	43.77	15.1	25.12

Results Table - No 1 Shaft FA

Row	Distance (m)	Dry Bulb (°C)	Wet Bulb (°C)	Pressure (kPa)	Sigma Heat (kJ/kg)	Density (kg/m³)	Humidity (%)	VRT (°C)	MST (°C)
53	520	8.92	4.19	106.638	16.26	1.315	43.61	15.3	25.20
54	530	9.00	4.25	106.745	16.36	1.316	43.46	15.4	25.29
55	540	9.09	4.31	106.853	16.45	1.317	43.31	15.6	25.37
56	550	9.18	4.37	106.960	16.55	1.317	43.16	15.7	25.46
57	560	9.27	4.43	107.067	16.65	1.318	43.01	15.9	25.54
58	570	9.36	4.49	107.175	16.75	1.319	42.86	16.1	25.63
59	580	9.44	4.55	107.282	16.85	1.320	42.71	16.2	25.72
60	590	9.53	4.61	107.390	16.95	1.321	42.57	16.4	25.81
61	600	9.62	4.67	107.498	17.05	1.322	42.42	16.5	25.89
62	610	9.71	4.73	107.605	17.15	1.323	42.28	16.7	25.98
63	620	9.79	4.79	107.713	17.24	1.324	42.14	16.8	26.06
64	630	9.88	4.85	107.821	17.34	1.325	41.99	17.0	26.15
65	640	9.97	4.91	107.930	17.44	1.326	41.85	17.2	26.23
66	650	10.06	4.97	108.038	17.54	1.327	41.71	17.3	26.31
67	660	10.14	5.03	108.146	17.64	1.328	41.57	17.5	26.40
68	670	10.23	5.09	108.255	17.74	1.328	41.44	17.6	26.48
69	680	10.32	5.15	108.363	17.84	1.329	41.30	17.8	26.57
70	690	10.41	5.21	108.472	17.94	1.330	41.16	17.9	26.65
71	700	10.49	5.27	108.581	18.04	1.331	41.03	18.1	26.73
72	710	10.58	5.33	108.690	18.13	1.332	40.89	18.3	26.82
73	720	10.67	5.39	108.799	18.23	1.333	40.76	18.4	26.90
74	730	10.75	5.45	108.908	18.33	1.334	40.63	18.6	26.99
75	740	10.84	5.51	109.017	18.43	1.335	40.49	18.8	27.07
76	750	10.93	5.57	109.126	18.53	1.336	40.36	18.9	27.15
77	760	11.02	5.63	109.236	18.63	1.337	40.23	19.1	27.24
78	770	11.10	5.68	109.345	18.73	1.338	40.10	19.2	27.32
79	780	11.19	5.74	109.455	18.83	1.339	39.98	19.4	27.41
80	790	11.28	5.80	109.565	18.93	1.340	39.85	19.5	27.49
81	800	11.36	5.86	109.675	19.03	1.340	39.72	19.7	27.57
82	810	11.45	5.92	109.785	19.12	1.341	39.60	19.9	27.66
83	820	11.54	5.98	109.895	19.22	1.342	39.47	20.0	27.74
84	830	11.62	6.04	110.005	19.32	1.343	39.35	20.2	27.82
85	840	11.71	6.10	110.115	19.42	1.344	39.22	20.3	27.91
86	850	11.80	6.16	110.226	19.52	1.345	39.10	20.5	27.99
87	860	11.88	6.21	110.336	19.62	1.346	38.98	20.6	28.08
88	870	11.97	6.27	110.447	19.72	1.347	38.86	20.8	28.16
89	880	12.06	6.33	110.557	19.82	1.348	38.74	21.0	28.24
90	890	12.14	6.39	110.668	19.92	1.349	38.62	21.1	28.33
91	900	12.23	6.45	110.779	20.02	1.350	38.50	21.3	28.41
92	910	12.32	6.51	110.890	20.12	1.351	38.38	21.4	28.49
93	920	12.40	6.56	111.001	20.21	1.352	38.27	21.6	28.57
94	930	12.49	6.62	111.113	20.31	1.353	38.15	21.8	28.66
95	940	12.58	6.68	111.224	20.41	1.354	38.04	21.9	28.74
96	950	12.66	6.74	111.335	20.51	1.355	37.92	22.1	28.82
97	960	12.75	6.80	111.447	20.61	1.355	37.81	22.2	28.91
98	970	12.83	6.86	111.559	20.71	1.356	37.69	22.4	28.99
99	980	12.92	6.91	111.670	20.81	1.357	37.58	22.6	29.07
100	990	13.01	6.97	111.782	20.91	1.358	37.47	22.7	29.16
101	1000	13.09	7.03	111.894	21.01	1.359	37.36	22.9	29.24
102	1010	13.18	7.09	112.006	21.11	1.360	37.25	23.0	29.32
103	1020	13.26	7.15	112.119	21.21	1.361	37.14	23.2	29.41
104	1030	13.35	7.20	112.231	21.31	1.362	37.03	23.4	29.49

Results Table - No 1 Shaft FA

Row	Distance (m)	Dry Bulb (°C)	Wet Bulb (°C)	Pressure (kPa)	Sigma Heat (kJ/kg)	Density (kg/m³)	Humidity (%)	VRT (°C)	MST (°C)
105	1040	13.44	7.26	112.343	21.41	1.363	36.92	23.5	29.57
106	1050	13.52	7.32	112.456	21.51	1.364	36.81	23.7	29.65
107	1060	13.61	7.38	112.569	21.60	1.365	36.71	23.8	29.74
108	1070	13.69	7.44	112.681	21.70	1.366	36.60	24.0	29.82
109	1080	13.78	7.49	112.794	21.80	1.367	36.50	24.1	29.90
110	1090	13.86	7.55	112.907	21.90	1.368	36.39	24.3	29.99
111	1100	13.95	7.61	113.020	22.00	1.369	36.29	24.5	30.07
112	1110	14.04	7.67	113.133	22.10	1.370	36.18	24.6	30.15
113	1120	14.12	7.72	113.247	22.20	1.371	36.08	24.8	30.23
114	1130	14.21	7.78	113.360	22.30	1.372	35.98	24.9	30.32
115	1140	14.29	7.84	113.474	22.40	1.373	35.88	25.1	30.40
116	1150	14.38	7.90	113.587	22.50	1.374	35.78	25.3	30.48
117	1160	14.46	7.95	113.701	22.60	1.375	35.68	25.4	30.56
118	1170	14.55	8.01	113.815	22.70	1.376	35.58	25.6	30.65
119	1180	14.63	8.07	113.929	22.80	1.376	35.48	25.7	30.73
120	1190	14.72	8.13	114.043	22.90	1.377	35.38	25.9	30.81
121	1200	14.80	8.18	114.157	23.00	1.378	35.28	26.1	30.89
122	1210	14.89	8.24	114.271	23.10	1.379	35.18	26.2	30.97
123	1220	14.98	8.30	114.386	23.20	1.380	35.09	26.4	31.06
124	1230	15.06	8.35	114.500	23.30	1.381	34.99	26.5	31.14
125	1240	15.15	8.41	114.615	23.39	1.382	34.89	26.7	31.22
126	1250	15.23	8.47	114.730	23.49	1.383	34.80	26.8	31.30
127	1260	15.32	8.53	114.844	23.59	1.384	34.70	27.0	31.39
128	1270	15.40	8.58	114.959	23.69	1.385	34.61	27.2	31.46
129	1280	15.49	8.64	115.074	23.79	1.386	34.52	27.3	31.54
130	1290	15.57	8.70	115.190	23.89	1.387	34.42	27.5	31.62
131	1300	15.66	8.75	115.305	23.99	1.388	34.33	27.6	31.70
132	1310	15.74	8.81	115.420	24.09	1.389	34.24	27.8	31.78
133	1320	15.83	8.87	115.536	24.19	1.390	34.15	27.9	31.86
134	1330	15.91	8.92	115.651	24.29	1.391	34.06	28.1	31.95
135	1340	15.99	8.98	115.767	24.39	1.392	33.97	28.3	32.03
136	1350	16.08	9.04	115.883	24.49	1.393	33.88	28.4	32.11
137	1360	16.16	9.09	115.999	24.59	1.394	33.79	28.6	32.19
138	1370	16.25	9.15	116.115	24.69	1.395	33.70	28.8	32.27
139	1380	16.33	9.21	116.231	24.79	1.396	33.61	28.9	32.35
140	1390	16.42	9.26	116.347	24.89	1.397	33.53	29.1	32.43
141	1400	16.50	9.32	116.464	24.99	1.398	33.44	29.2	32.50
142	1410	16.59	9.38	116.580	25.09	1.399	33.35	29.4	32.55
143	1420	16.67	9.43	116.697	25.19	1.400	33.27	29.5	32.60
144	1430	16.76	9.49	116.813	25.29	1.401	33.18	29.7	32.64
145	1440	16.84	9.54	116.930	25.39	1.402	33.10	29.9	32.68
146	1450	16.92	9.60	117.047	25.49	1.403	33.01	30.0	32.72
147	1460	17.01	9.66	117.164	25.59	1.404	32.93	30.2	32.75
148	1470	17.09	9.71	117.281	25.69	1.405	32.84	30.3	32.78
149	1480	17.18	9.77	117.398	25.79	1.406	32.76	30.5	32.81
150	1490	17.26	9.82	117.516	25.89	1.407	32.68	30.6	32.85
151	1500	17.35	9.88	117.633	25.99	1.408	32.60	30.8	32.87
152	1510	17.43	9.94	117.751	26.09	1.409	32.51	31.0	32.90
153	1520	17.51	9.99	117.869	26.19	1.410	32.43	31.1	32.93
154	1530	17.60	10.05	117.986	26.29	1.411	32.35	31.3	32.95
155	1540	17.68	10.10	118.104	26.39	1.412	32.27	31.4	32.98
156	1550	17.77	10.16	118.222	26.49	1.413	32.19	31.6	33.00

Results Table - No 1 Shaft FA

Row	Distance (m)	Dry Bulb (°C)	Wet Bulb (°C)	Pressure (kPa)	Sigma Heat (kJ/kg)	Density (kg/m³)	Humidity (%)	VRT (°C)	MST (°C)
157	1560	17.85	10.22	118.341	26.59	1.414	32.11	31.8	33.03
158	1568	17.92	10.26	118.435	26.67	1.415	32.05	31.9	33.04
159	Strata heat totals: sensible heat = -823.34 kW, latent heat = 925.20 kW								
160	Other heat totals: sensible heat = 0.00 kW, latent heat = 0.00 kW								
161	Metabolic rate = 200 W/m², Skin temperature limit value = 34.98 °C								

Results Table - 5400L No 1 FA

Row	Distance (m)	Dry Bulb (°C)	Wet Bulb (°C)	Pressure (kPa)	Sigma Heat (kJ/kg)	Density (kg/m³)	Humidity (%)	VRT (°C)	MST (°C)
1	0	17.92	10.26	118.435	26.67	1.415	32.03	28.6	33.03
2	10	18.00	10.32	118.552	26.76	1.416	31.95	28.8	33.05
3	20	18.09	10.37	118.669	26.86	1.417	31.87	28.9	33.08
4	30	18.17	10.43	118.786	26.96	1.418	31.80	29.1	33.10
5	40	18.25	10.48	118.903	27.06	1.419	31.72	29.3	33.12
6	50	18.34	10.54	119.020	27.16	1.420	31.64	29.5	33.14
7	60	18.42	10.59	119.138	27.26	1.420	31.57	29.6	33.16
8	70	18.50	10.65	119.255	27.36	1.421	31.49	29.8	33.18
9	80	18.59	10.70	119.373	27.46	1.422	31.42	30.0	33.20
10	90	18.67	10.76	119.490	27.56	1.423	31.34	30.1	33.22
11	100	18.75	10.81	119.608	27.66	1.424	31.27	30.3	33.24
12	110	18.84	10.87	119.726	27.76	1.425	31.19	30.5	33.26
13	120	18.92	10.92	119.844	27.86	1.426	31.12	30.7	33.27
14	130	19.00	10.98	119.962	27.96	1.427	31.05	30.8	33.29
15	140	19.09	11.03	120.081	28.06	1.428	30.97	31.0	33.31
16	151	19.18	11.09	120.211	28.17	1.430	30.89	31.2	33.33
17	Strata heat totals: sensible heat = -111.62 kW, latent heat = 125.41 kW								
18	Other heat totals: sensible heat = 0.00 kW, latent heat = 0.00 kW								
19	Metabolic rate = 200 W/m², Skin temperature limit value = 34.98 °C								

Results Table - 5900L No 1 FA

Row	Distance (m)	Dry Bulb (°C)	Wet Bulb (°C)	Pressure (kPa)	Sigma Heat (kJ/kg)	Density (kg/m³)	Humidity (%)	VRT (°C)	MST (°C)
1	0	19.18	11.09	120.211	28.16	1.429	30.86	30.6	33.42
2	10	19.26	11.15	120.340	28.26	1.431	30.79	30.8	33.44
3	20	19.35	11.20	120.470	28.36	1.432	30.73	30.9	33.45
4	30	19.43	11.26	120.600	28.46	1.433	30.66	31.1	33.47
5	40	19.51	11.31	120.730	28.56	1.434	30.59	31.3	33.48
6	50	19.59	11.37	120.860	28.66	1.435	30.53	31.5	33.50
7	60	19.68	11.42	120.990	28.77	1.436	30.46	31.6	33.52
8	70	19.76	11.48	121.120	28.87	1.437	30.40	31.8	33.53
9	80	19.84	11.54	121.250	28.97	1.439	30.33	32.0	33.55
10	90	19.93	11.59	121.381	29.07	1.440	30.27	32.1	33.56
11	100	20.01	11.65	121.511	29.17	1.441	30.20	32.3	33.58
12	107	20.07	11.69	121.603	29.24	1.442	30.16	32.4	33.59
13	Strata heat totals: sensible heat = -57.07 kW, latent heat = 67.27 kW								
14	Other heat totals: sensible heat = 0.00 kW, latent heat = 0.00 kW								
15	Metabolic rate = 200 W/m², Skin temperature limit value = 34.98 °C								

Results Table - 6200L No 1 FA

Row	Distance (m)	Dry Bulb (°C)	Wet Bulb (°C)	Pressure (kPa)	Sigma Heat (kJ/kg)	Density (kg/m³)	Humidity (%)	VRT (°C)	MST (°C)
1	0	20.07	11.69	121.603	29.25	1.442	30.17	33.7	33.64
2	10	20.15	11.75	121.738	29.35	1.443	30.11	33.9	33.66
3	20	20.24	11.80	121.872	29.45	1.444	30.05	34.1	33.67
4	30	20.32	11.86	122.007	29.55	1.445	29.99	34.3	33.69
5	40	20.40	11.91	122.142	29.65	1.446	29.93	34.4	33.70
6	50	20.49	11.97	122.277	29.75	1.448	29.86	34.6	33.71
7	60	20.57	12.03	122.412	29.86	1.449	29.80	34.8	33.73
8	70	20.65	12.08	122.548	29.96	1.450	29.74	35.0	33.74
9	80	20.74	12.14	122.683	30.06	1.451	29.68	35.1	33.76
10	90	20.82	12.19	122.819	30.16	1.452	29.62	35.3	33.77
11	100	20.90	12.25	122.954	30.26	1.453	29.56	35.5	33.76
12	110	20.98	12.31	123.090	30.36	1.455	29.50	35.7	33.78
13	120	21.07	12.36	123.226	30.47	1.456	29.45	35.9	33.79
14	130	21.15	12.42	123.362	30.57	1.457	29.39	36.1	33.80
15	140	21.23	12.47	123.498	30.67	1.458	29.33	36.3	33.82
16	150	21.32	12.53	123.635	30.77	1.459	29.27	36.4	33.83
17	160	21.40	12.59	123.771	30.87	1.461	29.21	36.6	33.84
18	170	21.48	12.64	123.907	30.97	1.462	29.15	36.8	33.85
19	180	21.57	12.70	124.044	31.08	1.463	29.10	37.0	33.87
20	183	21.59	12.71	124.085	31.11	1.463	29.08	37.0	33.87
21	Strata heat totals: sensible heat = -77.02 kW, latent heat = 98.12 kW								
22	Other heat totals: sensible heat = 0.00 kW, latent heat = 0.00 kW								
23	Metabolic rate = 200 W/m², Skin temperature limit value = 34.98 °C								

Results Table - 6950L No 1 FA

Row	Distance (m)	Dry Bulb (°C)	Wet Bulb (°C)	Pressure (kPa)	Sigma Heat (kJ/kg)	Density (kg/m³)	Humidity (%)	VRT (°C)	MST (°C)
1	0	21.59	12.71	124.085	31.10	1.463	29.05	34.1	33.91
2	10	21.67	12.77	124.224	31.20	1.465	29.00	34.3	33.92
3	20	21.75	12.82	124.363	31.30	1.466	28.95	34.5	33.93
4	30	21.84	12.88	124.502	31.40	1.467	28.89	34.6	33.94
5	Strata heat totals: sensible heat = -11.17 kW, latent heat = 14.20 kW								
6	Other heat totals: sensible heat = 0.00 kW, latent heat = 0.00 kW								
7	Metabolic rate = 200 W/m², Skin temperature limit value = 34.98 °C								

Results Table - Sump No 1 FA

Row	Distance (m)	Dry Bulb (°C)	Wet Bulb (°C)	Pressure (kPa)	Sigma Heat (kJ/kg)	Density (kg/m³)	Humidity (%)	VRT (°C)	MST (°C)
1	0	21.84	12.88	124.502	31.41	1.467	28.90	34.8	33.94
2	10	21.70	12.94	124.641	31.52	1.469	29.94	35.0	33.93
3	20	21.56	12.99	124.780	31.62	1.471	30.98	35.2	33.91
4	30	21.79	13.21	124.920	32.09	1.472	31.31	35.4	33.94
5	40	21.66	13.27	125.059	32.19	1.474	32.33	35.5	33.93
6	50	21.54	13.32	125.199	32.30	1.476	33.34	35.7	33.92
7	60	21.42	13.38	125.339	32.40	1.478	34.34	35.9	33.90
8	71	21.29	13.44	125.493	32.52	1.481	35.42	36.1	33.89
9	Electric heat source at 29 m, sensible heat = 90.00 kW								
10	Strata heat totals: sensible heat = -403.75 kW, latent heat = 415.56 kW								
11	Other heat totals: sensible heat = 90.00 kW, latent heat = 0.00 kW								
12	Metabolic rate = 200 W/m², Skin temperature limit value = 34.98 °C								

Results Table - 6850L Access

Row	Distance (m)	Dry Bulb (°C)	Wet Bulb (°C)	Pressure (kPa)	Sigma Heat (kJ/kg)	Density (kg/m³)	Humidity (%)	VRT (°C)	MST (°C)
1	0	21.84	12.88	124.502	31.41	1.467	28.90	34.2	34.15
2	10	21.82	12.89	124.502	31.43	1.467	29.05	34.2	34.15
3	20	21.80	12.90	124.501	31.45	1.467	29.20	34.2	34.15
4	27	21.79	12.90	124.501	31.46	1.467	29.31	34.2	34.15
5	Strata heat totals: sensible heat = -2.69 kW, latent heat = 5.17 kW								
6	Other heat totals: sensible heat = 0.00 kW, latent heat = 0.00 kW								
7	Metabolic rate = 200 W/m², Skin temperature limit value = 34.98 °C								

Results Table - 6850L 1

Row	Distance (m)	Dry Bulb (°C)	Wet Bulb (°C)	Pressure (kPa)	Sigma Heat (kJ/kg)	Density (kg/m³)	Humidity (%)	VRT (°C)	MST (°C)
1	0	21.79	12.90	124.501	31.46	1.467	29.28	34.2	34.15
2	10	21.78	12.91	124.501	31.48	1.467	29.42	34.2	34.15
3	20	21.76	12.92	124.500	31.50	1.467	29.57	34.2	34.15
4	25	26.22	14.90	124.500	36.00	1.445	22.67	34.2	34.54
5	Electric heat source at 20 m, sensible heat = 225.00 kW								
6	Strata heat totals: sensible heat = -1.87 kW, latent heat = 4.77 kW								
7	Other heat totals: sensible heat = 225.00 kW, latent heat = 0.00 kW								
8	Metabolic rate = 200 W/m², Skin temperature limit value = 34.98 °C								

Results Table - 6850L 2

Row	Distance (m)	Dry Bulb (°C)	Wet Bulb (°C)	Pressure (kPa)	Sigma Heat (kJ/kg)	Density (kg/m³)	Humidity (%)	VRT (°C)	MST (°C)
1	0	26.22	14.90	124.500	35.99	1.445	22.64	34.2	34.55
2	10	26.81	15.17	124.500	36.63	1.443	21.98	34.2	34.58
3	20	26.77	15.18	124.499	36.65	1.443	22.14	34.2	34.58
4	31	27.36	15.45	124.499	37.29	1.440	21.52	34.2	34.62
5	Electric heat source at 1 m, sensible heat = 30.00 kW								
6	Electric heat source at 29 m, sensible heat = 30.00 kW								
7	Strata heat totals: sensible heat = -5.09 kW, latent heat = 7.47 kW								
8	Other heat totals: sensible heat = 60.00 kW, latent heat = 0.00 kW								
9	Metabolic rate = 200 W/m², Skin temperature limit value = 34.98 °C								

Results Table - 6850L 3

Row	Distance (m)	Dry Bulb (°C)	Wet Bulb (°C)	Pressure (kPa)	Sigma Heat (kJ/kg)	Density (kg/m³)	Humidity (%)	VRT (°C)	MST (°C)
1	0	27.36	15.45	124.499	37.29	1.440	21.51	34.2	34.55
2	10	27.32	15.45	124.498	37.30	1.440	21.67	34.2	34.55
3	20	27.28	15.46	124.498	37.31	1.440	21.82	34.2	34.54
4	Strata heat totals: sensible heat = -5.36 kW, latent heat = 6.78 kW								
5	Other heat totals: sensible heat = 0.00 kW, latent heat = 0.00 kW								
6	Metabolic rate = 200 W/m², Skin temperature limit value = 34.98 °C								

Results Table - 6850L 4

Row	Distance (m)	Dry Bulb (°C)	Wet Bulb (°C)	Pressure (kPa)	Sigma Heat (kJ/kg)	Density (kg/m³)	Humidity (%)	VRT (°C)	MST (°C)
1	0	27.28	15.46	124.498	37.32	1.440	21.85	34.2	34.58
2	10	27.24	15.47	124.498	37.33	1.440	22.01	34.2	34.58
3	20	27.21	15.47	124.497	37.34	1.441	22.17	34.2	34.58
4	30	27.17	15.48	124.497	37.36	1.441	22.32	34.2	34.57
5	40	27.13	15.48	124.496	37.37	1.441	22.48	34.2	34.57
6	50	27.10	15.49	124.496	37.38	1.441	22.64	34.2	34.57
7	60	27.06	15.49	124.496	37.40	1.441	22.80	34.2	34.56
8	70	27.03	15.50	124.495	37.41	1.441	22.96	34.2	34.56
9	80	26.99	15.50	124.495	37.43	1.441	23.12	34.2	34.56
10	90	26.95	15.51	124.494	37.44	1.442	23.27	34.2	34.56
11	94	26.94	15.51	124.494	37.44	1.442	23.34	34.2	34.55
12	Strata heat totals: sensible heat = -19.15 kW, latent heat = 25.97 kW								
13	Other heat totals: sensible heat = 0.00 kW, latent heat = 0.00 kW								
14	Metabolic rate = 200 W/m², Skin temperature limit value = 34.98 °C								

Results Table - 6850L 5

Row	Distance (m)	Dry Bulb (°C)	Wet Bulb (°C)	Pressure (kPa)	Sigma Heat (kJ/kg)	Density (kg/m³)	Humidity (%)	VRT (°C)	MST (°C)
1	0	26.94	15.51	124.494	37.45	1.442	23.34	34.2	34.59
2	10	26.91	15.52	124.494	37.46	1.442	23.50	34.2	34.59
3	20	26.87	15.52	124.493	37.48	1.442	23.67	34.2	34.59
4	30	26.84	15.53	124.493	37.49	1.442	23.83	34.2	34.58
5	40	26.80	15.54	124.493	37.51	1.442	23.99	34.2	34.58
6	50	26.77	15.54	124.493	37.53	1.442	24.15	34.2	34.58
7	60	26.74	15.55	124.492	37.55	1.442	24.31	34.2	34.57
8	70	26.70	15.56	124.492	37.56	1.443	24.47	34.2	34.57
9	80	26.67	15.56	124.492	37.58	1.443	24.64	34.2	34.57
10	90	26.64	15.57	124.492	37.60	1.443	24.80	34.2	34.56
11	100	26.61	15.58	124.491	37.61	1.443	24.96	34.2	34.56
12	105	26.59	15.58	124.491	37.62	1.443	25.04	34.2	34.56
13	Strata heat totals: sensible heat = -16.08 kW, latent heat = 23.94 kW								
14	Other heat totals: sensible heat = 0.00 kW, latent heat = 0.00 kW								
15	Metabolic rate = 200 W/m², Skin temperature limit value = 34.98 °C								

Results Table - 6850L 4r1

Row	Distance (m)	Dry Bulb (°C)	Wet Bulb (°C)	Pressure (kPa)	Sigma Heat (kJ/kg)	Density (kg/m³)	Humidity (%)	VRT (°C)	MST (°C)
1	0	26.94	15.51	124.494	37.45	1.442	23.34	34.2	34.82
2	10	26.92	15.54	124.494	37.51	1.442	23.56	34.2	34.82
3	20	26.90	15.57	124.494	37.58	1.442	23.78	34.2	34.82
4	29	26.89	15.59	124.494	37.64	1.442	23.98	34.2	34.81
5	Strata heat totals: sensible heat = -0.55 kW, latent heat = 2.58 kW								
6	Other heat totals: sensible heat = 0.00 kW, latent heat = 0.00 kW								
7	Metabolic rate = 200 W/m², Skin temperature limit value = 34.98 °C								

Results Table - 6850L 4r2

Row	Distance (m)	Dry Bulb (°C)	Wet Bulb (°C)	Pressure (kPa)	Sigma Heat (kJ/kg)	Density (kg/m³)	Humidity (%)	VRT (°C)	MST (°C)
1	0	26.89	15.59	124.494	37.64	1.442	23.96	34.2	34.81
2	10	26.87	15.62	124.494	37.71	1.442	24.18	34.2	34.81
3	20	26.85	15.65	124.494	37.77	1.442	24.40	34.2	34.81
4	30	26.84	15.67	124.494	37.84	1.442	24.62	34.2	34.81
5	40	45.16	22.55	124.494	56.36	1.359	9.07	34.2	36.49
6	50	45.63	22.76	124.494	57.01	1.357	9.00	34.2	36.68
7	60	45.38	22.74	124.494	56.94	1.358	9.26	34.2	36.62
8	70	45.14	22.72	124.494	56.88	1.359	9.52	34.2	36.57
9	80	44.90	22.69	124.494	56.81	1.360	9.79	34.2	36.52
10	90	44.66	22.67	124.494	56.75	1.361	10.06	34.2	36.46
11	100	44.43	22.65	124.494	56.69	1.362	10.33	34.2	36.42
12	110	44.20	22.63	124.494	56.63	1.363	10.60	34.2	36.37
13	120	43.97	22.61	124.494	56.58	1.364	10.88	34.2	36.32
14	130	43.75	22.59	124.494	56.52	1.364	11.16	34.2	36.27
15	140	43.53	22.57	124.494	56.47	1.365	11.44	34.2	36.22
16	Electric heat source at 30 m, sensible heat = 195.00 kW								
17	Electric heat source at 40 m, sensible heat = 7.50 kW								
18	Strata heat totals: sensible heat = -25.62 kW, latent heat = 21.74 kW								
19	Other heat totals: sensible heat = 202.50 kW, latent heat = 0.00 kW								
20	Metabolic rate = 200 W/m², Skin temperature limit value = 34.98 °C								

Results Table - 6850L 3r1

Row	Distance (m)	Dry Bulb (°C)	Wet Bulb (°C)	Pressure (kPa)	Sigma Heat (kJ/kg)	Density (kg/m³)	Humidity (%)	VRT (°C)	MST (°C)
1	0	27.28	15.46	124.498	37.32	1.440	21.85	34.2	34.81
2	10	27.26	15.49	124.515	37.38	1.440	22.04	34.2	34.81
3	20	27.25	15.51	124.532	37.44	1.441	22.23	34.2	34.81
4	30	27.23	15.54	124.549	37.50	1.441	22.43	34.3	34.80
5	40	27.22	15.57	124.566	37.56	1.441	22.62	34.3	34.80
6	50	27.20	15.59	124.582	37.62	1.441	22.81	34.3	34.80
7	60	27.19	15.62	124.599	37.69	1.442	23.00	34.3	34.80
8	70	27.18	15.65	124.616	37.75	1.442	23.19	34.4	34.80
9	80	27.16	15.67	124.633	37.81	1.442	23.38	34.4	34.80
10	90	27.15	15.70	124.650	37.87	1.442	23.57	34.4	34.79
11	100	27.14	15.73	124.667	37.94	1.443	23.76	34.4	34.79
12	110	27.13	15.75	124.684	38.00	1.443	23.95	34.4	34.79
13	120	27.11	15.78	124.701	38.06	1.443	24.13	34.5	34.79
14	130	27.10	15.81	124.718	38.13	1.443	24.32	34.5	34.79
15	140	27.09	15.83	124.735	38.19	1.444	24.51	34.5	34.79
16	150	27.08	15.86	124.752	38.25	1.444	24.69	34.5	34.78
17	160	27.07	15.89	124.769	38.32	1.444	24.88	34.5	34.78
18	170	27.06	15.92	124.785	38.38	1.444	25.06	34.6	34.78
19	180	27.05	15.94	124.802	38.45	1.444	25.24	34.6	34.78
20	190	27.04	15.97	124.819	38.51	1.445	25.43	34.6	34.78
21	200	27.03	16.00	124.836	38.57	1.445	25.61	34.6	34.78
22	210	27.02	16.03	124.853	38.64	1.445	25.79	34.7	34.77
23	220	27.02	16.05	124.870	38.70	1.445	25.97	34.7	34.77
24	230	27.01	16.08	124.887	38.77	1.445	26.15	34.7	34.77
25	240	27.00	16.11	124.904	38.84	1.446	26.33	34.7	34.77
26	250	26.99	16.14	124.921	38.90	1.446	26.51	34.7	34.77
27	259	26.99	16.16	124.936	38.96	1.446	26.67	34.8	34.77
28	Strata heat totals: sensible heat = -8.43 kW, latent heat = 27.08 kW								
29	Other heat totals: sensible heat = 0.00 kW, latent heat = 0.00 kW								
30	Metabolic rate = 200 W/m², Skin temperature limit value = 34.98 °C								

Results Table - Shaft bottom ramp

Row	Distance (m)	Dry Bulb (°C)	Wet Bulb (°C)	Pressure (kPa)	Sigma Heat (kJ/kg)	Density (kg/m³)	Humidity (%)	VRT (°C)	MST (°C)
1	0	21.29	13.44	125.493	32.52	1.481	35.43	35.4	33.75
2	10	21.23	13.42	125.430	32.49	1.480	35.62	35.3	33.74
3	20	21.17	13.40	125.366	32.46	1.480	35.81	35.3	33.73
4	30	21.12	13.38	125.303	32.43	1.479	36.00	35.2	33.72
5	40	21.06	13.37	125.240	32.39	1.479	36.19	35.1	33.71
6	50	21.00	13.35	125.176	32.36	1.478	36.39	35.0	33.71
7	60	20.95	13.33	125.113	32.33	1.478	36.58	35.0	33.70
8	70	20.89	13.31	125.050	32.30	1.478	36.77	34.9	33.69
9	80	20.83	13.29	124.987	32.27	1.477	36.96	34.9	33.68
10	90	20.78	13.27	124.923	32.24	1.477	37.16	34.8	33.67
11	100	20.72	13.25	124.860	32.20	1.476	37.35	34.7	33.67
12	105	20.69	13.24	124.829	32.19	1.476	37.45	34.7	33.66
13	Strata heat totals: sensible heat = -53.02 kW, latent heat = 67.26 kW								
14	Other heat totals: sensible heat = 0.00 kW, latent heat = 0.00 kW								
15	Metabolic rate = 200 W/m², Skin temperature limit value = 34.98 °C								

Results Table – FA xfr BAC

Row	Distance (m)	Dry Bulb (°C)	Wet Bulb (°C)	Pressure (kPa)	Sigma Heat (kJ/kg)	Density (kg/m³)	Humidity (%)	VRT (°C)	MST (°C)
1	0	20.69	13.24	124.829	32.18	1.476	37.42	34.8	33.65
2	10	20.49	13.24	124.820	32.19	1.477	38.59	34.8	33.62
3	20	20.29	13.24	124.811	32.20	1.478	39.75	34.8	33.59
4	30	20.10	13.25	124.802	32.20	1.478	40.90	34.8	33.56
5	40	19.92	13.25	124.793	32.21	1.479	42.03	34.8	33.53
6	50	19.74	13.25	124.785	32.22	1.480	43.16	34.8	33.51
7	60	19.56	13.25	124.776	32.23	1.481	44.27	34.8	33.48
8	70	19.39	13.25	124.767	32.24	1.481	45.38	34.8	33.45
9	80	19.23	13.26	124.758	32.24	1.482	46.47	34.8	33.42
10	90	19.07	13.26	124.749	32.25	1.483	47.54	34.8	33.39
11	100	18.91	13.26	124.740	32.26	1.483	48.61	34.8	33.36
12	110	18.76	13.26	124.731	32.27	1.484	49.66	34.8	33.34
13	120	18.61	13.27	124.722	32.28	1.484	50.69	34.8	33.31
14	130	18.47	13.27	124.713	32.28	1.485	51.72	34.8	33.28
15	140	18.33	13.27	124.705	32.29	1.485	52.73	34.8	33.25
16	150	18.20	13.27	124.696	32.30	1.486	53.72	34.8	33.22
17	160	18.07	13.27	124.687	32.31	1.487	54.70	34.8	33.19
18	170	17.94	13.28	124.678	32.32	1.487	55.67	34.8	33.17
19	180	17.82	13.28	124.669	32.32	1.487	56.62	34.8	33.14
20	190	17.70	13.28	124.660	32.33	1.488	57.55	34.8	33.11
21	200	17.58	13.28	124.651	32.34	1.488	58.47	34.8	33.08
22	210	17.47	13.28	124.643	32.35	1.489	59.38	34.8	33.05
23	Strata heat totals: sensible heat = -861.64 kW, latent heat = 902.11 kW								
24	Other heat totals: sensible heat = 0.00 kW, latent heat = 0.00 kW								
25	Metabolic rate = 200 W/m², Skin temperature limit value = 34.98 °C								

Results Table - Ramp 6850-5 to 7350

Row	Distance (m)	Dry Bulb (°C)	Wet Bulb (°C)	Pressure (kPa)	Sigma Heat (kJ/kg)	Density (kg/m³)	Humidity (%)	VRT (°C)	MST (°C)
1	0	26.59	15.58	124.491	37.62	1.443	25.04	34.2	34.55
2	10	26.57	15.59	124.514	37.65	1.443	25.18	34.2	34.55
3	20	26.56	15.61	124.536	37.68	1.444	25.32	34.3	34.54
4	30	26.54	15.62	124.559	37.72	1.444	25.46	34.3	34.54
5	40	26.53	15.64	124.582	37.75	1.444	25.60	34.3	34.54
6	50	26.51	15.65	124.604	37.78	1.445	25.74	34.4	34.54
7	60	26.50	15.67	124.627	37.81	1.445	25.88	34.4	34.54
8	70	26.48	15.68	124.650	37.85	1.445	26.01	34.4	34.54
9	80	26.47	15.70	124.672	37.88	1.446	26.15	34.4	34.53
10	90	26.45	15.71	124.695	37.91	1.446	26.29	34.5	34.53
11	100	26.44	15.73	124.718	37.95	1.446	26.43	34.5	34.53
12	110	30.66	17.47	124.740	42.24	1.426	20.77	34.5	34.76
13	120	30.63	17.48	124.762	42.27	1.427	20.92	34.5	34.76
14	130	30.60	17.49	124.785	42.30	1.427	21.07	34.6	34.76
15	140	30.57	17.51	124.807	42.32	1.428	21.22	34.6	34.75
16	150	30.54	17.52	124.830	42.35	1.428	21.37	34.6	34.75
17	160	30.50	17.53	124.852	42.37	1.428	21.52	34.7	34.75
18	170	30.47	17.54	124.874	42.40	1.429	21.67	34.7	34.75
19	180	30.44	17.55	124.897	42.43	1.429	21.81	34.7	34.74
20	190	30.41	17.56	124.919	42.45	1.430	21.96	34.8	34.74
21	200	30.38	17.58	124.942	42.48	1.430	22.11	34.8	34.74
22	210	30.98	17.83	124.964	43.14	1.427	21.48	34.8	34.76
23	220	30.94	17.85	124.986	43.16	1.428	21.63	34.9	34.76
24	230	30.91	17.86	125.009	43.19	1.428	21.78	34.9	34.76
25	240	30.88	17.87	125.031	43.21	1.428	21.92	34.9	34.76
26	250	30.85	17.88	125.054	43.24	1.429	22.07	34.9	34.75
27	260	30.82	17.89	125.076	43.27	1.429	22.22	35.0	34.75
28	270	30.79	17.90	125.098	43.29	1.430	22.37	35.0	34.75
29	280	30.75	17.92	125.121	43.32	1.430	22.52	35.0	34.75
30	290	30.72	17.93	125.143	43.35	1.430	22.66	35.0	34.74
31	300	30.69	17.94	125.166	43.37	1.431	22.81	35.1	34.74
32	310	30.66	17.95	125.188	43.40	1.431	22.96	35.1	34.74
33	320	30.63	17.96	125.211	43.43	1.432	23.10	35.1	34.74
34	330	30.60	17.97	125.233	43.45	1.432	23.25	35.2	34.73
35	340	30.58	17.99	125.256	43.48	1.432	23.40	35.2	34.73
36	350	30.55	18.00	125.278	43.51	1.433	23.54	35.2	34.73
37	360	30.52	18.01	125.301	43.54	1.433	23.69	35.3	34.73
38	370	30.49	18.02	125.323	43.56	1.433	23.84	35.3	34.72
39	380	30.46	18.03	125.345	43.59	1.434	23.98	35.3	34.72
40	390	30.43	18.05	125.368	43.62	1.434	24.13	35.4	34.72
41	400	30.41	18.06	125.390	43.65	1.434	24.27	35.4	34.72
42	410	30.38	18.07	125.413	43.67	1.435	24.42	35.4	34.71
43	420	30.35	18.08	125.435	43.70	1.435	24.56	35.4	34.71
44	430	30.33	18.10	125.458	43.73	1.436	24.70	35.5	34.71
45	440	30.30	18.11	125.481	43.76	1.436	24.85	35.5	34.71
46	450	30.27	18.12	125.503	43.79	1.436	24.99	35.5	34.70
47	460	30.25	18.13	125.526	43.81	1.437	25.14	35.6	34.70
48	470	30.22	18.14	125.548	43.84	1.437	25.28	35.6	34.70
49	480	30.20	18.16	125.571	43.87	1.437	25.42	35.6	34.70
50	490	30.17	18.17	125.593	43.90	1.438	25.56	35.6	34.70
51	500	30.15	18.18	125.616	43.93	1.438	25.71	35.7	34.69
52	510	34.36	19.79	125.638	48.22	1.419	20.36	35.7	34.88

Results Table - Ramp 6850-5 to 7350

Row	Distance (m)	Dry Bulb (°C)	Wet Bulb (°C)	Pressure (kPa)	Sigma Heat (kJ/kg)	Density (kg/m³)	Humidity (%)	VRT (°C)	MST (°C)
53	520	34.31	19.80	125.660	48.24	1.419	20.51	35.7	34.87
54	530	34.27	19.81	125.683	48.26	1.420	20.66	35.8	34.87
55	540	34.23	19.82	125.705	48.28	1.420	20.81	35.8	34.87
56	550	34.18	19.83	125.727	48.31	1.420	20.96	35.8	34.87
57	560	34.14	19.84	125.749	48.33	1.421	21.11	35.9	34.86
58	570	34.10	19.85	125.772	48.35	1.421	21.26	35.9	34.86
59	580	34.06	19.86	125.794	48.37	1.422	21.41	35.9	34.86
60	590	34.02	19.87	125.816	48.40	1.422	21.56	35.9	34.85
61	600	33.98	19.88	125.839	48.42	1.422	21.71	36.0	34.85
62	610	33.93	19.89	125.861	48.44	1.423	21.86	36.0	34.85
63	620	33.89	19.90	125.883	48.47	1.423	22.01	36.0	34.85
64	630	33.85	19.91	125.906	48.49	1.424	22.16	36.1	34.84
65	640	33.81	19.92	125.928	48.51	1.424	22.31	36.1	34.84
66	650	33.78	19.93	125.950	48.54	1.425	22.46	36.1	34.84
67	660	33.74	19.94	125.973	48.56	1.425	22.61	36.1	34.84
68	670	33.70	19.95	125.995	48.58	1.425	22.76	36.2	34.83
69	680	33.66	19.96	126.017	48.61	1.426	22.91	36.2	34.83
70	690	33.62	19.97	126.040	48.63	1.426	23.06	36.2	34.83
71	700	33.58	19.98	126.062	48.65	1.427	23.21	36.3	34.82
72	710	33.55	19.99	126.084	48.68	1.427	23.36	36.3	34.82
73	720	33.51	20.00	126.107	48.70	1.427	23.51	36.3	34.82
74	730	33.47	20.01	126.129	48.73	1.428	23.65	36.4	34.82
75	740	33.44	20.02	126.151	48.75	1.428	23.80	36.4	34.81
76	750	33.40	20.03	126.174	48.77	1.429	23.95	36.4	34.81
77	760	33.37	20.04	126.196	48.80	1.429	24.10	36.4	34.81
78	770	33.33	20.05	126.219	48.82	1.429	24.24	36.5	34.81
79	780	33.30	20.06	126.241	48.85	1.430	24.39	36.5	34.80
80	790	33.26	20.07	126.264	48.87	1.430	24.54	36.5	34.80
81	800	33.23	20.08	126.286	48.90	1.431	24.68	36.6	34.80
82	810	33.19	20.09	126.308	48.92	1.431	24.83	36.6	34.80
83	820	33.16	20.10	126.331	48.95	1.431	24.98	36.6	34.79
84	830	33.12	20.12	126.353	48.97	1.432	25.12	36.6	34.79
85	840	33.09	20.13	126.376	49.00	1.432	25.27	36.7	34.79
86	850	33.06	20.14	126.398	49.02	1.433	25.41	36.7	34.79
87	860	33.03	20.15	126.421	49.05	1.433	25.56	36.7	34.79
88	870	32.99	20.16	126.443	49.08	1.433	25.70	36.8	34.78
89	880	32.96	20.17	126.466	49.10	1.434	25.85	36.8	34.78
90	890	32.93	20.18	126.488	49.13	1.434	25.99	36.8	34.78
91	900	32.90	20.19	126.511	49.15	1.434	26.14	36.9	34.78
92	910	33.41	20.40	126.533	49.73	1.432	25.50	36.9	34.80
93	920	33.38	20.41	126.556	49.75	1.433	25.64	36.9	34.80
94	930	33.34	20.42	126.578	49.78	1.433	25.79	36.9	34.79
95	940	33.31	20.43	126.601	49.80	1.433	25.93	37.0	34.79
96	950	33.28	20.44	126.623	49.83	1.434	26.08	37.0	34.79
97	Electric heat source at 100 m, sensible heat = 209.00 kW								
98	Electric heat source at 200 m, sensible heat = 30.80 kW								
99	Electric heat source at 500 m, sensible heat = 209.00 kW								
100	Electric heat source at 900 m, sensible heat = 26.80 kW								
101	Strata heat totals: sensible heat = -219.67 kW, latent heat = 266.35 kW								
102	Other heat totals: sensible heat = 475.60 kW, latent heat = 0.00 kW								
103	Metabolic rate = 200 W/m², Skin temperature limit value = 34.98 °C								